Modelling and Analysis of ER Fluid Dampers: with application to tremor suppression

By

Geoffrey Walsh, B.Eng.

Submitted for the degree of

Doctor of Philosophy

Dublin City University

Department of Mechanical & Manufacturing Engineering

July 2006

Supervisors

Dr. Harry Esmonde and Prof. Saleem Hashmi

I hereby certify the this material, which I now submit for assessment on the programme of study leading to the award of Doctor of Philosophy is entirely my own work and has not been taken from the work of others save and to the extent that such work has been cited and acknowledged within the text of my work.

Signed: Geoff Walsh . ID No: 97085359

Candidate

Date: 7th of July 2006

Abstract

The most commonly used definition for human tremor is as an involuntary, roughly sinusoidal oscillation of one or more parts of the body. It has been established that the application of viscous damping can significantly reduce the amplitude of tremor related oscillations, but that the level of damping required also impedes voluntary motion. Evidence would suggest that if a controllable damper were used, then it may be possible to modulate the damping so as to provide a significant level of tremor suppression, while allowing voluntary motion. A candidate for the construction of such a damper is electrorheological (ER) fluid. When an electric field is applied to a volume of ER fluid, its material properties change from that of a Newtonian fluid to that of an elastic-plastic solid. These structural changes occur within milliseconds and are completely reversible, making ER fluids an attractive option when designing controllable dampers. The analysis and design of control strategies for ER dampers requires the development of suitable mathematical models. In particular, models should be capable of predicting the dominant behaviour of the device when coupled to other physical systems. In this thesis, well known thermomechanical principles are used to develop simple, physically intuitive models which are well suited for analysis and control design. The simplest of these damper models is then coupled with a forced, second order oscillator, representing the human forearm/elbow subject to tremor. A detailed analysis of the qualitative behaviour of this system is then performed, using traditional energy based and Liapunov type techniques. Sufficient conditions for the existence and stability of periodic solutions are also presented. A result of this analysis is the development of a novel control strategy for the attenuation of periodic oscillations. In the final section of the thesis, the feasibility of using the above mentioned control strategy for suppression of human tremor is investigated. The theoretical results are quite favourable and are supported by numerous simulation results.

Acknowledgements

To begin with, I would like to thank my supervisor Dr. Harry Esmonde for his advice, friendship and for never loosing faith in me. I would like to express my gratitude to the members of my examination committee, Dr. Anthony Holohan and Dr. Neil Sims, for taking the time and pains to review my thesis and for their many useful suggestions. I would also like to thank all the staff and postgraduates of the Mechanical Engineering Department for their friendship and encouragement. I cannot find the words to articulate how much I have valued the continual support and encouragement given to me by Mom, Dad, my sister Sile and my close friends. The best I can do is "thanks lads".

Dedication

I would like to dedicate this thesis to my good friends

Jim J. Jerrily
Ann Jar
John "JJ" Jobine
Seth Bowlyllow
Sminey A. Smoney

"Thanks for all the Eulidanes"

Table of Contents

Table of Contents

Appendices

List of Figures

Chapter 1

Chapter 2

Chapter 3

List of Figures

Chapter 4

Chapter 5

Symbols and notation

Mathematical symbols

$\forall$	for all
$\mid$	such that
$=$	left is equal to right
$:=$	left is by definition equal to right
$<(>)$	less (greater) than
$\leq(\geq)$	less (greater) than or equal to
$\Leftrightarrow$	left is equivalent to right
$\Rightarrow$	left implies right
$\mapsto$	maps to
$\rightarrow$	tends to
$\in$	belongs to
$\notin$	does not belong to
$\subset$	is a subset of
$\bigcap$	intersection
$\bigcup$	union
max(min)	maximum (minimum)
sup(inf)	supremum, least upper bound (infimum, greatest lower bound)
$\mathrm{osc}_T x$	oscillation of the T-periodic function $x:\Re_+ \rightarrow \Re$ over the interval $[0,T]$
$\Re$	real numbers
$\Re_+$	nonnegative real numbers
$\Re^n$	n-dimensional Euclidean space
$\langle x,y\rangle$	Euclidean inner product
$\lvert x\rvert$	norm in $\Re^n$, $\sqrt{\langle x,x\rangle}$
int $\mathbf{C}$, bd$\mathbf{C}$	interior, boundary of the set $\mathbf{C}\subset\Re^n$
$\mathrm{B}(x;r)$	closed ball $\{y\in\Re^n \mid \lvert y-x\rvert\leq r\}$
$f:S_1\mapsto S_2$	a function mapping the set S_1 into the set S_2
$f_1\circ f_2$	the composition of two functions
$f^{-1}(\cdot)$	inverse function
$\dot{x}(\ddot{x})$	first (second) derivative of the function $x:\Re\rightarrow\Re^n$, with respect to time
∇f	gradient of the function $f:\Re^n\rightarrow\Re$
$\frac{\partial f(x)}{\partial x_i}$	partial derivative of the function $f:\Re^n\rightarrow\Re$ with respect to $x_i\in x$
$\partial f(x)$	subderivative of the convex function $f:\Re^n\rightarrow\Re$, at $x\in\Re^n$
$N(x;\mathbf{C})$	normal cone to the convex set $\mathbf{C}\subset\Re^n$, at $x\in\Re^n$
$I(x;\mathbf{C})$	indicator function of the convex set $\mathbf{C}\subset\Re^n$ evaluated at $x\in\Re^n$
$Q(x;\mathbf{C})$	projection of $x\in\Re^n$ onto the set $\mathbf{C}\subset\Re^n$, if $\mathbf{C}=[-r,r]$, with $r\in\Re_+$, then the notation $Q(x;r)$ will be used

$P(x;\mathbf{C})$	dual of the projection operator $P(x;r) = x - Q(x;r)$
sgn(·)	signum function
SGN(·)	set valued signum function

Function spaces (see Appendix A for details)

For some interval $J \subset \Re_+$

$L_\infty(J;\Re^n)$	the space of essential bounded functions $x : J \mapsto \Re^n$
$\|x\|_\infty$	(essential) supremum norm, $\|x\|_\infty = \operatorname{ess\,sup}_{t\in J}\|x(t)\|$
$L_1(J;\Re^n)$	the space of integrable functions $x : J \mapsto \Re^n$
$L_2(J;\Re^n)$	the space of square integrable functions $x : J \mapsto \Re^n$
$C(J;\Re^n)$	the space of continuous functions $x : J \mapsto \Re^n$
$C^k(J;\Re^n)$	the space of k-times continuously differentiable functions $x : J \mapsto \Re^n$
$C^{0,1}(J;\Re^n)$	the space of Lipschitz continuous functions $x : J \mapsto \Re^n$
$C^{k,1}(J;\Re^n)$	the space of k-times continuously differentiable functions $x : J \mapsto \Re^n$, with Lipschitz continuous k^{th} derivative

Thermomechanics and damper modelling

α	internal variables
A	thermodynamic force conjugate to α
χ	observable thermodynamic state variables or modified Bingham plastic function
X	thermodynamic force conjugate to the state variable χ
U	internal energy
W	free energy
Φ	dissipation function
D	dissipation potential
D^*	flow potential (Legendre dual of D)
σ	shear stress
e	shear strain
r	yield stress
$\bar{r}$	upper bound for variable yield stress
r_e	yield strain
E	electric field (scalar)
G	elastic modulus (spring stiffness)
η	viscosity
f	yield function

Damper model Abbreviations

EP	elastic plastic model
Π(EP)	multiple element elastic plastic model
EVP	elastic viscous plastic model
VP	viscoplastic model
MVP	modified viscoplastic model
GnF	model of Gamota and Filisko

General modelling and systems

Σ_X	forearm model
Σ_Z	damper model (EP model)
Σ	coupled system , between Σ_X and Σ_Z
Σ_S	reference damper model in dissipation shaping (EVP model)
Σ_D	coupled system , between Σ_X and Σ_S
Σ_F	Dahl friction model
q	actual angle of forearm (elbow angle)
q^*	desired angle of the forearm (desired elbow angle)
x	(shifted) state of forearm model or state of general ordinary differential equation
z	state of damper model (EP model)
x_a	state of coupled system, $x_a = (x, z)$
s	state of reference damper model in dissipation shaping
J	inertia
m	mass
R	viscous coefficient associated with forearm model
K	stiffness coefficient associated with forearm model
$h(\cdot)$	nonlinear restoring force due to gravitational forces and the feed forward control acting on the forearm
$h_K(\cdot)$	$h_K(x) = Kx + h(x)$
b	tremor torque
r	controllable yield stress of damper model Σ_Z (damper control)
r_s	controllable yield stress of reference damper model Σ_S
F	external torque acting on the forearm
T	period associated with tremor or interval for OT -recurrent control
φ	test function used in variational inequalities
H	total stored energy
V	Liapunov function
$\Omega(x)$	positive limit set (ω -limit set) of a function $x : \Re_+ \to \Re^n$

Main Stability Abbreviations (see Appendix B for details)

GAS	globally asymptotically stable
GUAS	globally uniformly asymptotically stable
ES	exponentially stable
GES	globally exponentially stable
UB	uniformly bounded
UUB	uniformly ultimately bounded

Referencing

§x.y	chapter x section y
(x.y.z)	equation z, appearing in section y of chapter x
Fig x.y	figure y appearing in chapter x
[x]	literary reference x

Chapter 1

Introduction and Motivation

Pathological tremor usually manifests itself as an involuntary oscillation of a limb or limbs. In its mild forms it can be a nuisance and in severe cases it can occur with such severity that the sufferer is unable to perform the basic activities involved in daily living. Drug treatment and surgery have not been very successful in treating some of the more severe forms of tremor. This has led to the search for alternative approaches to the problem of tremor suppression. Section.1 of this chapter briefly discusses the various types/causes of tremor and reviews some of the devices which have been developed for tremor suppression. It is known that the application of viscous damping can significantly reduce the amplitude of tremor related oscillations, but that the level of damping required also impedes voluntary motion. Evidence would suggest that if a controllable damper were used, then it may be possible to modulate the damping so as to provide a significant level of tremor suppression, while allowing voluntary motion.
A candidate for the construction of such a damper is electrorheological (ER) fluid. ER fluid is a class of smart material whose resistance to shear can be rapidly increased by applying an electric field. In order to investigate the feasibility of using an ER damper to suppress tremor, a model is required which captures the highly nonlinear behaviour exhibited by ER fluid dampers. Section.2 provides an introduction to ER fluids and reviews some of the models which have been developed for ER fluid dampers. Unfortunately many of the available models, which do capture the qualitative behaviour of ER fluid dampers are not well suited for analysis and control design. This thesis attempts to address this problem.

1.1 Tremor

The most commonly used definition of tremor is as an involuntary, roughly sinusoidal oscillation of one or more parts of the body. Tremor mainly affects the hands and arms, though certain forms may effect the legs, trunk, head and even one's speech, [1][2][3]. Human tremor is initially categorised as being either physiological or pathological. Physiological tremor is an 8-12 Hz oscillation, which is inherent in all human motion,

both voluntary and involuntary. It is generally confined to the hands, with an amplitude low enough for it to be barely visible. As such, it only becomes a nuisance during highly dexterous tasks. Pathological tremor however is a potentially disabling symptom that occurs as a result of numerous neurological disorders such as Parkinson's disease and Multiple Sclerosis (MS). For many individuals who suffer from pathological tremor in their arms and hands, independent function during daily activities can be difficult if not impossible.

During a medical diagnosis, pathological tremor is typically classified according to the behavioural circumstances under which it occurs, see Table 1. Rest tremor appears when the affected limb is relaxed and fully supported against gravity. Postural tremor occurs when the sufferer tries to maintain a posture against gravity, such as when holding the arms out in front of the body. Action tremor, as its name would suggest, occurs during voluntary movement of the affected limb. Action tremor is usually further classified as either kinetic or intention tremor. Kinetic tremor occurs during arbitrary movements of the limb from point to point, whereas with intention tremor, the amplitude of the tremor increases as the affected limb approaches the intended goal [1][2][3]. It is also possible to characterize different forms of tremor by performing a quantitative analysis of an individual's tremor, based on the amplitude, phase, frequency and the activation pattern of the agonistic muscles (alternating or synchronous).

Tremor	Frequency	Occurrence	Typical Cause
Postural tremor	**5 to 9 Hz**	**When limb is positioned against gravity**	**Essential tremor**
Rest tremor	**3 to 6 Hz**	**When limb is wholly supported against gravity and muscles are not voluntarily activated**	**Parkinson's disease, Wilson's disease, Essential tremor.**
Action tremor	**3 to 10 Hz**	**During voluntary muscle contraction**	**Multiple Sclerosis, Head injury**

Table 1.1, taken from [3].

Possibly the most disabling form of tremor is the low frequency (2.5-4Hz), large amplitude kinetic tremor frequently affecting those with MS. The tremor can occur with sufficient amplitude to obscure all underlying intentional motion [5]. The effect for the sufferer is that every day tasks, essential for an independent lifestyle, cannot be completed unaided. Fig 1.1 shows the EMG recordings taken from the triceps and bicep

(main muscle group controlling flexion and extension of the elbow) of a patient suffering from severe kinetic tremor due to Multiple Sclerosis. As this form of tremor is only observed during voluntary motion, the patient was asked to slowly flex and extend the elbow while the recordings were being taken. It can clearly be seen that the muscles are activated in an alternating pattern, with a constant phase relationship. Analysis of the recording showed the tremor to have a mean frequency of 2.9 Hz. Recordings taken several months later revealed a decrease in the mean frequency to 2.6 Hz. As these were only short time recordings, nothing can be concluded from this shift in frequency, as it may be a daily occurrence. It can also be seen that the amplitude of the EMG varies significantly, this was confirmed by the observed variations in the physical amplitude of the tremor.

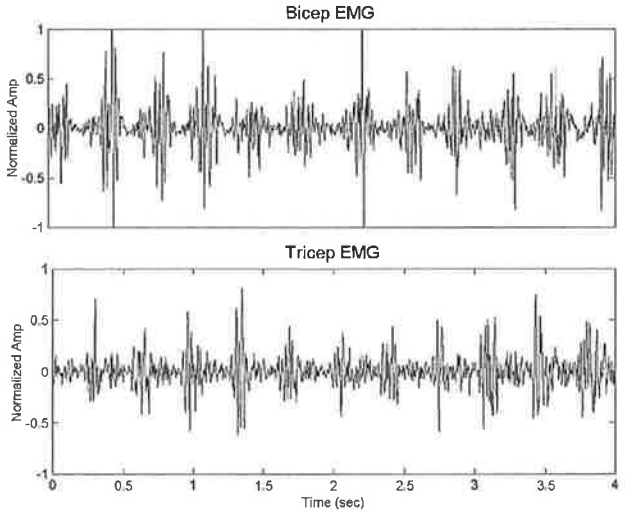

Fig 1.1 EMG recordings from patient with MS (recorded by the author)

When a person is initially diagnosed with a disabling form of tremor the first line of treatment is oral medication. The prescription of medication for the relief of tremor is generally based on the cause of the tremor (associated neurological disorder). While medication may provide relief for milder forms of tremor, for the most severely affected patients, there is no consistently effective treatment. Even if some relief is found, the resulting side effects may be more debilitating than the tremor itself, [2][3].

In cases of severely disabling drug resistant tremor, there are a number of surgical treatments available. However these are generally only considered when all other options have failed to provide relief. A thalamotomy involves permanently destroying targeted nerve tissue in the thalamus, the region of the brain believed responsible for causing tremor. The effects of the surgery are often only short lived however, with

many people finding that their tremor returns [2][3]. Another option is Thalamic stimulation. This involves implanting a tiny electrode in the thalamus area of the brain, during open-skull surgery. A wire attached to the electrode is then tunnelled under the scalp and down the neck to a pulse generator (similar to a pace maker) located under the skin below the collarbone. The pulse generator sends electrical pulses to the electrode, which cancel the nerve signals responsible for causing tremor. Thalamic stimulation was originally developed for the treatment of Parkinson's disease but has also proved successful in alleviating the effects of essential tremor. It is still a new therapy however and is not yet approved for MS tremor [2][5].

An alternative approach to restoring functionality during certain tasks is to develop assistive devices. To date the design of aids for those with tremor has been approached in two ways. The first is to design specific signal processing algorithms to remove tremor related inputs from a computer mouse, a joystick or a digital pen. Thus allowing patients to successfully operate electronic equipment such as computers and electric wheelchairs, [6][7][8]. The second approach is to suppress the effect of tremor using some form of external mechanical device. These devices act mechanically in parallel with the user and are based on evidence that viscous and inertial damping can dramatically reduce the amplitude of severe action tremor and help to restore functional limb control, [4][9][10]. It is known that the frequency content of the voluntary motion involved in activities of daily living is lower than the frequency content of most tremors. Thus, the success of adding viscous damping could be attributed to a form of low pass filtering of the motion. The external mechanical devices which have been developed by various research groups have followed two different approaches, active or passive compensation based on a grounded or wearable orthosis. Grounded devices have been developed to assist in various daily tasks such as eating and controlling an electric wheel chair.

To the knowledge of the author the only commercially available eating aid is the Neater Eater [11]. In its most basic form, the Neater Eater is a two degree of freedom linkage with a viscous damper at the base. The base can be rigidly attached to a table or wheelchair. It is designed to support various utensils, which assist in eating and other personal care activities.

The same company also produces a device called the Mousetrap. This uses a set of viscous restraints, designed to attach to a standard computer mouse and restrain jerky movements from transferring to the computer.

The authors of [12] investigated methods for designing non-adaptive force feedback tremor suppression systems, using a small grounded robotic arm. The methods utilized quantitative frequency domain performance criteria for the selection of feedback gains to achieve a specified reduction in tremor amplitude, much like standard process control. The feedback coefficients are chosen to increase attenuation at a specified tremor frequency, while preserving the low frequency response, so as to preserve voluntary movement. This technique was found to be unsuitable for individuals with low frequency tremor, such as action tremor due to Multiple Sclerosis.

A research group at the Massachusetts Institute of Technology has obtained patents on several devices for tremor suppression. The first of these, called the Controlled Energy Dissipation Orthosis (CEDO) is a three degree of freedom device that can be attached to a wheelchair or table, to facilitate eating and other tabletop activities [13]. Each degree of freedom is damped by a magnetic particle brake, which is controlled in real time by an onboard computer. Tests with the CEDO have shown up to 80% reduction of tremor in severe cases, though it is unclear what effect this had on the intended motion. One of the developers is quoted as saying that the user gets the overall feeling of "moving your arm through molasses". A problem with using fixed levels of viscous damping is that the level of damping required to suppress severe action tremor, such as in MS, will also make intentional motion difficult. Another development by the same group is the MIT damped joystick, designed to allow people with tremors operate electric wheelchairs [14]. Results show that the joystick provides considerable improvement in pursuit tracking tasks for persons with tremor.

The first wearable tremor suppression device to have been published is the Viscous-Beam-Wrist-Orthosis developed in [15]. The orthosis applies a viscous resistance to the wrist in flexion and extension using a constrained-layer-damping (CLD) system. The CLD linearly converts wrist flexion/extension into rectilinear translation within the damper. The damper is coupled to the user by hand and forearm cuffs and is small enough to be worn under the sleeve. Results have shown it to be successful in attenuating the effects of tremor at the wrist.

It was noted however, that as it was only a passive device, in cases of severe tremor, increasing the resistance to achieve tremor reduction was impossible without adversely affecting the intentional motion. In addition for cases where there is tremor present in the elbow and/or shoulder an additional orthosis would be required.

More recently, the DRIFTS "Dynamical Responsive Intervention For Tremor Suppression" project was financed by the European Commission's Fifth Framework Program, a complete overview of which can be found in [16]. The main aim of the project is to create proof of concept prototypes of wearable orthoses for the suppression of upper limb tremor. As part of the project the WOTAS (Wearable Orthosis for Tremor Assessment and Suppression) was developed to measure upper-extremity tremor and as a prototyping platform for evaluating control strategies, actuators, and sensors for tremor suppression [17]. The WOTAS comprises an adjustable exoskeleton with articulated joints incorporating actuators (DC motors) at wrist and elbow, kinematic sensors and kinetic sensors. Using the WOTAS, tremor measurement and suppression strategies can be investigated in three different degrees of freedom: elbow flexion/extension, wrist flexion/extension and wrist pronation/supination. A recent result of the DRIFTS project is a prototype orthosis, similar in some respects to the Viscous-Beam-Wrist-Orthosis described above, see Fig 1.2. It is an articulated brace worn over the forearm and wrist. The orthosis incorporates a viscous-beam-actuator, which applies a controlled damping force in proportion to the tremor force across the wrist joint [18]. Changes in the tremor pattern are instantaneously detected by miniature electronic gyroscopes and digital filters are used to distinguish between the intended motion and tremor. Feedback and control algorithms are then used to determine the amount of damping required to suppress the tremor. The controllable damping is provided by a double-viscous-beam (DVB) actuator, an electronically controlled damping mechanism using magnetorheological fluids [18]. The specific details of the construction and operation of the DVB actuator can be found in [19]. Unfortunately specific details of the model and control strategies used and on experimental results with the device, do not seem to have been published yet.

Electrorheological (ER) and magnetorheological (MR) fluids belong to the class of smart fluids. They have the ability to rapidly alter their resistance to shear in response to the application of an electric or magnetic field (more details will be given in the next section). By constructing tremor suppression devices from these fluids, it should be

possible to modulate the resistance in such a way, so as to attenuate the oscillations caused by severe forms of action tremor, but with a minimal amount of resistance to intentional motion. Based on the success of the DVB actuator, a suitable next step towards a full arm orthosis, would be to develop a damper using ER or MR fluids for the suppression of tremor at the elbow. As will be described in the next section, dampers constructed from ER and MR fluids display highly nonlinear behavior. A significant hindrance to the development and analysis of control systems for such devices is the lack of well behaved models which capture their nonlinear behaviour. This fact will be discussed in greater detail in the next section of this chapter.

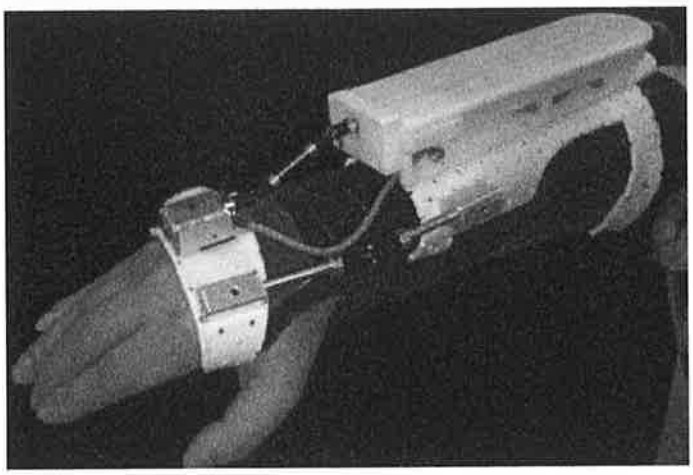

Fig 1.2 Drifts orthosis (picture taken from [18]).

1.2 ER fluid dampers

Electrorheological (ER) fluids are characterised by the ability to adjust their mechanical properties through application of a sufficiently strong electric field. In particular, application of an electric field causes an increase in the force (yield force) required to induce unbounded flow of the fluid. This change in resistance to flow occurs rapidly and is completely reversible, upon removal of the electric field. These properties make ER fluids an attractive means for the construction of controllable dampers and other force transfer devices. Furthermore, while the electric fields required to induce this change in resistance are quite high, ER fluids draw very little current, resulting in low power requirements. Unlike active control devices, when an ER fluid device is coupled with a mechanical system, it can only dissipate and store energy by reacting to its

motion. As a result the term "semi-active" is often used for ER devices, however the term "controllable passive" is probably more appropriate [20].

A typical ER fluid consists of a suspension of tiny polarisable particles in a viscous nonconducting liquid. Consider the case where a volume of ER fluid is confined between two parallel electrodes. When an electric field is applied to the fluid, the particles become polarized and form into chains that span the gap between the field generating electrodes. The mechanical behaviour of a sheared ER fluid is similar to an elastic-plastic solid, with a yield stress which is an increasing function of the electric field [21]. When the shear stress is less than this yield stress, the fluid behaves like an elastic solid, capable of sustaining stress in the absence if flow. This behavior is associated with the reversible stretching and deformation of the particle chains.

For unbounded shear to occur, the shear stress needs to be maintained at a level greater than or equal to the yield stress. In this case, the deformations are dissipative and can be associated with dynamic equilibrium between chain snapping and reformation [21]. Thus the behaviour of sheared ER fluid can be characterized into two distinct regimes: preyield and postyield. Magnetorheological (MR) fluid is another controllable fluid, the behaviour of which is quantitatively identical to that of ER fluid. In this case however, a magnetic field is responsible for the formation of particle chains by inducing a magnetic moment in the particles. When a damper or other controllable device is constructed using ER/MR fluids, the behaviour of the device resembles that of the controllable fluid. Fig 1.3 shows the response of an activated, large scale MR damper subject to a sinusoidal displacement, taken from [22]. This form of response is typical of most ER and MR dampers (after appropriate scaling).Note that the force displacement hysteresis loop is traversed in the clockwise direction, while the force velocity loop is traversed in the anticlockwise direction.

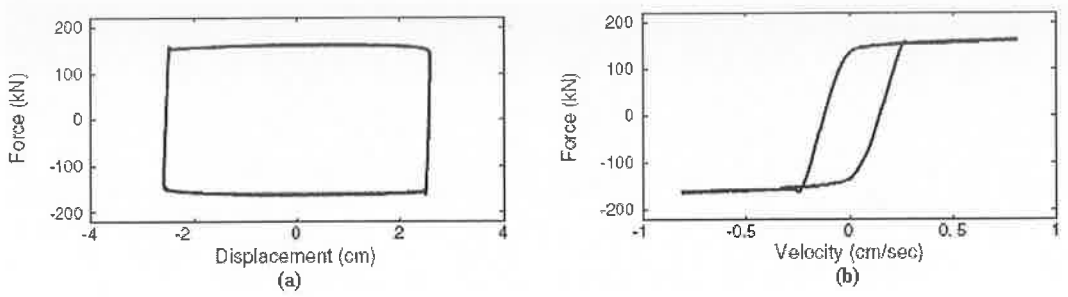

Fig 1.3 Typical response characteristic of an activated ER/MR fluid Damper [22]

In constructing controllable dampers using ER fluids, there are three main modes of operation: shear mode, flow mode and squeeze mode [20]. Shear mode involves the direct shearing of the fluid between translating of rotating electrodes. Fig 1.4(a) shows a simple model of a couette-type ER fluid damper, consisting of a fixed electrode and a rotating electrode with ER fluid in between them. The two cylinders also act as a pair of electrodes. If a voltage difference is generated between the cylinders an electric field builds up in the gap, which is perpendicular to the flow. The ER fluids resistance to shear increases with increasing level of electric field strength, as does the torque exerted on the outer cylinder. In flow mode the fluid is forced between a pair of stationary electrodes. The fluids resistance to flow is increased by increasing the electric filed strength, creating a sort of "flow control valve". Fig 1.4(b) show a typical flow mode ER damper. The piston rod moves up and down in a chamber filled with fluid, forcing the fluid to flow through the valve. The accumulator compensates for the change in volume of the chamber caused by motion of the piston and also prevents cavitation.
The accumulator affects the behaviour of the damper, acting like a spring from a phenomenological point of view [23].

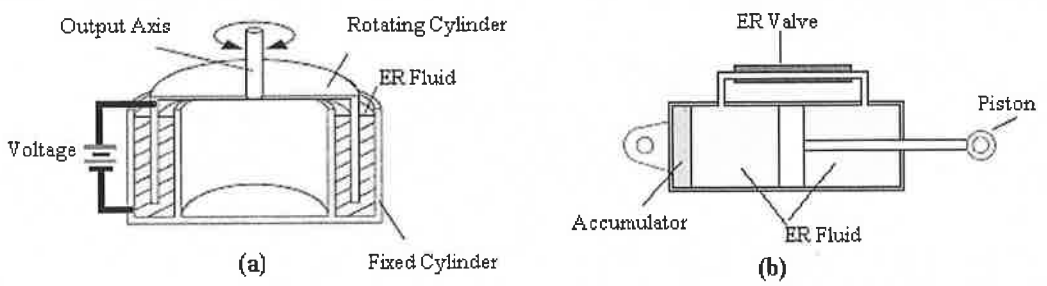

Fig 1.4 Typical geometries for ER dampers

In order to take advantage of ER/MR fluid devices in control applications, mathematical models are required to describe their dynamical behaviour and which are suitable for coupling with other mechanical system models. To date, there have been dozens of studies focusing on the characterization of the fluids and the development of suitable models for dampers and other devices. Phenomenological models are one class of model which is quite popular and appealing because of their intuitive nature. These models are usually constructed from idealized mechanical elements such as elastic springs, viscous dashpots and rigid friction elements. The elements are arranged in such a way so as to capture the essential macroscopic behaviour of the damper under study. Due to their qualitatively similar behaviour, phenomenological models for ER and MR fluid devices can usually be applied to either case. A brief review of some of the more

successful phenomenological models to appear in the literature will now be given. For a more comprehensive review, the reader is referred to the excellent papers [24][25].

Let $x(t)$ denote the displacement of the damper and $F(t)$ the reactive force. For the damper in Fig 1.4(a), $x(t)$ corresponds with the angular displacement of the rotating cylinder and $F(t)$ is the torque on the corresponding shaft. One of the first models to be developed for an ER damper consisted of a rigid friction element and a viscous damper in parallel [26]. This model is commonly referred to as the Bingham model in analogy with the Bingham plastic model from continuum mechanics (more details in §3). The equations describing this model are simply

$$F(t) = R\dot{x}(t) + F_Y(t)\mathrm{SGN}(\dot{x}(t)) \tag{1.2.1}$$

the viscous damping coefficient $R > 0$ accounts for the base fluid viscosity and $F_Y(t) \geq 0$ is the controllable (field dependent) yield force, Fig 1.4(a). The function $\mathrm{SGN}(\dot{x})$ is the set valued signum function given by

$$\mathrm{SGN}(\dot{x}) \in \begin{cases} 1 & \text{if } \dot{x} > 0 \\ [-1,1] & \text{if } \dot{x} = 0 \\ -1 & \text{if } \dot{x} < 0 \end{cases}. \tag{1.2.2}$$

It is widely accepted that the Bingham model captures the dominant behaviour of ER/MR fluid dampers in postyield, i.e. for fully developed flow. However, it assumes that the fluid remains rigid in the preyield region, that is if $|F(t)| \leq F_Y(t)$, then $\dot{x}(t) = 0$. Thus, the Bingham model does not account for the essentially viscoelastic behaviour of the fluid in the preyield region. In order to facilitate analysis and to allow for motion in the preyield region numerous smooth approximations of the Bingham model have been presented. For example, in [27] and [28] the function $\mathrm{SGN}(\dot{x})$ was replaced by the smooth hyperbolic tangent function and the inverse hyperbolic sine function respectively. Possibly the most popular approximation is the biviscous model [20][29][30].

$$F(t) = R\dot{x}(t) + \begin{cases} F_Y(t)\mathrm{sgn}(\dot{x}(t)) & \text{if } |\dot{x}(t)| > F_Y(t)/R_p, \\ R_p\dot{x}(t) & \text{otherwise}. \end{cases} \tag{1.2.3}$$

The fundamental problem with these smooth approximations is that they are fluid models, which is to say that that they are incapable of sustaining a force at zero velocity.

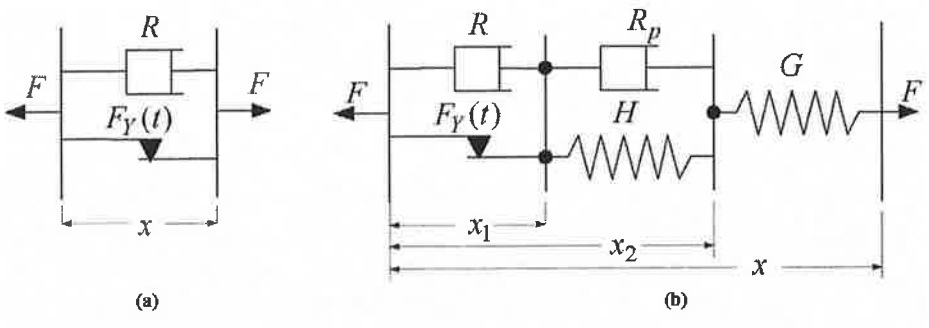

Fig 1.5 (a) Bingham Model, (b) extended Bingham model .

In order to account for the viscoelastic behaviour of ER fluid in preyield, in [31] the Bingham plastic was placed in series with the standard model for solid viscoelasticity, to create the extended Bingham model in Fig 1.5(b). The governing equations for this model, as presented in [23] and [24], are

$$F(t)=\begin{cases} G(x-x_2) \\ H(x_2-x_1)+R_p(\dot{x}_2-\dot{x}_1), \quad if \quad |F(t)|>F_Y(t), \\ R\dot{x}_1+F_Y(t)\,\mathrm{sgn}(\dot{x}_1) \\ \\ G(x-x_2) \\ H(x_2-x_1)+R_p\dot{x}_2, \qquad otherwise. \end{cases} \tag{1.2.4}$$

In [32] the parameters defining the model were fitted to experimental data from a shear mode ER damper. It was found that the elastic moduli G , H and the viscous coefficients R, R_p were independent of the electric field (above some small value). As expected the yield force $F_Y(t)$ was found to be a strictly increasing function of the electric field strength. The extended Bingham model was also found to capture all the qualitative behaviour of an MR damper in [23]. The main criticism of the model in both of these studies was that the model was very difficult to deal with numerically, due to the presence of the friction element. In [27] this difficulty was overcome by replacing the friction element by the smooth approximation $F_Y(t)\tanh(\dot{x}_1(t)/V_r)$, where V_r is some reference velocity governing the sharpness of the yielding. Again, the problem with this is that the model becomes a fluid model, incapable of sustaining a stress without motion.

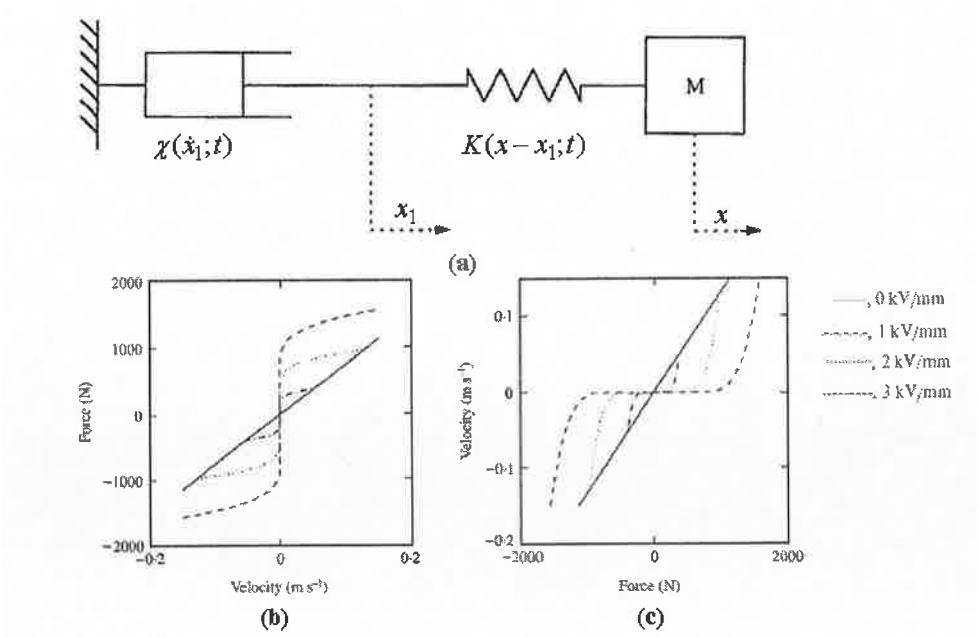

Fig 1.6 Model for a long stroke ER fluid damper, (b) modified Bingham plastic function, (c) inverse of modified Bingham plastic function (taken from[33]).

The phenomenological model in Fig 1.6(a) was developed in [33] to capture the behaviour of a long stroke ER fluid damper. The mass m is included to account for the effect of fluid inertia and $K(x-x_1;t)$ is a bilinear spring function given by

$$K(x;t)=\begin{cases}2Gx & if \quad |x|\le F_Y(t)/2G,\\ Gx-F_Y(t)/2 & if \quad |x|<-F_Y(t)/2G,\\ Gx+F_Y(t)/2 & if \quad |x|>F_Y(t)/2G.\end{cases} \tag{1.2.5}$$

The function $\chi(\dot{x}_1;t)$ is referred to as the modified Bingham plastic function, and accounts for the dampers behaviour in preyield, the graph of $\chi(\dot{x}_1;t)$ is shown in Fig 1.6(b). The resulting equations of motion are given by

$$\begin{aligned}&\chi(\dot{x}_1;t)=K(x-x_1;t),\\ &m\ddot{x}+K(x-x_1;t)=F(t).\end{aligned} \tag{1.2.6}$$

In order to solve the equations of motion, the modified Bingham plastic function is inverted as in Fig 1.6(c), to obtain the differential equation $\dot{x}_1=\chi^{-1}(K(x-x_1;t);t)$. For simulation purposes, the inverse of the modified Bingham plastic function was implemented using a lookup table. In a later study [30], this model was applied to a MR damper, replacing (1.2.5) with a linear spring and the modified Bingham plastic function by the biviscous model in (1.2.3).

In order to obtain a numerically tractable and versatile model, in [23] a Bouc type hysteresis model [34] was used to characterizes an MR damper such as the one in Fig 1.4(b). The simplest such model presented in [23] is given by

$$\begin{aligned} F(t) &= R\dot{x}(t) + \alpha(t)z, \\ \dot{z} &= -\gamma|\dot{x}(t)|z|z|^{n-1} - \beta|z|^{n}\dot{x}(t) + A\dot{x}(t). \end{aligned} \tag{1.2.7}$$

By adjusting the parameters γ, β, A and n it is possible to control the shape of the hysteresis loops generated by the internal variable z. In modelling MR dampers the model is generally implemented using $A > 0$ and $\beta = \gamma > 0$ [23][35]. In this case, for steady unidirectional flow the internal variable approaches the value $z = \sqrt[n]{A/(\gamma+\beta)}\,\mathrm{sgn}(\dot{x}(t))$. The value of the field dependent control variable $\alpha(t) \geq 0$ can then be used to control the level of the rate independent yield stress.

The last model to be described is the nonlinear viscoelastic-plastic model, originally proposed in [36]. The model is based on the knowledge that in preyield ER/MR fluids behave like viscoelastic solids and in postyield like a Bingham plastic. The idea is to use two separate models to capture the preyield and postyield behaviour and then to smoothly transition between them using suitable switching functions. In preyield the fluid/damper is modelled using a spring and dashpot in parallel, $F_{pr}(t) = R_p\dot{x}(t) + Kx(t)$. In postyield the fluid/damper response is modelled using a viscous dashpot $F_{po}(t) = R\dot{x}(t)$ and a friction element with yield force $F_y(t)$. To effect a smooth transition between these regimes the following switching function are used

$$\begin{aligned} S_{pr}(t) &= \frac{1}{2}\left(1 - \tanh\left(\frac{|\dot{x}(t)| - v_y}{4\varepsilon_y}\right)\right), \\ S_{po}(t) &= \frac{1}{2}\left(1 + \tanh\left(\frac{|\dot{x}(t)| - v_y}{4\varepsilon_y}\right)\right), \\ S_{y}(t) &= \frac{1}{2}\tanh\left(\frac{\dot{x}(t)}{4\varepsilon_y}\right). \end{aligned} \tag{1.2.8}$$

where the parameters ε_y and v_y are used to control the rate at which the transition takes place. The total reactive force generated by the damper is then given by

$$F(t) = S_{pr}(t)F_{pr}(t) + S_{po}(t)F_{po}(t) + S_y(t)F_y(t). \tag{1.2.9}$$

For the purposes of identification all six parameters $R_p, K, R, F_y, \varepsilon_y$ and v_y are assumed to be functions of the applied field. In [29] it was also demonstrated that the nonlinear

viscoelastic-plastic model can capture the behaviour MR dampers when subject to sinusoidal excitation.

Given that so many models have already been developed for ER/MR fluid dampers, why the need to develop new models. The purpose of this thesis is not so much to develop new models. Rather, it is present techniques which can be used to reformulate existing models, in a manner which is more amenable to analysis and control design. Based on the premise that modelling should always be performed in connection with the intended application, the application considered in this thesis will be reviewed to gain some insight into what might be required from a damper model. From the discussion in Section.1, the intended application could be stated as follows: To couple the damper model with a model of the human forearm with tremor (periodically forced second order oscillator) and to investigate the feasibility of using the damper to attenuate the effect of a tremor, on the motion of the forearm (tremor suppression).

A logical approach to tackling this problem might go as follows. First derive a model for the damper which captures all of the observed qualitative behaviour. Couple this model with the model of the second order system and show that the coupled model is wellposed. In other words, to show that it has a unique solution, depending continuously on the data of the problem. The next step would be to investigate the qualitative behaviour of the system, such as boundedness of solutions, stability of equilibria and the existence of periodic solutions. Since ER/MR dampers are essentially dissipative devices, a suitable next step would be to analyze the energy flow in the system. In particular, to analyze the effect that varying the electric field has on the energy dissipated by the damper. Based on the results of the investigation, one might try to devise a control strategy for the damper, to maximize (in some sense) the energy dissipated by the damper, while ensuring that the motions of the coupled system remain well behaved. Finally, derive efficient integration algorithms for the models and investigate the effectiveness of the control strategy through a simulation study.

Consider again the extended Bingham model in Fig 1.5(b). Based on the previous discussions it is clear that this model captures the dominant behaviour of ER fluid dampers. However, it would be very difficult (if not impossible) to use the standard theory for ordinary differential equations to establish existence and uniqueness of solutions for (1.2.4). Without this fundamental result it is very difficult to perform any

sort of meaningful analysis on the system or to develop integration algorithms. Of course, this difficulty could be overcome by replacing the friction element with a smooth approximation. However this modification transforms the model into a fluid model, loosing an essential behaviour of ER fluid devices. Alternatively, one could use one of the rather non-physical models (1.2.7) and (1.2.9). However (1.2.9) is only suitable for small oscillations and (1.2.7) can exhibit some very non-physical behaviour for time varying $\alpha(t)$. Now, it should not be expected that modelling and analysis tools, developed for smooth mechanical systems, can be applied without modification to systems exhibiting nonsmooth behaviours.

This fact was recognized over a hundred years ago, by scientists and engineers trying to model materials exhibiting elastic-plastic and viscoplastic type behaviours (see [37] for a historical perspective). As a result numerous modelling and analysis techniques have been developed specifically to deal with such materials. A particularly intuitive and interesting approach is the modern theory of "thermomechanics with internal variables", details of which can be found in the excellent texts [37]-[39]. This theory takes as its starting point, two functions expressing the stored internal energy and rate of energy dissipation. Then using some established principles from thermodynamics and some convex analysis, well behaved evolution equations are derived for the internal variables. In the context of the extended Bingham model, the internal energy corresponds with the energy stored in the springs, the dissipation rate is obtained from the dashpots and friction element , while the internal variables are simply x_1 and x_2. Due the importance of elastic-plastic and viscoplastic models in various engineering applications, numerous methods have been developed for establishing wellposedness of the resulting models [40] and developing efficient integration algorithms [41].

1.3 Thesis outline

The purpose of this thesis is two fold. Firstly, to present a method for constructing models of ER fluid dampers, which capture the mechanical behaviour of the devices and which are amenable to analysis and control design. Secondly, to investigate the feasibility of using an ER damper to suppress action tremor at the elbow, with as little effect on the voluntary motion as possible.

Chapter 2 develops a simple second order model for the human forearm, undergoing point-to-point reaching movements and subject to tremor. Stability and boundedness of solutions of the model are briefly discussed. The final section also provides some motivation for the developments presented in later sections. In particular, the feasibility of using a controllable damper to attenuate the effect of tremor is briefly investigated.

The purpose of §3 is to present a simple method for the modelling of shear mode ER dampers. The method itself is based on the method of "thermomechanics with internal variables", and uses some simple results from convex analysis to deal with the nonsmooth behaviour exhibited by ER fluid dampers. Before getting down to the actual modelling, some of the basic mechanisms governing the ER effect are reviewed. The interest in these mechanisms is not to predict the force levels or parameters values, but to gain some insight into the energy storage and dissipation properties of an ER fluid in shear. A simplified version of "thermomechanics with internal variables", is then presented along with the required tools from convex analysis. This theory is then used to reformulate some of the models for ER dampers which have appeared in the literature.

In §4 the simplest of the damper models developed in the previous chapter (the EP model) is coupled with the second order model for the forearm, developed in §2.
Following this, some basic internal and external stability results are established for the coupled system. Section 4.2 begins with a review of some known results for semi-active dampers. Finding that these results to be inappropriate for the present purposes, the notion of a OT-recurrent control is developed. Section 4.3 analyses the possibility of "linearizing" the response of the EP model through the use of a feedforward control. An outgrowth of the analysis is the novel concept of dissipation shaping. In some sense, the dissipation shaping control can be seen as a form of model reference control, in which

the response of the EP model is forced to track the response of a more desirable rheological model

The control objective was stated earlier as: devise a control strategy for an ER damper which will reduce the oscillations caused by the tremor, with out adversely affecting the intentional motion. In Chapter.5, the feasibility of achieving this objective is briefly considered, using some of the external stability results from §4 and Appendix D. The theoretical results are quite positive and are backed up by numerous simulations.

Finally, Chapter 6 provides a summery of the various results obtain in previous chapters, along with some possible extensions and generalisations of these results. Some interesting topics for future research are presented.

This thesis contains four appendices. Appendix A outlines some results from real analysis and convex analysis which are use through the thesis. Appendix B provides a summery of the main definitions and theorems relating to stability in the sense of Liapunov. Some useful results for investigating the asymptotic behaviour of ordinary differential equations are also presented. Appendix C develops some simple results for investigating the wellposedness of the damper models presented in §3, when in isolation and when coupled with other models for mechanical systems. Finally, Appendix D presents some results relating to the existence and stability of periodic solutions of the EP model, when in isolation and when the coupled with the forearm model. These results will prove particularly useful when discussing tremor attenuation in §5.

Chapter 2

Forearm Model and Semi-Active Damping

The purpose of this chapter is primarily to develop a simple model for the human forearm, under going point to point reaching movements and subject to tremor. The final section also provides some motivation for the developments presented in later sections. In particular, the feasibility of using an ER fluid damper to attenuate the effect of tremor is briefly investigated.

2.1 Model of the forearm

In this section a simple model for the human forearm, muscles and neural controller will be presented. Both experimental and theoretical motivation for the model can be found in the papers [42] and [43], to which the reader is referred for further details. In the present study, only fast, short duration, voluntary motions will be considered. The term point-to-point motion will be used when referring to fast voluntary motions of the arm from some initial position to a desired position. The arm is assumed to remain at the desired position for some time, before making the transition to the next desired position, and so on. In robotic systems, the use of feedback for motion control, is justifiable as sampling and control frequencies can be made very high, resulting in negligibly small feedback delays. However, the same cannot be said for biological systems. The delay incurred for visual feedback on motions of the arm, are typically in the range $150-250ms$ [44]. Even the fast spinal feedback loops (reflexes etc) incur delays of $30-50ms$. This is quite large compared with the typical duration of $150-500ms$, for point to point motions [44][45]. As a result biological feedback loops must have small gains if stability is to be ensured. In contrast, co-activation of agonist muscles may be used to provide proportional (stiffness) and derivative (viscous) gains about a fixed position, without any delay, [42][44].Furthermore, increasing the net stiffness and damping of the system will provide a certain robustness to unforeseen mechanical disturbances. Indeed, numerous studies have suggested for fast point-to-point motions, the CNS (central nervous system) uses a combination of internal models of the arm/environment and the ability to alter the arms impedance, in order to implement a purely feedforward control [42][45][46].

The forearm (and hand) will be modelled as a rigid link with inertia J and mass m. It is assumed that the arm is constrained by a brace, so that the axis of rotation can be considered as fixed. The joint angle q is defined as zero when pointing vertically downward and positive towards flexion, Fig 2.1(a). The numerous muscles acting on the forearm will be lumped into two opposing muscles, which will be referred to as the biceps and triceps for simplicity. The moment arm, r and the maximum extensive and reflexive torques which can be generated by the two muscles are assumed to be equal, see Fig 2.1.

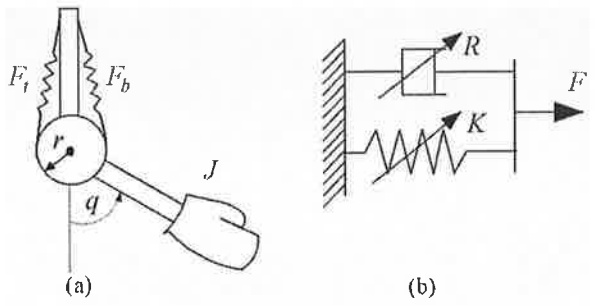

Fig 2.1 (a) forearm, (b) mechanical muscle

For a given neural excitation, the mechanical response of muscle is extremely complicated. However, for the present purposes only the dominant mechanical properties need be considered. In particular, neural activation determines both the contractile force generated by the muscle and the effective stiffness of the muscle (resistance to stretch). The observed static relationship between muscle force and stretch implies a controllable "spring like" behaviour, while the observed relationship between muscle force and the rate of stretch implies a controllable "viscous" behaviour [42]. The simplest mechanical model which captures this variable stiffness/damping type behaviour is a parallel combination of a variable spring and damper, Fig 2.1(b). Based on this model, the net moment of the two muscles will be modelled by [42]

$$\begin{aligned} \tau_b &= rF_b = (u_b(t) + 0.5\varepsilon_k)K_0(\bar{q} - q) - (u_b(t) + 0.5\varepsilon_R)R_0\dot{q}, \\ \tau_t &= rF_t = (u_t(t) + 0.5\varepsilon_k)K_0(\bar{q} + q) + (u_t(t) + 0.5\varepsilon_R)R_0\dot{q}, \end{aligned} \tag{2.1.1}$$

where the subscripts b and t refer to the biceps and triceps respectively. The constant $\bar{q}$ corresponds with the rest length of the muscles. The dimensionless constants ε_k and ε_R, capture the passive stiffness and damping of the muscles, in the sense that $\varepsilon_k K_0$ represents the passive muscle stiffness. Finally, the continuous variables $u_t(t), u_b(t) \geq 0, \forall t \geq 0$, represent the neural control signals. The physiological range of motion is assumed to be $[0, \pi]$ radians. While an explicit representation of this constraint will not be included in the present model, it is easily incorporated using the

penalty function type methods. In order to represent the fact that muscles cannot push, the rest angle $\bar{q}$ is assumed to be greater than π. This choice also captures the fact that the elbow can generate torque when fully extended/flexed. As the limb moves in the vertical plane there will also be a gravitational torque equal to $\tau_g = -mgl\sin(q)$, where g is the acceleration due to gravity and l is the distance from the centre of mass to the axis of rotation. Summing moments about the axis of rotation in Fig 2.1(a) gives

$$\begin{aligned} J\ddot{q} &= \tau_b - \tau_t + \tau_g + \tau_e(t), \\ &= -(u(t)+\varepsilon_R)R_0\dot{q} - (u(t)+\varepsilon_k)K_0 q - mgl\sin(q) + K_0\bar{q}\Delta u(t) + \tau_e(t), \end{aligned} \tag{2.1.2}$$

where $u(t) = u_t(t) + u_b(t)$, $\Delta u(t) = u_b(t) - u_t(t)$ and $\tau_e(t)$ is a torque resulting from interactions with the environment. It follows that at any given angle the torque about the joint and the stiffness/damping can be controlled independently via the sum and difference of the two muscle controls. For the purposes of control design it is more convenient to use the representation

$$\begin{aligned} J\ddot{q} &= -(u(t)+\varepsilon_R)R_0\dot{q} - (u(t)+\varepsilon_k)K_0(q-\delta(t)) - mgl\sin(q) + \tau_e(t), \\ \delta(t) &= \frac{\bar{q}\Delta u(t)}{u(t)+\varepsilon_k}, \end{aligned} \tag{2.1.3}$$

from which it can be seen that the combined activation of the two muscles results in a variable damper and a variable spring with adjustable threshold. The question now is, how to choose u and δ. Referring back to equation (2.1.3) and assuming for the moment that $\tau_e(t) \equiv 0$, the idea would be to choose fixed u and δ so that the desired position q^* is an asymptotically stable equilibrium point for the system (2.1.3). Then if necessary, increase u so as to ensure good transient behaviour. A sufficient condition for a mechanical system to have a unique, stable equilibrium at a position q^*, is that it corresponds with the global minimum of the system's potential energy. For a fixed level of muscle activation, the limb's potential energy is

$$U(q) = \frac{1}{2}(u+\varepsilon_k)K_0(q-\delta)^2 + mgl(1-\cos(q)). \tag{2.1.4}$$

$U(q)$ will have a minimum at $q = q^*$ if

$$\frac{\partial U(q^*)}{\partial q} = (u+\varepsilon_k)K_0(q^*-\delta) + mgl\sin(q^*) = 0, \tag{2.1.5}$$

or equivalently

$$\delta(q^*) = \frac{\bar{q}\Delta u}{u+\varepsilon_t} = q^* + \frac{mgl}{(u+\varepsilon_k)K_0}\sin(q^*). \tag{2.1.6}$$

A sufficient condition for q^* to be unique (global) minimum of $U(q)$ is that

$$\frac{\partial^2 U(q)}{\partial q^2} = (u+\varepsilon_k)K_0 + mgl\cos(q) > 0, \tag{2.1.7}$$

for all $q \in \Re$, which will be the case if u is chosen such that $u+\varepsilon_k > mgl/K_0$. Inserting (2.1.6) into (2.1.3) yields

$$J\ddot{q} = -(u+\varepsilon_R)R_0\dot{q} - (u+\varepsilon_k)K_0(q-q^*) - mgl\big(\sin(q)-\sin(q^*)\big). \tag{2.1.8}$$

Choosing u and δ to satisfy (1.6) and (1.7), the total system energy (kinetic and potential)

$$H(q,\dot{q}) = \frac{1}{2}J\dot{q}^2 + U(q), \tag{2.1.9}$$

is a strictly convex function of $(q,\dot{q})$ with minimum $(q^*,0)$. The derivative of $H(q,\dot{q})$ along the trajectories of (2.1.8) is

$$\dot{H}(q,\dot{q}) = \frac{\partial H}{\partial q}\dot{q} + \frac{\partial H}{\partial \dot{q}}\ddot{q} = -(u+\varepsilon_R)R_0\dot{q}^2 \le 0. \tag{2.1.10}$$

Inequality (2.1.10) implies that $H(q(t),\dot{q}(t))$ is nonincreasing as a function of time, which implies that all motions of (2.1.8) are bounded and that the equilibrium $(q^*,0)$ is stable (see §B for stability theorems and definitions). Because (2.1.8) is autonomous, the Krasovskii-LaSalle theorem (Theorem B.4) can be used to conclude that all motions of (2.1.8) are globally convergent to the largest invariant set contained in $\mathrm{E} = \{(q,\dot{q}) \mid \dot{q} = 0\}$. For any motion staying identically in E, $\dot{q} \equiv 0 \Rightarrow \ddot{q} \equiv 0$ implying that $(u+\varepsilon_k)K_0\left|q-q^*\right| = mgl\left|\sin(q)-\sin(q^*)\right| \le mgl\left|q-q^*\right|$, but $u+\varepsilon_k > mgl/K_0$, implying that $q = q^*$. It follows then that the equilibrium $(q^*,0)$ is GAS.

Thus the CNS can move the limb to a desired position $(q^*,0)$ by choosing u and δ to satisfy $u+\varepsilon_k > mgl/K_0$ and (2.1.6) respectively. For general point-to-point motions, consisting of a succession of equilibrium points, it has been suggested that the CNS shifts the threshold parameters between the required values (given by (2.1.6)) in a piecewise linear fashion [45][46].

For the purposes of simulation, the following parameter values were chosen based on the anthropometric data presented in [43][45][46], $J = 0.05kg\cdot m^2$, $mgl = 2.5kg.m^2/\sec^2$, $K_0 = 7Nm/rad$, $R_0 = 2.5Nm\cdot\sec/rad$, $\bar{q} = 1.3\pi rad$, $\varepsilon_K = 6/7$

$,\varepsilon_R = 16/7$ and for controlled trajectories $u = 6/7$. For small perturbations, the uncontrolled system behaves like an underdamped oscillator with natural frequency $\approx 8 rad/\sec$ and for controlled motions, an underdamped oscillator with natural frequency $\approx 12 rad/\sec$.

2.2 Incorporating tremor

The next step is to incorporate the effect of tremor into the arm model. In particular, the disabling, low frequency form of action tremor, affecting many individuals with multiple sclerosis (see §1.1 for discussion). Recall that action tremor occurs during the voluntary contraction of muscle and appears as an additive, rhythmic disturbance in the voluntary control signals sent to the muscle. At this point, the only assumptions which will be made, are that the tremor effects the antagonist muscles in an alternating pattern and is only present when $u(t) = u_b(t) + u_t(t) \neq 0$ (see Fig 1.1).

Consider the function $\rho \in C^{0,1}(\Re_+;\Re)$ taking both positive and negative values on each interval of $\Re_+$ with length greater than or equal to T (implying boundedness of ρ). On the assumption that the tremor has an alternating pattern, let $\rho_b(t) = \max(0, \rho(t))$ and $\rho_t(t) = \max(0, -\rho(t))$ define the tremorous contributions to the activation of the biceps and triceps respectively (see Fig.1.1). It follows that $\rho = \rho_b - \rho_t$ and $|\rho| = \rho_b + \rho_t$. The net moment of the individual muscles given in (1.1), now becomes

$$\begin{aligned} \tau_b &= (u_b(t) + \rho_b(t) + 0.5\varepsilon_k)K_0(\bar{q} - q) - (u_b(t) + \rho_b(t) + 0.5\varepsilon_R)R_0\dot{q}, \\ \tau_t &= (u_t(t) + \rho_t(t) + 0.5\varepsilon_k)K_0(\bar{q} + q) + (u_t(t) + \rho_t(t) + 0.5\varepsilon_R)R_0\dot{q}, \end{aligned} \tag{2.2.1}$$

and the equation of motion (1.2) (minus the external torque τ_e, to make things shorter)

$$J\ddot{q} = -\big(u(t) + |\rho(t)| + \varepsilon_R\big)R_0\dot{q} - \big(u(t) + |\rho(t)| + \varepsilon_K\big)K_0 q - mgl\sin(q) + K_0\bar{q}\big(\Delta u(t) + \rho(t)\big), \tag{2.2.2}$$

where $u(t) = u_t(t) + u_b(t)$ and $\Delta u(t) = u_b(t) - u_t(t)$. It can be shown that if $u(t)$ is constant and satisfies $2R_0(u + \varepsilon_R)(u + \varepsilon_k)/J > \|\dot{\rho}\|_\infty$, then all solutions of (2.2.2) will be uniformly bounded (UB). This result will now be used to simplify the system in (2.2.2). First of all, it will be assumed that u and Δu are constant, satisfying (2.1.6) and (2.1.7) for some $q^* \in [0, \pi]$, so that (2.2.2) becomes

$$J\ddot{q} = -\big(u + \varepsilon_R\big)R_0\dot{q} - \big(u + \varepsilon_K\big)K_0(q - q^*) - mgl\big(\sin(q) - \sin(q^*)\big) + Jb(t), \tag{2.2.3}$$

where

$$b(t) = \frac{1}{J}\left(K_0 \bar{q}\rho(t) - |\rho(t)|R_0\dot{q}(t) - |\rho(t)|K_0 q(t)\right). \tag{2.2.4}$$

Now, assuming that u satisfies $2R_0(u+\varepsilon_R)(u+\varepsilon_k)/J > \|\dot{\rho}\|_\infty$, then all solutions of the system (2.2.3)–(2.2.4) are UB. It follows that for each set of initial conditions $(q(0),\dot{q}(0)) \in \Re^2$, there exits a positive constant $\bar{B}$ such that $|b(t)| \le |\rho(t)|\bar{B}$, for all $t \ge 0$. From this point on, $b(t)$ will be considered as a lumped, bounded "tremor torque" and its particular dependence on $(q,\dot{q})$ will be ignored. This simplification is not as unreasonable as it may seem at first, as the relationship between (action) tremor related muscle activation, the state of the muscle and the voluntary muscle activation, is poorly understood [1][5].

To facilitate later analysis, (2.2.3) will now be transformed into a first order differential equation, with state variables $x_1 = q - q^*, x_2 = \dot{q}$. Using the assumption that u satisfies (2.1.7), define the constants

$$\begin{aligned} K &= \frac{1}{J}\left(K_0(u+\varepsilon_k) - mgl\right) > 0, \\ R &= \frac{1}{J}R_0(u+\varepsilon_k) > 0, \end{aligned} \tag{2.2.5}$$

and the functions $F(t) = \tau_e(t)/J$ and

$$h(x_1) = \frac{mgl}{J}\left(x_1 + \sin(x_1+q^*) - \sin(q^*)\right) = \frac{mgl}{J}\left(x_1 + 2\cos\left(\frac{x_1}{2}+q^*\right)\sin\left(\frac{x_1}{2}\right)\right). \tag{2.2.6}$$

From (2.2.6) it can be seen that $h(x_1)$ is a nondecreasing function of x_1, $h(0) = 0$ and

$$0 \le \left(h(x_1) - h(y_1), x_1 - y_1\right) \le L(x_1 - y_1)^2 \tag{2.2.7}$$

where $L = 2mgl/J$. Substituting $x_1 = q - q^*, x_2 = \dot{q}$, (2.2.5) and (2.2.6) into (2.2.3) yields the forced "pendulum type" system (with $F(t) = \tau_e(t)/J$ added back in)

$$\Sigma_X \begin{cases} \dot{x}_1 = x_2 \\ \dot{x}_2 = -Rx_2 - Kx_1 - h(x_1) + b(t) + F(t). \end{cases} \tag{2.2.8}$$

Assuming that $b(t)$ and $F(t)$ are continuous and bounded, then for each set of initial conditions $(t_0, x_0) \in \Re_+ \times \Re^2$, (2.2.8) has a unique solution $x(t) = x(t;t_0,x_0)$, $x \in C^1(\Re_+;\Re^2)$, which depends continuously on the initial conditions. Before moving onto the next section, a basic inequality for the solutions of (2.2.8) will be developed.

Consider the Liapunov function

$$V(x)=\left(\frac{1}{2}(R^2+2K)x_1^2+Rx_1x_2+x_2^2\right)+2\int_0^{x_1}h(s)ds. \tag{2.2.9}$$

The quadratic term in brackets is positive definite and due to (2.2.7), the integral term is at least positive semidefinite (see §B.1 for definitions). Furthermore, using the fact that $|h(x_1)|\le L|x_1|$, it is easily shown that there exists two positive constants c_1,c_2 such that $c_1|x|^2\le V(x)\le c_2|x|^2$ for all $x\in\Re^2$. For simplicity $F(t)$ will be dropped from (2.2.8) temporarily. Taking the derivative of $V(x)$ along the trajectories of (2.2.8) gives

$$\begin{aligned}\dot{V}(x)&=-RKx_1^2-Rh(x_1)x_1-Rx_2^2+(Rx_2+2x_1)b(t),\\&\le-\left(RKx_1^2+Rx_2^2\right)+\left(R|x|_2+2|x_1|\right)|b(t)|,\\&\le-2c_3V(x)+2c_4\sqrt{V(x)}|b(t)|,\end{aligned} \tag{2.2.10}$$

where $c_3=0.5\min(R,RK)/c_2$ and $c_4=0.5\max(R,2)/\sqrt{c_1}$. Letting $W(t)=\sqrt{V(x(t))}$, then $W(t)$ is differentiable except when $x(t)=0$, but has a directional derivative even there. It follows that the right hand derivative $\dot{W}_+(t)=\lim_{d\to0_+}\left(W(t+d)-W(t)\right)/d$ exits for all $t\in\Re_+$ and

$$\dot{W}_+(t)\le-c_3W(t)+c_4|b(t)|. \tag{2.2.11}$$

Applying the comparison lemma in §B.2 to (2.2.11), one obtains

$$W(t)\le W(t_0)e^{-c_3(t-t_0)}+c_4\int_{t_0}^{t}e^{-c_3(t-s)}|b(s)|ds, \tag{2.2.12}$$

and using $\sqrt{c_1}|x(t)|\le W(t)\le\sqrt{c_2}|x(t)|$

$$\begin{aligned}|x(t)|&\le\sqrt{\frac{c_2}{c_1}}|x(t_0)|e^{-c_3(t-t_0)}+\frac{c_4}{\sqrt{c_1}}\int_{t_0}^{t}e^{-c_3(t-s)}|b(s)|ds,\\&\le\sqrt{\frac{c_2}{c_1}}|x(t_0)|e^{-c_3(t-t_0)}+\frac{c_4}{\sqrt{c_1c_3}}\|b\|_\infty\left(1-e^{-c_3(t-t_0)}\right).\end{aligned} \tag{2.2.13}$$

From (2.2.13) it can be concluded that all solutions of (2.2.8) are UB, uniformly ultimately bounded (UUB) and converge to a ball of radius $c_4\|b\|_\infty/\sqrt{c_3c_1}$. Clearly if $b(t)\equiv0$, then the origin is globally exponentially stable (GES). Also, applying Lemma B.5 in §B.2 to the integral term in (2.2.13), it can be concluded that if either $b\in L_1(\Re_+;\Re)$ or $b(t)\to0$ as $t\to\infty$, than all solutions converge to zero. Of particular interest is the case where b is T-periodic, i.e. $b(t+T)=b(t),\forall t\in\Re_+$. In this case UUB implies that (2.2.8) has at least one T-periodic solution, which is to say that there exists

at least one point $x_T \in \Re^2$ such that $x(T+t_0;t_0,x_T)=x_T$. In §D it will be shown that sufficient conditions for the periodic solution to be GES and hence unique is that either $L<R^2$ or that there exists a T-periodic solution such that $\|x_2\|_\infty < 2RK/L$. From inequality (2.2.13) it can be concluded that any periodic solution must satisfy $\|x\|_\infty \le c_4\|b\|_\infty/\sqrt{c_3}c_1$, so that the final condition will be satisfied if $\|b\|_\infty$ is small enough.

2.3 Tremor suppression

As noted in §1, it has been established that by applying fixed levels of viscous damping to the effected limb, the tremor related motions can be significantly reduced. However, as one would expect, a concurrent resistance to voluntary motion also occurs. Motivated by this result it was suggested that if an ER damper were attached to the limb using a suitable brace/orthosis, then it may be possible to modulate the damping in such a way, so as to reduce the amplitude of the tremor related oscillations, with a minimal degradation of the voluntary motion.

It is widely accepted that ER dampers fall into the category of passive control devices, to quote [20], "It is important to note that in ER actuators, only the dissipation and possibly some storage of energy is possible. Consequently the term semi–active is often applied to ER devices although the term controllable-passive is probably more descriptive". From an energetic viewpoint a passive system is usually defined as one which cannot store more energy than is supplied externally, with the difference between the stored and supplied energy, being the dissipated energy. This property is important as it implies that the use of an ER damper for tremor suppression is safe, in the sense that the net flow of energy must be in the direction from the user to the damper.

In order to explore the implications of passivity more closely, a more precise definition is required. Consider the dynamical system with state $x \in \Re^n$, input $u \in \Re^m$ and output $y \in \Re^m$

$$\begin{aligned} \dot{x} &= f(t,x,u) \\ y &= c(t,x,u), \end{aligned} \tag{2.3.1}$$

and $f(t,0,0)=0, c(t,0,0)=0$ for all $t \in \Re_+$. It is assumed that f is such that (3.1) has a unique solution, $x(t;t_0,x_0,u)$. The following definition will suffice for the present purposes, the reader is referred to [48] and references therein for further details.

Passivity definition The system (2.3.1) is said to be passive if there exists a positive definite function $H \in C^1(\Re^n;\Re_+)$ (called the storage function) and a nonnegative, integrable function $\Phi(t)=\Phi(t,x(t),u(t))$ (called the dissipation function) such that for all $u \in C(\Re_+;\Re^m), x(t_0) \in \Re^n$ and $t \geq t_0 \geq 0$

$$\underbrace{H(x(t))-H(x(t_0))}_{\text{stored energy}}+\underbrace{\int_{t_0}^{t}\Phi(s)ds}_{\text{dissipated}}=\underbrace{\int_{t_0}^{t}\langle y(s),u(s)\rangle ds}_{\text{supplied}}, \tag{2.3.2}$$

or in differential form

$$\dot{H}(x(t))=-\Phi(s)+\langle y(t),u(t)\rangle \leq \langle y(t),u(t)\rangle. \tag{2.3.3}$$

Moreover, depending on the form of the dissipation function (2.3.1) is said to be

- lossless if $\Phi \equiv 0$,
- input strictly passive if $\Phi(t) \geq \varphi(u(t))$ for some positive definite function $\varphi : \Re^m \to \Re_+$,
- output strictly passive if $\Phi(t) \geq \varphi(y(t))$ for some positive definite function $\varphi : \Re^m \to \Re_+$,
- strictly passive if $\Phi(t) \geq \varphi(x(t))$ for some positive definite function $\varphi : \Re^n \to \Re_+$,
- to have finite gain if $\Phi(t) \geq k|y(t)|^2$ for some constant $k>0$.

Passive systems are often referred to as defining a passive map from u to y ($u \mapsto y$). For memoryless systems, that is with no state space, the above definition reduces to $y=c(t,u)$ and $\langle y,u\rangle \geq 0$ for all $t \in \Re_+$. In the scalar case this is equivalent to saying that the graph of $c(t,\cdot):\Re \to \Re$ lies in the first and third quadrants for all $t \in \Re_+$. Passivity is a rather abstract concept, however, for physical systems the natural choice of storage function is the system's energy. In this case the product of the inputs and outputs will have the units of power, i.e. forces and velocities for mechanical systems. An extremely useful property of passive systems is that passivity is preserved under

negative feedback interconnection, with the sum of the individual storage functions acting as a storage function for the connected system.

For the purposes of analysis the system Σ_X (2.2.8) can be viewed as a forced pendulum type system with unit inertia, so that the natural storage function is the system energy

$$H_X(x) = \frac{1}{2}\left(x_2^2 + Kx_1^2\right) + \int_0^{x_1} h(s)ds\,. \tag{2.3.5}$$

Taking derivative of $H_X(x)$ along the trajectories of Σ_X yields

$$\dot{H}_X(x) = -Rx_2^2 + \langle x_2, b(t) + F(t)\rangle, \tag{2.3.6}$$

which when compared with (2.3.3) shows that Σ_X with output $y = x_2$, is passive with finite gain. Note that taking the Liapunov function (2.2.9) as storage function, (2.2.10) implies that Σ_X with output $y = 2x_2 + Rx_1$ is strictly passive.

Now consider coupling an ER damper to the forearm via a rigid brace. The brace consists of two components rigidly fixed to the upper arm and forearm respectively. For simplicity the damper is assumed to be of the rotary couette type, similar to Fig.1.4 (a) in §1.2. It will consist of two concentric cylinders with ER fluid filling the small gap between them. The outer cylinder (casing) is rigidly attached to the upper-arm component of the brace and will not affect the dynamics of the forearm. The inner cylinder (rotor) is attached to the forearm component of the brace, the axis of rotation coinciding with that of the elbow. The rotor is assumed to be symmetric about the axis of rotation, so that its inertia is independent of angle and can thus be lumped in with the forearm's inertia. The two cylinders also act as electrodes. When a voltage is applied across them, an electric field will build up perpendicular to the couette flow, thus activating the ER fluid. When the elbow rotates the rotor is forced to rotate relative to the casing, shearing the fluid. The fluids resistance to shear is transmitted through the rotor/brace to the elbow in the form of a reactive torque, $-F(t)$ in (2.3.6). The idea is that by increasing the voltage, the fluid's resistance to shear increases, hence increasing the elbow's resistance to rotation.

The most commonly used model is ER devices in the Bingham plastic model (see equation (1.2.1). Neglecting the linear viscous term, it is basically an ideal, scalar, coulomb friction model. In this case the reactive force is given by $-F(t) \in r(t)\mathrm{SGN}(x_2)$, where $r(t) = F_Y(t)$ is a nonnegative control variable related to the applied voltage and $\mathrm{SGN}(x_2)$ is the set valued signum function, given in equation (1.2.2). Note that $\mathrm{SGN}(x_2)$ arises naturally as the subdifferential of $|x_2|$ (see §3.2). It is easily seen that this model satisfies the passivity requirement since $r(t)\mathrm{SGN}(x_2)x_2 = r(t)|x_2| \geq 0$. The coupled system is defined by

$$\begin{aligned} \dot{x}_1 &= x_2 \\ \dot{x}_2 &\in -Rx_2 - Kx_1 - h(x_1) - r(t)\mathrm{SGN}(x_2) + b(t). \end{aligned} \tag{2.3.7}$$

Using the properties of the function $\mathrm{SGN}(\cdot)$ it can be shown that if $b(t)$ and $r(t)$ are continuous and bounded for all $t \geq 0$ and if $r(t)$ is a nonnegative, then (2.3.7) has a unique solution $x \in C^{0,1}(\Re_+;\Re^2)$ for each $(t_0, x_0) \in \Re_+ \times \Re^2$. The next question is, how to choose $r(t)$ so as to attenuate the effect of $b(t)$ on the solutions of (2.3.7). In what follows it will assumed that $b(t)$ is a nontrivial T-periodic function taking both positive and negative values on each interval of length T.

The derivative of $H_X(x)$ along the trajectories of (2.3.7) is

$$\begin{aligned} \dot{H}_X(x) &= -Rx_2^2 - r(t)|x_2| + b(t)x_2, \\ &\leq -Rx_2^2 - |x_2|\big(r(t) - |b(t)|\big). \end{aligned} \tag{2.3.8}$$

For the purpose of illustration it will be assumed that $b(t)$ is known, so setting $r(t) = |b(t)|$ gives

$$\dot{H}_X(x) \leq -Rx_2^2. \tag{2.3.9}$$

Applying Theorem B.3 in §B to (2.39), it can be concluded that all solutions of (2.3.7) are uniformly bounded. Inequality (2.3.9) can be used to show that $x_2 \in L_2(\Re_+;\Re) \cap C^{0,1}(\Re_+;\Re)$, so that Barbalat's lemma (§B.2 lemma B.3) can be used to infer that $x_2(t) \to 0$ as $t \to \infty$. Based on this and the fact that (2.3.7) is a T-periodic system, it follows that the positive limit set $\Omega(x)$ (§B.2 lemma B.2) is nonempty, invariant and contained in the largest invariant subset of $\mathrm{E} = \{x \in \Re^2 \mid x_2 = 0\}$. Since $x_2 \equiv 0$ implies $\dot{x}_2 \equiv 0$, any solution of (2.3.7) remaining identically in E must satisfy $x_1 \equiv a$, for some constant a and from equation (2.3.7) $Ka + h(a) \in b(t) + |b(t)|[-1,1]$ for

all $t \geq 0$. But by assumption, $b(t)$ takes both positive and negative values, so there exists a $t \in [0,T]$ such that $b(t) = 0$ and hence $Ka + h(a) = 0$, implying $a = 0$. It follows that no solution can remain in E other that the zero solution, thus implying $\Omega(x) = 0$ and global asymptotic stability follows.

This is a nice result, unfortunately it relies on the set valued nature of the idealised Bingham plastic model at $x_2 = 0$. In other words, when $x_2 = 0$ the damper force can take any value in the set $|b(t)|[-1,1]$. Fig 2.2 compares the force velocity plots for the idealized Bingham plastic model and experimental force-velocity cycles for an ER damper subject to sinusoidal displacements with frequencies 0.25 Hz and 1.0 Hz respectively and various levels of the electric field (taken from [28]). Clearly, for each level of the electric field, the damper response is not set valued at $x_2 = 0$. Rather, it can take one of two distinct values, depending on the displacement history. This combined with the frequency dependency of the hysteresis loops, this indicates that some form of dynamic model is required. Note that the force velocity hysteresis loops are traversed in an anticlockwise direction.

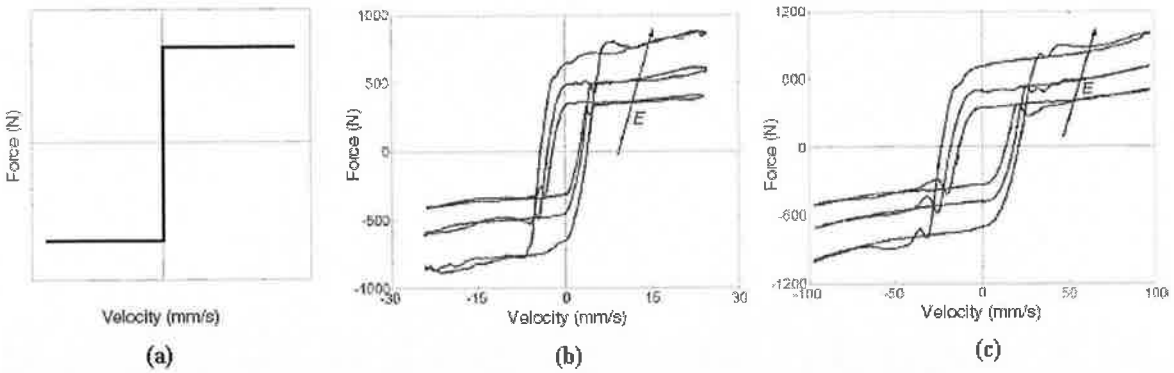

Fig 2.2 (a) shows the force velocity relation for the idealized Bingham plastic model, while (b) and (c) show experimental force velocity cycles for an ER damper subject to sinusoidal displacements with frequencies 0.25 Hz and 1.0 Hz respectively and for various levels of the electric field *E*. (taken from [28])

Consider now the case where the damper response is modelled using a scalar differential inclusion

$$\Sigma_Z \{ \quad \dot{z} \in G(r(t), z, x_2) \tag{2.3.10}$$

with $F = -z$ in (2.2.8) and where $r(t)$ is a nonnegative control variable related to the applied voltage. It is assumed that the set valued map G satisfies $G(r,0,0) = 0, \forall r \in \Re_+$

and is such that if $x_2 \in C^{0,1}(\Re_+;\Re)$ and $r \in C^{0,1}(\Re_+;\Re_+)$ then (2.3.10) has a unique solution $z \in C^{0,1}(\Re_+;\Re)$. The coupled system is now given by

$$\begin{aligned} \dot{x}_1 &= x_2 \\ \dot{x}_2 &= -Rx_2 - Kx_1 - h(x_1) - z + b(t) \\ \dot{z} &= G(r(t), z, x_2) \end{aligned} \tag{2.3.11}$$

Based on the definition of passivity and the discussion preceding it, it seems reasonable to expect that Σ_Z would define a passive map from x_2 to z, that is

$$\dot{H}_Z(z) = -\Phi(r(t), z) + zx_2 \le zx_2, \tag{2.3.12}$$

where the positive definite function H_Z represents the stored energy and the nonnegative function $\Phi(r(t), z)$ (dissipation function) is the rate at which Σ_Z dissipates energy along a given trajectory. Unfortunately many of the dynamic models which have been devised for ER dampers do not define a passive map from x_2 to z, making useful analysis and control design very difficult .

Assuming that Σ_Z is a passive system then integrating (2.3.11) and rearranging yields

$$-\int_{t_0}^{t} z(s)x_2(s)ds \le H_Z(z(t_0)), \tag{2.3.13}$$

which simply says that the maximum amount of energy which can be extracted from Σ_Z is finite, thus ensuring the safety of the user. Combining (2.3.6) and (2.3.12) yields the power balance (note that $ab \le Ra^2/2 + b^2/2R$)

$$\begin{aligned} \dot{H}(x,z) &= -Rx_2^2 - \Phi(r(t), z) + b(t)x_2, \\ &\le -\frac{R}{2}x_2^2 - \Phi(r(t), z) + \frac{1}{2R}b(t)^2, \end{aligned} \tag{2.3.14}$$

where $H(x,z) = H_X(x) + H_Z(z)$, implying that the coupled system with output x_2, is passive with finite gain. Unlike the Bingham plastic model, the passivity of (2.3.10) implies that $x = 0$ can not be rendered GAS by suitable choice of control $r(t)$. To see this note that for $x = 0$ to be a (partial) equilibrium for (2.3.11) would require that for $x_2 = 0$, there exist a control $r(t)$ such that (2.3.10) has a nontrivial periodic solution $z(t) = b(t), \forall t \ge 0$. Since $b(t)$ takes both positive and negative values, so must $z(t)$, implying the existence of a time $\tau \in [0,T)$ such that $z(\tau) = 0$. Setting $x_2 = 0$ in (2.3.12) gives $\dot{H}_Z(z(t)) \le 0$, implying that the stored energy H_Z is nonincreasing along this solution. Since H_Z is positive definite and nonincreasing, if $H_Z(z(\tau)) = 0$ then

$H_Z(z(t)) = 0$ for all $t \geq \tau$. But this implies that $z(t) = 0$ for $\forall t \geq \tau$, contradicting the assumption $z(t) = b(t), \forall t \geq 0$. So what can be achieved ?.

Assume for the moment that both $r(t)$ and $b(t)$ are T-periodic and that (2.3.11) has at least one T-periodic solution, say $(\hat{x}(t), \hat{z}(t))$. Integrating (2.3.14) along this T-periodic solution and using $H(\hat{x}(t+T), \hat{z}(t+T)) = H(\hat{x}(t), \hat{z}(t))$ for all $t \geq 0$, yields (need only consider the interval $[0, T]$ due to periodicity)

$$\int_0^T \hat{x}_2^2(s)ds \leq \frac{1}{R^2}\int_0^T b(s)^2 ds - \frac{2}{R}\int_0^T \Phi(r(s), \hat{z}(s))ds. \qquad (2.3.15)$$

It follows that if $r(t)$ could be chosen so as to maximise (in some sense) the energy dissipated by Σ_Z, over the interval $[0, T]$, this would reduce the upper bound on the L_2 norm of $\hat{x}_2$ over $[0, T]$. Note that this is equivalent to reducing the bound on the averaged kinetic energy for any T-periodic solution of (2.3.11). Furthermore, using the identity $\dot{\hat{x}}_1 = \hat{x}_2$ and applying Holder's inequality (§A.1) to the left hand side of (2.3.15) gives

$$\sqrt{T\int_0^T \hat{x}_2^2(s)ds} \geq \int_0^T \left|\dot{\hat{x}}_1(s)\right| ds \geq \mathrm{osc}_T \hat{x}_1, \qquad (2.3.16)$$

where $\mathrm{osc}_T \hat{x}_1 = \max_{t\in[0,T]} \hat{x}_1(t) - \min_{t\in[0,T]} \hat{x}_1(t) > 0$ is the oscillation of the periodic function $\hat{x}_1$.

It follows that maximising the energy dissipated by Σ_Z would also reduce the upper bound on the oscillation of the periodic motion $\hat{x}_1$. Of course, for this result to be useful it would have to be shown that all solutions of (2.3.13) converge to a T-periodic solution. This would in turn, require that the damper model be well behaved and amenable to analysis.

Recall that the original objective was to analyse the feasibility of using an ER damper to attenuate the tremor related motions of the limb, with a minimal degradation of the intentional motion. Also, in Section.2 it was stated that for each T-periodic tremor $b(t)$, the undamped (in the ER sense) arm model had a GES T-periodic solution. Based on this and inequalities (2.3.15) and (2.3.16), a suitable starting point would be to attempt to devise a control strategy for $r(t)$ which would ensure that for each T-periodic tremor $b(t)$, (2.3.11) has a GES T-periodic solution, whose oscillation is smaller than that for the undamped solution (in the ER sense).

Furthermore, the rate of convergence to the damped T-periodic solution should not be less than the rate of convergence to the undamped T-periodic solution (minimal degradation of the intentional motion). In order to attempt this, a damper model will need to be derived, which captures the dominant behaviour of ER fluid dampers, is well behaved and amenable to analysis.

In §3, thermomechanical principles and a bit of convex analysis are used to develop some simple, physically intuitive damper models, which are well suited for analysis and design. In §4, the simplest of these damper models is then coupled to the arm model (Σ_X) and the qualitative behaviour of the system is analysed using Liapunov type techniques. §D investigates conditions on $r(t)$, which will ensure the existence and exponential stability of periodic solutions. A result of this analysis is the development of some novel control strategies. Finally in §5, the feasibility of using these control strategies to achieve the control objectives, will be investigated both theoretically and numerically.

Chapter 3

Phenomenological modelling of ER fluids in shear

The purpose of this chapter is to demonstrate that the well known method of "thermomechanics with internal variables" is well suited to developing phenomenological models for ER fluid dampers. The chapter begins with a review of ER fluids and some of the physics-based micromechanical models which have been developed. A simplified version of "thermomechanics with internal variables" is then presented along with an intuitive model for the inelastic behaviour of ER fluids. The theory is then used to reformulate some of the models for ER dampers which have appeared in the literature.

3.1 Introduction to ER fluids

As early as the 1940's an experimentalist named Winslow noticed that when a suspension of dielectric particles in oil was placed between two electrodes and subjected to an electric field, the particles rapidly aggregated into fibrous chains running parallel to the field (see Fig 3.1). An even greater surprise was that this change in structure resulted in an equally dramatic change in the fluid's resistance to shear flow (perpendicular to the field) and which disappeared as soon as the field was removed. Further work showed that this controllable resistance was more akin to the yield stress associated with coulomb friction than with standard Newtonian viscosity. Aware of the potential for such a fluid, Winslow rapidly obtained patents for all manner of electromechanical devices including controllable dampers, clutches and brakes [49][50]. Despite their apparent promise, the early ER fluids were highly criticised due to problems with thermal breakdown, particle settling and abrasiveness. Since then the ER effect has been observed for numerous combinations of particles and fluid including cornstarch, silica, alumina, flour and semiconductors in a hydrophobic liquid such as silicone or corn oil (and even molten chocolate) [52][53].

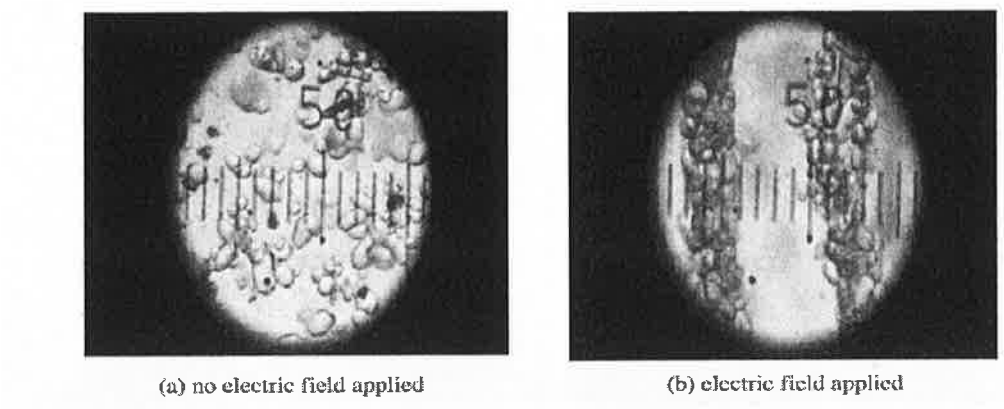

(a) no electric field applied (b) electric field applied

Fig 3.1 Electrorheological behaviour of PMA particles dispersed in silicone oil. Taken from [51].

Typically ER fluids consist of 1-100μm polarisable particles with volume fractions of particles to fluid ranging from 0.05 to 0.50. That said, very few combinations have the properties required of a commercially viable product. It is only in the last two decades or so that the above mentioned problems have been overcome (to some extent at least), sparking a renewed interest in the development of semi-active dampers and force transfer devices. Applications which have been investigated include automotive suspensions, vibration control, haptic interfaces and large scale dampers for the seismic protection of multi-storey buildings, [20][54][55]. Strangely enough, none of these have made the transition from laboratory curiosity to supermarket shelf.

The shear stress, σ, in a sheared ER fluid (or device) is usually modelled using the Bingham plastic model (compare with equation (1.1.1))

$$\begin{aligned} \sigma &= \sigma_y \operatorname{sgn}(\dot{e}) + \eta_v \dot{e} \quad \text{for } \dot{e} \neq 0, \\ \sigma &\in \sigma_y[-1,1] \quad \text{for } \dot{e} = 0, \end{aligned} \tag{3.1.1}$$

where η_v is the plastic viscosity, $\dot{e}$ is the shear rate and σ_y is the Bingham or dynamic yield stress. The yield stress is assumed proportional to the square of the applied electric field, while η_v is generally taken to be field independent. In equation (3.1.1), σ_y is interpreted as the dynamic yield stress, while the static yield stress is defined as the minimum shear stress required to produce continuous shearing flow in an originally static sample of activated fluid. In general these two definitions are not equivalent, though closely related [21]. That the material is capable of supporting a stress in the absence of flow would suggest the definition of a solid rather than a fluid. For example, the simplest experiment that can be performed with an ER fluid is to dip two electrodes into a sample, switch on the electric field and then remove the electrodes. The ER fluid

between the electrodes will be solidified and will remain stationary until the field is removed. Thus implying that the activated fluid is capable of supporting self weight in the absence of flow.

For ER fluids to become a truly attractive alternative to more conventional technologies, the fluid needs to display rapid response times (transformation from liquid to semi-solid) and achieve a large yield stress with a minimum of electric power consumption. At present commercially available ER fluids are typically designed to obtain a maximum dynamic yield stress of about 4-5 kPa at 4kV/mm [57], with typical activation time scales in the order of 1-50ms. Although the electric field required may is very high, ER fluids usually maintain a current density of about $10\mu A/cm^2$ (of electrode surface area) for applied electric field of 4kV/mm at room temperature. As a result the power consumption is still extremely low. While σ_y could theoretically be made extremely large by further increasing the electric field, all ER fluids are slightly conductive and too high an electric field will either result in large energy dissipation (due to current) causing the fluid to over heat, or the fluid will simply break down resulting in arcing between the electrodes.

In the design of any rehabilitation device or technological aid, the safety of the user should be given the highest priority. The main concern when designing ER fluid dampers, which are to interact with people, is the need for high voltages to develop the required damping forces. For this reason, extreme care should be taken so as to ensure the device itself is well insulated and that the power supply has sufficient safety features. Furthermore, in the design process every effort should be made to reduce the current consumption at maximum voltage, which will reduce the maximum power requirement and therefore the risk of injury.

At about the same time that ER fluids were discovered, their magnetic analogue called Magnetorheological (MR) fluid was also discovered. While MR fluids exhibit much the same behaviour as ER fluids under the influence of a magnetic field, there are some important differences. At present commercially available MR fluids offer a maximum controllable yield stress an order of magnitude greater than that attainable with ER fluids and remain stable over a wider range of temperatures. For this reason MR fluids have taken over as the controllable fluid of choice for experimentalists and developers [22][23][24]. For example several MR devices have become commercially available in the last few years, the most popular of which is a retrofit semi-active damper for long

haulage truck seats. Despite the advantages of MR fluids, the reasons for picking ER fluid for the current application is that ER fluids generally have a lower no field resistance, the particles are lighter meaning they are less likely to settle. Most importantly MR fluids require a controllable magnet for activation, which can add considerable weight to the device and are extremely difficult to design into small and complex geometries.

As pointed out in §1.2, a substantial obstacle for the design and development of control systems capable of taking full advantage of these fluids has been the fact that they exhibit all sorts of highly nonlinear hysteretic behaviour, little of which is captured by the Bingham model. As an example Fig 3.2 shows the experimental responses obtained from [22], for an MR damper subject to a sinusoidal displacement and for a range control currents applied to the electromagnet. Unfortunately good experimental data for ER dampers is hard to come by, though this response is qualitatively typical of most ER and MR dampers. It should be noted that the force displacement loops run clockwise, while the force velocity loops run counter-clockwise. The first thing to notice is that as the applied current is increased the area enclosed by the force-displacement loop also increases, indicating an increase in the energy dissipated per cycle.

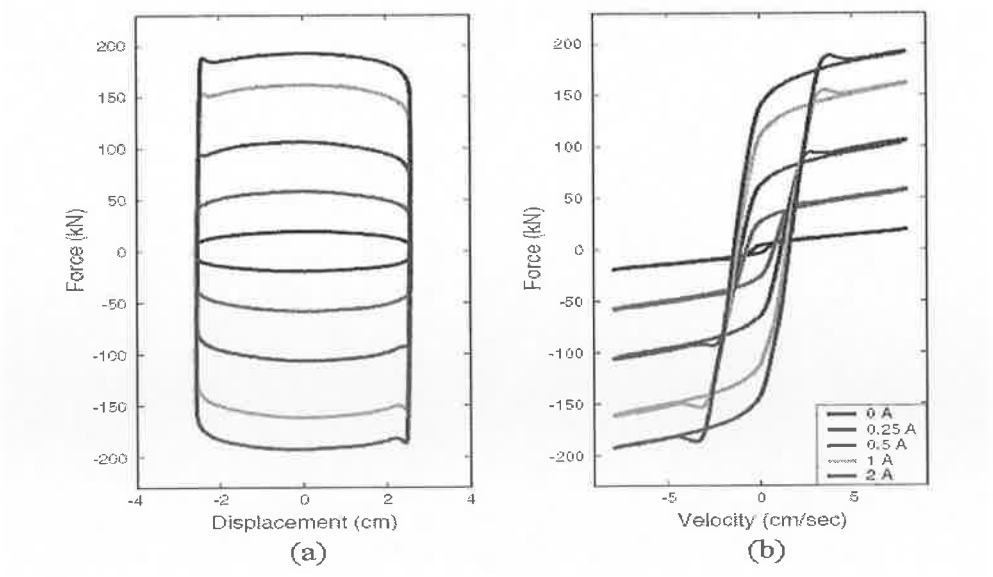

Fig 3.2 Experimental Force-displacement and Force-velocity relationships under sinusoidal displacement excitation, taken from [22].

While the Bingham model captures the basic features of force-displacement loop quite well, the main problem is in the representation of the force-velocity loop. Referring back to (1.1.1), the Bingham model presumes that the fluid remains rigid when the

applied force is less that the yield force, which is clearly not the case. When fitting the Bingham model to such a response it is usual to project the high velocity asymptote back to the force axis and take this to be σ_y while the average slope of the asymptote is taken as the plastic viscosity, η_v. Using the terminology from §1.2, when the damper force is less than the yield force, it is said to be operating in the pre-yield region. When the force is greater than the yield force it is said to be in the post-yield region. As noted in §1.2, numerous studies have come to the conclusion that ER fluids behave qualitatively similar to a nonlinear viscoelastic solid in the pre-yield region and like a Bingham plastic in the post-yield region, [21][25][31][32][36][56]. An interesting feature of Fig 3.2 is the peak in the force appearing in the upper left and lower right of the force-displacement loop, which correspond to the apparent over shoot in the force velocity curve. This strange behaviour might be attributed to the presence of a higher static yield force, which gets 'recharged' when the fluid is in the pre-yield region and begins to degrade as soon the fluid enters the post-yield region [60]. Alternatively the over shoot could be a result of fluid inertia. That is, non-negligible inertia would lead to a second order response. The above discussion should be enough to convince the reader that controllable fluid dampers are highly nonlinear devices.

To date there have been two main approaches to the modelling of controllable fluid dampers, which can be categorised as parametric and non-parametric [24]. The aim of the non-parametric approach is to replicate the input-output data exactly, without concern for the underlying phenomena. The modelling procedure can involve such things as fitting polynomials to the force-velocity curves, constructing fuzzy logic sets to discriminate between the pre and post yield regions or training neural networks on selected input-output data. As such nonparametric models rarely generalise to dynamics, which are not contained in the experimental data. In addition engineers are usually concerned with the physical nature of systems, so their usefulness as tools for control design and stability analysis is questionable.

Parametric models on the other hand, make use of prior knowledge about the physics and kinetics of the device to construct a constitutive model relating the input-output data. As shown in §1.2, a popular approach to the construction of a constitutive model is to use some interconnection of linear and nonlinear springs, dampers and friction elements (rheological elements). While the modelling of semi-active dampers with rheological elements is basically sound enough, to date the method of application has

been too ad-hoc, resulting in models that can exhibit very unrealistic behaviour. The main problems are in the construction of functions to determine whether the damper is in the pre or post yield region and the manner in which the effects of varying electric/magnetic fields are incorporated in the model. A consequence of the latter problem is that some of the models developed to date do not define a passive map between the imposed velocity and the reactive force (see §2.3 for definition of a passive system). As a result, it can be shown that these models are capable of generating "energy" under certain loading/control conditions (not a passive system). Consider first the model shown in Fig 1.6, which was developed in [33]. The total energy storage for this model consists of a kinetic component due to the presence of the mass and a potential energy due to the nonlinear spring (see equation (1.2.5))

$$H_1(\dot{x},x,x_1;t)=\frac{1}{2}m\dot{x}^2+\int_0^{x-x_1}K(s;t)ds. \tag{3.1.2}$$

The derivative of $H_1(\dot{x},x,x_1;t)$ along the solutions of the system in (1.2.6) satisfies

$$\dot{H}_1(\dot{x},x,x_1;t)=\begin{cases} F\dot{x}+\left(\dfrac{\dot{F}_y(t)}{2}|x-x_1|-\chi(\dot{x}_1;t)\dot{x}_1\right) & \text{if} \quad |x-x_1|>\dfrac{F_y(t)}{2G}, \\ F\dot{x}-\chi(\dot{x}_1;t)\dot{x}_1 & \text{if} \quad |x-x_1|\le\dfrac{F_y(t)}{2G}. \end{cases} \tag{3.1.3}$$

From the description of the modified Bingham plastic function, $\chi(\dot{x}_1;t)$, in Fig 1.6(b) it can be seen that the term $\chi(\dot{x}_1;t)\dot{x}_1$ is nonnegative. It follows that if $F_y(t)$ is constant (constant electric field) then the model does define a passive map from $\dot{x}$ to F. However if $|x-x_1|>F_y(t)/2G$ and $\dot{F}_y(t)|x-x_1|/2>\chi(\dot{x}_1;t)\dot{x}_1$, then the term in brackets will be positive (internal energy production) implying that the model does not define a passive map from $\dot{x}$ to F for arbitrarily time varying electric field. Note that in a later study [30], the field dependent nonlinear spring (1.2.5) was replaced with a linear spring with constant coefficient, leading to a passive model.

Next consider the Bouc-type model described by (1.2.7), generalizations of which are used in [22], [23] and [35]. When used for modelling MR dampers, this model is generally implemented using $A>0$ and $\beta=\gamma>0$, [23][35]. The total stored energy for this model can be taken as $H_2(z;t)=\alpha(t)z^2/2A$ (the state variable z has the dimensions of length [23]). The derivative of $H_2(z;t)$ along the solutions of the system in (1.2.7) (with $\beta=\gamma>0$) satisfies

$$\dot{H}_2(z;t) = \begin{cases} F\dot{x} + \left(\dfrac{\dot{\alpha}(t)z^2}{2A} - R\dot{x}^2 - \gamma 2\dfrac{\alpha(t)}{A}|\dot{x}\|z|^{n+1} \right) & \text{if } \dot{x}z > 0, \\ F\dot{x} + \left(\dfrac{\dot{\alpha}(t)z^2}{2A} - R\dot{x}^2 \right) & \text{if } \dot{x}z \le 0. \end{cases} \tag{3.1.4}$$

Clearly if either $\dot{x}z > 0$ and $\dot{\alpha}(t)z^2 > 2AR\dot{x}^2 - \gamma 4\alpha(t)|\dot{x}\|z|^{n+1}$ or $\dot{x}z \le 0$ and $\dot{\alpha}(t)z^2 > 2AR\dot{x}^2$, then the variations in the control parameter $\alpha(t)$ causes a net increase in the stored energy (internal power generation). It follows that the model does not define a passive map from $\dot{x}$ to F for arbitrarily time varying control. Similar calculations show that the models in [22],[23] and [35] do not define passive maps from $\dot{x}$ to F.

As a final example, the nonlinear viscoelastic-plastic model presented in [29] and [36] will be considered (see (1.2.8) and (1.2.9)). The model is based on the knowledge that ER/MR fluids behave like viscoelastic solids in preyield and like a Bingham plastic in postyield. The idea is to use two separate models to capture the preyield and postyield behaviour and then to smoothly transition between them using suitable switching functions. For small velocities (preyield) the fluid/damper is modelled by a spring and dashpot in parallel, so that the total reaction force is approximately $F(t) = R_p\dot{x}(t) + Kx(t)$. Both the spring stiffness K and the dashpot viscosity R_p are assumed to be increasing functions of the electric field. In this case the total stored energy corresponds with the energy stored in the spring, $H_3(x;t) = K(t)x^2/2$, the time derivative of which satisfies

$$\dot{H}_3(x;t) = F\dot{x} + \left(\dot{K}(t)x^2/2 - R\dot{x}^2\right). \tag{3.1.5}$$

Equation (3.1.5) implies that there is internal power generation whenever $\dot{K}(t)x^2/2 > R(t)\dot{x}^2$, from which it follows that the model does not define a passive map from $\dot{x}$ to F for arbitrarily time varying electric field.

Not only can this from of non-passive behaviour produce very strange results in any form of stability analysis, it can in fact give unrealistically good results in simulation studies of vibration or disturbance control. In addition it goes against the usual definition of a semi-active damper, as a control device with properties that can be

adjusted in real time, but cannot input energy into the system being controlled (see §1.2, §2.3).

The purpose of this chapter is to present a simple method for modelling shear mode electrorheological dampers, which avoids the above mentioned problems and produces models which are easy to analyse and numerical friendly. The method itself is based on the method of "thermodynamics with internal variables" and uses some simple results from convex analysis to ensure the transition between pre and post yield behaviour is physically consistent. It will also be shown that with a bit of insight into the underlying mechanisms, many of the observed nonlinear behaviours can be incorporated into the model in a systematic and easy to follow manner. Before getting down to the actual modelling, some of the basic theories presumed to govern the ER effect will first be reviewed. It is important to point out at this stage, that the interest in these models is not to predict the force levels or the actual values of parameters, but merely gain some insight into the relationships between observable variables such as the electric field, shear rate and bulk resistance of the fluid.

Microstructural Mechanisms

In order to formulate realistic models capable of predicting the behaviour of ER fluid based devices, it is important to have a basic understanding of the solidification kinetics and how an activated fluid responds to applied mechanical strains, especially in the case where substantial flow is induced. While numerous different phenomena have been proposed as the origin for the ER effect, many of these make specific assumptions about the chemical and physical nature of the ER fluid and are thus too specific to aid in the formulation of a general modelling procedure. For example, in [58] the author attributes the large increase in an ER fluid resistance to the formation of water bridges between particles. The idea here is that that these water bridges must be broken (overcome interfacial tension) for the fluid to flow. This mechanism originally received a lot of attention as the responses of many early ER fluids were found to depend on the moisture content of the particles. However many of the newer ER fluid formulations are essentially anhydrous, which rules out the water bridge as a fundamental mechanism [53].

The simplest and most general electrorheological mechanism is the polarisation model originally proposed by Winslow [50], which attributes the chaining of particles to their field induced polarisation relative to the base fluid. The usefulness of the polarization model lies in the fact that it can be easily modified to account for the attributes and operating conditions of a specific fluid composition, without greatly altering the qualitative nature of the equations. Application of the polarization model to the study of ER fluids has basically followed two paths, particle level simulations and single chain models.

Possibly the most interesting of the single chain models is the kinetic chain model developed in [59], to describe the evolution of a single particle width chain in oscillatory shear and over a range of strain amplitudes. While the chain model does lend some insight into the microscopic dynamics of an activated ER fluid, the assumption of single width particle chains is only justifiable for very small volume fractions. It has been shown both numerically and experimentally that ER fluids suitable for practical applications (with large controllable yield stress and low power consumption), require a volume fraction of between 30 and 40%. At such large concentrations the structure of an activated fluid is known to consist of thick fibrous clusters (Fig 3.1), which evolve continuously under non-stationary flow conditions. Under such conditions, the behaviour of ER fluid can be more accurately represented through particle level simulations. The basic idea here is to integrate the equation of motion for each individual particle in order to determine the evolution of the overall microstructure and then to evaluate the properties of interest. For a detailed discussion on the various components and aspects of the numerous microscopic models for ER fluids, the reader is referred to the references, [21][52][53][56][60]. Here, only some of the basic features will be considered.

The concept of electrostatic polarization as the origin of the ER effect still remains the fundamental building block for most successful micro-structural models. In its original form the induced electrostatic polarization forces were attributed to the dielectric mismatch between the ER particles and the base fluid (though it turns out that this is only valid for high frequency ac electric fields [53], for low frequency ac and dc fields, the important quantity is the ratio of particle to fluid conductivities). The basic idea being that if an uncharged particle, in a fluid of different dielectric constant is subjected to an electric field, it will develop an induced dipole due to the difference in polarizability of the two materials. The dipole itself can be seen as a concentration of

positive charge at one end of the particle and negative charge at the other end, see Fig 3.3.

For the purposes of analysis, a sample of ER fluid is usually treated as N neutrally-buoyant, hard spheres of radius b, dispersed in an incompressible Newtonian fluid of viscosity η. Both the particle size and the fluid Reynolds numbers are assumed to be small enough so that inertial effects can be ignored (apparently justifiable for $b < 10\mu m$ [52]). It is also assumed that Brownian/thermal forces are negligible, as these would only act to disrupt the particle chains vital for the ER effect. The exact electrostatic interpartical forces for a particular ER fluid could be calculated, in theory, however it would be an extremely difficult task due to the number of phenomena influencing the potential field. As a result, calculation of the electrostatic forces is usually only possible after a number of simplifications have been employed. The most common simplifications are to approximate the dipole on each sphere, as a point dipole located at the sphere centre, and to assume that the dipole moment on each particle is independent of it neighbours [53]. With this simplification and the aid of Fig 3.3, it is possible to qualitatively explain why ER fluids form particle chains parallel to the electric field. Consider two spheres who's line of centres is parallel to the electric field (i.e. $\theta_{ij} = 0$), there will be a net attraction between the positive and negative charges, pulling the spheres together.

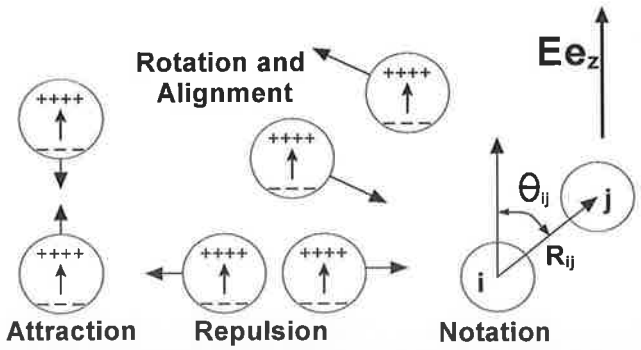

Fig 3.3 Electrostatic interaction between two dipoles, i and j. R_{ij} is the centre-to-centre spacing and θ_{ij} is the angle between the line of centres and the electric field, E.

Similarly for spheres with their line of centres perpendicular to the electric field, there is a net repulsion along their line of centres. If their line of centres is at any other angle with respect to the applied field, the pair will experience a net torque, causing them to translate and rotate into alignment with the electric field. Thus the forces due to polarization will cause the formation of particle chains running parallel to the electric field. That the model also predicts the formation of thick clusters requires a bit more thought, since the polarization model predicts that particle pairs with θ_{ij} greater than 55

degrees will repel each other. However, when a particle approaches an initially single particle width chain, it will experience attractive forces from the particles above and below its opposite in the chain. There will still be a net attractive force drawing the particle toward the chain. This net attractive force has other consequences, as it means that an electrode-spanning cluster can deform (as a result of moving the top electrode, relative to the lower) due to slight rearrangements and sliding of particles, without actually breaking any particle contacts.

In [60] the authors analysed the structural dynamics of ER suspensions under oscillatory shear (the fluid is contained between two parallel electrodes and shear is induced by moving one electrode relative to the other).The analysis was based on simulation results using a particle level model similar to that described above and experimental results using a 20wt % suspension of acidic alumina particles in polydimethylsiloxane (PDMS). The simulation results agreed, at least qualitatively with the experimental. The basic conclusions are best summarised using the Pipkin diagram in Fig 3.4, for ER fluids in laminar oscillatory shear flow (taken from [60]). The flow regimes are mapped in terms of the normalised frequency $\omega_E = \omega / AE^2$, (where A is a constant of suitable dimensions and E is the applied electric field) and the strain amplitude γ_o (i.e. for oscillatory strain $\gamma = \gamma_o \sin(\omega t)$). In keeping with [60], the strain will be denoted by γ rather than e. For fixed ω_E, very small strain amplitudes result in small affine particle displacements (from their equilibrium state), which are completely reversible/elastic. That is, if the stress is removed, the particles will return to their original position, restoring the energy that was stored during the original deformation. In this region dissipation will be small and of a purely viscous nature. As the amplitude increases above γ_1^{crit} the elastic response becomes nonlinear due to slight rearrangements and deformations of the particle clusters. In this region the strain will not be entirely recoverable due to the occurrence of permanent/irreversible rearrangements of particles. These rearrangements will dissipate energy due to viscous resistance opposing their motion and surface friction encountered as they slide over each other. Increasing the strain amplitude beyond γ_2^{crit} sends the fluid into the viscoplastic region.

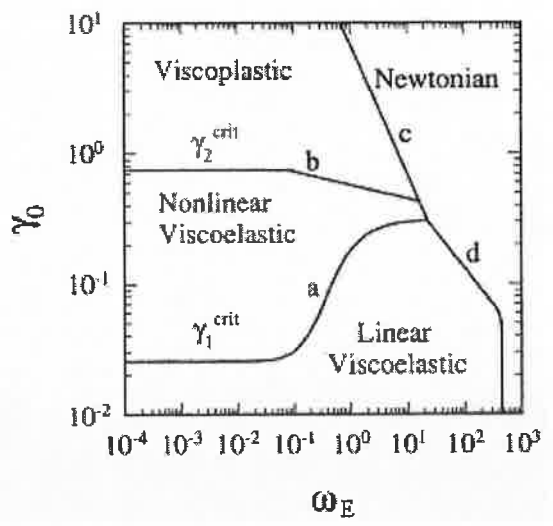

Fig 3.4 Pipkin diagram of dynamic rheological behaviour of ER fluids, the curves separating regions of different rheological behaviour, [60].

The fluid is no longer capable of accumulating additional elastic strain, resulting in a purely dissipative response. From a structural point of view, the viscoplastic response is characterised by continual rupture and reformation of particle clusters, giving rise to an apparent yield stress. Now running the other way, for a fixed γ_o, as the frequency increases, hydrodynamic forces will begin to degrade the electrode spanning clusters, allowing plastic deformation to occur at lower strain amplitudes. At even larger frequencies, the hydrodynamic forces will dominate completely and the response will appear to be purely viscous/Newtonian.

While the basic polarization model does lend some insight into the behaviour of ER fluids, it is still an over simplification of the actual behaviour. For example, when highly polarisable particles are in close proximity, the disturbance fields created by the neighbouring particles act to further polarise one another, resulting in electrostatic moments beyond the dipole approximation. In reality the ER fluid and electrodes should be treated as a leaky dielectric with a capacitance that depends on the instantaneous state of the fluid. The main failing of many of the micro-structural models to date is that the applied electric field is only treated as a constant parameter and thus, they do not give any insight into the effect of an arbitrarily varying field. The reason for this would seem to be that incorporating a varying electric field places the model in the realm of electrodynamics (as oppose to electrostatics), requiring consideration of the conduction current, charge densities on the electrodes and induced magnetic fields. Those models which have successfully incorporated these effects [62], are extremely complicated and difficult to interpret.

3.2 Thermomechanics

System Assumptions

The purpose of this section is to describe a simple method for the construction of one dimensional models for ER dampers, based on the observed energy storage and dissipation characteristics of ER fluid. The method itself is based on a simplified version of the method of "thermomechanics with internal variables", a detailed development of which can be found in the excellent texts, [37][38][39]. Of course, a one-dimensional model can hardly be expected to provide an in anyway accurate description of a complex system such as ER fluid. However, a good model should be constructed with the application in mind and should describe the real physics only as far as needed for that application. By using an approach rooted in thermodynamics, it is hoped that the resulting models will be capable of describing the qualitative energy storage and dissipation properties, without being overly complicated. While the presentation given below may seem rather abstract at first, in later sections it will be shown that the models can be interpreted using idealised rheological elements (springs, dampers etc). This allows for a clear interpretation of the physical effects taken into account.

To simplify matters, it will be assumed that the typical levels of shear to which the damper is subject are sufficiently small, so as to justify ignoring inertial effects. While a massless model does not make much physical sense, it should be kept in mind that the ultimate goal is to couple the model with the oscillator described in §2. From a thermodynamical point of view, it will be assumed that the instantaneous state of the damper can be adequately described using a vector of macroscopic variables $\chi \in \Re^n$, a vector of internal variables $\alpha \in \Re^m$ and the thermodynamic temperature $\theta > 0$. The macroscopic variables will include those quantities which can be observed externally, such as the strain and stored charge etc. The internal variables will be used to account for a lack of precise description of the complex phenomena occurring at a microscopic level, but which are macroscopically evident in certain observable irreversibilities. In particular to account for the structural rearrangements and deformations of particle chains, which occur when an activated ER fluid is subject to shear. The internal variables should be viewed as a form of "average", representing mean measures of the structural rearrangements. In consequence, the number of variables required to obtain a

satisfactory description, should be finite and independent of the volume of ER fluid under consideration.

Thermodynamic Potential

In what follows, the object of study will be a system Σ, whose state is completely determined by the variables $\chi \in \Re^n, \alpha \in \Re^m$ and $\theta > 0$, collectively referred to as the state, or state variables. Any function of them will be referred to as a state function, examples of which include the internal energy $U(\chi,\alpha,\theta)$, the entropy $S(\chi,\alpha,\theta)$ and the free energy, defined by $W(\chi,\alpha,\theta) = U - \theta S$. Following [39], the fundamental laws of thermodynamics can be stated as follows.

First Law The total increase of the internal energy per unit time balances the power of the forces, X, conjugate to χ and the heat supply $\dot{Q}$ per unit time,

$$\dot{U} = \langle \mathrm{X}, \dot{\chi} \rangle + \dot{Q}. \tag{3.2.1}$$

Second Law The rate of increase in entropy $\dot{S} = \dot{S}^r + \dot{S}^i$, consists of a reversible contribution

$$\dot{S}^r = \dot{Q}/\theta \tag{3.2.2}$$

called the external entropy supply, and a non-negative irreversible contribution

$$\dot{S}^i \geq 0 \tag{3.2.3}$$

referred to as the internal entropy production. If (3.2.3) holds with equality, i.e. $\dot{S}^i = 0$, then the system is said to be reversible and otherwise irreversible.

Combining (3.2.1)-(3.2.3) and using the definition $W = U - \theta S$, one obtains the inequality

$$\theta \dot{S}^i = \langle \mathrm{X}, \dot{\chi} \rangle - \dot{W} - \dot{\theta} S \geq 0. \tag{3.2.4}$$

Since W is a state function, $\dot{W}$ can be expanded to obtain

$$\theta \dot{S}^i = \left\langle \mathrm{X} - \frac{\partial W}{\partial \chi}, \dot{\chi} \right\rangle - \left\langle \frac{\partial W}{\partial \alpha}, \dot{\alpha} \right\rangle - \left\langle S + \frac{\partial W}{\partial \theta}, \dot{\theta} \right\rangle \geq 0. \tag{3.2.5}$$

By considering the case in which Σ is subject to a process of pure heating or cooling (i.e. $\dot{\chi} = 0, \dot{\alpha} = 0$) and noting that (3.2.5) must hold for both increasing and decreasing temperature, one obtains the state law [39],

$$S = -\frac{\partial W}{\partial \theta}. \tag{3.2.6}$$

Now, decompose the force X into a quasi-conservative component X^q, a dissipative component $\mathrm{X}^d = \mathrm{X} - \mathrm{X}^q$, and define

$$\mathrm{X}^q = \frac{\partial W}{\partial \chi}, \quad \mathrm{A} = -\frac{\partial W}{\partial \alpha}, \tag{3.2.7}$$

where A is the thermodynamic force conjugate to α. Inserting (3.2.6) and (3.2.7) into (3.2.5) yields the inequality

$$\theta \dot{S}^i = \left\langle \mathrm{X}^d, \dot{\chi} \right\rangle + \left\langle \mathrm{A}, \dot{\alpha} \right\rangle \geq 0, \tag{3.2.8}$$

which is the rate of energy dissipation resulting from the evolution of Σ. For simplicity, only isothermal processes will be considered from this point on ($\dot{\theta} = 0$), so that θ can be dropped from the list of state variables and simply absorbed into the definition of the state functions. Being a contribution to $\dot{S}$, the entropy production $\dot{S}^i$ is not a state variable, but a function of both $\chi_\alpha = (\chi, \alpha)$ and $\dot{\chi}_\alpha = (\dot{\chi}, \dot{\alpha})$. It is now possible to define the dissipation function $\Phi(\dot{\chi}_\alpha; \chi_\alpha) = \theta \dot{S}^i$ and write the well know dissipation inequality

$$\Phi(\dot{\chi}, \dot{\alpha}; \chi_\alpha) = \left\langle \mathrm{X}, \dot{\chi} \right\rangle - \dot{W} = \left\langle \mathrm{X}^d, \dot{\chi} \right\rangle + \left\langle \mathrm{A}, \dot{\alpha} \right\rangle \geq 0. \tag{3.2.9}$$

Systems satisfying inequality (3.2.9) will be referred to as thermodynamically consistent. Inequality (3.2.9) should be compared with the definition of a passive system given in §2.3. From the definition, it can be seen that the quasi-conservative forces X^q are state functions, whereas, being subject to inequality (3.2.9), the dissipative forces X^d and A, also depend strongly on $\dot{\chi}$ and $\dot{\alpha}$ respectively. Note that the dissipative power $\left\langle \mathrm{X}^d, \dot{\chi} \right\rangle$ results from the interaction between Σ and its environment, whereas $\left\langle \mathrm{A}, \dot{\alpha} \right\rangle$ represents the dissipation rate resulting from the internal evolution of Σ, (i.e. $\left\langle \mathrm{A}, \dot{\alpha} \right\rangle$ does not appear explicitly in the first law). For reasons of stability, it will henceforth be assumed that the free energy $W(\chi, \alpha)$ is convex in both it arguments and satisfies $W(0,0) = 0$.

Dissipation Potentials

In the previous section it was shown that knowledge of the free energy provides sufficient information to determine the relationship between the quasi-conservative force and the state variables, (3.2.7). However, the free energy provides no information

on the structure of the dissipative force X^d and if internal variables are included, the free energy provides only a definition of the associated force, A. It follows that in order to model dissipative systems, and in particular, to obtain evolution equations for the internal variables, a complementary formalism will be required. In [39] it is argued that the required relationships can be obtained (after suitable scaling) from the only element characterizing the difference between reversible and irreversible systems, the dissipation function.

In what follows it will be assumed that the dissipation function can be decomposed as $\Phi(\dot{\chi}_\alpha;\chi_\alpha)=\Phi_\chi(\dot{\chi};\chi_\alpha)+\Phi_\alpha(\dot{\alpha};\chi_\alpha)$, with Φ_χ and Φ_α being continuous in both arguments, convex with respect to $\dot{\chi}$ and $\dot{\alpha}$ respectively (uniformly in $\chi_\alpha=(\chi,\alpha)$), and satisfying $\Phi_\chi(0;\cdot)=0,\Phi_\alpha(0;\cdot)=0$. Thus, without loss of generality, the following discussion will focus on the properties of Φ_α with the appropriate extensions for Φ_χ being given at the end of this section (Table 3.1). A review of some definitions and results from convex analysis are given in §A.2.

Consider first, the case where Φ_α is continuously differential with respect to $\dot{\alpha}$. In [39] it was shown that the relationship between A and Φ_α can be obtained by applying a version of the maximum dissipation principle: for a given value of the thermodynamic force A, the actual velocity $\dot{\alpha}$, maximises the dissipation rate $\langle A,\dot{\alpha}\rangle$, subject to the constraint $\Phi_\alpha(\dot{\alpha};\chi_\alpha)=\langle A,\dot{\alpha}\rangle\geq 0$. The analytical formulation of this problem can be obtained by transforming the constrained maximisation into an unconstrained minimisation problem using the method of Lagrange multipliers. Consider the convex Lagrangian function

$$L(\dot{\alpha},\lambda)=-\langle A,\dot{\alpha}\rangle+\lambda\left(\Phi_\alpha(\dot{\alpha};\chi_\alpha)-\langle A,\dot{\alpha}\rangle\right) \tag{3.2.10}$$

where A and χ_α are considered fixed and $\lambda\in\Re$ is the Lagrange multiplier. A sufficient condition for $(\dot{\alpha},\lambda)$ to be a minimum of (3.2.10), is that $(\dot{\alpha},\lambda)$ solve the equations $\partial L/\partial\dot{\alpha}=0,\partial L/\partial\lambda=0$, which yields

$$A=\gamma\frac{\partial\Phi_\alpha(\dot{\alpha};\chi_\alpha)}{\partial\dot{\alpha}},\quad \gamma=\frac{\lambda}{1+\lambda}=\Phi_\alpha\left\langle\frac{\partial\Phi_\alpha}{\partial\dot{\alpha}},\dot{\alpha}\right\rangle^{-1}. \tag{3.2.11}$$

Using the fact that Φ_α is convex in $\dot{\alpha}$ and satisfies $\Phi_\alpha(0;\cdot)=0$, it can be shown that $\gamma \in [0,1]$. From a geometric point of view, (3.2.11) implies that at each instant the force A, corresponding to $\dot{\alpha}$, is an outward normal to the surface of constant dissipation $\Phi_\alpha = \text{const.}$. It can be seen that if Φ_α is positively homogenous of order $n>1$ in $\dot{\alpha}$ (i.e. $\Phi_\alpha(p\dot{\alpha},\cdot) = p^n \Phi_\alpha(\dot{\alpha},\cdot), \forall p>0$) , then $\gamma = 1/n$. The case where $n=1$ is more difficult and will be discussed in some detail later. As a quick example, consider the free energy and dissipation $W = 0.5G(\chi-\alpha)^2$ and $\Phi_\alpha = R\dot{\alpha}^2$, then $\gamma = 2$ and (3.2.7),(3.2.11) yield

$$\mathrm{A} = G(\chi-\alpha), \quad \dot{\alpha} = \frac{G}{R}(\chi-\alpha), \tag{3.2.12}$$

which is the Maxwell rheological model.

The inclusion of γ in (3.2.11) means that Φ_α is not a true potential for A, but instead is what is sometimes called a pseudopotential. If Φ_α is positively homogenous of order $n>1$ in $\dot{\alpha}$, then γ does not cause a problem. However if Φ_α is not a homogenous function of $\dot{\alpha}$ then the presence of γ can make things a bit awkward. Consider the case where the Φ_α can be written as $\Phi_\alpha = \langle \partial D/\partial\dot{\alpha}, \dot{\alpha}\rangle$, where $D(\dot{\alpha};\chi_\alpha)$ is convex in $\dot{\alpha}$ and satisfies $D(0;\cdot)=0$. It follows that D will serve as a true potential for A, and is referred to as the dissipation potential [38]. It follows that if Φ_α can be written in the form $\Phi_\alpha = \sum_1^N \Phi_\alpha^k$, where each of the N functions Φ_α^k are positively homogenous of order $n_k>1$ in $\dot{\alpha}$, then $D = \sum_1^N \frac{1}{n_k}\Phi_\alpha^k$. As D is a potential for A, the dual or flow potential $D^*(\mathrm{A};\chi_\alpha)$ can be obtained using the Legendre transform

$$D^*(A;\chi_\alpha) = \langle \mathrm{A}, \dot{\alpha}\rangle - D(\dot{\alpha};\chi_\alpha), \tag{3.2.13}$$

so that

$$\dot{\alpha} = \frac{\partial D^*(\mathrm{A};\chi_\alpha)}{\partial \mathrm{A}}. \tag{3.2.14}$$

From (3.2.7), (3.213) and (3.2.14) it can be seen that knowledge of the potentials W and D is sufficient to determine the evolution equation for the internal variables. The formalism presented above is sufficient for the modelling of simple systems exhibiting relaxation effects (viscoelastic etc). However, as pointed out in Section.1 and §1.2, the

qualitative behaviour of a shear mode ER damper is dominated by the presence of a dynamic yield stress and not by a characteristic time scale. This situation corresponds to the case in (3.2.11) for which $\gamma = 1$, implying that $D(\dot{\alpha};\chi_\alpha) = \Phi_\alpha(\dot{\alpha};\chi_\alpha)$. It follows that A must be positively homogeneous of degree zero in $\dot{\alpha}$ and hence insensitive to the magnitude of $\dot{\alpha}$ (i.e. rate independence). This property is typical of systems exhibiting plastic or hysteretic type behaviours [37]. This situation requires special attention as the dissipation potential will no longer have classical derivative for all $\dot{\alpha}$. For example $r|\dot{\alpha}|$ is not differentiable at $\dot{\alpha} = 0$. Furthermore, (3.2.13) would imply that the dual potential $D^*(\mathrm{A};\chi_\alpha)$ is identically equal to zero. It would appear that some additional mathematical apparatus is required to deal with these complexities. The appropriate tool is convex analysis, a brief summery of the relevant aspects being contained in §A.2. Recall that the subdifferential of convex function $f : \Re^m \to \Re$ at the point x is

$$\partial f(x) = \left\{ z \in \Re^m \mid f(\bar{x}) - f(x) \geq +\langle z, \bar{x} - x \rangle, \forall \bar{x} \in \Re^m \right\} \tag{3.2.15}$$

and the outward normal cone to a closed convex set $\mathbf{C}$ at x is defined by

$$N(x;\mathbf{C}) = \left\{ z \in \Re^m \mid \langle z, x - \bar{x} \rangle \geq 0, \forall \bar{x} \in \mathbf{C} \right\} \tag{3.2.16}$$

The normal cone $N(x;\mathbf{C})$, is the subdifferential of the indicator function, $I(x;\mathbf{C})$, of the convex set $\mathbf{C}$, see §A.2 and references therein for details.

Assume that $D(\dot{\alpha};\chi_\alpha) = \Phi_\alpha(\dot{\alpha};\chi_\alpha)$ is continuous in both arguments, convex and positively homogeneous of order one in $\dot{\alpha}$. Assume also that $D(0;\cdot) = 0$ and $D(\dot{\alpha};\cdot) \geq 0$, for all $\dot{\alpha} \in \Re^m$ .Define the closed convex set $\mathbf{C}(\chi_\alpha)$ by

$$\mathbf{C}(\chi_\alpha) = \left\{ \mathrm{A} \in \Re^m \mid \langle \mathrm{A}, \dot{\alpha} \rangle \leq D(\dot{\alpha};\chi_\alpha), \forall \dot{\alpha} \in \Re^m \right\}, \tag{3.2.17}$$

(see [65] for details)

Lemma 3.2.1

(a) D is the support function of $\mathbf{C}(\chi_\alpha)$: $D(\dot{\alpha};\chi_\alpha) = \sup\left\{ \langle \mathrm{A}, \dot{\alpha} \rangle \mid \mathrm{A} \in C(\chi_\alpha) \right\}$,

(b) The Legendre-Fenchel dual of D is the indicator function of $\mathbf{C}(\chi_\alpha)$:

$$D^*(\mathrm{A};\chi_\alpha) = I(\mathrm{A};\mathbf{C}(\chi_\alpha)) = \begin{cases} 0, & \mathrm{A} \in C(\chi_\alpha) \\ +\infty, & \mathrm{A} \notin C(\chi_\alpha) \end{cases} \tag{3.2.18}$$

(c) $\mathbf{C}(\chi_\alpha) = \partial_{\dot{\alpha}} D(0;\chi_\alpha)$,

(d) $\mathrm{A} \in \partial_{\dot{\alpha}} D(\dot{\alpha};\chi_\alpha) \Leftrightarrow \dot{\alpha} \in \partial_{\mathrm{A}} D^*(\mathrm{A};\chi_\alpha) = N(\mathrm{A};\mathbf{C}(\chi_\alpha))$, and from (3.2.16)

$$\left\langle \dot{\alpha}, \mathrm{A}-\hat{\mathrm{A}} \right\rangle \geq 0, \qquad \forall \hat{\mathrm{A}} \in \mathbf{C}(\chi_\alpha). \tag{3.2.19}$$

In plasticity theory, the variational inequality (3.2.19) is sometimes referred to as the Hill's maximum dissipation principle. The geometric interpretation of (3.2.19) is that the angle between the vectors $(\mathrm{A}-\hat{\mathrm{A}})$ and $\dot{\alpha}$ is acute ($\leq \pi/2$). From examination of (3.2.19) it can be seen that if $\mathrm{A} \in \operatorname{int} \mathbf{C}(\chi_\alpha)$ (interior) then $\dot{\alpha}=0$, implying that the dissipation is zero and the response reversible. Evolution of the internal variable, and hence positive dissipation, is only possible if A has reached a boundary point of $\mathbf{C}(\chi_\alpha)$ (yield surface), that is $\mathrm{A} \in \mathrm{bd}\mathbf{C}(\chi_\alpha)$. As an example, consider the case of a scalar internal variable with $D(\dot{\alpha};\chi_\alpha)=\Phi_\alpha(\dot{\alpha};\chi_\alpha)=r(\chi_\alpha)|\dot{\alpha}|$, where $r(\chi_\alpha)$ is Lipschitz function satisfying $r(\chi_\alpha)\geq 0, \forall \chi_\alpha \in \Re^{n+m}$.

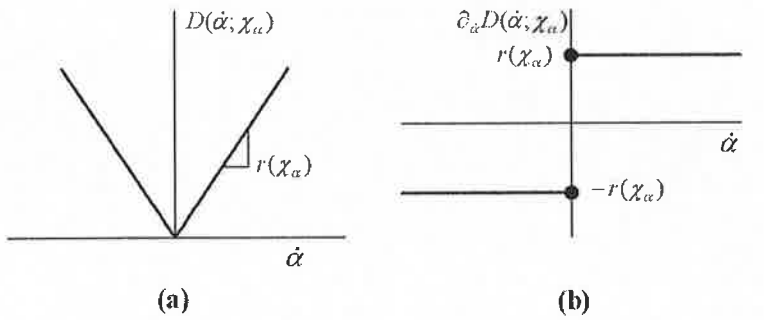

Fig 3.5 (a) support function of the convex set $\mathbf{C}=r(\chi_\alpha)[-1,+1]$ and (b) the corresponding subdifferential

It follows from either (3.2.17) or Lemma 3.2.1(c) that $\mathbf{C}(\chi_\alpha)=r(\chi_\alpha)[-1,1]$ and from Lemma 3.2.1(d), $\mathrm{A} \in r(\chi_\alpha)\partial|\dot{\alpha}|$, see Fig 3.5(a) .The dual potential is the indicator function of $\mathbf{C}(\chi_\alpha)$ and the evolution equation for the internal variable is given by part (c)

$$\dot{\alpha} \in N(\mathrm{A};\mathbf{C}(\chi_\alpha)) = \begin{cases} \Re_-, & \text{if } -\mathrm{A}=r(\chi_\alpha)>0 \\ 0, & \text{if } |\mathrm{A}|<r(\chi_\alpha), r(\chi_\alpha)>0 \\ \Re_+, & \text{if } \mathrm{A}=r(\chi_\alpha)>0 \\ \Re, & \text{if } \mathrm{A}=r(\chi_\alpha)=0 \end{cases}. \tag{3.2.20}$$

Comparing Fig 3.5(b) and Fig 3.6(b) it can be seen that $\partial_{\mathrm{A}} D^* = (\partial_{\dot{\alpha}} D)^{-1}$ and that the mapping $\mathrm{A} \leftrightarrow \dot{\alpha}$ is not one-to-one (for each values of A there may be numerous acceptable values of $\dot{\alpha}$). As it stands (3.2.20) is rather abstract. However, if $\mathbf{C}(\chi_\alpha)$ is closed convex and nonempty, it may be possible to construct a yield function $f(\mathrm{A};\chi_\alpha)$,

such that $f(\mathrm{A};\chi_\alpha)<0 \Leftrightarrow \mathrm{A}\in \operatorname{int}\mathbf{C}(\chi_\alpha)$ and $f(\mathrm{A};\chi_\alpha)=0 \Leftrightarrow \mathrm{A}\in \operatorname{bd}\mathbf{C}(\chi_\alpha)$, (see [65] for details).

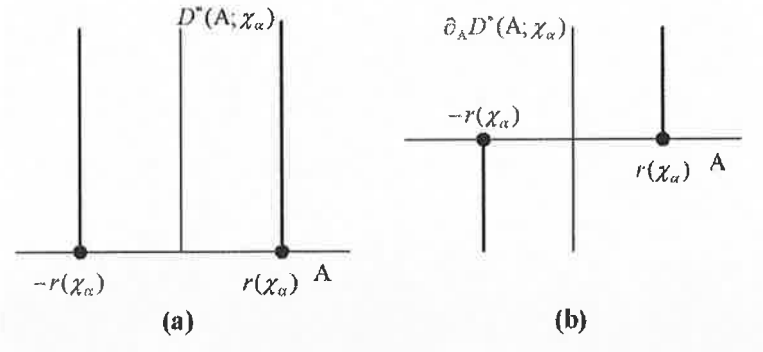

Fig 3.6 (a) indicator function of the convex set $\mathbf{C}=r(\chi_\alpha)[-1,+1]$ and (b) the corresponding subdifferential

For the example given above, $f(\mathrm{A};\chi_\alpha)=|\mathrm{A}|-r(\chi_\alpha)\le 0$ will do the trick. Now, if $f(\mathrm{A};\chi_\alpha)$ is continuously differentiable with respect to A when $\mathrm{A}\in \operatorname{bd}\mathbf{C}(\chi_\alpha)$ (requires $r(\chi_\alpha)>0$), then the normality law (3.2.20) can be expressed as

$$\dot{\alpha}=\lambda\frac{\partial f(\mathrm{A};\chi_\alpha)}{\partial A}, \tag{3.2.21}$$

where $\lambda\ge 0$ is a nonnegative scalar . That is, when $f(\mathrm{A};\chi_\alpha)=0$ the gradient of the yield function points in the normal direction to the convex set $\mathbf{C}(\chi_\alpha)$. The multiplier λ, often referred to as the plastic multiplier, belongs to the solution of the evolution problem and can be evaluated using the following conditions, (referred to as the loading-unloading conditions in plasticity)

$$\lambda\ge 0, f(\mathrm{A};\chi_\alpha)\le 0 \tag{3.2.22}$$

$$\lambda f(\mathrm{A};\chi_\alpha)=0 \tag{3.2.23}$$

$$\lambda\dot{f}(\mathrm{A};\chi_\alpha)=0 \tag{3.2.24}$$

or equivalently,

$$\begin{aligned}&\lambda\ge 0 \quad \textit{if } f=0 \textit{ and } \dot{f}=0\\ &\lambda=0 \quad \textit{if } f<0 \textit{ or } f=0 \textit{ and } \dot{f}<0\end{aligned} \tag{3.2.25}$$

Equations (3.2.21)-(3.2.23) can be obtained from consideration of the physical problem or by transforming the constrained maximisation problem in Lemma 3.2.1(a), into an unconstrained minimisation problem, with Lagrangian function

$$L(A,\lambda)=-\langle \mathrm{A},\dot{\alpha}\rangle+\lambda f(\mathrm{A};\chi_\alpha). \tag{3.2.26}$$

Applying the classical Karush-Kuhn-Tucker optimality conditions to (3.2.26) then yields (3.2.21)-(3.2.23), [41]. Condition (3.2.24) is referred to as the consistency (or persistency) condition and derives from the fact that if $A \in \text{bd}\mathbf{C}(\chi_\alpha)$, the yield function should necessarily satisfy $\dot{f} \le 0$, since $\dot{f} > 0$ would imply that A was leaving $\mathbf{C}(\chi_\alpha)$. Depending on the specific model, the consistency condition can usually be used to obtain a specific parameterisation of λ. Equations (3.2.22)-(3.2.24) are most easily interpreted in the form (3.2.24). That is, $\lambda \ge 0$ and hence $\dot{\alpha} \ge 0$ can only occur if $f = 0 \Leftrightarrow A \in \text{bd}\,\mathbf{C}$ and is persisting on $\text{bd}\mathbf{C}$ ($\dot{f} = 0$). Similarly $\lambda = 0$ and hence $\dot{\alpha} = 0$ if $f < 0 \Leftrightarrow A \in \text{int}\,\mathbf{C}$ or $A \in \text{bd}\,\mathbf{C}$ and is evolving towards the interior of $\mathbf{C}$ ($\dot{f} < 0$).

Now the problem of modelling the ER damper boils down to finding suitable expressions for the free energy $W(\chi,\alpha)$ and for the dissipation potential $D(\dot{\chi},\dot{\alpha};\chi_\alpha) = D_\chi(\dot{\chi};\chi_\alpha) + D_\alpha(\dot{\alpha};\chi_\alpha)$, with $\chi_\alpha = (\chi,\alpha)$, and then applying the fundamental equations,Table 3.1 . Recall that $\chi_\alpha = (\chi,\alpha)$ and $\dot{\chi}_\alpha = (\dot{\chi},\dot{\alpha})$.

1) Conservative Forces	$\mathrm{X}^q = \dfrac{\partial W}{\partial \chi}$ and $\mathrm{A} = -\dfrac{\partial W}{\partial \alpha}$
2) Normality Laws	$\mathrm{X}^d \in \partial_{\dot{\chi}} D_\chi(\dot{\chi};\chi_\alpha)$ and $\mathrm{A} \in \partial_{\dot{\alpha}} D_\alpha(\dot{\alpha};\chi_\alpha)$
3) Total Force	$\mathrm{X} = \mathrm{X}^d + \mathrm{X}^r$
4) Flow potential	$D_\alpha^*(\mathrm{A};\chi_\alpha) = \sup\left\{\langle \mathrm{A},\dot{\alpha}\rangle - D_\alpha(\dot{\alpha};\chi_\alpha) \mid \dot{\alpha} \in \Re^m\right\}$
5) Evolution equation	$\dot{\alpha} \in \partial_{\mathrm{A}} D_\alpha^*(A;\chi_\alpha) = N(A;\mathbf{C}(\chi_\alpha)$, *or* $\dot{\alpha} = \lambda \dfrac{\partial f(A;\chi_\alpha)}{\partial \mathrm{A}} \begin{cases} \lambda \ge 0 & \text{if } f = 0 \text{ and } \dot{f} = 0 \\ \lambda = 0 & \text{if } f < 0 \text{ or } f = 0 \text{ and } \dot{f} < 0 \end{cases}$
6) Dissipation inequality	$\Phi(\dot{\chi},\dot{\alpha};\chi_\alpha) = \langle \mathrm{X},\dot{\chi}\rangle - \dot{W} = \langle \mathrm{X}^d,\dot{\chi}\rangle + \langle \mathrm{A},\dot{\alpha}\rangle \ge 0.$

Table 3.1

3.3 A deformation mechanism

The purpose of this section is to develop a qualitative model relating the experimentally observed mechanical stress-strain relationships for an ER suspension in shear, with its mechanical energy storage and dissipation properties. The following section draws heavily from the papers [21] and [56]. Consider an ER suspension confined between

two parallel plates a distance L apart, across which a constant electric field E has been applied, Fig 3.7 . It is assumed that sufficient time has been allowed for the particles to form a "steady state" microstructure consisting of particle chains running parallel to the electric field. The lower plate is immobile and the upper plate translates with a steady infinitesimal velocity. Since the deformation is simple shear, both the shape and size of the control volume are assumed to be constant.

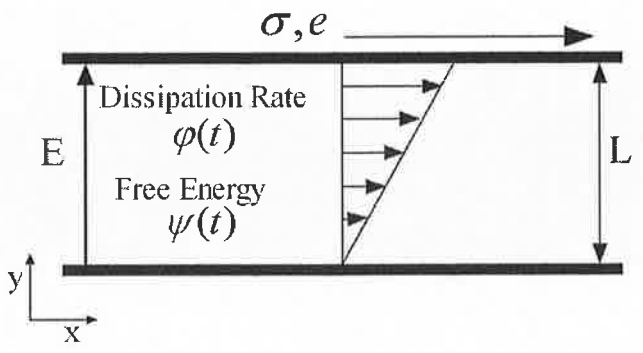

Fig 3.7 Control volume under consideration

In addition, all deformations will be considered to be isothermal. The shear rate in this simple shear flow will be denoted by $\dot{e} \in \Re$ and the shear stress on the plane parallel to the deformation by $\sigma \in \Re$. Now the electrostatic energy of the suspension can be written (see [21] and [56] for details)

$$U_E = -\frac{1}{2} n \left\langle E, \hat{C} \right\rangle E = -\frac{1}{2} n \left\langle \hat{P}, E \right\rangle , \tag{3.3.1}$$

where n is the number density of particles , E is the applied electric field and $\hat{C}$ is the ensemble average of the suspension capacitance matrix . This capacitance matrix is the proportionality relating the average polarization of the suspension to the electric field, $\hat{P} = \left\langle E, \hat{C} \right\rangle$ and is a function of the instantaneous particle positions [56]. When the particles are chained and aligned with the electric field, the average particle dipole is very large (due to mutual interactions) and so is the capacitance matrix. Since U_E is proportional to $-\hat{C}$, it follows that the U_E will be quite small in this state. If a small force is applied to the top plate the chains will stretch and deform, causing a decrease in the average polarization (particles cannot interact as strongly), and hence an increase in the electrostatic energy. That is to say, as the chains are deformed, the strain energy will increase due to the input of stress work necessary for the particles to be pulled apart from their preferred, chained configuration. Now this increase in stored energy can be interpreted as an increase in an equivalent, strain dependent, free energy $W(e)$, due to the work performed during deformation. For fixed E, the free energy can be defined as,

$$W(e) = U_E(e) - U_E(0), \tag{3.3.2}$$

where $U_E(e)$ is the electrostatic energy in (3.3.1), defined as a function of the shear strain e. It follows that $W(0) = 0$ and that the shear stress σ can be defined as,

$$\sigma = \frac{\partial W(e)}{\partial e}. \tag{3.3.3}$$

In order to form a qualitative picture of the relationship between $W(e)$ (and hence σ) and a monotonically increasing strain e, consider the idealized microstructure in Fig 3.8(a), [21],[53]. It consists of a simple monolayer of single width particle chains spanning the electrodes and periodically repeated along the electrode length. If the upper electrode translates slowly relative to the lower, the chains will deform affinely, Fig 3.8(b), storing energy, until some critical strain $e_y << 1$ is reached Fig 3.8(c). At $e = e_y$, the chains will snap releasing the stored energy. The upper chain segments will then connect with the adjacent lower chain segments (in the direction of shear) repeating the original, undeformed microstructure. Assuming e continues to increase, the process will simply repeat in a periodic fashion. It follows that in this idealized model, the particle chains under go two distinct motions [21], slow elastic/reversible affine deformations of the initially aligned chains, followed by a rapid rearrangement of the microstructure, in which the chains snap and reconnect with adjacent chain segments. In the above model and for monotonically increasing strain e, the free energy will be a periodic function of e, with period e_y.

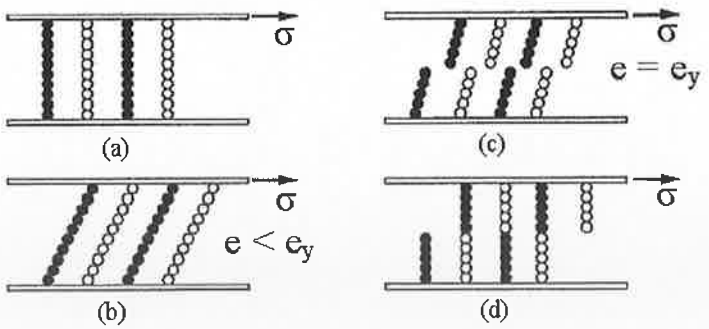

Fig 3.8 Idealized microstructure for an ER suspension.

Furthermore, it has been shown in [63], that the critical strain e_y of a particle chain, is an increasing function of the chain thickness. As an extension of the previous model, consider N monolayer's, with increasing particle thickness and hence increasing critical strain $0 < e_{y1} < e_{y2} \ldots e_{yN} << 1$, arranged across the width of the control volume, see

Fig 3.9. At each instant the total free energy W, will be the sum of the free energies W_i, corresponding to the individual monolayers. For constant shear rate $\dot{e} > 0$, each contribution, W_i, to the total free energy will be a periodic function of the strain, with period e_{yi}. Therefore, one would expect W to be an almost periodic function, with nonzero mean corresponding to the average stored energy.

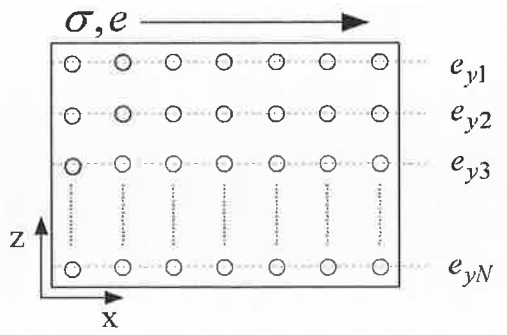

Fig 3.9 N monolayer's, with increasing critical strain, $0 < e_{y1} < e_{y2} \ldots e_{yN} << 1$.

Now the next step will be to relate the dynamics of the idealized microscopic model described above with the macroscopically observed dissipation in the control volume. Intuitively one would expect that the macroscopic dissipation would contain a component which is in some way related to the energy released by the snapping of the particle chains. What is not so intuitive is that this component of the dissipation is responsible for the macroscopically observed "Bingham" type yield stress, in equation (3.1.1).

In order to develop a qualitative description of the total dissipation in an ER suspension subject to constant shear, a dissipation inequality similar to (3.2.9) is required for the control volume in Fig 3.7. In [21] and [66], it has been shown that for a statistically homogeneous suspension, the areal average instantaneous shear stress, $\sigma(t)$, is constant throughout the control volume and is thus equal to the volume averaged instantaneous shear stress. While the ER suspension is a highly ordered structure, it is still statistically homogenous [21]. It follows that the volume average dissipation inequality for the control volume, subject to a constant electric field and constant shear rate $\dot{e} > 0$, can be written as

$$\Phi(t) = \sigma(t)\dot{e} - \dot{W}(t) \geq 0 \tag{3.3.4}$$

where Φ and W are the volume averaged dissipation rate and free energy for the control volume. That is, the rate of dissipation in the fluid is equal to the rate of work done on the fluid by the moving plate minus the increase in the free energy for the

system. Based on the previous discussion, one would expect $\sigma(t)$, $W(t)$ and hence $\Phi(t)$ to be almost periodic functions, however the yield stress is a time averaged quantity since it appears constant on a macroscopic time scale. Choosing a time period T large enough so as to include numerous change snapping events, but macroscopically short, the time average of the dissipation inequality is,

$$\frac{1}{T}\int_0^T \Phi(t)dt = \frac{1}{T}\int_0^T \sigma(t)\dot{e}dt - \frac{1}{T}\int_0^T \dot{W}(t)dt \geq 0. \tag{3.3.5}$$

Denoting by $\sigma_{av} = (1/T)\int_0^T \sigma(s)ds$, the time average shear stress and evaluating the last integral yields,

$$\frac{1}{T}\int_0^T \Phi dt = \sigma_{av}\dot{e} - \frac{W(T)-W(0)}{T} \geq 0. \tag{3.3.6}$$

Since W is bounded above and below in steady shear, the quantity $[W(T)-W(0)]/T$ will be negligibly small for large enough T and so that (3.6) can be approximated by (3.7).

$$\Phi_{av} = \frac{1}{T}\int_0^T \Phi(t)dt = \sigma_{av}\dot{e} \geq 0 \tag{3.3.7}$$

In [21] it is shown that the time averaged dissipation Φ_{av} can be further approximated by

$$\Phi_{av} = \eta\dot{e}^2 + \frac{n}{T}\Delta W \geq 0, \tag{3.3.8}$$

where η is the hydrodynamic viscosity of the suspension, n is the average number of chain snapping episodes occurring in a time interval of length T and ΔW is the time averaged amount of energy released when the chains snap. Thus, the ratio n/T is the average temporal frequency at which the chain snapping episodes occur. Taking e_y as the average critical strain of the chains in the control volume, then the snapping frequency n/T, is simply $|\dot{e}|/e_y$ and so that

$$\Phi_{av} = \sigma_{av}\dot{e} = \eta\dot{e}^2 + \frac{\Delta W}{e_y}|\dot{e}| \geq 0. \tag{3.3.9}$$

Note that the energy release during chain snapping occurs very rapidly so that the energy dissipation for a monolayer can be approximated by a series of delta functions in time. It follows that taking ΔW to be a constant (for constant E) is only valid if the microstructural rearrangements occur on a time scale which is much shorter than the macroscopic time scale, which will be proportional to $1/|\dot{e}|$ (see [38] for a discussion on time scales). It would be expected that the averaged energy release ΔW and the

averaged yield strain e_y would be functions of the electric field strength E. For simplicity in what follows, the ratio $\Delta W/e_y$ will be replaced by a function of the electric field, $r(E) = \Delta W/e_y \geq 0$. The manner in which $r(E)$ might depend on E will be explored in the next section. Now decomposing the average stress σ_{av} into a dissipative component σ^d and a conservative component $\sigma^q = \partial W/\partial e$, the dissipation inequality (3.3.9) can be rewritten

$$\Phi_{av} = \sigma^d \dot{e} + \sigma^q \dot{e} = \sigma^d \dot{e} + r(E)|\dot{e}| \geq 0 \ , \tag{3.3.10}$$

or

$$\Phi_v = \sigma^d \dot{e} = \eta \dot{e}^2 \geq 0 , \tag{3.3.11}$$

$$\Phi_p = \sigma^q \dot{e} = r(E)|\dot{e}| \geq 0 . \tag{3.3.12}$$

where Φ_v is the viscous dissipation and Φ_p will be referred to as the plastic dissipation since it is homogenous of degree one in $\dot{e}$. It follows from the discussions in Section.2 that (3.3.12) implies the existence of a closed convex set $\mathbf{C}$ defined by $\mathbf{C} = [-r(E), r(E)]$. In the discussions above it was assumed that the ER suspension was in steady shear and that the chains were continuously undergoing the process of snapping and reformation. Consider however the case when the activated suspension is initially in a state of zero stress, $\sigma^q = 0$ and hence $W = 0$, and is subsequently subjected to a constant shear rate. In this case all of the chains will have to be brought up to the corresponding critical strain before the process of snapping and reformation can begin. It follows that during this initial loading process, $\sigma^q \in \text{int}\,\mathbf{C}$ and that $\Phi_p = 0$. It is only when σ^q has reached bd$\mathbf{C}$, that there will be plastic dissipation, $\Phi_p > 0$. A similar case occurs when $\sigma^q \in \text{bd}\mathbf{C}$ and the shear rate $\dot{e}$ changes direction. In this case the suspension will initially unload its stored energy before beginning to stretch out in the opposite direction. During this period, $\sigma^q \in \text{int}\,\mathbf{C}$ and hence $\Phi_p = 0$. It is only when σ^q has reached bd$\mathbf{C}$ again (in the opposite direction) that the plastic dissipation will resume. To overcome this singularity in (3.3.12), $\dot{e}$ will be replaced by an internal variable rate $\dot{\alpha}$ and σ^q by its thermodynamic conjugate, A. It follows that $\dot{\alpha} = \dot{e}$ when $\text{A} \in \text{bd}\mathbf{C}$ and $\dot{\alpha} = 0$ when $\text{A} \in \text{int}\,\mathbf{C}$, so that the plastic dissipation can be replaced by ,

$$\Phi_p(\dot{\alpha}) = \sup\{\langle \text{A}, \dot{\alpha} \rangle \mid \text{A} \in \mathbf{C}\} = r(E)|\dot{\alpha}| \geq 0 \tag{3.3.13}$$

(see Lemma 3.2.1 (a) in Section.2) and the total dissipation by ,

$$\Phi(\dot{e},\dot{\alpha}) = \sigma^d \dot{e} + r(E)|\dot{\alpha}| \geq 0 . \qquad (3.3.14)$$

The thermomechanical formulation for this phenomenological model will be made more rigorous in the next section.

3.4 Simple Phenomenological models for ER fluids

In the following sections a number of phenomenological models will be developed for ER suspensions in shear, using the thermomechanical framework of Section.2. The models will be derived on the assumption that the particle and fluid Reynolds numbers are small enough so that inertia forces can be considered negligible (quasi-static's, or Stokesian dynamics in the fluids literature [56]). In addition all deformations are assumed to be isothermal and isochoric (unavoidable in one dimension). The models will be constructed using idealised "linear" rheological elements, along the lines of generalised standard materials, [37]. The primary reason is that this approach will greatly simplify later analysis and allows for the development of closed form, absolutely stable integration algorithms [41]. Due to the rather singular nature of elastic-plastic type models, questions of existence and uniqueness of solutions is quite a bit more complicated than in the smooth case. So as not to complicate the presentation, the required theorems are given in §C.

Simple elastic-plastic model

Consider the case where a fixed electric field has been applied to a static ER suspension (undeformed and stress free). After sufficient time for the suspension chain structure to achieve a steady state has elapsed, a monotonically increasing strain is applied to the movable electrode (at a sufficiently slow rate). At first the response will be predominantly elastic, due to reversible stretching and deformation of the particle chains. In the vicinity of some critical strain, the particle chains will begin the process of breakage and reformation. At this point the storage of mechanical energy will cease and there will be a large increase in the mechanical dissipation. The dissipation can be broken up into two "almost" independent components (3.3.11) and (3.3.12). The first component, which is homogenous of degree two in the strain rate, is due to the shear flow of the base fluid. The second component is positively homogenous of degree one in the shear rate and is due to the continuous process of breakage and reformation of the

electrode spanning chains. In this idealised case the latter component is singular in the sense that it only occurs when the applied strain has reached some critical value.

Now consider the case, where the suspension is already in steady shear and the chains are snapping and reforming continuously. If at some point the strain rate reverses, the chains will cease the process of breakage and reformation and will comove with the fluid until they are once again aligned with the electric field. During this phase the rate independent dissipation will cease and the chains will return the stored elastic type energy, in the form of stress work. Subsequently the chains will stretch out in the opposite direction (storing energy) until they are once again in the vicinity of the critical strain and the process repeats.

The simplest rheological model which captures the basic behaviours described above consists of a series combination of a linear elastic element and a plastic element (EP) in parallel with a linear viscous element Fig 3.10. The case of constant electric field will be considered first, so that the elastic modulus $G > 0$, viscous friction coefficient $\eta_v > 0$, the yield stress $r > 0$ of the friction element, can be considered constant. It is assumed that the model initially possess unit length (and unit area). The system is subject to a total strain e, which can be decomposed into an elastic/reversible strain s across the elastic element and a plastic/irreversible strain α on the friction element.

$$e = s + \alpha \tag{3.4.1}$$

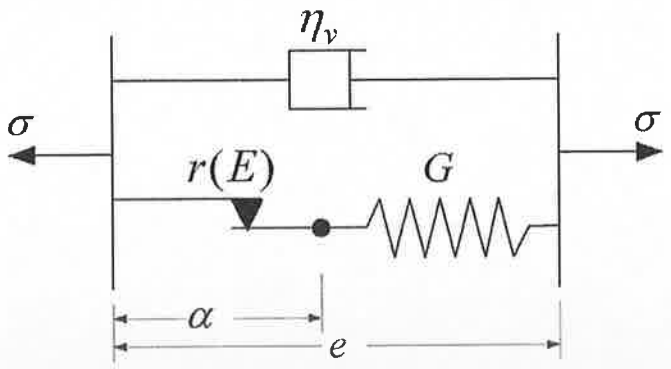

Fig 3.10 Elastic-plastic (EP) model in parallel with linear viscous element

Placed in the thermodynamic framework of Section.2, the total strain e, and total stress σ, take the place of the observable variable χ and its associated force X. Likewise the plastic strain takes the place of the internal variable. From Fig 3.10 it can be seen that the elastic element provides the only means of storing energy, while both the viscous and friction elements can only dissipate energy. It follows that the free energy and the dissipation function describing this model are,

$$W(e,\alpha)=\frac{1}{2}Gs^2=\frac{1}{2}G(e-\alpha)^2, \tag{3.4.2}$$

$$\Phi(\dot{e},\dot{\alpha})=\Phi_v(\dot{e})+\Phi_p(\dot{\alpha})=\eta_v\dot{e}^2+r|\dot{\alpha}|. \tag{3.4.3}$$

Since the viscous component Φ_v, is homogenous of degree two in $\dot{e}$, and the plastic component Φ_p, is positively homogenous of degree one in $\dot{\alpha}$, the corresponding dissipation potential is

$$D(\dot{e},\dot{\alpha})=D_v(\dot{e})+D_p(\dot{\alpha})=\frac{1}{2}\eta_v\dot{e}^2+r|\dot{\alpha}|. \tag{3.4.4}$$

The constitutive equations describing the model can now be obtained from (3.4.2) and (3.4.4) by applying the formula in Table 3.1

$$\sigma^q=\frac{\partial W}{\partial e}=G(e-\alpha),\qquad \sigma^d=\frac{\partial D_v}{\partial \dot{e}}=\eta_v\dot{e},$$
$$\sigma=\sigma^q+\sigma^d, \tag{3.4.5}$$

$$\mathrm{A}=-\frac{\partial W}{\partial \alpha}=G(e-\alpha)=\sigma^q, \tag{3.4.6}$$

$$\mathrm{A}\in\partial D_p=r\partial|\dot{\alpha}|, \tag{3.4.7}$$

Using the inclusion (3.4.7) it is possible to construct the yield function $f(\mathrm{A})=|\mathrm{A}|-r\le 0$, and the closed convex set (closed line segment) of admissible forces $\mathbf{C}=[-r,r]=\{\mathrm{A}\in\Re\,|\,f(\mathrm{A})\le 0\}$. Applying Lemma 3.2.1, the dual plastic potential $D_p^*(\mathrm{A})$, is the indicator function $I(\mathrm{A};\mathbf{C})$ of the convex set $\mathbf{C}$. The evolution equation for α is given by

$$\dot{\alpha}\in\partial D_p^*(\mathrm{A})=N(\mathrm{A};\mathbf{C}). \tag{3.4.8}$$

Using $G\alpha=Ge-\mathrm{A}$, and the definition of the normal cone in (3.2.16), it follows that (3.4.8) is equivalent to the variational inequality , $|\mathrm{A}(t)|\le r,\forall t\ge 0$

$$G\langle\dot{\alpha}(t),\mathrm{A}(t)-\varphi\rangle=\langle G\dot{e}(t)-\dot{\mathrm{A}}(t),\mathrm{A}(t)-\varphi\rangle\ge 0\quad\forall|\varphi|\le r, \tag{3.4.9}$$

with initial condition $\mathrm{A}(0)=\mathrm{A}_0\in r[-1,1]$. In §C.3, it is shown that for each $e\in C^{0,1}(\Re_+;\Re)$ (where $C^{0,1}(\Re_+;\Re)$ is the space if Lipschitz functions $\Re_+\mapsto\Re$), and each initial condition $\mathrm{A}_0\in[-r,r]$, (3.4.9) has a unique solution $\mathrm{A}\in C^{0,1}(\Re_+;\Re)$ (implying existence and uniqueness of α). Due to the assumption that $r>0$, the yield function $f(\mathrm{A})$ is differentiable at $f(\mathrm{A})=0$, so that the evolution equation (3.4.8) can be written as

$$\dot{\alpha} = \lambda \frac{\partial f(\mathrm{A})}{\partial \mathrm{A}} = \lambda \mathbf{n}(\mathrm{A}), \tag{3.4.10}$$

(i.e. $\mathbf{n}(\mathrm{A}) = \mathrm{A}/|\mathrm{A}|$) subject to the complimentary conditions

$$\lambda \geq 0, f \leq 0, \lambda f = 0 \text{ and } \lambda \dot{f} = 0. \tag{3.4.11}$$

The conditions above imply that $\lambda \geq 0$ is permitted only if $f(\mathrm{A}) = 0$ and $\dot{f}(\mathrm{A}) = 0$. Evaluating $\dot{f}(\mathrm{A})$ at $f(\mathrm{A}) = 0$ yields $\dot{f}(\mathrm{A}) = \mathbf{n}(\mathrm{A})G\dot{e} - G\lambda = 0$. Thus, if $\mathbf{n}(\mathrm{A})\dot{e} \leq 0$ then $\lambda = 0$. Similarly if $\mathbf{n}(\mathrm{A})\dot{e} > 0$ then $\lambda = \mathbf{n}(\mathrm{A})\dot{e}$ ensures $\dot{f}(\mathrm{A}) = 0$. Combining the above results, with (3.4.6), yields the discontinuous differential equation

$$\dot{\mathrm{A}} = \begin{cases} 0 & \text{if } |\mathrm{A}| = r \text{ and } \mathrm{A}\dot{e}(t) > 0, \\ G\dot{e}(t) & \text{otherwise.} \end{cases} \tag{3.4.12}$$

In a similar fashion the dissipation (3.4.3) can be written as

$$\Phi = \begin{cases} \eta_v \dot{e}^2 + r|\dot{e}| & \text{if } |\mathrm{A}| = r \text{ and } \mathrm{A}\dot{e}(t) > 0, \\ \eta_v \dot{e}^2 & \text{otherwise,} \end{cases} \tag{3.4.13}$$

which should be compared with (3.3.11), (3.3.12) and the subsequent discussion. To obtain more insight into irreversible behaviour of the model, the loading/unloading behaviour of the elastic-plastic element will be examined in isolation.

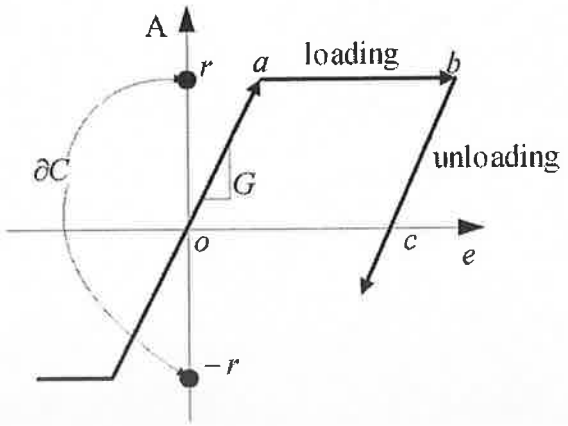

Fig 3.11 Loading-unloading behaviour of the elastic-plastic model

Referring to Fig 3.11, if a positive strain rate is applied to the EP model (initially at (0,0)), the stress will initially increase linearly with e, storing energy in the elastic element. When the strain reaches the point $a = r/G$, (the elastic yield strain), A will be at the boundary of the set $\mathbf{C}$ and equal to $r\,\mathrm{sgn}(\dot{\alpha})$. The system will thus stop storing energy and start dissipating at a rate $\Phi_p = r|\dot{e}|$. If at point b, the strain rate reverses sign, the friction element will lock up and the stress will begin to decrease (unloading) re-entering int $\mathbf{C}$. As the stress decreases back to zero, all of the stored energy will be

restored in the form of stress work. When $A = 0$, the system will have accumulated a plastic strain α, corresponding to the point c. Comparing the above description with that given at the start of this section, it can be seen that the E-P element reproduces the response of the idealized micro-structural model of Section.3. Note that the important difference between the EP element and rheological models of the relaxation type is that the absence of a characteristic time (rate independence), which allows the EP model to sustain a stress in the absence of flow ($\dot{e} = 0$), as apparent in (3.4.12).

Time varying electric field

The next question is, how should a time varying electric field be incorporated into the simple EP model. For the present purposes it will be assumed that the electric field satisfies $E \in C^{0,1}(\Re_+;\Re) \cap [0, \overline{E}]$, where $\overline{E}$ is some positive constant possibly corresponding with the dielectric breakdown of the fluid. The Lipschitz constant for E is assumed to be small enough, so that the corresponding polarization dynamics (chain formation) can be considered as instantaneous and completely reversible.

In addition the purely viscous component of the stress $\eta_v \dot{e}$, will be ignored, since it is assumed to be field independent and can always be added to the model later. That r must be an increasing function of E is obvious, if the dissipation is to match that of the Bingham model. However this does not answer the question since the yield stress can be equivalently defined as $r = Ge_r$. Thus there are two independent quantities available, the elastic modulus G and the elastic yield strain e_r. Unfortunately there is little conclusive evidence to guide the choice. The most popular method for analysing the effect of different levels of electric field on the response of ER fluids, is to subject the fluid to oscillatory shear and use some form of harmonic analysis to calculate the fluid storage and loss moduli, over a range of frequencies, strain amplitudes and field strengths [52]. A common conclusion of such analysis, is that the elastic modulus varies quadraticaly with E, while the strain amplitude at which the fluid response transitions from reversible to irreversible behaviour, remains relatively constant for E greater than some threshold, say E_T, [53][60]. On the other hand, in [61] and [32] it was concluded that the elastic modulus remains constant for E greater that some small threshold E_T, and that it is the yield strain which varies quadraticaly for $E \in [E_T, \overline{E}]$. However, it is difficult to compare those results that are available, due to the differing chemical compositions of the ER suspensions and the different experimental apparatus used.

Furthermore, to make conclusions based on linear harmonic analysis seems a bit dubious given the obvious nonlinear nature of the system. In order to gain some insight, the thermodynamic implications of each choice will be analyzed briefly.

$G \propto E^2$

In this case the observable variables are chosen as the suspension polarization per unit volume P (conjugate to E) and the elastic strain e. The internal variable once again corresponds with the irreversible strain across the plastic element. Using the partial Legendre transform $\overline{W}(e,E,\alpha) = W(e,P,\alpha) - PE$ and inequality (6) of Table 3.1 leads to the dissipation inequality

$$\Phi = \sigma\dot{e} - P\dot{E} - \dot{\overline{W}}(e,E,\alpha) \geq 0 \ , \tag{3.4.14}$$

which yields the state laws,

$$\sigma = \frac{\partial \overline{W}}{\partial e}, P = -\frac{\partial \overline{W}}{\partial E} \quad \text{and} \quad \mathrm{A} = -\frac{\partial \overline{W}}{\partial \alpha}. \tag{3.4.15}$$

Based on (3.3.1) and (3.3.2) a simple choice for $\overline{W}$ is

$$\overline{W}(e,E,\alpha) = -\frac{1}{2}\chi E^2[\delta - (e-\alpha)^2], \tag{3.4.16}$$

where χ and $\delta >> e_r^2$ are suitably dimensioned positive constants. Comparing (3.4.16) with (3.3.1)-(3.3.2) it can be seen that $\chi[\delta - (e-\alpha)^2]$ represents the deformation dependent, averaged capacitance of the suspension (per unit volume). Recalling that the polarization dynamics are assumed to be instantaneous and reversible, a suitable dissipation function is

$$\Phi(\dot{\alpha};E) = D_p(\dot{\alpha};E) = \chi E^2 e_r \mid \dot{\alpha} \mid \geq 0 \ , \tag{3.4.17}$$

(i.e. $G = \chi E^2$), in which the electric field acts as a parameter. The corresponding constitutive equations are as follows,

$$P = -\frac{\partial \overline{W}}{\partial E} = \chi E[\delta - (e-\alpha)^2], \tag{3.4.18}$$

$$\sigma = \frac{\partial \overline{W}}{\partial e} = \chi E^2 (e-\alpha), \tag{3.4.19}$$

$$\mathrm{A} = -\frac{\partial \overline{W}}{\partial \alpha} = \chi E^2 (e-\alpha) = \sigma, \tag{3.4.20}$$

$$\mathrm{A} \in \partial_{\dot{\alpha}} D_p = \chi E^2 e_r \partial|\dot{\alpha}|, \tag{3.4.21}$$

Equation (3.4.21) leads to the definition of the set of admissible stresses $\mathbf{C} = \{\mathrm{A} \in \Re \mid f(\mathrm{A};E) = \mid \mathrm{A} \mid -\chi E^2 e_r \le 0\}$. For the present purposes the constraints on the system are more conveniently defined in terms of a closed convex set of admissible elastic strains $s = (e-\alpha)$, $\mathbf{C}_s = \{s \in \Re \mid f_s(s;E) = \mid s \mid -e_r \le 0\}$. Now following the same reasoning as before, the evolution equation for α is, $\dot{\alpha} \in N(s;\mathbf{C}_s)$ or equivalently $|s(t)| \le r, \forall t \ge 0$

$$\langle \dot{\alpha}(t), s(t)-\varphi \rangle = \langle \dot{e}(t) - \dot{s}(t), s(t)-\varphi \rangle \ge 0 \quad \forall |\varphi| \le e_r, \tag{3.4.22}$$

with initial condition $s(0) \in [-e_r, e_r]$. For this model to make any physical sense, the yield strain e_r must also tend to zero with E, since otherwise the elastic strain would continue to evolve even as $E \to 0$. This issue will be tactfully ignored at present, but can be dealt with using methods presented shortly. Because the model automatically satisfies the dissipation inequality (3.4.14), it is technically, thermodynamically admissible. This is slightly deceiving however as will now be shown. Consider the mechanical strain energy, which is obtained from (3.4.16) as,

$$\overline{W}_m(e,\alpha;E) = \overline{W}(e,E,\alpha) - \overline{W}(0,E,0) = \frac{1}{2}\chi E^2 (e-\alpha)^2, \tag{3.4.23}$$

in which E acts as a parameter. The purely mechanical dissipation inequality,

$$\Phi_m = \sigma \dot{e} - \dot{\overline{W}}_m(e,\alpha;E), \tag{3.4.24}$$

$$\Phi_m = \mathrm{A}\dot{\alpha} - \chi E \dot{E}(e-\alpha)^2 = \chi E^2 e_r |\dot{\alpha}| - \chi E \dot{E}(e-\alpha)^2, \tag{3.4.25}$$

is sign indefinite. In particular, when $|\dot{\alpha}| = 0$ the dissipation will be negative for $\dot{E} > 0$. The consequence of this is that the map $\dot{e} \to \sigma$ is no longer passive, for $\dot{E} > 0$, which is due to the additional energy supply rate $P\dot{E}$ appearing in (3.4.14).

To examine the physical consequences of such behaviour, consider coupling the damped oscillator, $\ddot{x} + 2\dot{x} + x = 0$ with the EP model. Setting $s = (e-\alpha)$, $G = E^2$ and $e_r = 1$ yields

$$\ddot{x} + 2\dot{x} + x + E(t)^2 s = 0\ , \tag{3.4.26}$$

$$\langle \dot{x} - \dot{s}, s - \bar{s} \rangle \ge 0 \quad \forall |\bar{s}| \le 1, \tag{3.4.27}$$

If the initial conditions are taken to be $\dot{x}(0) = 0$, $x(0) = .4$, $s(0) = -.4$, $E(0) = 1$ and $\dot{E}(0) = 0$, the system will be in equilibrium. Now if E is varied according to $E(t) = 1$ for $0 \le t < 2$ and $E(t) = 1 + .2(t-2)$ for $t \ge 2$, the EP model will displace the oscillator,

overcoming the restoring force $-x$, Fig 3.12. While ER fluids may display this form of behaviour, to the author's knowledge experimental evidence has never been reported. Indeed ER fluid dampers are usually regarded as providing a passive or dissipative map between $\dot{e}$ and σ, whose dissipative properties alone can be modulated by varying the electric field strength (see §2.3).

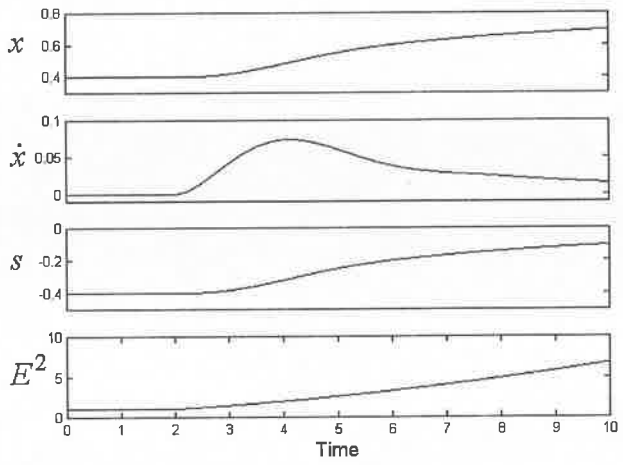

Fig 3.12 Affect of time varying stiffness

Recall that a model with positive definite free energy, W, defines a passive map between $\dot{e}$ and σ if it satisfies the dissipation inequality

$$\sigma\dot{e} - \dot{W} \geq 0. \tag{3.4.28}$$

A sufficient condition for a model to satisfy inequality (3.4.28) is that the free energy depends only on the strain and the internal variables and that the dissipation potential, $D(\dot{e},\dot{\alpha};E)$, is nonnegative, satisfies $D(0,0;E)=0$ and is convex in $\dot{e}$ and $\dot{\alpha}$ uniformly in the electric field, E. This statement can be verified using the formula in Table 3.1

$$\begin{aligned}\sigma\dot{e} - \dot{W} &= \sigma\dot{e} - \frac{\partial W}{\partial e}\dot{e} - \frac{\partial W}{\partial \alpha}\dot{\alpha} \\ &= \sigma^d\dot{e} + \mathrm{A}\dot{\alpha} \\ &= \partial_{\dot{e}} D\dot{e} + \partial_{\dot{\alpha}} D\dot{\alpha} \geq 0\end{aligned} \tag{3.4.29}$$

where non-negativity of the final term follows from the assumption that $D(0,0;E)=0$, the definition of the subdifferential of a convex function in (3.2.15). This will be the approach taken through out the remainder of this chapter.

$G = \text{const}, r \propto E^2$

Consider now the effect of varying e_r in proportion to E^2, while keeping the modulus G constant (once again the purely viscous stress will ignored). Since G is constant, this has the same effect as varying $r(E) = Ge_r(E)$ in proportion to E^2. Referring back to (3.4.2) and (3.4.6) it can be seen that the mechanical free energy and the stress no longer depend explicitly on E. Instead the value of the electric field controls the size of the set of admissible elastic strains $\mathbf{C}_s = [-e_r, e_r]$ and hence the set of admissible stresses, since $\mathbf{C} = G\mathbf{C}_s$. In consequence, the value of E places an upper bound on the available energy storage, equal to $W = Ge_r^2(E)/2 = r^2(E)/2G$. Note however, that the energy itself must be supplied by the environment in the form of stress work. An apparent inconsistency in the model is that in the postyield regime $W = r^2(E)/2G \propto E^4$, however in this case the yield stress can also be written as $r(E) = 2W/e_r(E) \propto E^2$, which should be compared with (3.3.9).

The next step is to formulate the model. Since the purely viscous component can be decoupled from the EP element, it will be ignored with the knowledge that it can be added in later. The free energy and dissipation function are

$$\begin{aligned} W(e,\alpha) &= \frac{1}{2}Gs^2 = \frac{1}{2}G(e-\alpha)^2, \\ \Phi_p(\dot{\alpha};E) &= D_p(\dot{\alpha};r) = r(E)|\dot{\alpha}|. \end{aligned} \tag{3.4.30}$$

The corresponding constitutive equations can be obtained from the differentials of the potentials as follows.

$$\sigma = \frac{\partial W}{\partial e} = G(e-\alpha), \tag{3.4.31}$$

$$\mathrm{A} = -\frac{\partial W}{\partial \alpha} = G(e-\alpha) = \sigma, \tag{3.4.32}$$

$$\mathrm{A} \in \partial_{\dot{\alpha}} D_p = r(E)\partial|\dot{\alpha}|. \tag{3.4.33}$$

Inclusion (3.4.33) and equation (3.4.32) leads to the definition of the time varying set of admissible stresses, $\mathbf{C}(E) = [-r(E), r(E)] = \{\sigma \in \Re \mid f(\sigma;E) = |\sigma| - r(E) \le 0\}$. Using the duality results from Section.2 and equation (3.4.30), the dual dissipation potential is the indicator function $I(\sigma;\mathbf{C}(E))$ of the convex set $\mathbf{C}(E)$ and the evolution equation for α is thus given by

$$\dot{\alpha} \in N(\sigma;\mathbf{C}(E)). \tag{3.4.34}$$

For simplicity in what follows, the field dependent yield stress will be replaced by the time varying composite function $r(t) = r(E(t)) \in [0, \bar{r}], \forall t \in \Re_+$. Using $G\alpha = Ge - \sigma$, and the definition of the normal cone in (3.2.16), it follows that (3.4.34) is equivalent to the variational inequality , $|\sigma(t)| \le r(t), \forall t \ge 0$

$$\langle G\dot{e}(t) - \dot{\sigma}(t), \sigma(t) - \varphi \rangle \ge 0 \quad \forall |\varphi| \le r(t), \tag{3.4.35}$$

with initial condition $\sigma_0 \in [-r(0), r(0)]$. In §C.3, it is shown that for each $e \in C^{0,1}(\Re_+; \Re)$, $r \in C^{0,1}(\Re_+; \Re_+) \bigcap [0, \bar{r}]$ and each initial condition $\sigma_0 \in [-r(0), r(0)]$, (3.4.33) has a unique solution $\sigma \in C^{0,1}(\Re_+; \Re)$.

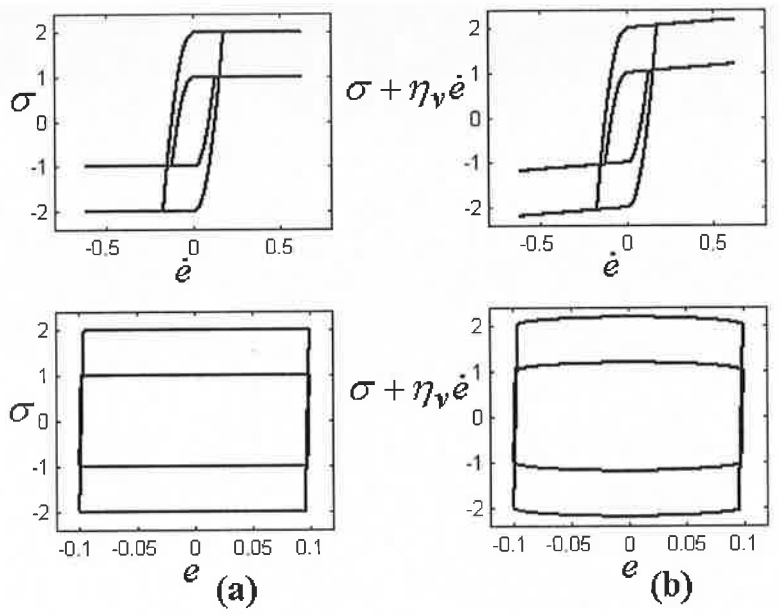

Fig 3.13 (a) Typical stress/strain rate and stress/ strain loops for the system (3.4.34) subject to a sinusoidal strain and for two values of the yield stress, (b) with additional linear viscous term.

Fig 3.13 (a) shows typical stress/strain rate and stress/strain loops for the variational inequality in (3.4.34), when subject to a sinusoidal strain and for two values of the yield stress. Fig 3.13 (b) shows the same loops as Fig 3.13 (a) but with an additional linear viscous term. Comparing Fig 3.13 with Fig 1.3, Fig 2.2 and Fig 3.2 it would appear that the EP model captures the hysteric behaviour of ER/MR fluid dampers for sinusoidal strains and constant electric field. The next step will be to derive the corresponding discontinuous differential equation, which will prove useful in interpreting solutions of the variational inequality (3.4.35).

Unfortunately the procedure used to obtain (3.4.12) cannot be applied, as the yield function $f(\sigma; r(t)) = |\sigma| - r(t) \le 0$, will not be differentiable with respect to σ when

$f(\sigma;r(t))=0$ and $r(t)=0$. However with a bit of extra work it can be seen that the variational inequality (3.4.33) is equivalent to the discontinuous differential equation

$$\dot{\sigma}(t)=\begin{cases}\dot{r}(t) & \text{if } \sigma(t)=r(t) \text{ and } G\dot{e}(t)>\dot{r}(t),\\ -\dot{r}(t) & \text{if } \sigma(t)=-r(t) \text{ and } -G\dot{e}(t)>\dot{r}(t),\\ G\dot{e}(t) & \text{otherwise.}\end{cases} \tag{3.4.36}$$

Note that time derivatives appear on both sides of (3.4.36), implying the evolution of σ is rate independent, with respect to the input e and r. As this controllable EP model, will form a basis for much of the stability analysis in later chapters, it will be worthwhile to give an energetic description of its evolution. From (3.4.231) the free energy can be expressed in terms of σ as $W(\sigma)=\sigma^2/2G$. Rearranging the dissipation inequality $\Phi_p=\sigma\dot{e}-\dot{W}$ and integrating over $[t_0,t]$, yields the integral energy balance

$$\underbrace{W(\sigma(t))-W(\sigma(t_0))}_{\text{Stored}}=\underbrace{\int_{t_0}^{t}\sigma(s)\dot{e}(s)ds}_{\text{Supplied}}-\underbrace{\int_{t_0}^{t}\Phi_p(s)ds}_{\text{Dissipated}}. \tag{3.4.37}$$

When $\sigma(t)\dot{e}(t)>0$ the EP model is receiving energy from the environment (loading) and when $\sigma(t)\dot{e}(t)<0$ energy is being returned to the environment (unloading). An important point is that varying r can only modulate the dissipation when $\dot{\alpha}\neq 0$, (3.4.30) and cannot add energy into the system. This implies that the map $\dot{e}\mapsto\sigma$ is passive, irrespective of variations in r. Furthermore, it places the instantaneous upper bound $W(r(t))=r(t)^2/2G$, on the available energy storage. Thus, using (3.4.34) the dissipation rate can be expresses as

$$\Phi_p(t)=\begin{cases}\sigma(t)\dot{e}(t)-\dot{W}(r(t)) & \text{if } W(\sigma(t))=W(r(t)) \\ & \text{and } \sigma(t)\dot{e}(t)>\dot{W}(r(t)),\\ 0 & \text{otherwise.}\end{cases} \tag{3.4.38}$$

From (3.4.38) it can be seen that dissipation can only occur when the stored energy is at it instantaneous maximum and the rate of energy supply is greater than the rate of change of this maximum. Note that $\sigma(t)\dot{e}(t)>0$ is not required for dissipation to occur. If the system is in the process of unloading ($\sigma(t)\dot{e}(t)<0$), dissipation can still occur if $W(r)$ is decreasing faster than the energy can be extracted by the environment. If $\dot{e}=0$, then the stored energy will be nonincreasing and can in fact be brought to zero in finite time by bringing $W(r)$ to zero (cannot occur infinitely quickly as $r\in C^{0,1}(\Re_+;\Re_+)$). If this is the case then all of the stored energy will be dissipated. In terms of the electrorheological response, the scenario described above might correspond to the

relaxation and eventual disintegration of all the chains that were in tension. It is also conceivable that originally reversible deformations of electrode spanning chains would become irreversible, as the electric field would no longer be strong enough to overcome the particle-particle friction and restore the particles to their original configuration. From a thermodynamic perspective, it could be viewed as a controlled increase in entropy, due to the loss of ability to do useful work on the environment during natural unloading. To ensure that the model is in some way realistic, an important restriction must be placed on the relationship between E and $r(E)$. All of the experimental and numerical analyses cited so far require/indicate that the maximum elastic strain should satisfy $e_r(\overline{E}) = r(\overline{E})/G << 1$.

3.5 Viscoplastic models

The viscous contributions to the "output resistance" of any practical ER device, will be numerous and will to a large extent depend on the type of ER fluid (viscosity, volume fraction etc.) and on the geometry of the device. The relative importance of each contribution will depend on the range of shear rates that the fluid experience's during operation and as such, only those deemed important need be included in the model (to maintain simplicity). For example, as only low to moderate shear rates are expected in the current application (people move relatively slowly) the effects of turbulence, complete degradation of chain structures (loss of yield) due to hydrodynamic forces etc., will not be covered here. The most obvious and probably most dominant viscous contribution to the stress in a shear mode device will be the viscous drag produced on the moving electrode, which has been modelled using the electric field independent term $\eta_v \dot{e}$ in (3.4.6) (η_v is proportional to the base fluid viscosity). Of course, if the assumption of field independence does not coincide with the experimental data, then η_v can be made a function of E (or any of the state variables) without affecting the previous developments. The purpose of this section is to show how additional viscous effects can be easily incorporated into the ER fluid model by considering different forms of dissipation function.

Simple Viscoplastic model

Consider the simple modification of the EP model shown in Fig 3.14, which will be referred to as the viscoplastic model. The reason for incorporating the linear viscous element η_p in the model is to capture the effect of free chains on the system response. Based on the discussions in Section.3, once the process of breakage and reformation begins, there will be a certain distribution of chain segments attached to a single electrode and with no opposing segment in the flow path, with which to connect (free chains). In the presence of sufficient shear rate, it seems reasonable to assume that the free chains will not remain parallel with E , but will tilt in the direction of shear flow.

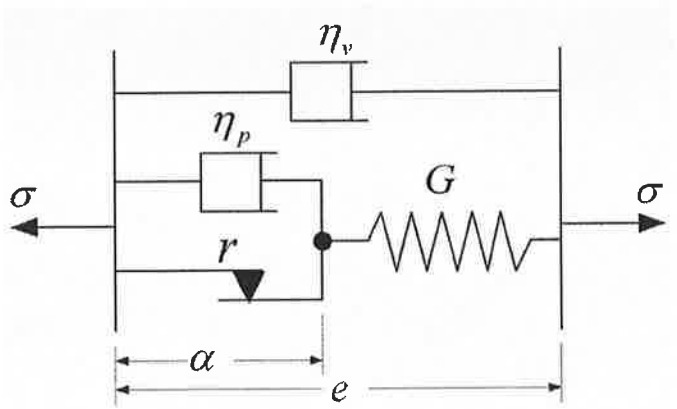

Fig 3.14 Simple viscoplastic model (VP)

The equilibrium angle of the chains would be a competition between the electrostatic forces trying to align the chains with the electric field and the hydrodynamic forces trying align the chain with the shear in the fluid. The chains would thus contribute to the viscous resistance/stress during plastic flow and also to the stored energy (due to misalignment with the field).The presence of these free chains would also account for the relaxation phenomena observed in the response of ER fluid when the imposed strain rate is suddenly brought to zero, [52][53][60].

The model in Fig 3.14 is subject to a total strain e, which can be decomposed into an elastic/reversible strain s across the elastic element and a viscoplastic strain α, which will be used as the internal variable. It will be assumed that the elastic modulus G is constant, the field dependent yield stress $r(E)$ is an increasing function of E, mapping $[0,\overline{E}]$ onto $[0,\overline{r}]$ and that the plastic viscosity $\eta_p(E)$ is also an is an increasing function of E, mapping $[0,\overline{E}]$ onto $[\delta,\overline{\eta}_p]$, for some $\delta > 0$. To simplify the derivation, the shear viscosity η_v will be taken as zero, with the knowledge that it can be added in later.

Now from examination of Fig 3.14, the free energy and dissipation function are given by,

$$W(e,\alpha)=\frac{1}{2}Gs^2=\frac{1}{2}G(e-\alpha)^2, \tag{3.5.1}$$

$$\Phi_{vp}(\dot{\alpha};E)=\eta_p(E)\dot{\alpha}^2+r(E)|\dot{\alpha}|. \tag{3.5.2}$$

The dissipation function the sum of two positively homogenous functions of degree one and two, so that the dissipation potential is given by

$$D_{vp}(\dot{\alpha};E)=\frac{1}{2}\eta_p(E)\dot{\alpha}^2+r(E)|\dot{\alpha}|. \tag{3.5.3}$$

The differentials of the potentials yield

$$\sigma=\frac{\partial W}{\partial e}=G(e-\alpha), \tag{3.5.4}$$

$$\mathrm{A}=-\frac{\partial W}{\partial \alpha}=G(e-\alpha)=\sigma, \tag{3.5.5}$$

$$\mathrm{A}\in\partial_{\dot{\alpha}}D_{vp}=\eta_p(E)\dot{\alpha}+r(E)\partial|\dot{\alpha}|. \tag{3.5.6}$$

Comparing (3.5.5) and (3.5.6) it can be seen that if $\dot{\alpha}=0$, then $\sigma\in\mathbf{C}(E)=[-r(E),r(E)]$. It follows that if $\sigma\in\operatorname{int}\mathbf{C}$, the response is purely elastic, as it was for the EP model. However, if $\dot{\alpha}\neq 0$ then $\sigma=\eta_p(E)\dot{\alpha}+r(E)\mathbf{n}(\dot{\alpha})$ implying that $|\sigma|>r$ and hence $\dot{\alpha}=\eta_p^{-1}\left(\sigma-r(E)\mathbf{n}(\sigma)\right)$. It follows that unlike the EP model, the stress is no longer constrained to take values in the convex set $\mathbf{C}$.Based on the above discussion, the dual potential is easily obtained from the Legendre-Fenchel transform (recall $\sigma=\mathrm{A}$),

$$D_{vp}^*(\mathrm{A};E)=\sup\left\{\mathrm{A}\dot{\alpha}-D_{vp}(\dot{\alpha};E)\mid\dot{\alpha}\in\Re\right\}, \tag{3.5.7}$$

which after a little bit of work yields

$$D_{vp}^*(\mathrm{A};E)=\frac{1}{2\eta_p(E)}\left(P(\mathrm{A};r(E))\right)^2=\frac{1}{2\eta_p(E)}\left(\mathrm{A}-Q(\mathrm{A};r(E))\right)^2, \tag{3.5.8}$$

where $Q(\mathrm{A};r)$ is the projection onto the set $\mathbf{C}=[-r,r]$ and $P(\mathrm{A};r)=\mathrm{A}-Q(\mathrm{A};r)$ (see §A.2 for details). Consequently

$$\dot{\alpha}=\partial_{\mathrm{A}}D_{vp}^*=\frac{1}{\eta_p(E)}P(\mathrm{A};r(E)), \tag{3.5.9}$$

and hence (for simplicity , dropping the dependence on E)

$$\dot{\sigma}=G\dot{e}-\frac{G}{\eta_p}P(\sigma;r)=G\dot{e}-\frac{G}{\eta_p}\left(\sigma-Q(\sigma;r)\right). \tag{3.5.10}$$

The fact that (3.5.10) defines a passive map from $\dot{e}$ to σ follows from (3.5.5) and (3.5.9)

$$\sigma\dot{e} - \dot{W}(e,\alpha) = \mathrm{A}\dot{\alpha} = \frac{1}{\eta_p(E)} P(\sigma; r(E))\sigma \geq 0 \qquad (3.5.11)$$

where non-negativity of the final term in (3.5.11) follows from the definition of the operator P (see §A.2). It should be clear that (3.5.9)-(3.5.10) represents rather regular behaviour in comparison with (3.4.34). Interestingly it can be shown that as $\eta_p \to 0$, the dual potential D_{vp}^* converges to the indicator function of the convex set $\mathbf{C}(E)$ [37] (physically, the viscous element simply disappears). The regularization becomes more apparent when the graph of the dissipation potentials (3.5.3) and (3.5.8) in Fig 3.15, are compared with their plastic counterparts in Fig 3.5 and Fig 3.6. The differentials in Fig 3.15 (b) and (d) should also be compared with the modified Bingham plastic function in Fig 1.5 (b) and (c). Due to the fact that the operator P in (3.5.10) is Lipschitz in both arguments (§A.2), existence and uniqueness of solutions can be obtained using standard results for ordinary differential equations (§C.2). Indeed, suppose the composite functions $r(t) = r(E(t))$ and $\eta_p(t) = \eta_p(E(t))$ satisfy $r \in L_\infty(\Re_+;\Re_+) \bigcap [0, \bar{r}]$ and $\eta_p \in L_\infty(\Re_+;\Re_+) \bigcap [\delta, \bar{\eta}_p]$ respectively. Then for any $e \in C^{0,1}(\Re_+;\Re)$ and any initial condition $\sigma(0) \in \Re$, the differential equation (3.5.10) has a unique solution $\sigma \in C^{0,1}(\Re_+;\Re)$. When compared with the results for the EP model, the significance here is that the requirements on $r(t)$ have been weakened from Lipschitz continuity to measurability. Thus it would appear that the viscoplastic model offers a nice alternative to the EP model. However, for small δ, the differential equation becomes very stiff and much more difficult to handle numerically than the EP model.

Fig 3.16 shows typical stress/strain and stress/strain rate loops for the ordinary differential equation in (3.5.10), when subject to a sinusoidal strain and for two values of the yield stress. Comparing Fig 3.16 with Fig 3.13 (b) it can be seen that the hysteresis loops traced out be the EP and VEP models are almost identical. However, the two models have quite different energy storage and dissipation properties, as will now be shown.

Consider a test at constant electric field and constant shear rate, $\dot{e}(t) = \dot{e}_c > 0$, for $t > 0$, with initial condition $\sigma(0) = 0$. The response of (3.5.10) is given by,

$$\sigma(t)=\begin{cases} G\dot{e}_c t & \text{for} \quad 0\le t\le r/G\dot{e}_c, \\ r+\eta_p\dot{e}_c\left[1-\exp\left(-(t-r/G\dot{e}_c)/\tau\right)\right] & \text{for} \quad r/G\dot{e}_c<t<\infty, \end{cases} \tag{3.5.12}$$

where $\tau=\eta_p/G$ is the characteristic time constant. It follows that the stress $\sigma(t)$ will tend to $r+\eta_p\dot{e}_c$ as $t\to\infty$, implying that the elastic strain and free energy are unbounded functions of the strain rate.

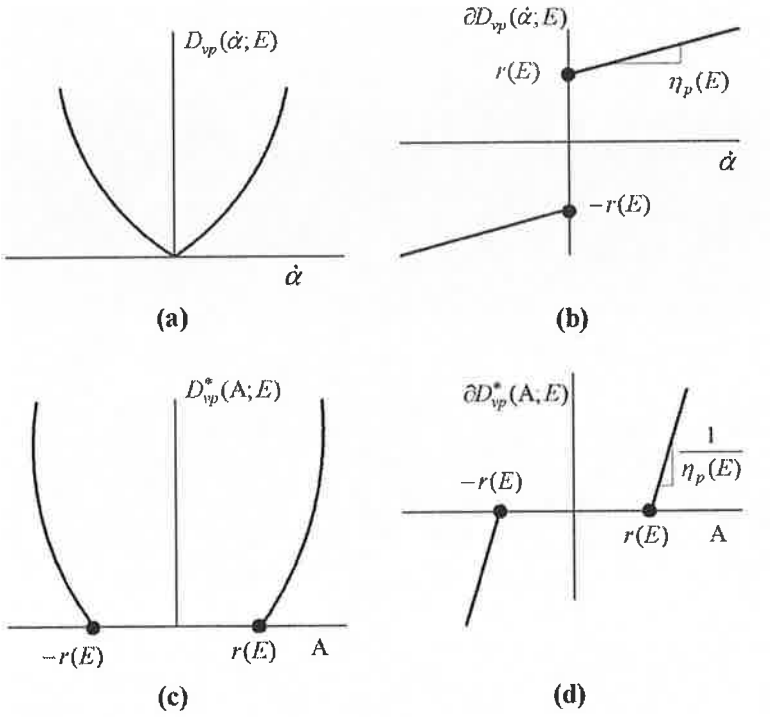

Fig 3.15 Dissipation potentials (3.5.3) and (3.5.8), and the corresponding subdifferential's.

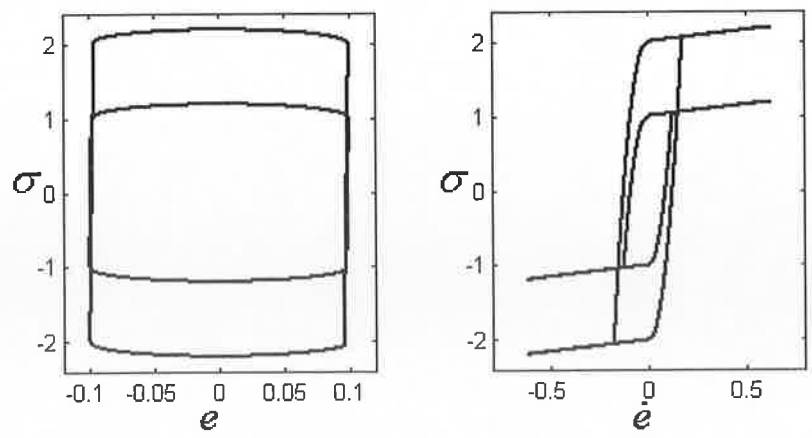

Fig 3.16 Typical stress/strain and stress/ strain rate loops for the system (3.5.10) subject to a sinusoidal strain and for two values of the yield stress.

However as noted earlier, the maximum tilt angle for a chain is 55 degrees, after which neighbouring particles will repel each other (actually for single chains in the point

dipole approximation the critical angle is closer to 21 degrees [53][52]). It would seem reasonable to assume that for sufficiently large shear rate, the free chains would approach this critical angle. The particles at the end of the chains would then fragment, so as to reduce the hydrodynamic forces and allow for better alignment with the electric field. This would imply that the contribution of the viscous element to the total stress should be bounded independently of $\dot{e}$.

As a remedy to this problem, consider the modified viscoplastic model in Fig 3.17.

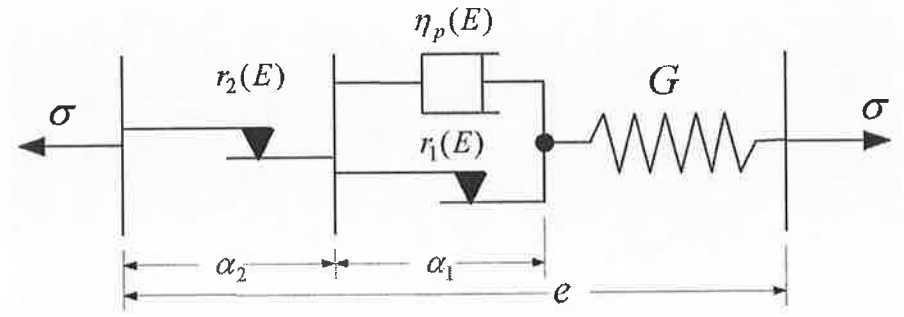

Fig 3.17 Modified viscoplastic model (MVP).

For this model to make any sense it is required that $r_2(E) > r_1(E) \geq 0, \forall E \in [0, \overline{E}]$. This condition can be satisfied trivially by taking $r_1(E) = \rho r_2(E)$, for some positive constant $\rho \in (0,1)$. Unlike previous models, the modified viscoplastic model requires two internal variables to formulate the complete response. Referring to Fig 3.17, the strain across the elastic element is now given by $s = e - \alpha_1 - \alpha_2$, so that the free energy and dissipation function can be written as,

$$W(e,\alpha) = \frac{1}{2}Gs^2 = \frac{1}{2}G(e-\alpha_1-\alpha_2)^2, \tag{3.5.13}$$

$$\Phi_{vp}(\dot{\alpha};E) = \eta_p(E)\dot{\alpha}_1^2 + r_1(E)|\dot{\alpha}_1| + r_2(E)|\dot{\alpha}_2|. \tag{3.5.14}$$

Following the same reasoning as before, leads to the variational inequality $|\sigma(t)| \leq r_2(t), \forall t \geq 0$

$$\left\langle G\dot{e}(t) - \frac{G}{\eta_p(t)}P(\sigma(t);r_1(t)) - \dot{\sigma}(t), \sigma(t) - \varphi \right\rangle \geq 0 \quad \forall |\varphi| \leq r_2(t) \tag{3.5.15}$$

with initial condition $\sigma_0 \in r_2(0)[-1,1]$. Similar to (3.12), the variational inequality the (3.5.15) satisfies the dissipation inequality (confirming passivity)

$$\begin{aligned} \sigma\dot{e} - \dot{W} &= \frac{1}{G}\left\langle G\dot{e} - \frac{G}{\eta_p}P(\sigma;r_1) - \dot{\sigma}, \sigma \right\rangle + \frac{1}{\eta_p}P(\sigma;r_1)\sigma \\ &\geq \frac{1}{\eta_p}P(\sigma;r_1)\sigma \geq 0. \end{aligned} \tag{3.5.16}$$

Note that the variational inequality (3.5.15) can also be written in the form of an ODE coupled with the EP model

$$\dot{x}(t) = \dot{e}(t) - \frac{1}{\eta_p(t)} P(\sigma(t); r_1(t)),$$
$$\langle G\dot{x}(t) - \dot{\sigma}(t), \sigma(t) - \varphi \rangle \geq 0 \quad \forall |\varphi| \leq r_2(t). \tag{3.5.17}$$

so that Corollary C.3.1 can be used to obtain sufficient condition for the existence and uniqueness of solutions.

Model of Gamota and Filisko

As discussed in §1.2 , the authors of [31] presented an extension of the Bingham plastic, formulated in order to describe the viscoelastic behaviour of an ER suspension subject to low amplitude oscillatory strains and the viscoplastic behaviour when subject to oscillations of larger amplitude. The GnF model shown in Fig 3.18, consists of the standard model for viscoelastic solids in series with the Bingham plastic model (plastic element in parallel with a linear viscous element).

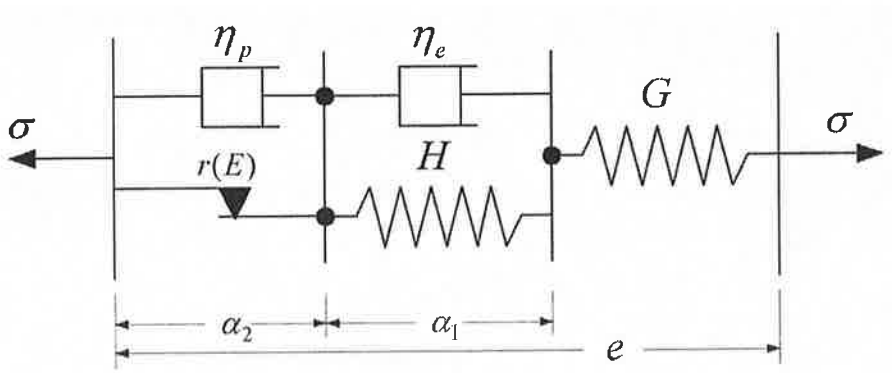

Fig 3.18 The model of Gamota and Filisko (GnF)

In [32] the model parameters were fit to the experimental data obtained from an ER suspension subject to oscillatory shear. The elastic moduli G and H were found to be independent of the electric field, while the viscosities η_e, η_p and the yield stress r were found to be increasing functions of E, with $r \propto E^2$. The constitutive equations describing this model will be derived briefly using the present thermodynamic framework. It will be assumed that the elastic moduli G and H are constant, the field dependent yield stress $r(E)$ is an increasing function of E, mapping $[0, \overline{E}]$ onto $[0, \overline{r}]$ and that the viscosities $\eta_e(E)$ and $\eta_p(E)$ are also increasing functions of E, mapping $[0, \overline{E}]$ onto $[\delta, \overline{\eta}_e]$ and $[\delta, \overline{\eta}_p]$ respectively, for some $\delta > 0$. The free energy and dissipation function are given by

$$W(e,\alpha)=\frac{1}{2}G(e-\alpha_1-\alpha_2)^2+\frac{1}{2}H\alpha_1^2, \tag{3.5.18}$$

$$\Phi(\dot{\alpha};E)=\eta_e(E)\dot{\alpha}_1^2+\eta_p(E)\dot{\alpha}_2^2+r(E)|\dot{\alpha}_2|\geq 0, \tag{3.5.19}$$

and the corresponding dissipation potentials,

$$\begin{aligned} D(\dot{\alpha};E)&=\frac{1}{2}\eta_e(E)\dot{\alpha}_1^2+\eta_p(E)\dot{\alpha}_2^2+r(E)|\dot{\alpha}_2|,\\ D^*(\mathrm{A};E)&=\frac{1}{2\eta_e(E)}\mathrm{A}_1^2+\frac{1}{2\eta_p(E)}\left(P(\mathrm{A}_2;r(E))\right)^2. \end{aligned} \tag{3.5.20}$$

Taking the differentials of the potentials then provides

$$\sigma=\frac{\partial W}{\partial e}=G(e-\alpha_1-\alpha_2), \tag{3.5.21}$$

$$\mathrm{A}_1=-\frac{\partial W}{\partial \alpha_1}=G(e-\alpha_1-\alpha_2)-H\alpha_1=\sigma-H\alpha_1, \tag{3.5.22}$$

$$\mathrm{A}_2=-\frac{\partial W}{\partial \alpha_2}=G(e-\alpha_1-\alpha_2)=\sigma, \tag{3.5.23}$$

and the evolution equations

$$\begin{aligned} \dot{\alpha}_1&=\partial_{\mathrm{A}1}D^*=\frac{1}{\eta_e(E)}\mathrm{A}_1,\\ \dot{\alpha}_2&=\partial_{\mathrm{A}2}D^*=\frac{1}{\eta_p(E)}P(\mathrm{A}_2;r(E)). \end{aligned} \tag{3.5.24}$$

Combining (3.5.21)-(3.5.24) yields the nonautonomous ordinary differential equation (using the composite functions $\eta_e(t)=\eta_e(E(t))$, $\eta_p(t)=\eta_p(E(t))$ and $r(t)=r(E(t))$)

$$\begin{aligned} \dot{\sigma}&=G\dot{e}+\frac{G}{\eta_e(t)}\left(H\alpha_1-\sigma\right)-\frac{G}{\eta_p(t)}P(\sigma;r(t)),\\ \dot{\alpha}_1&=\frac{1}{\eta_e(t)}\left(\sigma-H\alpha_1\right). \end{aligned} \tag{3.5.25}$$

which should be compared with the representation in equation (1.2.4). Unlike the previous models, all motions of the GnF model are dissipative, due to the addition of η_e. Using equations (3.5.18) and (3.5.21) the free energy can be written as

$$W(\sigma,\alpha_1)=\frac{1}{2}\sigma^2+\frac{1}{2}H\alpha_1^2, \tag{3.5.26}$$

which leads to the dissipation inequality

$$\begin{aligned} \sigma\dot{e}-\dot{W}(\sigma,\alpha_1)&=\frac{1}{\eta_p}P(\sigma;r)\sigma+\frac{1}{\eta_e}\left(\sigma^2-2H\alpha_1\sigma+H^2\alpha_1^2\right),\\ &=\frac{1}{\eta_p}P(\sigma;r)\sigma+\frac{1}{\eta_e}\left(\sigma-H\alpha_1^2\right)^2\geq 0, \end{aligned} \tag{3.5.27}$$

thus confirming passivity of the GnF model. As noted in §1.2, the main criticism of the GnF model given in is that the system differential equations are extremely stiff (due to the plastic element) making it unsuitable for use in simulation studies, due to the small time steps required. However recent advances in numerical integration algorithms for plasticity based constitutive equations means that this is no longer a problem. Indeed, applying the projection based integration methods described in [41], leads to a closed form integration algorithm capable of producing more than sufficient results with a time step three orders of magnitude larger than those required in [23].

All of the models presented so far exhibit a transition between elastic/viscoelastic and plastic flow which is instantaneous. Based on the discussions in sections one and three, it would be expected that the onset of plastic flow would be more gradual. That is, for an applied monotonic strain, the thinner/weaker chains will begin to snap and reform first followed by the snapping of thicker chains until eventually fully developed plastic flow is achieved. One method of representing this form of behaviour, is to include additional plastic elements, with different yield stresses into the model. Referring back to Fig 3.18, an additional friction element could be placed in parallel with η_e and H. Then an additional "layer" of viscous, elastic and plastic elements could be placed in series with these, until N "layers" have been incorporated. Each layer would have its own internal variable, which would begin to evolve when the stress had exceeded threshold on the corresponding plastic element. In this way the transition from viscoelastic to plastic behaviour can be broken down into a finite number of steps, through a suitable choice of parameter values. The actual number required would depend on the desired smoothness of the transition. The model described above does not lend itself to obvious interpretation in terms of the inner workings of an ER fluid. However the dual of this model, obtained by arranging a finite number of elementary models (i.e. EP) in parallel allows for a simple interpretation and as such will be taken up next.

3.6 A Multiple element model

As noted previously, the main drawback of the models presented so far is that for fixed electric field, the transition between elastic and plastic flow is instantaneous. In a "real" ER fluid one would expect the transition to be more gradual, implying the simultaneous

occurrence of both elastic and plastic deformation. Consider the situation where an electric field is applied to a fluid initially at rest (no flow, stress free), at a rate sufficiently slow so that viscous effects can be ignored. Suppose that after sufficient time for chain formation has elapsed, an increasing strain is applied to the movable electrode, at a rate sufficiently slow so that viscous effects can be ignored. At first the response would be predominantly elastic due to reversible stretching and deformation of electrode spanning particle chains. There would also be some irreversible deformation of the chains (plastic response), due to the friction experienced by particles as they slide over one another during the deformation. As the strain increases further, the irreversible deformations would also increase and would be accompanied by the snapping and reformation of weaker particle chains (see Section.3). Further increase in the strain will cause more and more of the chains to begin the process of rupture and reformation, decreasing the ratio of reversible to irreversible deformation. This process would continue with increasing strain until the effective elastic response had disappeared and fully developed plastic flow is achieved.

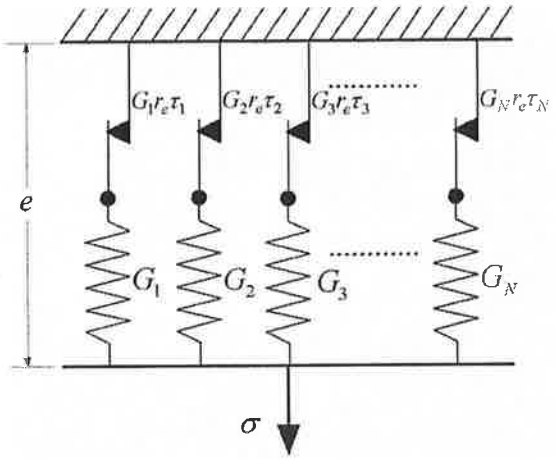

Fig 3.19 Generalized elastic plastic model Π(EP)

One approach to modelling such behaviour is to combine a finite number of elastic-plastic models in parallel, Fig 3.19. The total strain across each of the elements is the same and the total stress is the sum of the stresses on the individual springs. Each element has a constant elastic modulus $G_i > 0$ and a field dependent yield strain $e_r(E)\tau_i$. The sequence $\{\tau_i\}$ is assumed to satisfy $0 = \tau_o < \tau_1 < \tau_2 ..... < \tau_N < \infty$ with uniform partition $\Delta\tau = \tau_i - \tau_{i-1}$ for all $i = 1,2,\cdots,N$. It will also be assumed that $e_r(E)$ is an increasing function of the electric field mapping $[0,\overline{E}]$ onto $[0,\overline{e}_r]$ and that the composite function $e_r(t) = e_r(E(t))$ is Lipschitz continuous. Using this model it will be possible to break up the transition from elastic to purely plastic flow into a finite

number of steps. In the literature on hysteresis operators this sort of model is usually referred to as the Prandtl-Ishlinskii model (of the stop type) [67][68], however in what follows it will simply be referred to as the $\prod$(EP) model.

The free energy and dissipation function for a model consisting of N (EP) elements are simply,

$$W(e,\alpha)=\frac{1}{2}\sum_{i=1}^{N}G_i(s_i)^2=\frac{1}{2}\sum_{i=1}^{N}G_i(e-\alpha_i)^2, \tag{3.6.1}$$

$$\Phi(\dot{\alpha};E)=\sum_{i=1}^{N}\Phi_i(\dot{\alpha}_i;E)=\sum_{i=1}^{N}G_i e_r(E)\tau_i\,|\,\dot{\alpha}_i\,|\geq 0\,. \tag{3.6.2}$$

where $\alpha=[\alpha_1,\alpha_2,\ldots,\alpha_N]^{\mathrm{T}}$ is the vector of internal variables, corresponding with the strains across the individual plastic elements. Since the dissipation function is homogenous of first order in the internal variable rates, the individual dissipation potentials satisfy $D_i(\dot{\alpha}_i;E)=\Phi_i(\dot{\alpha}_i;E)$. Now taking differentials of the potentials yields,

$$\sigma=\frac{\partial W}{\partial e}=\sum_{i=1}^{N}G_i(e-\alpha_i)=\sum_{i=1}^{N}G_i(s_i), \tag{3.6.3}$$

$$\mathrm{A}_i=-\frac{\partial W}{\partial \alpha_i}=G_i(e-\alpha_i)=G_i s_i, \tag{3.6.4}$$

$$\mathrm{A}_i=\partial D_i=G_i e_r(E)\tau_i\partial|\dot{\alpha}_i|. \tag{3.6.5}$$

Applying Lemma 3.2.1, the dual dissipation potential is simply $D^*(\mathrm{A};E)=\sum_1^N I(\mathrm{A}_i;\mathbf{C}_i(E))$, where $I(\mathrm{A}_i;\mathbf{C}_i(E))$ is the indicator function of the convex set $\mathbf{C}_i(E)=\{\mathrm{A}_i\in\Re\,|\,f_i(\mathrm{A}_i;e_r(E))=|\mathrm{A}_i|-G_i e_r(E)\tau_i\leq 0\}$. The evolution equation for $\dot{\alpha}_i$ is given by

$$\dot{\alpha}_i\in N(\mathrm{A}_i;\mathbf{C}_i(E)). \tag{3.6.6}$$

Using (3.6.4) and the definition of the normal cone in (3.2.16), it follows that (3.6.6) is equivalent to a family of N variational inequalities (in terms of the composite function $e_r(t)=e_r(E(t))$), $|s_i(t)|\leq e_r(t)\tau_i,\forall t\geq 0$

$$\langle\dot{e}(t)-\dot{s}_i(t),\dot{s}_i(t)-\varphi_i\rangle\geq 0\quad\forall|\varphi_i|\leq e_r(t)\tau_i \tag{3.6.7}$$

with initial condition $|s_i(0)|\leq e_r(0)\tau_i$. Applying the results in §C.3, it follows that for each $e\in C^{0,1}(\Re_+;\Re)$, $e_r\in C^{0,1}(\Re_+;\Re_+)\bigcap[0,e_r]$, each of the N variational inequalities

has a unique solution $s_i \in C^{0,1}(\Re_+;\Re)$. Define the total initial stiffness $G_T = \sum_1^N G_i$ and the stiffness ratio $\beta_i = G_i/G_T$, so that $\sum_1^N \beta_i = 1$. The total stress in (3.6.3) can now be rewritten as,

$$\sigma = G_T\left(e - \sum_{i=1}^{N} \beta_i \alpha_i\right) = G_T \sum_{i=1}^{N} \beta_i s_i . \tag{3.6.8}$$

The i[th] element can be interpreted as representing all the chains with yield strain $e_r(E)\tau_i$, while β_i can be interpreted as representing the total fraction (per unit volume) of chains with yield strain $e_r(E)\tau_i$. Passivity of the model (3.6.7)-(3.68) follows from the fact that each the individual EP elements define passive maps from $\dot{e}$ to s_i (see (3.4.37)). An important practical question is the possibility of identifying G_T and the individual β_i from physical experiments. Consider applying a fixed electric field $(\dot{e}_r(\cdot) = 0)$ to a static control volume of ER fluid (as in Section.3) and assume that $e(t)$ increases slowly on $\Re_+$ from initial condition $e(0) = 0$. It may be possible to model the stress response model using a memoryless function of the applied strain, $\sigma = L(e)$. In solid mechanics $L(e)$ is often referred to as the initial loading curve [37]. For simplicity it will be assumed that $L \in C^{1,1}(\Re_+;\Re_+)$ is an increasing, concave function (softening) satisfying $L(0) = 0$ and $\lim_{e\to\infty} L(e) < \infty$. Once a parameterization of $L(e)$ has been obtained for a given E (either in parametric form or from experimental data), the total yield stress and initial stiffness can be obtained from,

$$r(E) = \lim_{e\to\infty} L(e), \quad G_T = \left.\frac{dL(e)}{de}\right|_{e=0} . \tag{3.6.9}$$

To simplify developments, set $e_r(E) = r(E)/G_T$, which corresponds with the yield strain for single EP element with yield stress $r(E)$ and elastic modulus G_T. It follows that in fully developed plastic flow (all elements yielding)

$$r(E) = G_T e_r(E)\sum_{i=1}^{N} \beta_i\tau_i = r(E)\sum_{i=1}^{N} \beta_i\tau_i \;\Rightarrow\; \sum_{i=1}^{N} \beta_i\tau_i = 1. \tag{3.6.10}$$

Now, for fixed $e_r(E) > 0$, assume that $e(t)$ increases slowly on $\Re_+$ from initial condition $e(0) = 0$ and that $s_i(0) = 0, \forall i = 1,\ldots,N$. The response of each (E-P) element will be given by

$$s_i(t) = \min(e(t), e_r\tau_i), \quad i = 1,\ldots,N , \tag{3.6.11}$$

so that the total stress response can be written as

$$\sigma(t) = L(e(t)) = G_T e(t) \sum_{i=n+1}^{N} \beta_i + G_T e_r \sum_{i=1}^{n} \beta_i \tau_i \quad \text{for} \quad e(t) \in e_r[\tau_n, \tau_{n+1}), \tag{3.6.12}$$

A simple least square method for identifying the individual β_i so as to accurately approximate the smooth loading curve $L(e)$ is easily deduced. It is also possible to extend the $\prod$(EP) so as to include an infinite number of EP elements, this model is referred to as the continuous $\prod$(EP). As an example, in [69] the authors proposed the phenomenological relation in (3.6.13) as a response for an ER fluid subject to monotonic shear, i.e. $e, \dot{e} \geq 0$.

$$\sigma = r(E)(1 - \exp(-G_T e / r(E)) + \eta \dot{e} \tag{3.6.13}$$

where G_T is the constant shear modulus and $r(E)$ is the field dependent yield stress. To simplify maters the linear viscosity η will be ignored for the present. Now it can easily be seen that (3.6.13) saturates to $\sigma = r(E)$ as $e \to \infty$, so the domain of τ is $\Re_+$. Using $e_r(E) = r(E)/G_T$, the stress-strain relation in (3.6.13) can be written as $\sigma = G_T e_r(1 - \exp(-e/e_r))$, from which it can be seen that e_r plays the role of a space constant (as opposed to a time constant), governing the rate of saturation with increasing e. Setting $L(e) = G_T e_r(1 - \exp(-e/e_r))$ for $e \in [0, \infty)$, it can be seen that $L(e)$ is increasing and concave as required. Fig 3.20(a) shows a single (clockwise) stress-strain loop for the simple EP model and the continuous $\prod$(EP) obtained from the loading curve (3.6.13). Fig 3.20 (b) shows the stress-strain loop for a 5 element approximation of the continuous $\prod$(E-P) model. While the E-P model predicts a very unrealistic instantaneous transition between elastic and plastic behaviour, the continuous $\prod$(EP) model predicts a smooth, asymptotic transition (the elastic modulus used in the simulations is unrealistically small and was used simply to illustrate the effects more clearly). Examination of Fig 3.20(b), shows that even using 5 elements, the improvement over the EP model is quite considerable.

At this stage two important (though probably obvious) remarks need to be made. For fixed E, the shape of the hysteresis loops in Fig 3.20 are independent of the rate at which they are traversed. Also, for monotonic loading nothing distinguishes the continuous $\prod$(EP) from a nonlinear elastic solid with the same $L(e)$. It is only when unloading, after a change in sign of the strain rate, that the irreversible/plastic behaviour will become apparent.

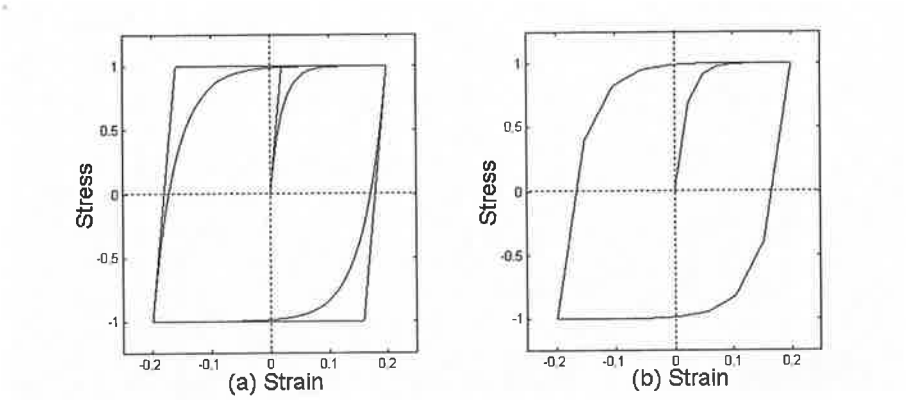

Fig 3.20 Stress-strain loop for (a) EP model and continuous ∏(EP) model, (b) 5 element approximation to continuous ∏(EP).

Fig 3.21(b) and (c) show the hysteresis loops generated by the EP model and a 20 element ∏(EP) model, for a fixed electric field and a sinusoidal strain with monotonically increasing amplitude Fig 3.21 (a). Fig 3.22 shows the responses of the two models to a sinusoidal applied strain $e = A\sin(2\omega t)$ and a time varying yield strain $r(E) = B + C\sin(\omega t)$. While a model consisting of twenty or more EP elements may seem overly complicated and inefficient for control implementation or simulation, the actual integration algorithms are remarkably simple, accurate and absolutely stable [41].

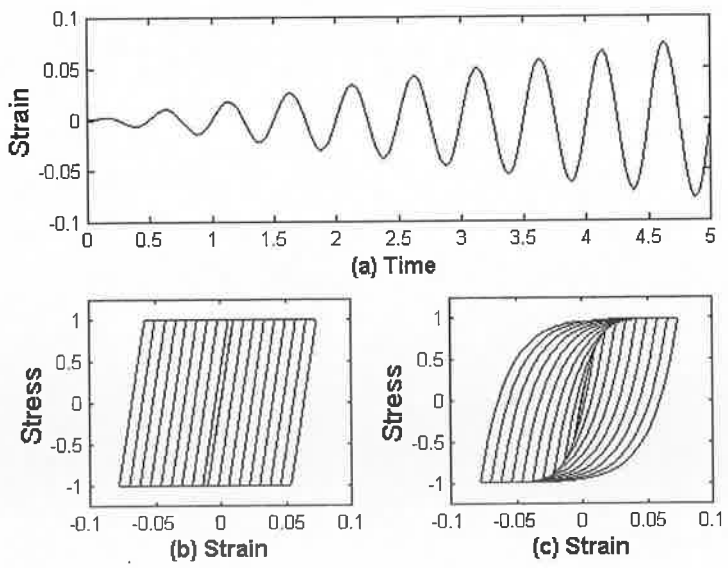

Fig 3.21 (a) Applied strain time history , (b) stress strain loops generated by EP model, (c) stress strain loops generated by 20 element ∏(EP).

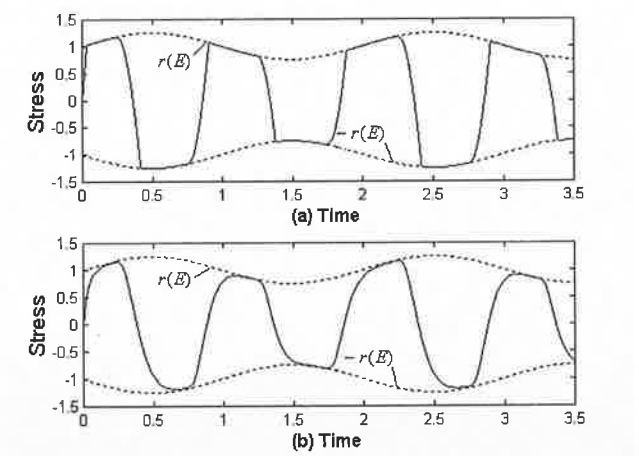

Fig 3.22 Response of (a) E-P model and (b) 20 element ∏(EP) model to a sinusoidal strain and a time varying yield strain.

Note that all of the models presented above define a passive mapping between $\dot{e}$ and σ, even in the presence of a time varying electric field. It was noted previously, that this is a consequence of the fact that the electric field does not appear as a variable in the free energy, only as a parameter in the dissipation potential. Its overall effect is to control the size of the set of admissible reversible strains, thus placing an upper bound on the achievable dissipation rate and on the available energy storage.

3.7 Summary

The primary purpose of this chapter was to demonstrate that the well-known method of "thermomechanics with internal variables" provides an intuitive and systematic approach for modelling the mechanical behaviour of shear mode ER fluid dampers.

The chapter begins with a brief review of some of the present approaches for the modelling of ER dampers/fluids. It was shown that some of these approaches can produce models which do not define a passive map between the imposed velocity and the predicted damper resistance. Not only can this form of non-passive behaviour lead to strange results when performing qualitative analysis on the models, it can also lead to unrealistically good results in simulation studies of vibration or disturbance control. The basic mechanisms believed to govern the ER effect were then reviewed. The interest in these mechanisms is not to predict the force levels or parameters values, but to gain some insight into the energy storage and dissipation properties of an ER fluid in shear.

A simplified version of the theory of "thermomechanics with internal variables" was then presented along with the necessary tools from convex analysis. Through the use of examples, it was shown that a simple and intuitive approach to applying the theory is first construct a phenomenological model, using idealised rheological elements such as springs and friction elements, which conceptually captures the mechanical behaviour of a given damper. This model is used to construct two functions, the free energy and the dissipation function, which represent the energy stored by the rheological elements and the rate at which energy is dissipated by the elements respectively. Applying a systematic procedure to these two functions, one then obtains an evolution equation for the phenomenological damper model.

It is also shown that if the electric field (control variable) appears only as a parameter in the dissipation function, the resulting model will automatically define a passive map from the imposed velocity to the resulting force. In terms of rheological elements this results states that the stiffness coefficients of the springs should be independent of the electric field, while the nonnegative viscous coefficients and yield stresses associated with dashpots and friction elements respectively, are allowed to depend on the electric field. A number of simple elastic-plastic and viscoplastic type models were then presented, all of which follow this caveat.

It was noted that the main drawback of these simple models is that for fixed electric field, the transition between preyield and postyield behaviour is instantaneous. In a "real" ER fluid one would expect the transition to be more gradual. It was shown that one approach to modelling such behaviour is to combine a finite number of simple models in parallel. Using this approach it will be possible to break up the transition preyield to postyield behaviour into a finite number of steps.

Sufficient conditions for establishing existence and uniqueness of solutions for each of the damper models were also presented. The proofs for these results are contained in Appendix C. In the present literature on ER and MR fluids, little or no attention is paid to questions of existence and uniqueness of solutions of damper models. This is surprising, as many of the models which have been proposed are highly nonlinear and often discontinuous.

Chapter 4

Stability Analysis

The primary focus of the present chapter is the qualitative analysis of a simple second order oscillator from §2, coupled with the controllable EP model from §3. The system is defined by the ordinary differential equation and variational inequality

$$\Sigma\begin{cases}\Sigma_X\begin{cases}\dot{x}_1 = x_2\\ \dot{x}_2 = -Rx_2 - Kx_1 - h(x_1) - z + b(t)\end{cases}\\ \Sigma_Z\begin{cases}\langle Gx_2 - \dot{z}, z - \varphi\rangle \geq 0, \quad \forall |\varphi| \leq r(t),\\ |z(t)| \leq r(t), \quad \forall t \geq 0.\end{cases}\end{cases}$$

where x_1 and x_2 represent the position and velocity of the oscillator and z represents the damper reaction force. The time dependent variables $r(t)$ and $b(t)$ represent the controllable yield force associated with the damper and a bounded disturbance (tremor). The reasons for focusing on the EP model, over the other, possibly more realistic damper models developed in §3, are twofold. First the EP model is relatively simple and as such, easier to analyse. However, when viewed as the model of a controllable damper, the EP model has some rather undesirable input-output properties, not present in more complex models, making it a sort of worst case scenario.

Section 4.1, first develops the model presented above. Following this, some basic internal and external stability results are established for Σ. Section 4.2 focuses on the internal stability properties of the coupled system (i.e. $b(\cdot) \equiv 0$). The section begins with a review of some know results for semi-active dampers. Finding these results to be inadequate for the present purposes, the notion of a OT-recurrent control is developed. Section 4.3 analyses the possibility of "linearizing" the response of the EP model through a "feedforward" control. An outgrowth of the analysis is the novel concept of dissipation shaping. In some sense, the dissipation shaping control can be seen as a form of model reference control, in which the response of the EP model is forced to track the response of a more desirable rheological model.

4.1 Basic stability analysis

The first thing to do is to couple the forearm model given by equation (2.2.8)

$$\Sigma_X \begin{cases} \dot{x}_1 = x_2 \\ \dot{x}_2 = -Rx_2 - Kx_1 - h(x_1) + b(t) + F(t). \end{cases} \tag{4.1.1}$$

with the controllable EP model defined by equation (3.4.35), $|\sigma(t)| \le r(E(t)), \forall t \ge 0$

$$\langle G\dot{e}(t) - \dot{\sigma}(t), \sigma(t) - \varphi \rangle \ge 0 \quad \forall |\varphi| \le r(E(t)) \quad \text{for a.e. } t > 0. \tag{4.1.2}$$

The ER damper is assumed to be of the rotary couette type and that the axis of the rotor is located at the elbow. For simplicity it is assumed that the shear strain can be approximated by $e = x_1$ and the reactive torque by $-F(t) = \sigma/J =: z$. Setting $e = x_1$, the purely viscous contribution of the damper force can simply be absorbed in to the damping coefficient R, in (4.1.1). It is assumed that the yield stress (torque) $r(E)$ is a known, increasing function of the controllable electric field $E(t)$ that maps $[0, \bar{E}]$ onto $[0, \bar{r}]$, where $\bar{E}$ is the maximum electric field level. To simplify notation in what follows, only the composite function $r(t) = r(E(t))$ will be used. Now, absorbing the inertia J into the elastic modulus G and the controllable yield stress $r(t)$ yields the coupled system

$$\Sigma \begin{cases} \Sigma_X \begin{cases} \dot{x}_1 = x_2 \\ \dot{x}_2 = -Rx_2 - Kx_1 - h(x_1) - z + b(t) \end{cases} \\ \Sigma_Z \begin{cases} \langle Gx_2 - \dot{z}, z - \varphi \rangle \ge 0, \quad \forall |\varphi| \le r(t), \\ |z(t)| \le r(t), \quad \forall t \ge 0. \end{cases} \end{cases} \tag{4.1.3}$$

with state vector $x_a = (x, z)$. Recall that the nonlinear function $h : \Re \mapsto \Re$ satisfies $h(0) = 0$ and the inequality

$$0 \le \big(h(x_1) - h(y_1), x_1 - y_1\big) \le L(x_1 - y_1)^2. \tag{4.1.4}$$

Using inequality (2.2.13) it follows that for initial conditions $x(0) \in \Re^2$ and $|z(0)| \le r(0)$, any solution of Σ will satisfy $|z(t)| \le r(t) \le \bar{r}$ and

$$|x(t)| \le \beta |x(0)| e^{-ct} + \gamma \big(\|b\|_\infty + \bar{r} \big) \big(1 - e^{-ct} \big), \tag{4.1.5}$$

for some constants $\beta, \gamma, c > 0$. Based on (4.1.5) and corollary C.3.1, one obtains the following existence and uniqueness result. Let $b(t)$ and $r(t)$ be given functions such that $b \in C^{0,1}(\Re_+; \Re)$, $|b(t)| \le \bar{b}, \forall t \ge 0$ and $r \in C^{0,1}(\Re_+; \Re_+)$, $r(t) \le \bar{r}, \forall t \ge 0$. Then for each

set of initial conditions $x(0) \in \Re^2$ and $|z(0)| \le r(0)$, Σ has a unique solution $x_a(t; x_a(0), r(\cdot), b(\cdot)) = (x(t; x_a(0), r(\cdot), b(\cdot)), z(t; x_a(0), r(\cdot), b(\cdot)))$ such that $x \in C^{1,1}(\Re_+; \Re^2)$ and $z \in C^{0,1}(\Re_+; \Re)$. Moreover, the solution depends continuously on the initial conditions $x_a(0)$ and the functions $r(t), b(t)$. When this dependence is clear $x_a(t) = (x(t), z(t))$ will be used to refer to the state of Σ at time $t \ge 0$.

Having established existence and uniqueness of solutions, the next step is to look at the qualitative behaviour of Σ. A natural starting point is to obtain some expressions relating to the energy flow in the system. The reader is referred back to §2.3 for the required definitions. In §2.3 it was shown that Σ_X defines a passive, finite gain map $(b - z) \mapsto x_2$, with natural storage function and energy balance

$$H_X(x) = \frac{1}{2}(x_2^2 + Kx_1^2) + \int_0^{x_1} h(s)ds, \tag{4.1.6}$$

$$H_X(x(t)) - H_X(x(0)) + \int_0^t Rx_2^2(s))ds = -\int_0^t z(s)x_2(s)ds + \int_0^t b(s)x_2(s)ds. \tag{4.1.7}$$

By construction Σ_Z defines a passive map $x_2 \mapsto z$ with natural storage function and energy balance (see equation (3.4.37))

$$H_Z(z) = \frac{1}{2G}z^2, \tag{4.1.8}$$

$$H_Z(z(t)) - H_Z(z(0)) + \int_0^t \Phi(s)ds = \int_0^t z(s)x_2(s)ds. \tag{4.1.9}$$

The function $\Phi(t) = \Phi(z(t), x_2(t); r(t))$ is the nonnegative dissipation function, given by (see (3.4.38))

$$\Phi(z, x_2; r(t)) = \begin{cases} x_2 z - \dot{H}_Z(r(t)) & \text{if } H_Z(z) = H_Z(r(t)) \\ & \text{and } x_2 z > \dot{H}_Z(r(t)), \\ 0 & \text{otherwise,} \end{cases} \tag{4.1.10}$$

where $H_Z(r(t)) = r(t)^2/2G$ places an instantaneous upper bound on the energy which can be stored by (and hence extracted from) Σ_Z. In (4.1.7) $b(t)x_2(t)$ represents the rate of external energy supply, $z(t)x_2(t)$ represents the rate at which energy is transferred between Σ_X and Σ_Z, and $Rx_2^2(t)$ represents the rate at which energy is dissipated due to the motions of Σ_X. If $z(t)x_2(t) > 0$ then the energy transfer is from

Σ_X to Σ_Z (loading) and if $z(t)x_2(t) < 0$ the energy transfer is from Σ_Z to Σ_X (unloading).

The damper Σ_Z has no external power supply, rather its only source of energy is through its interaction with Σ_X. This energy flow is shown in Fig 4.1. The natural storage function for Σ is simply $H(x,z) = H_X(x) + H_Z(z)$ and the total energy balance is

$$\underbrace{H(x(t),z(t)) - H(x(0),z(0))}_{\text{Stored}} + \underbrace{\int_0^t Rx_2^2(s)ds + \int_0^t \Phi(s)ds}_{\text{Dissipated}} = \underbrace{\int_0^t b(s)x_2(s)ds}_{\text{Supplied}}, \qquad (4.1.11)$$

which defines a passive, finite gain, map from $b \mapsto x_2$ (passivity properties of Σ_X preserved). As the tremor, $b(t)$, provides the only external source of energy, the behaviour of Σ for nonzero $b(t)$ will be referred to as external behaviour, while if $b(t) \equiv 0$, the behaviour of Σ will be referred to as internal behaviour. Assume for the moment that the initial stored energy is zero ($H(x_a(0)) = 0$), so that any nontrivial evolution of Σ must be due to an external supply of energy. Rearranging (4.1.9) and (4.1.11) yields

$$\begin{aligned} \int_0^t \Phi(s)ds &\le \int_0^t z(s)x_2(s)ds, \\ &\le \int_0^t b(s)x_2(s)ds - \int_0^t Rx_2^2(s)ds. \end{aligned} \qquad (4.1.12)$$

Thus, Σ_Z cannot dissipate more energy than is supplied to it by Σ_X, which is in turn less than the energy supplied to Σ_X minus the energy dissipated due to the motion of Σ_X.

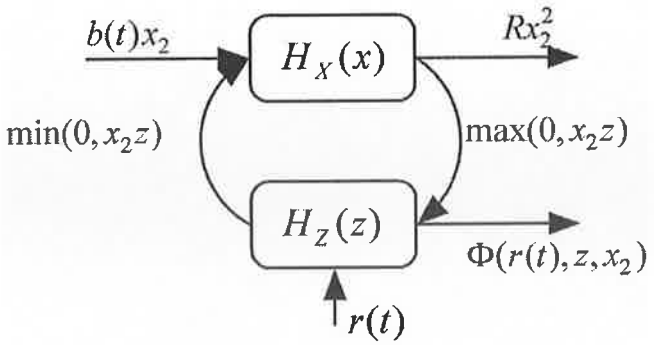

Fig 4.1 Energy flow in (4.1.12) with lossless interconnection

Now, energy transfer from Σ_X to Σ_Z requires nontrivial motion of Σ_X ($x_2 \neq 0$), and this motion will dissipate some of the supplied energy. As a result, the maximum amount of energy that Σ_Z can possibly dissipate is strictly less that that supplied to Σ_X

by $b(t)$. This is basically a statement of the fact (see §2) that no admissible control $r(t)$ ($r \in C^{0,1}(\Re_+;\Re_+)$) exists which can completely cancel the effect of a persistent disturbance, on the behaviour of Σ_X. To make this a bit more precise, consider the case where $b(t)$ is some nontrivial T-periodic disturbance. Then for $x = 0$ to be a partial equilibrium for Σ would require that for $x_2 = 0$, there exist a control $r(t)$, such that Σ_Z has a nontrivial T-periodic solution $z(t) = b(t), t \geq 0$. Setting $x_2 = 0$ in (4.1.9) implies that $H_Z(z(t))$ and hence $|z(t)|$ is nonincreasing as a function of time. Since $|z(t)|$ is bounded below by zero, it tends to a limit as $t \to \infty$, ruling out the possibility of a nontrivial T-periodic solution. For example, if $z(t)$ is T-periodic then there exist two times $t_1, t_2 \in [0,T)$, such that $t_2 > t_1$ and $|z(t_2)| < |z(t_1)|$. But by periodicity $|z(t_2)| < |z(t_1 + T)|$, which is impossible.

All is not lost however. Consider the case where both $b(t)$ and $r(t)$ are T-periodic and let $\bar{x}_a = (\bar{x}, \bar{z})$ be a T-periodic solution of Σ (proof of existence is given in §D.2). Then $H(x_a(t)) = H(x_a(t+T)), \forall t \geq 0$, so that applying the inequality $x_2 b \leq R x_2^2/2 + b^2/2R$ to (4.1.11) and rearranging yields

$$\int_t^{t+T} \bar{x}_2^2(s)ds \leq \frac{1}{R}\int_t^{t+T} b^2(s)ds - \frac{2}{R}\int_t^{t+T} \overline{\Phi}(s)ds. \qquad (4.1.13)$$

for all $t \geq 0$. Note that the left hand side of (4.1.13) represents the averaged kinetic energy over $[0,T)$. Thus by ensuring Σ_Z dissipates a positive amount of energy on each period, the upper bound on the averaged kinetic energy will be reduced. As noted in §2.3, this will also reduce the upper bound on the oscillation of $\bar{x}_1$.

Returning to the dissipation function (4.1.10), it can be seen that Σ_Z is not strictly passive and not lossless either (see §2.3 for passivity definitions). For example, if $H_Z(r(t_0)) = 0$ and $x_2(t) > 0, \forall t \in [t_0, t_1]$, then Σ_Z can store all of the energy supplied to it without any losses, provided $H_Z(z(t)) < H_Z(r(t)), \forall t \in [t_0, t_1]$. If after $t = t_1$, $x_2 < 0, \forall t \in (t_1, t_2]$, then all of this stored energy can be returned to Σ_X, again provided $H_Z(z(t)) < H_Z(r(t)), \forall t \in (t_1, t_2]$. Examination of (4.1.10) shows that Σ_Z will only dissipate energy if the stored energy is at its instantaneous maximum and if the rate of energy supply from Σ_X is greater than the rate of change of $H_Z(r(t))$. Note that the

condition $x_2 z > 0$ is not required for dissipation to occur. Indeed dissipation is possible if Σ_Z is in the process of returning stored energy to Σ_X due to the natural evolution of Σ, and if the available storage is decreasing faster than the natural energy extraction can take place. Now if $x_2 \equiv 0$ (say, clamped by some large multivalued friction force), then $x_2 z \equiv 0$ and $H_Z(z)$ will be nonincreasing. Now $H_Z(z)$ can still be brought to zero in finite time by bringing $H_Z(r(t))$ to zero (cannot be done infinitely fast due to the restriction $r \in C^{0,1}$). If this is the case, then all of the stored energy will be dissipated (which could be interpreted as a controlled increase in entropy, due to the loss of ability to do useful work on Σ_X). An interesting case occurs when $r(t) = r = \text{constant}$. From (4.1.10) it can be seen that dissipation will occur only if $H_Z(z) = H_Z(r) = \text{constant}$ and $x_2 z > 0$ (energy flowing from Σ_X to Σ_Z). It this is the case then the dissipation is given by $\Phi(t) = x_2 z > 0$, which can be interpreted as a sort of overflow condition. That is, Σ_Z is unable to store any more energy and so instantly dissipates all additional energy received (maximum dissipation principle). It can also be seen that dissipation requires Σ_X to exhibit nontrivial motion ($x_2 \neq 0$), while Σ_Z must remain stationery ($\dot{z} = 0$).

So far the discussion has focused on external properties of Σ. However tremor is not permanent, so ensuring nice internal stability properties is also important. In §2.2 it was shown that that if $b(t) \equiv 0$ and $r(t) \equiv 0$ (and hence $z(t) \equiv 0$) then the origin is a GES equilibrium for Σ_X. If the tremor does vanish, what conditions can be imposed on the function $r(t)$ so as to ensure that the origin (in $\Re^3$) is an internally GES equilibrium for Σ (other than the restriction $r(t) \equiv 0$). This is a bit tricky and will be taken up in the next two sections of this chapter. For the present, sufficient conditions for the origin to be an internally GAS equilibrium will suffice. A review of Liapunov stability concepts can be found in §B. Note that for $b(t) \equiv 0$, $x_a = 0$ is an equilibrium for Σ, irrespective of variations in $r(t)$. Using (4.1.4) it is easily shown that the natural storage function $H(x_a) = H_Z(z) + H_X(x)$ satisfies $c_1 |x_a|^2 \leq H(x_a) \leq c_2 |x_a|^2$ for some constants $c_2 \geq c_1 > 0$. Setting $b(t) \equiv 0$ in (4.1.11) gives

$$H(x_a(t)) \leq H(x_a(0)) - \int_0^t R x_2^2(s) ds, \tag{4.1.14}$$

and hence $|x_a(t)| \le \sqrt{c_2/c_1}|x_a(0)|$ for all $t \ge 0$, from which it follows that the origin (in $\Re^3$) is uniformly stable and that all solutions are uniformly bounded. Consequently the positive limit set $\Omega(x_a)$ (see §B.2) is nonempty, compact and is the smallest closed set approached by $x_a(t)$. Since the storage function $H(x_a(t))$ is nonincreasing as a function of time and bounded below by zero, it has a definite limit as $t \to \infty$, i.e. $\lim_{t\to\infty} H(x_a(t)) = l$, so

$$\int_0^\infty R x_2^2(s)ds \le H(x_a(0)) - l. \tag{4.1.15}$$

Combining (4.1.15) with the existence result given at the start of this section, it can be concluded that $x_2 \in L_2(\Re_+;\Re) \cap C^{1,1}(\Re_+;\Re)$. Barbalat's lemma (Lemma B.3) can now be used to show that $x_2(t) \to 0$ as $t \to \infty$. Since $x_2(t) \to 0$ as $t \to \infty$ and $\dot{x}_2 \in C^{0,1}(\Re_+;\Re)$, the second version of Barbalat's lemma (Lemma B.4) can be used to concluded that $\dot{x}_2(t) \to 0$ as $t \to \infty$. It follows from (4.1.3) that

$$\lim_{t\to\infty} |h_K(x_1(t)) + z(t)| = \lim_{t\to\infty} |Rx_2(t) + \dot{x}_2(t)| = 0, \tag{4.1.16}$$

where $h_K(x_1) = Kx_1 + h(x_1)$ is an increasing function. The limit in (4.1.16) implies a one to one correspondence between limits sets $\Omega(x_1)$ and $\Omega(z)$, which is provided by the function $h_K(\cdot)$. Now, using (4.1.16) and that fact that $x_2(t) \to 0$ as $t \to \infty$ gives

$$\begin{aligned} \lim_{t\to\infty} H(x_a(t)) &= \lim_{t\to\infty}\left(\frac{1}{2}Kx_1^2(t) + \frac{1}{2G}z^2(t) + \int_0^{x_1(t)} h(s)ds\right), \\ &= \lim_{t\to\infty}\left(\frac{1}{2}Kx_1^2(t) + \frac{1}{2G}h_K(x_1(t))^2 + \int_0^{x_1(t)} h(s)ds\right), \\ &= l, \end{aligned} \tag{4.1.17}$$

implying that $x_1(t)$ tends to a constant, say $x_1^* \in \Omega(x_1)$ and that $z(t)$ tends to a constant $z^* = -h_K(x_1^*) \in \Omega(z)$. It follows that for each divergent subsequence $\{t_n\}$ of $\Re_+$, it must be that $\lim_{n\to\infty} r(t_n) \ge \lim_{n\to\infty} |z(t_n)| = |z^*|$, which implies that $|z^*| \le \liminf_{t\to\infty} r(t) = r_m$. Putting all this together it can be concluded that $\Omega(x_a) \in \mathbf{M} = \{x_a \in \Re^3 \mid h_K(x_1) = -z^*, x_2 = 0, z = z^*, \forall z^* \in [-r_m, r_m]\}$. Clearly if $r_m = 0$, then $\Omega(x_a) = 0$, implying that $x_a = 0$ is a GAS equilibrium for Σ. For example if $r(t)$ is T-periodic and $\min_{t\in[0,T)} r(t) = 0$, then $r_m = 0$, implying the origin is GAS. Furthermore, in this case periodicy of Σ means that GAS can be strengthened to

GUAS (see §B.1). Of course if the control $r(t)$ is a nonzero constant, then $r(t) \equiv r_m$ and it can only be concluded that all solutions converge to the set $\mathbf{M}$.

Fig 4.2 shows some typical trajectories of Σ, for different initial conditions, with $b(t) \equiv 0$ and $r(t) \equiv r_m > 0$. The elastic modulus for the damper model will be taken as $1000 Nm/rad$, which when scaled by the inertia (see §2.2), gives $G = 20000$. All simulations of Σ have been performed in the Simulink/Matlab software package [83], using a fourth-order Runge-Kutta algorithm for Σ_X coupled with an implicit Euler algorithm for the Σ_Z. A fix time step of 0.0005 seconds was used along with the parameter values $R = 16, K = 90, L = 100$ and $G = 20000$. Notice that when the solutions are close to the corresponding limit point, the projection of the trajectories into the x-plane, behave as if the equilibrium was a stable focus. This is the sort of behaviour usually associated with a linear under damped oscillator. This form of oscillatory behaviour is undesirable and probably not what one would intuitively expect from an ER damper. However, it can be eliminated be using more complex models such as the multiple element EP model and the GnF model (see §3.5). As such, the EP model can be viewed as a worst case scenario, in terms of well behaved transients and thus a suitable start for the analysis.

So what can be concluded from the analysis presented above? In terms of disturbance attenuation, it was shown that complete cancellation of the effects of $b(t)$ is impossible. However, as $b(t)$ provides the only source of energy supply, it should be possible to a least reduce its effect on the resulting trajectories of Σ_X, by suitably modulating the dissipation function $\Phi(t)$. Now if a general control scheme for $r(t)$ could be devised, which would ensure that all solutions of Σ tend to a T-periodic solution, then Σ_Z would have a periodic supply of energy at its disposal (loading and unloading on each period of solution). It follows that if most of this energy could be periodically dissipated in some suitable manner, then the average of the system kinetic energy, over each period will be less than that of the system with the trivial control $r(\cdot) \equiv 0$. This would in turn imply that it should be possible to reduce the oscillation of the trajectory as compared to the trajectory resulting from $r(\cdot) \equiv 0$. The various aspects of the scenario presented above will be analysed in some detail in the sections that follow.

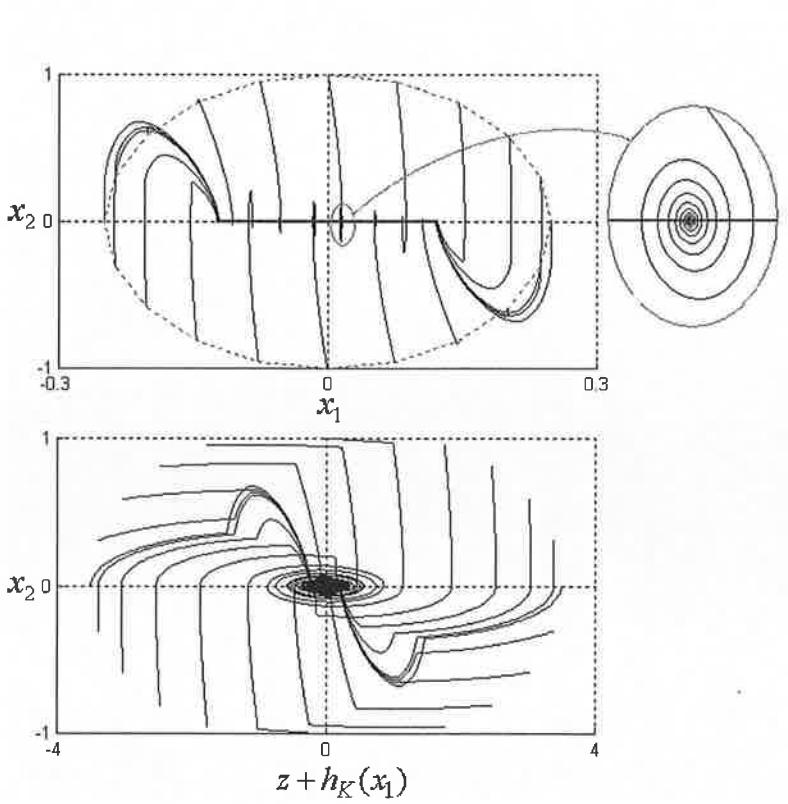

Fig 4.2 Example solution trajectories for Σ with $b(\cdot) = 0$ $r(t) = const. > 0$

4.2 Internal stability

The objective of this section will be to establish some internal stability results for Σ, for the case in which $r(t)$ is time varying. More precisely, the objective here is to obtain sufficient conditions on $r(t)$ which ensure that the origin is an internal GES equilibrium for Σ, while still allowing some scope for the development of disturbance attenuation schemes in later sections (thus ruling out the trivial control $r(\cdot) \equiv 0$).

The stability analysis of mechanical systems coupled with nonlinear/nonautonomous dissipative devices arises frequently in the literature on semi-active control. The problem is not restricted to hysteretic damping either. For example, consider the simple oscillator, $\ddot{x} + R(t)\dot{x} + Kx = 0$, with stiffness $K > 0$ and controllable damping coefficient $R(t) \geq 0, \forall t \geq 0$. The total energy for this systems is $H = 0.5(\dot{x}^2 + Kx^2)$, which is dissipated at the rate $\dot{H} = -R(t)\dot{x}^2 \leq 0$. If $R(\cdot) \geq a > 0$, then the system is stable and all of the system's kinetic energy $0.5\dot{x}^2$, will be dissipated as $t \to \infty$. Unfortunately, without further knowledge of $R(t)$, the same cannot be said for the potential energy. It can be shown that if $R(\cdot) \leq b < \infty$ is also enforced, then all of the

systems energy will be dissipated, rendering the equilibrium $\dot{x} = x = 0$, GAS. However if $R(t)$ is not bounded above, a little more care needs to be taken. The classical counter example arises with $R(t) = 2 + e^t$ and $K = 1$, which admits the solution $x(t) = c(1 + e^{-t})$, $\forall c \in \Re$ so that $\lim_{t\to\infty} x(t) = c$. An intuitive explanation for this sort of phenomena is that as the system is linear, so it cannot approach the origin faster than exponentially. Thus if $R(t)$ grows fast enough, then even if $\lim_{t\to\infty} \dot{x}(t) = 0$, it may occur that $\lim_{t\to\infty} -R(t)\dot{x}(t) \neq 0$. A necessary and sufficient condition for GAS was obtained in [71]: if $R(t) \geq a > 0, \forall t \geq 0$ and $c > 0$ is fixed, then the equilibrium $\dot{x} = x = 0$ asymptotically stable, if and only if $\sum_{n=1}^{\infty} \left[H(nc)^{-1} - H((n-1)c)^{-1}\right]^2 = \infty$, where $H(t) = \int_0^t R(s)ds$. Using this condition it can be shown that if $R(t) = at, a > 0$, then the origin is GAS, while GAS is lost if $R(t) = at^2$. The loss of GAS is not restricted to nonautonomous damping. For example if $R(t)\dot{x} = a\mathrm{SGN}(\dot{x})$, one obtains the much studied case of multivalued coulomb friction. A straight forward application of the Krasovskii-Lasalle theorem (§B.2) shows that all solutions will converge to the set $\mathbf{M} = \left\{(x, \dot{x}) \in \Re^2 \mid \dot{x} = 0, Kx \in a[-1,1]\right\}$. The similarity with the results of the previous section is due to the fact that the corresponding dissipation function is homogenous of degree one in $\dot{x}$.

There have been numerous works dedicated to the stability analysis of mechanical systems coupled with semi-active, hysteretic dampers, however many of the results developed to date are inapplicable in the present case. A common approach to modelling is to start with a variant of Bouc's hysteresis model [34] and then to equip it with time varying "control" parameters. These parameters account for the effect of variations in the electric field, normal force etc, [23],[35],[72]-[75]. The reason for the popularity of the Bouc-type models is their "smoothness", supposedly making subsequent analysis much easier. In autonomous form these models are usually thermodynamically consistent [76], however the indiscriminate placement of the time varying "control" parameters leads to models which are often inconsistent. As an example, the stability of Σ_X coupled with a simplified version of the Dahl friction model [77], modelling a friction damper [73],[74], will now be considered.

The Dahl friction model, Σ_F, can be seen as a special case of the Bouc-type hysteresis model given in equation (1.2.6), with $n=1, A=G, \gamma=G/F_C$ and $\beta=0$

$$\begin{aligned}\Sigma_X &= \begin{cases}\dot{x}_1 = x_2 \\ \dot{x}_2 = -Rx_2 - Kx_1 - h(x_1) - \theta(t)z\end{cases} \\ \Sigma_F &= \left\{\dot{z} = G\left(x_2 - \frac{|x_2|}{F_C}z\right)\right.\end{aligned} \tag{4.2.1}$$

In this case, the variable z represents the restoring force, resulting from the average deformation of the microscopic asperities between two contacting surfaces (in which case x_2 represents relative motion in the tangential direction). The constant $G>0$ is proportional to the average stiffness of the asperities and $F_C>0$ is the coulomb friction level (proportional to the normal force between the surfaces). If $x_2(\cdot)$ is not identically zero and sign definite, it can be seen that $\lim_{t\to\infty} z(t) = F_C \operatorname{sgn}(x_2)$, and if $|z(0)| \le F_C$ then $|z(t)| \le F_C, \forall t \ge 0$. The parameter $\theta(\cdot) \in [0, \bar{\theta}], \forall t \ge 0$, represents controllable variations in the normal force. While its placement in Σ_X may same a bit odd, it seems to be the placement of choice for the control parameters in [23],[35],[72]-[75],[80] (and many other such works). In isolation, the Dahl model is consistent in the sense that it describes a passive map $x_2 \mapsto z$, with storage function $H_D = 0.5\, z^2/G$. Now consider the total stored energy for the coupled system (4.2.1),

$H(x,z) = 0.5(x_2^2 + Kx_1^2 + z^2/G) + \int_0^{x_1} h(s)ds$, the directional derivative of which is

$$\begin{aligned}\dot{H}(x,z) &= -Rx_2^2 - \frac{1}{F_C}|x_2|z^2 + (1-\theta(t))x_2 z, \\ &= -Rx_2^2 + |x_2 z|\left((1-\theta(t))\operatorname{sgn}(x_2 z) - \frac{1}{F_C}|z|\right).\end{aligned} \tag{4.2.3}$$

It follows that if $\theta(t) \equiv 1$, then (4.2.3) becomes $\dot{H} \le -Rx_2^2 - |x_2|z^2/F_C \le -Rx_2^2 \le 0$, from which it can be concluded that the zero solution is stable and that all solutions are bounded. Application of the Krasovskii-Lasalle theorem shows that the system is globally convergent to the largest invariant set $\mathbf{M}$, contained in

$\mathbf{E} = \{(x,z) \in \Re^2 \times \Re \mid x_2 = 0\}$. A quick examination of (2.1) shows that

$\mathbf{M} = \{(x,z) \in \Re^2 \times \Re \mid x_2 = 0, x_1 = h_K^{-1}(-z), |z| \le F_C\}$, where $h_K(x_1) = Kx_1 + h(x_1)$. For arbitrarily time varying $\theta(\cdot) \in [0, \bar{\theta}]$, $\dot{H}(x,z)$ is indefinite so that no such conclusions are possible. The reason that this inconsistency seems to have gone unnoticed is that in

the control formulation and subsequent analysis, only the energy function for Σ_X is taken into account. The reasoning typically goes as follows [35][55][73][74]. The derivative of the energy function $H_X(x) = 0.5(x_2^2 + Kx_1^2) + \int_0^{x_1} h(s)ds$ along the solutions of Σ_X is

$$\dot{H}_X(x,z) = -Rx_2^2 - \theta(t)x_2 z\,. \tag{4.2.4}$$

The control objective is now to maximize the dissipation provided by the second term in (4.2.4), while ensuring Σ_X is GAS with respect to the origin. This leads to the discontinuous control law

$$\theta(t) = \begin{cases} \bar{\theta}, & if \quad zx_2 > 0, \\ 0, & otherwise. \end{cases} \tag{4.2.5}$$

Using (4.2.5), it can be seen that $\theta(t)z(t)x_2(t) \geq 0, \forall t \geq 0$, so that (2.4) implies that the system will converge to the largest invariant set, $\mathbf{M}$, contained in $\mathbf{E} = \{x \in \Re^2 \mid x_2 = 0\}$ (assuming (4.2.1) and (4.2.5) has a solution). Since $x_2 \equiv 0 \Rightarrow \theta = 0$, it can be seen that $\mathbf{M}$ corresponds with the origin, thus ensuring GAS of the origin for Σ_X. Justification for (4.2.5) is usually that since Σ_F can store energy, the control law (4.2.5) prevents the return of this stored hysteretic energy to Σ_X. This reasoning is a bit inconsistent, since if $x_2 z \leq 0$, the flow of energy is from $\Sigma_F \mapsto \Sigma_X$. However, $x_2 z \leq 0 \Rightarrow \theta(t) = 0$, which implies that Σ_F and Σ_X are decoupled, so where does the energy go?. To highlight the thermodynamic inconsistency of the system in (4.2.1), consider the reversed control law

$$\theta(t) = \begin{cases} 2, & if \; x_2 z < 0, \\ 0, & otherwise. \end{cases} \tag{4.2.6}$$

which when applied to (4.2.3) yields

$$\dot{H}(x,z) = -Rx_2^2 + |x_2 z|\left(1 - \frac{1}{F_C}|z|\right). \tag{4.2.7}$$

Recalling that $|z| \leq F_C$, it can be seen that second term in (4.2.7) is nonnegative, so that stability of the origin can no longer be concluded. Indeed $\dot{H} > 0$ if $|x_2| < \left(|z|/R - |z|^2/RF_C\right)$. However, since $\theta(t)|z(t)| \leq 2F_C$, inequality (4.1.5) (with $\bar{r}$ replaced by $2F_C$) can be used to show that all solutions of Σ_X are UB and UUB.

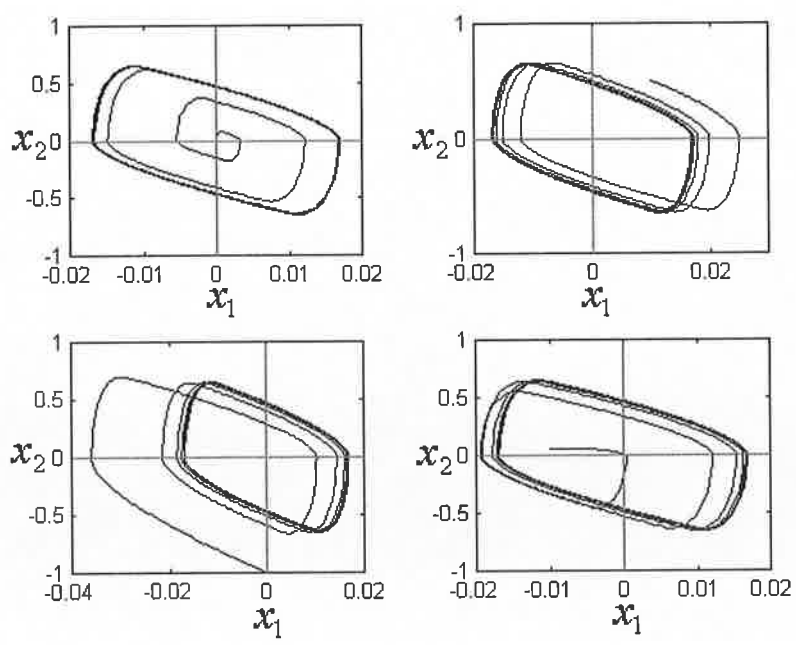

Fig 4.3 Examples of phase portrait of (2.1) with control law (2.6).

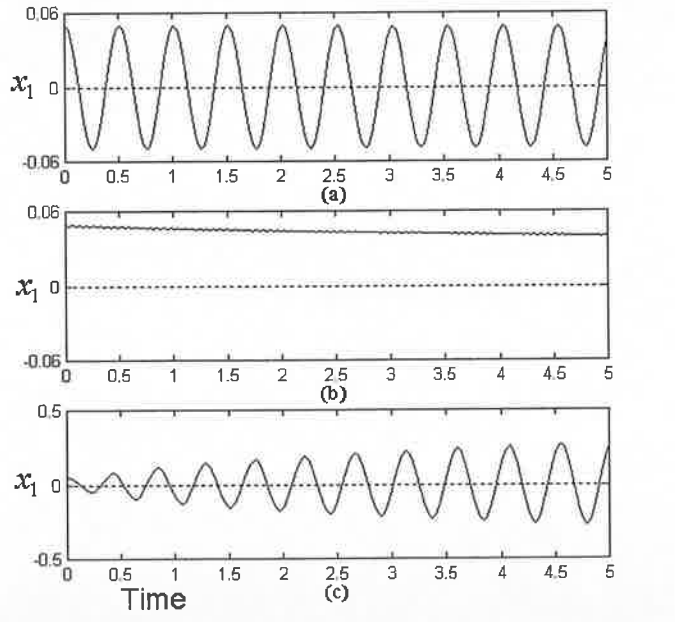

Fig 4.4 Example trajectories of x_1 with $R = 0$, (a) $\theta = 0$ (b) $\theta = 1$ and (c) control (4.2.6).

The fact that all solutions are uniformly bounded, means that the positive limit set $\Omega(x, z)$ is nonempty, compact and is the smallest closed set approached by $(x(t), z(t))$. Combining this with the possible instability of the origin, would seem to suggest that at least one solution will converge to a limit cycle. The physical interpretation is that if Σ_D injects more energy into Σ_X during each cycle, than it can dissipate naturally, the system will not "settle down".

Fig 4.3 shows some typical phase portraits of the system (4.2.1) with control (4.2.6). The parameter values used for Σ_X are the same as those in Section 4.1 and $G = 500Nm/rad$ and $F_C = 5Nm$ used for Σ_D. If $R = 0$ (Σ_X is lossless), it can be seen that $\dot{H}(x,z) \geq 0$ and $\dot{H}(x,z) > 0$ if $x_2 \neq 0$ and $|z| \in (0, F_C)$. This suggests that solutions with nonzero initial conditions could become unbounded. Fig 4.4 shows examples of solution trajectories for x_1 with initial condition $(x_0, z_0) = [.05,0,0]$, $R = 0$ and (a) $\theta = 0$ (b) $\theta = 1$ and (c) control law (4.2.6).

From the discussions above and §2.3, it is safe to conclude that the model (4.2.1) does not capture the expected behaviour of a semiactive damper. Indeed, the definition given in [35] is "semiactive devices can only absorb or store vibratory energy in a structure by reacting to its motion, they are considered to be stable in a bounded-input, bounded-output sense". Now return to the original system Σ in (4.1.3), (repeated for convenience)

$$\Sigma \begin{cases} \Sigma_X \begin{cases} \dot{x}_1 = x_2 \\ \dot{x}_2 = -Rx_2 - Kx_1 - h(x_1) - z + b(t) \end{cases} \\ \Sigma_Z \begin{cases} \langle Gx_2 - \dot{z}, z - \varphi \rangle \geq 0, \quad \forall |\varphi| \leq r(t), \\ |z(t)| \leq r(t), \quad \forall t \geq 0. \end{cases} \end{cases} \tag{4.2.8}$$

In Section 4.1 it was shown that if $r(t)$ is an admissible control then all solutions of the unforced system (i.e. $b(t) \equiv 0$) are UB and the positive limit set $\Omega(x,z)$ is contained in the set $\mathbf{M} = \{(x,z) \in \Re^2 \times \Re \mid x_2 = 0, x_1 = h_K^{-1}(-z), |z| \leq r_m\}$, where $r_m = \liminf_{t\to\infty} r(t)$. It follows that if $r_m = 0$ then all solutions converge to the origin. This condition is not as restrictive as it may seem, for example, any T-periodic control with $\min_{t\in[0,T)} r(t) = 0$ will suffice.

It would seem worth while to demonstrate why Bang-Bang type control laws (4.2.5), don't quite fit in with the present objectives of tremor suppression. Putting aside the question of existence and uniqueness of solutions for the moment (i.e. inadmissible control allowed), consider applying the control law (4.2.5) to Σ_Z, that is

$$r(t) = \begin{cases} \bar{r}, & \text{if} \quad zx_2 > 0, \\ 0, & \text{otherwise.} \end{cases} \tag{4.2.9}$$

The problem is that if there exists a time τ such that $z(\tau)x_2(\tau) \le 0$, then $r(\tau) = 0$ and hence $z(t) = 0, \forall t \ge \tau$, since it would impossible to obtain the condition $z(t)x_2(t) > 0$. This doesn't leave much scope for disturbance attenuation (the existence of τ being all the more likely if $b(t)$ is periodic). A possible modification to (4.2.9) would be to replace the condition $zx_2 > 0$ with $zx_2 \ge 0$. However in this case $x_2(\cdot) \equiv 0$ does not imply $z(\cdot) = 0$, so that is only possible to conclude that the positive limit set $\Omega(x,z)$ is contained in the set $\mathbf{M} = \left\{(x,z) \in \Re^2 \times \Re \mid x_2 = 0, x_1 = h_K^{-1}(-z), |z| \le \bar{r}\right\}$. Furthermore, even if it were possible to implement a discontinuous, bang-bang type control, it would probably lead to a jerky motion, which could be more debilitating than the tremor itself.

Recall that in §2.2 it was shown that if $b(t) \equiv 0$ and $r(t) \equiv 0$ (hence $z(t) \equiv 0$), then the origin is a GES equilibrium for Σ_X. It will now be shown that by strengthening the condition $\liminf_{t\to\infty} r(t) = 0$, the equilibrium $(x,z) = (0,0)$ can be rendered internally GES for Σ. There are numerous reasons why GES is more desirable than GAS. Besides the fact that it provides an explicit bound for the rate of convergence to zero, if a Liapunov function can be found which proves the system is internally GES, then this same Liapunov function can be used to establish certain nice external stability properties.

Suppose there exists a finite constant $T > 0$, such that on each interval of length T, there exists a time τ such that $r(\tau) = 0$ (and hence $z(\tau) = 0$). Consider the partition $J_n = T[n, n+1)$, $n = 0,1,2,\ldots$, so that for each n there exists a time $\tau_n \in J_n$ such that $r(\tau_n) = 0$. If $r(t)$ takes the value 0 repeatedly on any interval, set $\tau_n = \min\left\{s \in T[n,n+1) \mid r(s) = 0\right\}$. An admissible control satisfying these conditions will be referred to as a $0T$-recurrent control. To analyze the consequence of applying a $0T$-recurrent control, consider the energy like function $V(z) = z^2$, the directional derivative of which satisfies

$$\dot{V}(z) \le 2Gx_2 z - 2\langle \dot{z} - Gx_2, z\rangle \le 2G|x_2|\sqrt{V(z)}. \tag{4.2.10}$$

For $t \in [\tau_n, \tau_{n+1})$, integrating (4.2.10) over $[\tau_n, t]$ gives

$$|z(t)| \le |z(\tau_n)| + G\int_{\tau_n}^{t} |x_2(s)|ds \le G\int_{\tau_n}^{t} |x_2(s)|ds, \tag{4.2.11}$$

and if $n \ge 1$ (ensuring $t \ge T$)

$$|z(t)| \le G\int_{t-T}^{t} |x_2(s)|ds. \tag{4.2.12}$$

Using (4.2.12) it can be seen that if $x_2(t) \to 0$ as $t \to \infty$, then $z(t) \to 0$ as $t \to \infty$. Define the characteristic function χ_T by $\chi_T(s) = 1$ if $s \in [0,T]$ and $\chi_T(s) = 0$ otherwise. With out loss of generality, it will be assumed that $\tau_0 = 0$, so that combining (4.2.11) and (4.2.12) yields

$$|z(t)| \le G \int_0^t \chi_T(t-s)|x_2(s)|ds, \tag{4.2.13}$$

for all $t \ge 0$. Using the fact that $\chi_T(s)\chi_T(s) = \chi_T(s)$ and applying Holders inequality (see §A.1) to the left hand side of (4.2.13) gives

$$\begin{aligned} |z(t)| &\le G\left(\int_0^t \chi_T(t-s)ds \right)^{1/2} \left(\int_0^t \chi_T(t-s)|x_2(s)|^2 ds \right)^{1/2}, \\ &\le G(T)^{1/2} \left(\int_0^t \chi_T(t-s)|x_2(s)|^2 ds \right)^{1/2}, \end{aligned} \tag{4.2.14}$$

$$|z(t)|^2 \le G^2 T \int_0^t \chi_T(t-s)|x_2(s)|^2 ds. \tag{4.2.15}$$

Setting $t = \tau$ in (4.2.15) and integrating both sides of (4.2.15) from 0 to t

$$\begin{aligned} \int_0^t |z(\tau)|^2 d\tau &\le G^2 T \int_0^t \int_0^\tau \chi_T(\tau - s)|x_2(s)|^2 ds d\tau, \\ &= G^2 T \int_0^t |x_2(s)|^2 \int_s^t \chi_T(\tau - s) d\tau ds, \\ &\le G^2 T^2 \int_0^t |x_2(s)|^2 ds. \end{aligned} \tag{4.2.16}$$

It follows that if $x_2 \in L_2(\Re_+;\Re)$ then $z \in L_2(\Re_+;\Re)$. That Σ_Z now has finite L_2 gain can be seen as a consequence of the fact that the $0T$-recurrent control frequently dumps any energy stored by Σ_Z. With $x_a = (x,z)$ consider the Liapunov function

$$V(x_a) = \frac{1}{2}\left(2K + \rho R^2\right)x_1^2 + \rho R x_1 x_2 + x_2^2 + \frac{1}{G}z^2 + 2\int_0^{x_1} h(s)ds. \tag{4.2.17}$$

A sufficient condition for $V(x_a)$ to be positive definite is that $\rho \in (0,2)$ and furthermore, due to (1.4) there exists constants $c_2 > c_1 > 0$ such that $c_1|x_a|^2 \le V(x_a) \le c_2|x_a|^2$. Taking the derivative of $V(x_a)$ along the solutions of Σ one obtains

$$
\begin{aligned}
\dot{V}(x_a) &\le -(2-\rho)Rx_2^2 - \rho RKx_1^2 - \rho Rx_1 z + \left(2|x_2| + \rho R|x_1|\right)|b(t)|, \\
&\le -(2-\rho)Rx_2^2 - \frac{\rho}{2}RKx_1^2 - \frac{\rho}{2K}Rz^2 + \frac{\rho}{K}Rz^2 + \left(2|x_2| + \rho R|x_1|\right)|b(t)|, \\
&\le -(1-\rho)Rx_2^2 - \frac{\rho}{2}RKx_1^2 - \frac{\rho}{2K}Rz^2 \\
&\quad + R\left(\frac{\rho}{K}z^2 - x_2^2\right) + \left(2|x_2| + \rho R|x_1|\right)|b(t)|, \\
&\le -\left(\frac{1}{2}-\rho\right)Rx_2^2 - \frac{\rho}{4}RKx_1^2 - \frac{\rho}{2K}Rz^2 \\
&\quad + R\left(\frac{\rho}{K}z^2 - x_2^2\right) + \left(\frac{2}{R} + \frac{\rho R}{K}\right)|b(t)|^2.
\end{aligned}
\tag{4.2.18}
$$

where frequent use has been made of Young's inequality (see §A.1). Taking $\rho < 0.5$, setting $c_3 = R\min(0.5-\rho, 0.25\rho K, 0.5\rho/K)/c_2$ and $c_4 = 2/R + \rho R/K$ (2.18) becomes

$$
\dot{V}(x_a) \le -c_3 V(x_a) + c_4|b(t)|^2 + R\left(\frac{\rho}{K}z^2 - x_2^2\right). \tag{4.2.19}
$$

Integrating (4.2.19) from 0 to t and using (4.2.16)

$$
\begin{aligned}
V(x_a(t)) - V(x_a(0)) &\le -c_3\int_0^t V(x_a(s))ds + c_4\int_0^t |b(s)|^2 ds + R\int_0^t \frac{\rho}{K}z^2(s) - x_2^2(s)ds, \\
&\le -c_3\int_0^t V(x_a(s))ds + c_4\int_0^t |b(s)|^2 ds + R\left(\frac{\rho}{K}(GT)^2 - 1\right)\int_0^t x_2^2(s)ds.
\end{aligned}
\tag{4.2.20}
$$

Taking $\rho < \min\left(0.5, K/G^2T^2\right)$, the final term is negative and hence

$$
V(x_a(t)) - V(x_a(0)) \le -c_3\int_0^t V(x_a(s))ds + c_4\int_0^t |b(s)|^2 ds, \tag{4.2.21}
$$

which implies that

$$
V(x_a(t)) \le V(x_a(0))e^{-c_3 t} + c_4\int_0^t e^{-c_3(t-s)}|b(s)|^2 ds, \tag{4.2.22}
$$

and hence

$$
\begin{aligned}
|x_a(t)|^2 &\le \frac{c_2}{c_1}|x_a(t)|^2 e^{-c_3 t} + \frac{c_4}{c_1}\int_0^t e^{-c_3(t-s)}|b(s)|^2 ds, \\
&\le \frac{c_2}{c_1}|x_a(t)|^2 e^{-c_3 t} + \frac{c_4}{c_1 c_3}\|b\|_\infty^2\left(1 - e^{-c_3 t}\right).
\end{aligned}
\tag{4.2.23}
$$

It follows from (4.2.23) that if $b(t) \equiv 0$, that all solutions of Σ are GES with respect to the origin and if $\|b\|_\infty \neq 0$, then all solutions converge to a Ball in $\Re^3$, the radius of which depends on $\|b\|_\infty$. While this result was obtained without restriction on the size of T the same cannot be said for the quantitative properties. Fig 4.5 shows an example of

the transient behaviour of Σ with OT-recurrent control $r(t)=1-\cos(n2\pi t)$, (a) $n=0$, (b) $n=1$ and (c) $n=40$.

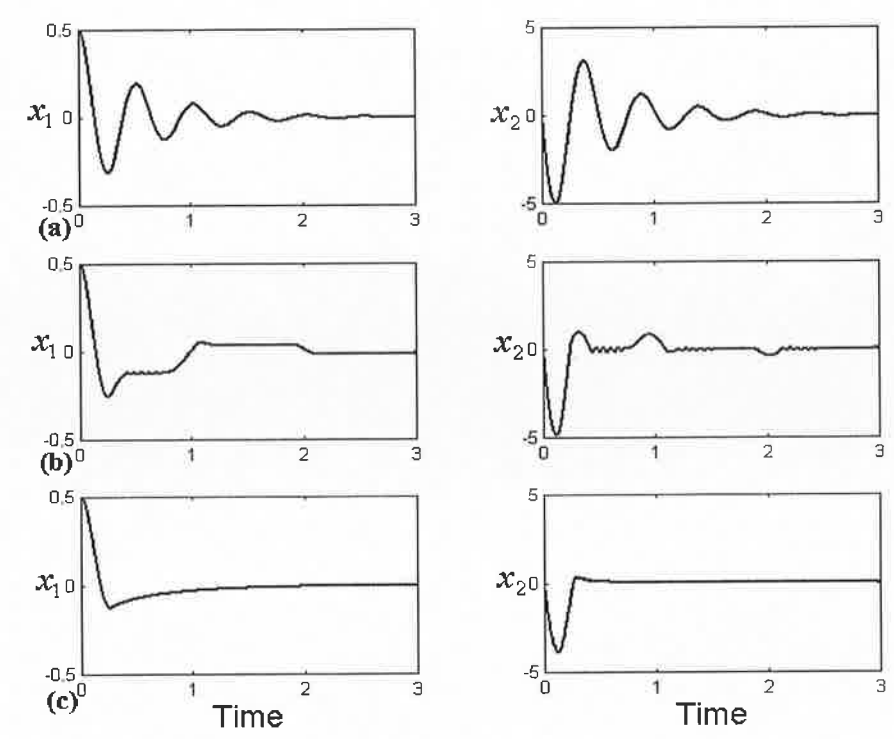

Fig 4.5 Transient behaviour of Σ with OT-recurrent $r(t)=1-\cos(n2\pi t)$, (a) $n=0$,(b) $n=1$ and (c) $n=40$

The qualitative behaviour of Σ with OT-recurrent control will be discussed further in §D, in connection with periodic trajectories and in §5, in connection with disturbance attenuation. Interestingly, it can be shown that for small enough T and large enough G, certain OT-recurrent controls have the effect of qualitatively transforming Σ_Z into a memoryless function of x_2 in an averaged sense. The whole idea is similar in spirit, to the use of dither to linearize nonsmooth control systems. Some further discussion on this point will be given in the final chapter of this thesis, as it would seem to be an interesting direction for future research.

4.3 Feedforward Dissipation Shaping

In addition to the bang-bang type control law, another popular approach to the control of semi-active dampers, is to attempt to linearize the dampers response using some form of feedback or feedforward control [78]-[81]. In the present discussion the terms feedback or feedforward control are used to distinguish between the cases in which the control does or does not use measurements of the damper force.

For example if the damper is modelled using a Bingham plastic (Coulomb friction) type model, the controllable damper response will be of the form $F(t) = -r(t)\mathrm{SGN}(x_2)$. In this case, setting $r(t) = R_c|x_2|$, with $R_c > 0$, yields the linear feedback law $F(t) = -R_c x_2$. An alternative would be to retain some controllability (for the purposes of disturbance attenuation) by using the control law $r(t) = Q\big(R_c|x_2|; r_s(t)\big)$, yielding the feedback law $F(t) = -Q\big(R_c x_2; r_s(t)\big)$ (where $Q(x; r_s)$ is the projection operator, see §A.2). In this case the controllable yield stress $r_s(t)$ can be regarded as the new control variable. Thus, if $R_c x_2(t) > r_s(t)$, then $F(t) = -r_s(t)\mathrm{sgn}(x_2)$, affording some controllability and if $R_c x_2(t) \le r_s(t)$, then $F(t) = -R_c x_2$, preserving GAS for the unforced system. Note that $F(t) = -Q\big(R_c x_2; r_s(t)\big)$ is equivalent to a linear viscous element in series with a controllable friction element.

Now, if the damper is modelled by a dynamic system, such as the EP model, then the term linearization is a bit misleading as the actual goal would be to force the systems output response to track a memoryless function of the velocity. Consider again the system

$$\Sigma\begin{cases}\Sigma_X\begin{cases}\dot{x}_1 = x_2\\ \dot{x}_2 = -Rx_2 - Kx_1 - h(x_1) - z + b(t)\end{cases}\\ \Sigma_Z\begin{cases}\langle Gx_2 - \dot{z}, z - \varphi\rangle \ge 0, \quad \forall|\varphi| \le r(t),\\ |z(t)| \le r(t), \quad \forall t \ge 0.\end{cases}\end{cases} \tag{4.3.1}$$

with the control law $r(t) = Q\big(R_c|x_2|; r_s(t)\big)$, where $r_s(t)$ is an admissible control, i.e. $r_s \in C^{0,1}(\Re_+; \Re_+) \cap [0, \bar{r}]$. If $b(t) \equiv 0$, it was shown in Section 4.1 that all solutions of Σ converge to the set $\mathbf{M} = \big\{x_a \in \Re^3 \mid h_K(x_1) = -z^*, x_2 = 0, z = z^*, \forall z^* \in [-r_m, r_m]\big\}$ where $h_K(x_1) = Kx_1 + h(x_1)$ and $r_m = \liminf_{t\to\infty} r(t)$. But if $r(t) = Q\big(R_c|x_2|; r_s(t)\big)$ then $x_2(t) \to 0$ as $t \to \infty$ implies that $r(t) \to 0$ as $t \to \infty$, which implies that $\mathbf{M} = 0$. It follows that the control $r(t) = Q\big(R_c|x_2|; r_s(t)\big)$ ensures that the origin is internally GAS. An important point about this result is that it was achieved without any restrictions on the size of R_c or on the variations of $r_s(t)$. This means that it would be possible to pick R_c very large, and since $r(t) = r_s(t)$, for all $|x_2| \ge \bar{r}/R_c$, almost all of the original controllability is recovered. If it could be shown that, $z(t) = Q\big(R_c|x_2(t)|; r_s(t)\big)$ for all

$t \geq 0$, then it would be possible to achieve some quantitative results relating to the achievable disturbance attenuation. Unfortunately it is impossible to guarantee such a result when Σ is subject to an arbitrary disturbance. As an example, consider the rather unrealistic case where $x_2(t) = A\omega \sin(\omega t)$ for some constants $A, \omega \geq 0$ and $r(t) = R_c|x_2(t)|$. A straightforward calculation shows the corresponding solution of Σ_Z is

$$z(t) = \begin{cases} Gx_1(t) - Gx_1(n\pi/\omega) & for \quad t \in [n\pi/\omega, n\pi/\omega + \Delta t), \\ R_c x_2(t) & for \quad t \in [n\pi/\omega + \Delta t, (n+1)\pi/\omega), \end{cases} \tag{4.3.2}$$

for $n = 0,1,2,\ldots$, where the time increment Δt is given by

$$\Delta t = \frac{1}{\omega} \cos^{-1}\left(\frac{G^2 - R_c^2\omega^2}{G^2 + R_c^2\omega^2} \right). \tag{4.3.3}$$

(under the assumption that $G^2 > R^2\omega^2$). Note that $\Delta t \to 0$ as $G \to \infty$ (i.e. EP model approaches coulomb friction) and $\Delta t \to \pi/\omega$ as $R \to \infty$. Fig 4.6 shows some simulation results for the EP model with, $x_2(t) = A\omega \sin(\omega t)$ and $r(t) = R_c|x_2(t)|$. The control described above suffers from several drawbacks. For example, it makes subsequent analysis of the closed loop system quite difficult and is impractical from an implementation point of view, in that it requires "clean" measurements of the velocity.

A more tractable scenario would be to replace the measurement x_2, with the output of a first order filter, that is $\dot{s} = (R_c x_2 - s)/\tau$ and set $r(t) = Q(|s(t)|; r_s(t))$. It can be seen that for sufficiently small τ, the filter will approximate $R_c x_2$. Furthermore, if $\lim_{t\to\infty} x_2(t) = 0$ then $\lim_{t\to\infty} s(t) = 0$ and hence $\lim_{t\to\infty} r(t) = 0$, thus achieving internal GAS of the equilibrium $x_a = 0$ for Σ. Consider the simpler case where $r(t) = |s(t)|$. It would be of interest to know how closely $z(t)$ tracks $s(t)$. To this end set $\tau = R_c/\hat{G}$, so that $\dot{s} = \hat{G}(x_2 - s/R_c)$, which is equivalent to Maxwell's viscoelastic model. Define the tracking error $\tilde{z}(t) = z(t) - s(t)$ and the error function $V(\tilde{z}) = (\tilde{z})^2 = (z-s)^2$, the directional derivative of which satisfies

$$\dot{V}(\tilde{z}) = 2(z - s, \dot{z} - Gx_2) + 2(z - s, \hat{G}x_2 - \dot{s}) + 2(z - s, Gx_2 - \hat{G}x_2). \tag{4.3.4}$$

The first term in (4.3.4) is negative due to the variational inequality (4.3.1) so that inserting $\dot{s} = \hat{G}(x_2 - s/R_c)$ yields

$$\dot{V}(\tilde{z}) \le -2\frac{\hat{G}}{R_c}(s, s-z) + 2\left|\tilde{G}\right\|\tilde{z}\|x_2|, \tag{4.3.5}$$

where $\tilde{G} = G - \hat{G}$.

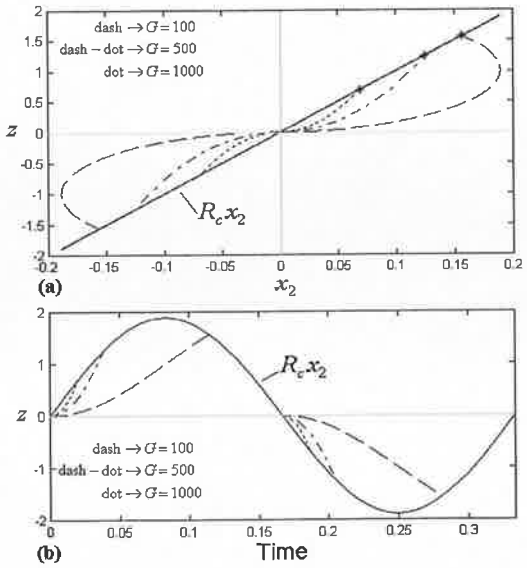

Fig 4.6 Simulation of EP model with $x_2(t) = A\omega\sin(\omega t)$ and $r(t) = R_c|x_2(t)|$, $A = .01, \omega = 6\pi, R_c = 10$. The stared points in (a) are given by $(x_2^*, R_c x_2^*)$, where $x_2^* = A\omega\sin(\omega\Delta t)$.

In order to proceed further, it needs to be shown that $2(s, s-z) \ge (s-z)^2$.

Suppose $2(s, s-z) < (s-z)^2$, then multiplying out both sides yields $s^2 < z^2$, contradicting the fact that $|z(t)| \le r(t) = |s(t)|$. Using the obtained inequality

$$\dot{V}(\tilde{z}) \le -\frac{\hat{G}}{R_c}(s-z)^2 + 2\left|\tilde{G}\right\|\tilde{z}\|x_2| \le -\frac{\hat{G}}{R_c}V(\tilde{z}) + 2\left|\tilde{G}\right\|x_2|\sqrt{V(\tilde{z})}, \tag{4.3.6}$$

and hence

$$|\tilde{z}(t)| \le |\tilde{z}(0)|e^{-(\hat{G}/2R_c)t} + 2R_c\left|1 - G/\hat{G}\right\|x_2\|_\infty\left(1 - e^{-(\hat{G}/2R_c)t}\right) \tag{4.3.7}$$

The tracking error can thus be made arbitrarily small by suitable choice of $\hat{G}$ and R_c. Indeed if $\hat{G} = G$, then the tracking error will converge to zero exponentially. Note that if $\hat{G} = G$, then the two systems have the same energy function, that is $H_Z(\cdot) = H_S(\cdot) = 0.5(\cdot)^2/G$. The power flow for each system is given by

$$\begin{aligned} \dot{H}_Z(z) &= x_2 z - \Phi(r(t), z, x_2) = x_2 z - r(t)|x_2 - \dot{z}/G|, \\ \dot{H}_Z(s) &= x_2 s - s^2/R_c. \end{aligned} \tag{4.3.8}$$

Thus if $\hat{G} = G$ and the control $r(t) = |s(t)|$ is applied, then (4.3.8) implies that the dissipation rate for the EP model $\Phi(|s(t)|, z(t), x_2(t))$ converges to the quadratic dissipation rate $z^2(t)/R_c$ as $t \to \infty$. The effect of this "feedforward" control is to shape the systems dissipation.

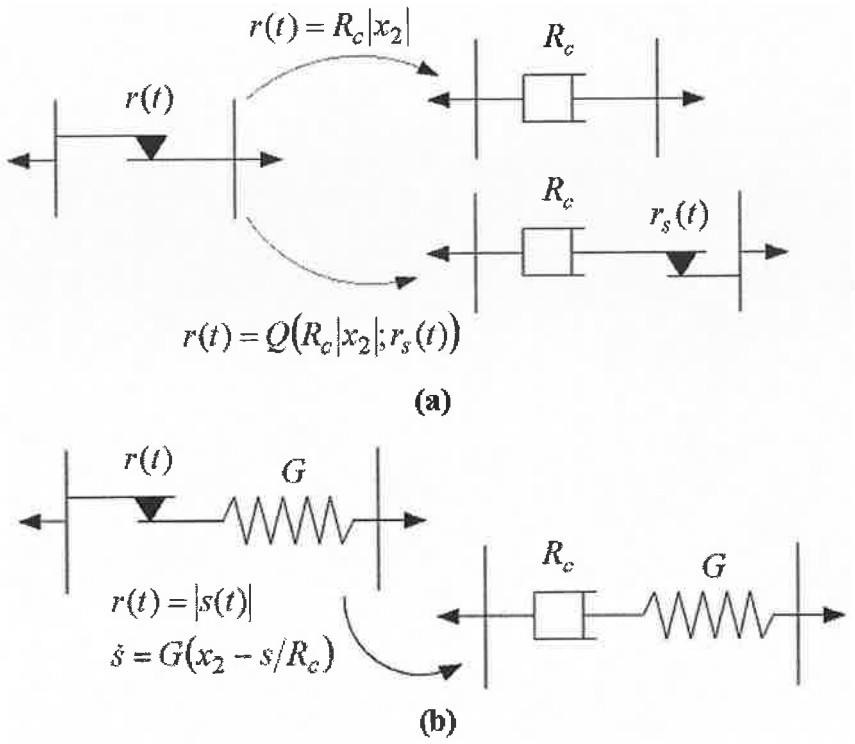

Fig 4.7 Illustration of dissipation shaping control.

To recap, a controllable friction element in isolation is purely dissipative, with dissipation rate $r(t)|x_2|$. By suitable choice of control the friction element can be made to behave exactly like other purely dissipative elements, for example, like a linear viscous element with dissipation rate $R_c x_2^2$, or a viscous element in series with a controllable friction element, with dissipation rate $Q(R_c|x_2|; r_s(t))|x_2|$, see Fig 4.7 (a).

The EP model on the other hand consists of a spring in series with a controllable friction element. That is, it consists of a fixed conservative element, capable of storing energy (has memory), in series with a purely dissipative element, whose behaviour can be controlled. The presence of the spring means that the EP model cannot behave exactly like a purely dissipative system. A more suitable goal would be to try an make the EP model behave like a system consisting of a fixed spring in series with a dissipative element, with a more desirable dissipation rate than the friction element. Indeed, it was shown above that by choosing the control $r(t) = |s(t)|$, where $s(t)$ is the solution of the

Maxwell model, the dissipation rate associated with the EP model converges to z^2/R_c, see Fig 4.7(b).

Now, in analogy with the constrained control $r(t) = Q\big(R_c|x_2|; r_s(t)\big)$, consider the constrained Maxwell type model in Fig 4.8. For simplicity, this model will be referred to as the EVP model (elastic-viscous-plastic). The corresponding constitutive equations will be derived using the internal variable formalism of §3.

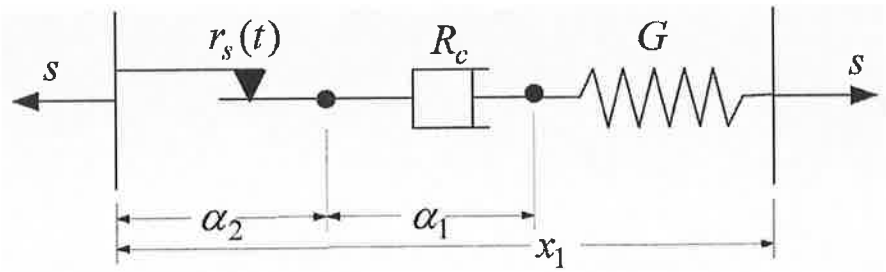

Fig 4.8 Constrained Maxwell or EVP model

From inspection of Fig 4.8 it can be seen that the model is completely defined by the internal energy and dissipations function

$$\begin{aligned} H_S(x_1,\alpha) &= \frac{1}{2}G(x_1-\alpha_1-\alpha_2)^2, \\ \Phi_S(\dot{\alpha};r_s(t)) &= R_c\dot{\alpha}_1^2 + r_s(t)|\dot{\alpha}_2|. \end{aligned} \tag{4.3.9}$$

Following the same reasoning as in §3, one obtains the dissipation potentials

$$\begin{aligned} D(\dot{\alpha};r_s(t)) &= \frac{1}{2}R_c\dot{\alpha}_1^2 + r_s(t)|\dot{\alpha}_2|, \\ D^*(\mathrm{A};r_s(t)) &= \frac{1}{2R_c}\mathrm{A}_1^2 + I\big(\mathrm{A}_2;\mathbf{C}_s(t)\big), \end{aligned} \tag{4.3.10}$$

where $C_s(t) = [-r_s(t), r_s(t)]$ and $\mathrm{A} = [\mathrm{A}_1, \mathrm{A}_2]^{\mathrm{T}}$ is the thermodynamic force conjugate to $\alpha = [\alpha_1, \alpha_2]^{\mathrm{T}}$. Taking the differentials of the potentials gives

$$\begin{aligned} s &= \frac{\partial H_S}{\partial x_1} = G(x_1-\alpha_1-\alpha_2), \\ \mathrm{A}_1 &= -\frac{\partial H_S}{\partial \alpha_1} = G(x_1-\alpha_1-\alpha_2) = s, \\ \mathrm{A}_2 &= -\frac{\partial H_S}{\partial \alpha_2} = G(x_1-\alpha_1-\alpha_2) = s. \end{aligned} \tag{4.3.11}$$

and

$$\dot{\alpha}_1 = \partial_{\mathrm{A}_1} D^*(\mathrm{A}; r_s(t)) = \frac{\mathrm{A}_1}{R_s},$$
$$\dot{\alpha}_2 \in \partial_{\mathrm{A}_2} D^*(\mathrm{A}; r_s(t)) = N(\mathrm{A}_2; \mathbf{C}_s(t)). \tag{4.3.12}$$

Combining (4.3.11) and (4.3.12) leads to the variational inequality

$$\Sigma_S \begin{cases} \langle Gx_2 - Gs/R_c - \dot{s}, s - \varphi \rangle \geq 0 & \forall |\varphi| \leq r_s(t), \\ |s(t)| \leq r_s(t) & \forall t \geq 0. \end{cases} \tag{4.3.13}$$

The integral energy balance for Σ_S is simply

$$H_S(s(t)) - H_S(s(0)) + \frac{1}{R_c}\int_0^t s^2(\tau)d\tau + \int_0^t \overline{\Phi}_S(\tau)d\tau = \int_0^t s(\tau)x_2(\tau)d\tau, \tag{4.3.14}$$

where the frictional dissipation rate $\overline{\Phi}_S(s, x_2; r_s(t)) = \Phi_S(s, x_2; r_s(t)) - s^2/R_c \geq 0$ is given by

$$\overline{\Phi}(s, x_2; r_s(t)) = \begin{cases} sx_2 - s^2/R_c - \dot{H}_s(r_s(t)) & \text{if } H_s(s(t)) = H_s(r_s(t)), \\ & \text{and } \langle s, x_2 - s/R_c \rangle > \dot{H}_s(r_s(t)), \\ 0 & \text{otherwise.} \end{cases} \tag{4.3.15}$$

From (4.3.14) and (4.3.15) it can be seen that Σ_S is strictly passive (fully dissipative state space), in contrast with the EP model. A simple calculation using $H_S(s)$ yields the estimate

$$|s(t)| \leq \min\left(r_s(t), |s(t_0)|e^{-G(t-t_0)/R_c} + G\int_{t_0}^t e^{-G(t-\tau)/R_c}|x_2(\tau)|d\tau \right), \tag{4.3.16}$$

from which it follows that if x_2 tends to zero with time, then so will s. Using the material in §C.3, it can be shown that if $x_1 \in C^{0,1}([0,T];\Re_+)$ and $r_s \in C^{0,1}([0,T];\Re_+) \cap [0,\bar{r}]$, for some $T > 0$ then (4.3.13) has a unique solution $s \in C^{0,1}([0,T];\Re_+)$, which depends continuously on the initial conditions. If the conditions on x_2 and r_s hold on each compact subset of $\Re_+$, then the solution $s(t; s(0), x_1(\cdot), r_s(\cdot))$ has a unique extension over $\Re_+$. It follows that $r(t) = |s(t)|$ defines an admissible control (note that since $|s(t)| \leq r_s(t) \leq \bar{r}$ inequality (4.1.5) still holds). Now setting $r(t) = |s(t)|$ and consider the error energy $V(\tilde{z}) = (z-s)^2$, the directional derivative of which satisfies

$$\dot{V}(\tilde{z}) = 2(z - s, \dot{z} - Gx_2) + 2\left(z - s, Gx_2 - \frac{G}{R_c}s - \dot{s} \right) + 2\frac{G}{R_c}(s, s - z). \tag{4.3.17}$$

Since $|z(t)| \le |s(t)| \le r_s(t), \forall t \ge 0$, the first two terms in (4.3.17) are negative and hence

$$\dot{V}(\tilde{z}) \le -2\frac{G}{R_c}(s, s-z) \le 0. \tag{4.3.18}$$

Using the inequality $2(s, s-z) > (s-z)^2$ in (4.3.18) shows that the tracking error converges to zero exponentially. However, it is also possible to prove finite time convergence. That is, for any admissible set of initial conditions $|z(0)| \le |s(0)| \le |r_s(0)|$ a, there exists a finite time τ, such that $z(t) = s(t), \forall t \ge \tau \ge 0$. There are two possibilities. First, if there exists a time t_1, such that $s(t_1) = 0$, then $z(t_1) = 0$ and by (4.3.18) $z(t) = s(t), \forall t \ge t_1$. The second possibility is that s remains nonzero (and sign definite by continuity), for all $t \ge 0$. In this case, there exits a positive constant $\varepsilon > 0$, such that $|s(t)| \ge \varepsilon$ for all $t \ge 0$. Suppose that $z(t) \ne s(t)$ for all $t \ge 0$, then $\text{sgn}(s(t)) = \text{sgn}(s(t) - z(t))$ since $|z(t)| \le |s(t)|$, and (4.3.18) can be rewritten as

$$\dot{V}(\tilde{z}) \le -2\frac{G}{R_c}|s\|s-z| \le -2\frac{G}{R_c}\varepsilon|\tilde{z}| = -2\frac{G}{R_c}\varepsilon\sqrt{V(\tilde{z})} \le 0, \tag{4.3.19}$$

integrating (4.3.19) and using $\sqrt{V(\tilde{z}(t))} = |\tilde{z}(t)|$ gives

$$|\tilde{z}(t)| \le |\tilde{z}(0)| - \varepsilon\frac{G}{R_c}t. \tag{4.3.20}$$

But the right hand side of (4.3.20) is negative for $t \ge \tau > R_c|z(0)|/G\varepsilon$, implying that $z(t) = s(t), \forall t \ge \tau$. In some sense this result is redundant, since $s(t)$ is a control variable and it is possible to simply set $s(0) = 0$. It follows that for the purposes of analysis, it is sufficient to consider the controlled system,

$$\Sigma\begin{cases}\Sigma_X\begin{cases}\dot{x}_1 = x_2\\ \dot{x}_2 = -Rx_2 - Kx_1 - h(x_1) - z + b(t)\end{cases}\\ \Sigma_Z\begin{cases}\langle Gx_2 - Gz/R_c - \dot{z}, z - \varphi\rangle \ge 0, \quad \forall|\varphi| \le r_s(t),\\ |z(t)| \le r_s(t), \quad \forall t \ge 0.\end{cases}\end{cases} \tag{4.3.21}$$

with $r_s(t)$ acting as the new control variable. Now consider the Liapunov function

$$V(x_a) = \left(\frac{1}{2}(2K + \rho R^2)x_1^2 + \rho R x_1 x_2 + x_2^2 + \frac{1}{G}z^2\right) + 2\int_0^{x_1} h(s)ds. \tag{4.3.22}$$

A sufficient condition for the term on brackets to be positive definite is that $\rho \in (0,2)$.

Assuming this to be the case and using (1.4), it is easily shown that there exist two constant $c_2 > c_1 > 0$ such that $c_1|x_a|^2 \le V(x_a) \le c_2|x_a|^2$ ($x_a = (x,z)$). Taking the directional derivative of $V(x_a)$ along the solutions of (4.3.21), and using (4.1.4) yields

$$\begin{aligned}\dot{V}(x_a) &= -\left((2-\rho)Rx_2^2 + \rho RKx_1^2 + \rho Rh(x_1)x_1 + \rho Rx_1 z + 2z^2/R_c\right) \\ &\quad 2\left\langle z, \dot{z} + Gz/R_c - Gx_2\right\rangle/G + \left(\rho Rx_1 + 2x_2\right)b(t), \\ &\le -\left((2-\rho)Rx_2^2 + \rho RKx_1^2 + \rho Rx_1 z + 2z^2/R_c\right) + \left(\rho R|x_1| + 2|x_2|\right)|b(t)|.\end{aligned} \tag{4.3.23}$$

A sufficient condition for the quadratic term in brackets to be positive definite is that $0 < \rho \le \min(2, 8K/RR_c)$. Choosing ρ to satisfy the proceeding inequality, and following the same procedures as in §2.2 it can be shown that there exist positive constants, $\beta, \gamma, c > 0$ (not the same as in (4.1.5)) such that

$$|x_a(t)| \le \beta|x_a(0)|e^{-ct} + \gamma\|b\|_\infty\left(1 - e^{-ct}\right). \tag{4.3.24}$$

From (4.3.24) it can be seen that if $b(t) \equiv 0$ then $x_a = 0$ is a GES equilibrium for (4.3.21). Furthermore, for nonzero $b(t)$, all solutions of (4.3.21) ($x_a(t) = x_a(t; x_a(0), r_s(\cdot), b(\cdot))$), converge to a ball in $\Re^3$, whose radius is proportional to $\|b\|_\infty$. The important point being that, compared with inequality (4.1.5), the radius of the ball is independent of $r_s(t)$, a point which will prove useful when discussing periodic solutions. It follows that the dissipation shaping control $r_s(t) = |s(t)|$, where $s(t; s(0), x_1(\cdot), r_s(\cdot))$ is a solution of (4.3.13), improves both the internal and external stability properties of Σ. In order to provide a comparison with the control $-F(t) = Q(R_c x_2; r_s(t))$, a simple singular perturbation type analysis will be performed on (4.3.21). The idea of the analysis to follow, is to show that if the constant R_c^2/G is sufficiently small, then it is reasonable to expected that the motions of Σ_X in (4.3.21) will converge into a cylinder about the motions of the system Σ_Y

$$\Sigma_Y \begin{cases} \dot{y}_1 = y_2 \\ \dot{y}_2 = -Ky_1 - Ry_2 - h(y_1) - Q(R_c y_2; r_s(t)) + b(t), \end{cases} \tag{4.3.25}$$

the radius of which is proportional to R_c^2/G. Now multiplying the variational inequality for Σ_Z in (4.3.21) by R_c/G and setting $\varepsilon = R_c/G$ yields

$$\left\langle R_c x_2 - z - \varepsilon\dot{z}, z - \varphi\right\rangle \ge 0, \quad \forall|\varphi| \le r_s(t). \tag{4.3.26}$$

Since G is assumed to be several orders of magnitude greater than all other parameters, $\varepsilon = R_c/G$ appears to be a suitable choice for the perturbation parameter. Note that $\varepsilon = R_c/G$ is the characteristic time scale associated with the Maxwell model.

From (4.3.26), it can be seen that when is ε sufficiently small, $z(t)$ will evolve on a much faster time scale than $x(t)$. Now, the basic idea of singular perturbation theory, is to first set $\varepsilon = 0$, and then to solve (4.3.26) for z in terms of x_2 and $r_s(t)$. This is called the quasi-steady state function. The quasi-steady state function is then substituted into $\sum_X$, in order to form a reduced order system. The next step is to show that for ε sufficiently small the solutions of the full model will converge into some neighbourhood of the solutions of the reduced model. If this can be achieved, it will also provide a justification for using the reduced model in subsequent analysis. Unfortunately, standard singular perturbation theory cannot be applied in the present case, as it requires that the differential equations satisfying certain strict smoothness properties, which are clearly absent is $\sum_Z$ (the reader is referred to [82] , for a nice development of singular perturbation theory). That said, it will still be possible to obtain some useful results.

Since $|z(t)| \le r_s(t) \le \bar{r}$, inequality (4.1.5) applies to all solutions of $\sum$. In particular, there exists a positive constant κ_X, independent of G and R_c, such that $\|\dot{x}\|_\infty \le \kappa_X$. The first step in the analysis is to set $\varepsilon = 0$ in (4.3.26) and to solve the resulting inequality in terms of x_2 and $r_s(t)$. The goal is to find the quasi-steady state function $z = f_z(x_2, r_s(t))$ such that

$$\langle R_c x_2 - f_z(x_2, r_s(t)), f_z(x_2, r_s(t)) - \varphi \rangle \ge 0, \quad \forall |\varphi| \le r_s(\tau), \tag{4.3.27}$$

and $|f_z(x_2, r_s(t))| \le r_s(t), \forall t \ge 0$. It is easily seen that $f_z(x_2, r_s(t)) = Q(R_c x_2; r_s(t))$ solves (4.3.27), which becomes $\langle P(R_c x_2; r_s(t)), Q(R_c x_2; r_s(t)) - \varphi \rangle \ge 0$, $\forall |\varphi| \le r_s(t)$, where $P(R_c x_2; r_s(t)) = R_c x_2 - Q(R_c x_2; r_s(t))$ (see §A.2 for details). The result is intuitively obvious, as the ratio $\varepsilon = R_c/G$ tends to zero, the EVP model in Fig 4.8 converges to the series combination of the viscous element and friction element shown in Fig 4.7(b).

Substituting $f_z(x_2, r_s(t)) = Q(R_c x_2; r_s(t))$ for z in (4.3.21) yields the reduced order system, which corresponds with $\sum_Y$ in (4.3.25). In order to prove that the asymptotic

distance between the solutions $x(t)$ of Σ_X and $y(t)$ of Σ_Y, can be made arbitrarily small, it needs to be shown that the error

$$p(t) = z(t) - Q(R_c x_2(t), r_s(t)), \tag{4.3.28}$$

is UUB, with an ultimate bound which is a continuous, increasing function of ε. Testing the inequality $\langle P(R_c x_2; r_s(t)), Q(R_c x_2; r_s(t)) - \varphi \rangle \geq 0$, $\forall |\varphi| \leq r_s(t)$, with $\varphi = z(t)$ and using (4.3.28) gives $\langle P(R_c x_2; r_s(t)), p(t) \rangle \leq 0$. The next step is to obtain a variational inequality defining the evolution of $p(t)$. A slight problem arises at this point because the function $Q(R_c x_2(t); r_s(t))$ does not have a classical derivative at the points $R_c x_2(t) = \pm r_s(t)$. However $Q(R_c x_2(t); r_s(t))$ does satisfy the Lipschitz type inequality (see §A.2)

$$|Q(R_c x_2(t); r_s(t)) - Q(R_c x_2(t'); r_s(t'))| \leq R_c |x_2(t) - x_2(t')| + |r_s(t) - r_s(t')|. \tag{4.3.29}$$

Combining (4.3.29) with the fact that $r_s(t)$ and $x_2(t)$ are Lipschitz continuous, implies that the composite function $\mathrm{Q}(t) = Q(R_c x_2(t); r_s(t))$ is Lipschitz and hence differentiable almost everywhere. Furthermore inequality (4.3.29) implies that at those points where the derivative does exist it satisfies the estimate $|\dot{\mathrm{Q}}(t)| \leq R_c \kappa_X + \kappa_r = \kappa_Q$, where κ_r is the Lipschitz constant for $r_s(t)$. Now, differentiating (4.3.28), inserting the result into (4.3.26) and using the identity $R_c x_2 = P(R_c x_2; r_s(t)) + Q(R_c x_2; r_s(t)), \forall t \geq 0$, gives

$$\langle P(R_c x_2; r_s(t)) - \varepsilon \dot{\mathrm{Q}}(t) - p - \varepsilon \dot{p}, p + Q(R_c x_2; r_s(t)) - \varphi \rangle \geq 0, \ \forall |\varphi| \leq r_s(t) \tag{4.3.30}$$

almost everywhere. Testing (4.3.30) with $\varphi = Q(R_c x_2(t); r_s(t))$ and using the inequality $\langle P(R_c x_2; r_s(t)), p(t) \rangle \leq 0$, yields

$$\langle -\varepsilon \dot{\mathrm{Q}}(t) - p - \varepsilon \dot{p}, p \rangle \geq 0, \tag{4.3.31}$$

which implies that

$$\frac{d}{dt} p^2 \leq -\frac{2}{\varepsilon} p^2 - 2\dot{\mathrm{Q}}(t) p \leq -\frac{2}{\varepsilon} p^2 + 2\kappa_Q |p|, \tag{4.3.32}$$

and hence

$$\begin{aligned} |p(t)| &\leq |p(0)| e^{-t/\varepsilon} + \varepsilon \kappa_Q \left(1 - e^{-t/\varepsilon}\right) \\ &= |p(0)| e^{-t/\varepsilon} + \frac{R_c}{G} \left(\kappa_X R_c + \kappa_r\right) \left(1 - e^{-t/\varepsilon}\right), \end{aligned} \tag{4.3.33}$$

implying that p is UUB with ultimate bound $\varepsilon\kappa_Q$. In particular, if $z(t)$ and $x_2(\tau)$ are periodic, then so is $p(t)$, in which case $|p(t)| \le \varepsilon\kappa_Q, \forall t \ge 0$. With inequality (4.3.33) in hand it is now possible to analyze the asymptotic behaviour of the error function $\tilde{x}(t) = x(t) - y(t)$, defining the distance between the solutions of Σ_X and Σ_Y. Using (4.3.21) and (4.3.25) it can be seen that the difference $\tilde{x}(t)$ satisfies

$$\begin{aligned} \dot{\tilde{x}}_1 &= \tilde{x}_2 \\ \dot{\tilde{x}}_2 &= -R\tilde{x}_2 - K\tilde{x}_1 - \tilde{h}(\tilde{x}_1,t) - \tilde{Q}(\tilde{x}_2,t) - p(t), \end{aligned} \tag{4.3.34}$$

where $\tilde{h}(\tilde{x}_1;t) = h(\tilde{x}_1 + y_1(t)) - h(y_1(t))$ and

$\tilde{Q}(\tilde{x}_2;t) = Q(\tilde{x}_2 + y_2(t);r_s(t)) - Q(y_2(t);r_s(t))$. By construction, these nonlinearities satisfy the estimates

$$0 \le \left(\tilde{h}(\tilde{x}_1;t),\tilde{x}_1\right) \le L\tilde{x}_1^2,\ 0 \le \left(\tilde{Q}(\tilde{x}_2;t),\tilde{x}_2\right) \le R_c\tilde{x}_2^2, \tag{4.3.35}$$

for all $t \ge 0$. Consider the Liapunov function $V(\tilde{x}) = 0.5\left(2K + aR^2\right)\tilde{x}_1^2 + aR\tilde{x}_1\tilde{x}_2 + \tilde{x}_2^2$, which is positive definite for $a \in (0,2)$. The derivative of $V(\tilde{x})$ along the solutions of (4.3.34) satisfies

$$\begin{aligned} \dot{V}(\tilde{x}) &= -(2-a)R\tilde{x}_2^2 - aRK\tilde{x}_1^2 - aR\tilde{h}(\tilde{x}_1;t)\tilde{x}_1 - 2\tilde{h}(\tilde{x}_1;t)\tilde{x}_2 \\ &\quad - 2\tilde{Q}(\tilde{x}_2;t)\tilde{x}_2 - aR\tilde{Q}(\tilde{x}_2;t)\tilde{x}_1 - \left(aR\tilde{x}_1 + 2\tilde{x}_2\right)p(t), \\ &\le -(2-a)R\tilde{x}_2^2 - aRK\tilde{x}_1^2 - \frac{aR}{L}\tilde{h}^2(\tilde{x}_1;t) - 2\tilde{h}(\tilde{x}_1;t)\tilde{x}_2 \\ &\quad - \frac{2}{R_c}\tilde{Q}^2(\tilde{x}_2;t) - aR\tilde{Q}(\tilde{x}_2;t)\tilde{x}_1 + \left(aR|\tilde{x}_1| + 2|\tilde{x}_2|\right)|p(t)|, \\ &\le -\frac{1}{aR}\left(a(2-a)R^2 - L\right)\tilde{x}_2^2 - aR\left(K - aRR_c/8\right)\tilde{x}_1^2 + \left(aR|\tilde{x}_1| + 2|\tilde{x}_2|\right)|p(t)|, \end{aligned} \tag{4.3.36}$$

where (4.3.35) has been used in passing to the second inequality and Young's inequality (see §A.1) has been used to obtain the final inequality. Tacitly assuming that $L < R^2$, set $a = \min\left\{\theta \in (0,1) \mid \theta(2-\theta)R^2 > L\right\}$, so that picking $R_c < 8K/aR$ will ensure that the coefficients of $\tilde{x}_1^2$ and $\tilde{x}_2^2$ are positive. Note that these conditions are only sufficient and by no means necessary, different results can be obtained using different Liapunov functions. Assuming that a suitable value for a exits, it follows from $c_1|\tilde{x}|^2 \le V(\tilde{x}) \le c_2|\tilde{x}|^2$, that there exists positive constants $c_3, c_4 > 0$ such that

$$\dot{V}(\tilde{x}) \le -2c_3V(\tilde{x}) + 2c_4\sqrt{V(\tilde{x})}|p(t)|. \tag{4.3.37}$$

and after the usual manipulations

$$|\tilde{x}(t)| \le \sqrt{\frac{c_2}{c_1}}|\tilde{x}(0)|e^{-c_3 t} + \frac{c_4}{\sqrt{c_1}}\int_0^t e^{-c_3(t-s)}|p(s)|ds. \tag{4.3.38}$$

Without loss of generality it will be assumed that $r_s(0)=0$, implying $p(0)=0$, so that inserting (4.3.33) into (4.3.38) yields

$$\begin{aligned}|\tilde{x}(t)| &\le \sqrt{\frac{c_2}{c_1}}|\tilde{x}(0)|e^{-\alpha_3 t} + \frac{\varepsilon c_4 \kappa_Q}{\sqrt{c_1 c_3}}(1-e^{-c_3 t}).\\ &= \sqrt{\frac{c_2}{c_1}}|\tilde{x}(0)|e^{-\alpha_3 t} + \frac{c_4}{G\sqrt{c_1 c_3}}\left(R_c^2\kappa_X + R_c\kappa_r\right)(1-e^{-c_3 t}).\end{aligned} \tag{4.3.39}$$

Note that $c_i, i=1,\ldots,4$, κ_X and κ_r are all independent of G. It follows from (4.3.39) that the solutions of Σ_X converge into a cylinder (in $\Re^2\times\Re_+$) surrounding the solutions of Σ_Y, the radius of which can be made arbitrarily small by making G suitably large. Ideally the stiffness, G, of the damper would be large enough to ensure that the response of $z(t)$ of (4.3.13) forms a close approximation of $Q(R_c x_2; r_s(t))$, over a range of values of R_c. Interestingly the bound on R_c can be reduced if $r_s(t)$ is $0T$-recurrent, for suitably small T. The usefulness of this result will become clearer in §5.

It is important to note that the analysis performed above is not restricted to the reference model (4.3.13). Indeed, it can be shown that perfect tracking is achievable if the reference model defines a passive map from the velocity, x_2, to the output, s and if it has a storage function which is identical to that of the EP model. This applies to models derived using the internal variable framework of §3, starting with the same internal energy function but with a more desirable dissipation function. For example consider replacing the internal energy and dissipation function in (4.3.9) with

$$\begin{aligned}H_S(x_1,\alpha) &= \frac{1}{2}G(x_1-\alpha_1-\alpha_2)^2 = \frac{1}{2G}s^2,\\ \Phi_S(\dot{\alpha};r_s(t)) &= g(\dot{\alpha}_1)\dot{\alpha}_1 + r_s(t)|\dot{\alpha}_2|.\end{aligned} \tag{4.3.40}$$

Where $g\in C(\Re;\Re)$ is an increasing function, satisfying $g(0)=0$. Let $\hat{g}\in C(\Re;\Re)$ denote the inverse of g, that is $g(\hat{g}(x))=x$ for all $x\in\Re$. In terms of rheological elements (4.3.40) represents a series combination of a linear spring, a nonlinear viscous damper and a friction element with control $r_s(t)$. Now, following the same reasoning as in §3 (or above) leads to the variational inequality

$$\Sigma_S\begin{cases}\langle Gx_2 - G\hat{g}(s) - \dot{s}, s-\varphi\rangle \ge 0 & \forall|\varphi|\le r_s(t),\\ |s(t)|\le r_s(t) & \forall t\ge 0.\end{cases} \tag{4.3.41}$$

The integral energy balance for Σ_S is simply

$$H_S(s(t)) - H_S(s(0)) + \int_0^t \hat{g}(s(\tau))s(\tau)d\tau + \int_0^t \overline{\Phi}_S(\tau)d\tau = \int_0^t s(\tau)x_2(\tau)d\tau, \quad (4.3.42)$$

where $\overline{\Phi}_S(s, x_2; r_s(t)) = \Phi_S(s, x_2; r_s(t)) - \hat{g}(s)s \geq 0$ is the nonnegative dissipation rate associated with the friction element. Since $\hat{g}(s)$ is an increasing function and satisfies $\hat{g}(0) = 0$, the dissipation rate $\hat{g}(s)s$ is positive definite. This combined with (4.3.42) implies that (4.3.41) defines a strictly passive map from x_2 to s. Set $r(t) = |s(t)|$ as the control for the EP model Σ_Z and consider the error energy $V(\tilde{z}) = (z-s)^2$, the directional derivative of which satisfies

$$\dot{V}(\tilde{z}) = 2\langle z - s, \dot{z} - Gx_2 \rangle + 2\langle z - s, Gx_2 - G\hat{g}(s) - \dot{s} \rangle + 2G\langle \hat{g}(s), s - z \rangle. \quad (4.3.43)$$

Since $|z(t)| \leq |s(t)| \leq r_s(t), \forall t \geq 0$, the first two terms in (4.3.43) are negative and hence

$$\dot{V}(\tilde{z}) \leq -2G\langle \hat{g}(s), s - z \rangle \leq 0. \quad (4.3.44)$$

Next the proof finite time convergence is given. That is, for any admissible set of initial conditions $|z(0)| \leq |s(0)| \leq |r_s(0)|$, there exists a finite time $\tau \in \Re_+$, such that $z(t) = s(t), \forall t \geq \tau \geq 0$. Obviously, if there exists a time t_1, such that $s(t_1) = 0$, then $z(t_1) = 0$ and by (4.3.48) $z(t) = s(t), \forall t \geq t_1$. Consider the alternative case where s remains nonzero (and sign definite by continuity), for all $t \geq 0$. In this case, there exists a positive constant $\varepsilon > 0$, such that $|\hat{g}(s(t))| \geq \varepsilon$ for all $t \geq 0$. Suppose $z(t) \neq s(t)$ for all $t \geq 0$, then since $\hat{g}(s)$ an increasing function satisfying $\hat{g}(0) = 0$, it follows that $\text{sgn}(\hat{g}(s(t))) = \text{sgn}(s(t) - z(t))$. Equation (4.3.44) can now be rewritten as

$$\dot{V}(\tilde{z}) \leq -2G|\hat{g}(s)||s - z| \leq -2G\varepsilon|\tilde{z}| = -2G\varepsilon\sqrt{V(\tilde{z})} \leq 0, \quad (4.3.45)$$

and hence

$$|\tilde{z}(t)| \leq |\tilde{z}(0)| - \varepsilon\frac{G}{R_c}t. \quad (4.3.46)$$

But the right hand side of (4.3.46) is negative for $t \geq \tau > R_c|z(0)|/G\varepsilon$, implying that $z(t) = s(t), \forall t \geq \tau$. The applicability of this method is not restricted to the EP model either. The author has also applied it with some success to the viscoplastic models §3.5. Some more will be said on this point in the discussions chapter of this thesis.

4.4 Summary

In Section 4.1 an ordinary differential equation, representing the forearm with tremor (Σ_X), was coupled with the controllable EP model (Σ_Z). It was shown that there does not exist an admissible damper control, which can completely cancel the effect of a persistent disturbance on the behaviour of Σ_X. However, using a simple energy based analysis it was shown that if both the tremor and the damper control are T-periodic and the system has a T-periodic solution, then along this periodic solution it is possible to reduce the upper-bound on the average kinetic energy by ensuring that the damper dissipates a suitable amount of energy over each period. Also, if the tremor should vanish, then the state of the system will converge to an equilibrium set, the size of which depends on the limit inferior if the damper control.

Based on these findings, it was conjectured that the goal of tremor suppression might be achieved if a control scheme could be devised which would ensure that if the tremor was periodic, then all solutions of the system would converge to a periodic solution and that along this solution, the damper dissipated a suitable amount of energy. Also, if the tremor should vanish, then the state of the system should converge to zero. In order to gain some insight into how this might be achieved, the influence of the damper control on the qualitative behaviour of the coupled system (Σ) was analyzed in detail using traditional energy-based and Liapunov type techniques.

The objective of Section 4.2 was to obtain sufficient conditions on the damper control which would ensure that the origin is an internal GES equilibrium for Σ, while still allowing some scope for the development of disturbance attenuation schemes. The section begins with a review of some know results for semi-active dampers, including a discussion on the popular bang-bang type control strategies. Finding these results to be inadequate, the notion of a OT-recurrent control was developed. A damper control is said to be OT-recurrent if in each interval of length T there exists a time for which the control is zero. It was shown that if the control is OT-recurrent, then the origin is an internal GES equilibrium for Σ. While this result was obtained without restriction on the size of T, the rate at which the state converges to zero is strongly dependent of the size of T.

Section 4.3 investigates the feasibility of making the EP model behave in a more desirable manner by suitable choice of control. The possibility of making the EP model behave exactly like a passive, memoryless function of the velocity (purely dissipative element) was investigated first. It was shown that this is not possible because he EP model consists of fixed spring in series with a controllable friction element. Which is to say, it consists of a fixed conservative element, capable of storing energy (implying the model has memory), in series with a purely dissipative element, whose behaviour can be controlled. A more suitable goal would be to try to make the EP model behave like a rheological model consisting if a fixed spring with the same stiffness in series with purely dissipative elements, such as the EVP model. Indeed, it was shown that by solving the differential equation for the EVP model and setting the yield stress equal to the absolute value of this solution, then the solution of the EP model will converge to the solution of the EVP model in finite time. More generally, it was shown that the EP model can be made to behave exactly like another rheological model consisting a linear spring with the same stiffness, in series with a dissipative element with more desirable dissipation function (hence the name dissipation shaping).The importance of finite time convergence is that the EP model can be replaced by the new "reference" model for the purposes of analysis. In contrast to the EP model, the dissipation function associated with the EVP model is a positive definite function of the reaction force. As a result, it was shown that by making the EP model behave exactly like the EVP model then the coupled system will be internally GES with respect to the origin, irrespective of variations in the new controllable yield stress. Some singular perturbation type results were also obtained, which will prove extremely useful when discussing tremor attenuation in the next chapter.

The question of existence and stability of the periodic solutions of the coupled system was studied in Appendix C. The approach taken was to establish sufficient conditions for the existence of at least one periodic solution using a suitable fixed point theorem and to then study the stability of these solutions using Liapunov type analysis. Using an asymptotic fixed point theorem, it was shown that if for each set of admissible initial conditions the state of the forearm model is UB and UUB, then the coupled system will have at least one periodic solution. Various conditions on the damper control which would ensure the periodic solution is GES and hence unique, were also investigated. In particular it was shown that if the dissipation shaping control was first used to transform the EP model into the EVP model with T-periodic yield stress, then it is always

possible to select a value for the viscous coefficient of the EVP model, so as to ensure the coupled system has a GES T-periodic solution. This result will be used when investigating tremor suppression in the next chapter.

The analysis performed in this chapter was also intended to illustrate that the variational formulation of the EP model is well suited for analysis and that the thermodynamic origins (well defined energy and dissipation functions) allow for a physical interpretation of many of the results. The importance of establishing existence and regularity results for the solutions of the model under investigation is also evident. For example, the application of the fixed point theorem in Appendix D. relied crucially on the assumption that the solutions depend continuously on the initial conditions.

Chapter 5

Tremor Attenuation

In §2 the control objective was stated as follows: Devise a control strategy for an ER damper which will reduce the oscillations caused by the tremor, without adversely affecting the intentional motion. In this chapter, the feasibility of achieving this objective is briefly tackled, using some of the external stability results from §4. The theoretical results are quite positive and are backed up with numerous simulations.

5.1 Basic results for Tremor attenuation

Consider again the feedback interconnection of the controlled EP model and the forced second order oscillator (see §4.1)

$$\Sigma\begin{cases}\Sigma_X\begin{cases}\dot{x}_1 = x_2\\ \dot{x}_2 = -Kx_1 - Rx_2 - h(x_1) - z + b(t),\end{cases}\\ \Sigma_Z\begin{cases}\langle Gx_2 - \dot{z}, z - \varphi\rangle \geq 0, \quad \forall|\varphi| \leq r(t),\\ |z| \leq r(t),\ \forall t \geq 0.\end{cases}\end{cases} \tag{5.1.1}$$

with total state $x_a(t) = (x(t), z(t))$ and initial condition $x_a(0) \in \Re^2 \times [-r(0), r(0)]$. The nonlinear function $h(x_1) = 0.5L\left(x_1 + \sin(x_1 + q^*) - \sin(q^*)\right)$, where $q^* \in [0, \pi]$ is the desired equilibrium for the system (2.1.8), satisfies $h(0) = 0$ and $0 \leq \big(h(x) - h(y)\big)(x - y) \leq L(x - y)^2$. The damper control r will be called admissible if $r \in C^{0,1}(\Re_+; \Re) \cap [0, \bar{r}]$ for some constant $\bar{r} \geq 0$. The input $b \in C^{0,1}(\Re_+; \Re)$ represents a $T-$periodic disturbance (tremor). Under the assumptions stated above, using inequality (4.1.5) and corollary C.3.1, it can be concluded that Σ has a unique solution $\big(x(t), z(t)\big) = \big(x(t; x_a(0), r(\cdot), b(\cdot)), z(t; x_a(0), r(\cdot), b(\cdot))\big)$ such that $x \in C^{1,1}(\Re_+; \Re^2)$ and $z \in C^{0,1}(\Re_+; \Re)$. Moreover, the solution depends continuously on the initial conditions $x_a(0)$, the input $b(t)$ and the control $r(t)$. For simplicity, the disturbance will be assumed to be sinusoidal, that is $b(t) = A\sin(\omega t + \varphi)$, the parameters A and ω taking values in the intervals $[0, \bar{A}]$ and $[6\pi, 10\pi] = [\underline{\omega}, \bar{\omega}]$ respectively (kinetic tremor see §1.1).

Furthermore, it will be assumed that $\bar{r} \le |\bar{A}|$, so that any solution of Σ will satisfy $|z(t)| \le r(t) \le \bar{A}$ and

$$|x(t)| \le \beta |x(0)| e^{-ct} + \gamma \bar{A}\left(1 - e^{-ct}\right), \tag{5.1.2}$$

for some constants $\beta, \gamma, c > 0$, depending only on R, K and L.

In order to simplify the discussions which follow, when $b(\cdot) = 0$ and $r(\cdot) = 0$ (hence $z(\cdot) = 0$) the motions of Σ_X, $x(t) = x(t; x(0))$, will be referred to as natural motions. When $b(\cdot) \neq 0$ and $r(\cdot) = 0$, the resulting motions of Σ_X, $x(t) = x(t; x(0), b(\cdot))$, will be referred to as perturbed motions. If $b(\cdot) \neq 0$ and $r(\cdot) \neq 0$, the resulting motions of Σ, $x(t) = x\left(t; x_a(0), r(\cdot), b(\cdot)\right)$ and $z(t) = z\left(t; x_a(0), r(\cdot), b(\cdot)\right)$, will be referred to as controlled. Specific "steady state" motions, such as a periodic trajectory, will be referred to as the perturbed or controlled periodic trajectory.

In §2 the control objective was stated as: devise a control strategy for the damper which will reduce the oscillations caused by the tremor, with out adversely affecting the intentional motion. Unfortunately it is very difficult to give a mathematically precise formulation of this objective. If exact cancellation of the tremor were possible, then a suitable objective might be, to devise a control strategy for $r(t)$, which would ensure that the controlled motion of Σ_X converged to the natural motion of Σ_X. While it is tempting to weaken this and suggest that the controlled motion should converge to some small cylinder centred on the natural motion, inside this cylinder the controlled motion could be very jerky or even chaotic, which could be worse than the smooth oscillations caused by the tremor. It has been shown in §2.2 that if $b(\cdot) = r(\cdot) \equiv 0$, then the origin is a GES equilibrium for Σ_X. Thus, for a given set of initial conditions, the natural motion of Σ_X corresponds with exponential convergence to the origin. If in addition $b(t) = A\sin(\omega t + \varphi)$ and $L < R^2$, then the perturbed motion of Σ_X will converge to a unique T-periodic trajectory ($T = 2\pi/\omega$).

All simulations of Σ have been performed in the Simulink/Matlab software package [83], using a fourth-order Runge-Kutta algorithm for Σ_X coupled with an implicit Euler algorithm for the Σ_Z.

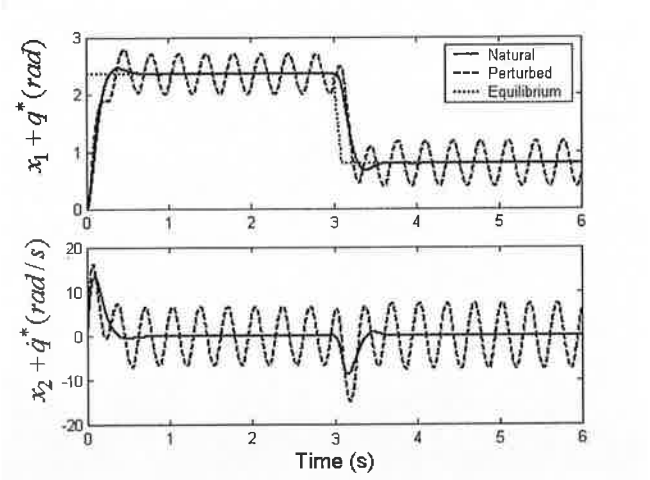

Fig 5.1Example of natural and perturbed motions. The equilibrium signal refers to the value of the desired equilibrium q^* , see §2.1.

A shift in equilibrium occurs between 3 and 3.1 seconds.

A fix time step of 0.0005 seconds was used along with the parameter values $R = 16, K = 90, L = 100$ and $G = 20000$. Fig 5.1 shows an example of the natural and perturbed motions of Σ_X. The equilibrium signal refers to the value of the desired equilibrium q^*, see §2.1 for details. For the purposes of illustration, a shift in equilibrium occurs between 3 and 3.1 seconds. During this period, the representation of Σ given in (5.1.1) is not valid, as there should be an additional disturbance term on the right hand side of Σ_X. However, since this disturbance disappears once the equilibrium shift is made, it will simply be ignored. With reference to Fig 5.1, the control objective might now be stated as: to select $r(\cdot)$ so as to ensure that the controlled motions of Σ_X converge to a periodic trajectory which is contained in a neighbourhood of the origin. The rate at which the controlled motion of Σ_X converges to this trajectory, should be close to the rate at which natural motion converges to origin. Furthermore the averaged kinetic energy for a controlled periodic trajectory should be smaller than that of the unique, perturbed periodic trajectory.

Recall that the natural storage function associated with Σ is given by

(i.e. $H(x,z) = H_X(x) + H_Z(z)$ see §4.1 for details)

$$H(x,z) = \frac{1}{2}(x_2^2 + Kx_1^2) + \int_0^{x_1} h(s)ds + \frac{1}{2G}z^2. \qquad (5.1.3)$$

If the tremor $b(t)$ is a nontrivial T-periodic function and $r(t)$ is an admissible, T-periodic control, the results of §D.2 can be used to show that Σ has at least one T-periodic solution, say $(\bar{x}(t), \bar{z}(t))$. It was also shown in §4.1, that $b([0,T]) \neq 0$

implies $\bar{x}([0,T]) \neq 0$, for all admissible, T-periodic damper controls (i.e. stabilization of the origin is impossible). At this point it will be worthwhile to recall some basic results from §2 and §4. Due to the periodicity of $(\bar{x}(t), \bar{z}(t))$, it follows that $H(\bar{x}(t+T), \bar{z}(t+T)) = H(\bar{x}(t), \bar{z}(t))$ for all $t \geq 0$, so that the energy balance equation (4.1.11) becomes (need only consider the interval $[0,T]$ due to periodicity)

$$\int_0^T b(s)\bar{x}_2(s)ds = \int_0^T R\bar{x}_2^2(s)ds + \int_0^T \overline{\Phi}(s)ds. \tag{5.1.4}$$

where $\overline{\Phi}(t)$ is the rate at which energy is dissipated by the periodic solution of Σ_Z, see equation (4.1.10). Equation (5.1.4) simply implies that the totality of the energy supplied to Σ over an interval of length T, can be partitioned into that dissipated by the motions of Σ_X and that dissipated by Σ_Z. Applying Young's inequality $ab \leq a^2/2R + b^2R/2$ to the left hand side of (5.1.4) and using the fact that $\bar{x}_2([0,T]) \neq 0$, yields

$$\int_0^T b(s)^2 ds \frac{1}{R^2} - \int_0^T \overline{\Phi}(t)ds \frac{2}{R} \geq \int_0^T \bar{x}_2^2(s)ds > 0. \tag{5.1.5}$$

Note that the right hand side of (5.1.5) represents the averaged kinetic energy over $[0,T]$. Now, using the identity $\dot{\bar{x}}_1 = \bar{x}_2$ and applying Holder's inequality (§A.1) to the right hand side of (5.1.5) gives

$$\int_0^T b(s)^2 ds \frac{T}{R^2} - \int_0^T \overline{\Phi}(s)ds \frac{2T}{R} \geq \left(\int_0^T \left|\dot{\bar{x}}_1(s)\right| ds \right)^2 > 0. \tag{5.1.6}$$

Recall that $\int_0^T \left|\dot{\bar{x}}_1(s)\right| ds$ is simply the arc length of the closed curve $\bar{x}_1([0,T])$ and that $\int_0^T \left|\dot{\bar{x}}_1(s)\right| ds \geq \mathrm{osc}_T \bar{x}_1$, where the oscillation is given by $\mathrm{osc}_T \bar{x}_1 = \max_{t\in[0,T)} \bar{x}_1(t) - \min_{t\in[0,T)} \bar{x}_1(t) > 0$. It follows that for a given periodic disturbance, it should at least be possible to reduce the upper bound on the averaged kinetic energy for a controlled T-periodic trajectory and the oscillation of the periodic motion $\bar{x}_1$, by ensuring that Σ_Z exhibits positive dissipation, i.e. $\overline{\Phi}([0,T)) \neq 0$.

The task now is to find an admissible damper control, which will guarantee that the controlled motions converge to a periodic trajectory, on which Σ_Z exhibits positive dissipation (without slowing down the initial transient response too much). If complete knowledge of $b(t) = A\sin(\omega t + \varphi)$ is assumed, then one would be tempted to simply put $r(\cdot) = A$. Referring to Fig 5.2 , it can be seen that effect of the tremor is greatly reduced,

however, the effect on the transient motion is far from favourable (compare Fig 5.1). Recall that the state variable $x_1(t) = q(t) - q^*$ is not measurable, since the desired equilibrium q^* is unknown. It follows that degradation of the convergence rate cannot be avoided by simply switching off the damper control until the $q(t)$ is in some pre-specified neighbourhood of the equilibrium. In addition, as tremor may disappear at some instant (see §2), the damper control should also ensure that if after some time, the tremor vanishes, all motions of Σ converge to the origin. Fig 5.3 compares the natural and controlled motions in the absence of tremor and with $r(\cdot) = E$. In this case it is only possible to conclude that all motions of Σ converge to the set $\mathbf{M} = \{(x, z) \in \Re^2 \times \Re \mid x_2 = 0, h_K(x_1) = -z, |z| \le E\}$, where $h_K(x_1) = Kx_1 + h(x_1)$.

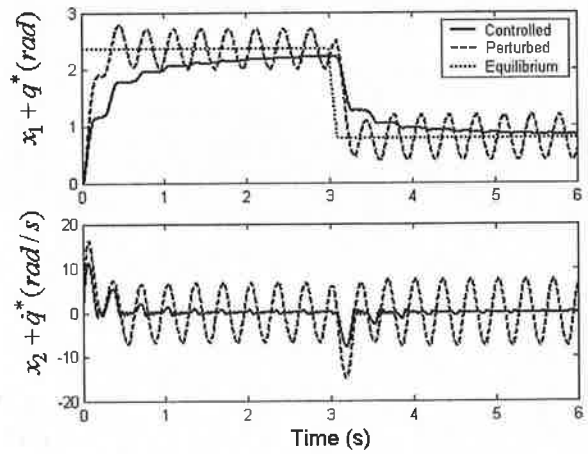

Fig 5.2 Example of perturbed and controlled motions with $r(\cdot) = A$.

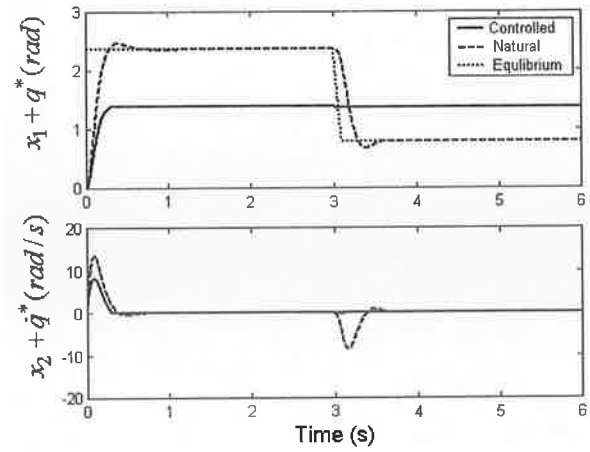

Fig 5.3 Example of natural motion and controlled motions in the absence of tremor and with $r(\cdot) = A$.

In order to gain some insight into possible control strategies, which might overcome these problems, consider replacing Σ_Z in (5.1.1) with a passive, memoryless velocity feedback, to obtain the system

$$\Sigma_Y \begin{cases} \dot{y}_1 = y_2 \\ \dot{y}_2 = -Ky_1 - Ry_2 - h(y_1) - \Theta(y_2;t) + b(t), \end{cases} \tag{5.1.7}$$

where the feedback function $\Theta(y_2;t)$ satisfies $\Theta(y_2;t)y_2 \geq 0$ and $\Theta(0;t) = 0$ for all $t \geq 0$. The derivative of the systems energy $H_Y(y) = 0.5(y_2^2 + Ky_1^2) + \int_0^{y_1} h(s)ds$ along the trajectories of Σ_Y is

$$\dot{H}_Y(y) = -Ry_2^2 - \Theta(y_2,t)y_2 + b(t)y_2. \tag{5.1.8}$$

The simplest choice of feedback is obviously the linear viscous feedback $\Theta(y_2;t) = R_c y_2$, for some constant $R_c > 0$. Let $\bar{y}(t)$ be a T-periodic trajectory Σ_Y. Inserting $\Theta(y_2,t) = R_c y_2$ into (5.1.8), applying Young's inequality and integrating yields the estimate

$$\int_0^T b(s)^2 ds \frac{1}{(R+R_c)^2} \geq \int_0^T \bar{y}_2^2(s)ds > 0. \tag{5.1.9}$$

It follows that the averaged kinetic energy of the T-periodic trajectory $\bar{y}(t)$, can be made arbitrarily small by making R_c suitably large. However, for arbitrary motions of Σ_Y, which are in the process of converging to $\bar{y}(t)$, making R_c too large will lead to an unacceptably slow rate of convergence. Assume for the moment that full knowledge of $b(t)$ is available. Ideally the controlled dissipation rate $\Theta(y_2;t)y_2$, should only be used to counteract the instantaneous supply rate $b(t)y_2$. While exact cancellation of $b(t)y_2$ is impossible using continuous passive feedback, it would make sense to ensure that the instantaneous, controlled dissipation is bounded by $|b(t)||y_2|$, for large y_2 at least.

If discontinuous control is permitted, then a suitable choice would be the controllable friction type feedback $\Theta(y_2;t) = |b(t)|\mathrm{SGN}(y_2)$, where $\mathrm{SGN}(\cdot)$ is the set valued signum function. In §2.3 it was shown that if $\Theta(y_2;t) = |b(t)|\mathrm{SGN}(y_2)$, then the origin is a GAS equilibrium for Σ_Y. Fig 5.4 compares the controlled motions of Σ_Y, corresponding to the linear feedback $\Theta(y_2;t) = R_c y_2$, with $R_c = 10R$, and the discontinuous $\Theta(y_2;t) = |b(t)|\mathrm{SGN}(y_2)$ feedback.

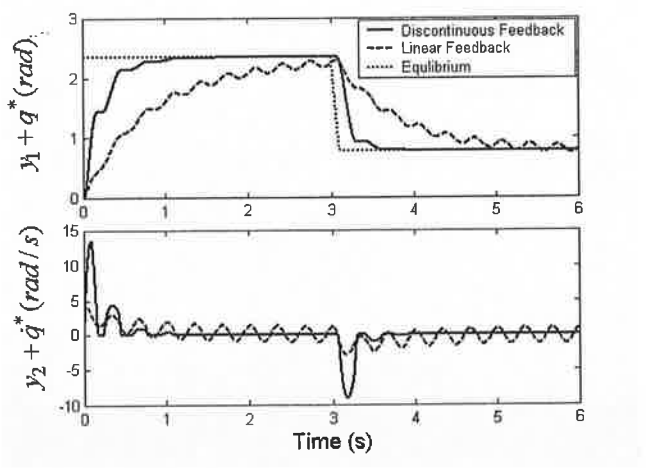

Fig 5.4 Comparison of controlled motions, corresponding to the linear $\Theta(y_2;t) = R_c y_2$ $(R_c = 10R)$ and discontinuous $\Theta(y_2;t) = |b(t)|\mathrm{SGN}(y_2)$, feedbacks.

Comparing with Fig 5.1, it can be seen that in both cases the effect of the disturbance is greatly reduced. However, the motion corresponding to the discontinuous feedback bears a much closer resemblance to the natural motion, than does the motion corresponding to the linear feedback. Fig 5.5 compares the tremor $b(t)$ with the values of linear and discontinuous feedbacks. Comparing with Fig 5.4, it can be seen that the slow rate of convergence, corresponding to the linear feedback, is a direct result of the fact that the feedback itself is unbounded as a function of y_2. It can also be seen that the discontinuous feedback converges to $b(t)$, as $y_2(t) \to 0$, in the sense that, $\lim_{t\to\infty} \int_t^{t+T} \big(b(s) - |b(s)|\mathrm{SGN}(y_2(s))\big) ds = 0$. The discontinuous, friction type, feedback would certainly appear to meet the control objectives (assuming knowledge of $b(t)$).

Motivated by these results, consider the continuous feedback $\Theta(y_2;t) = Q(R_c y_2; r(t))$, which corresponds with a linear viscous element is series with a controllable friction element (see Fig 4.7(a) in §4.3). This control can be seen as a continuous approximation of the discontinuous, friction type feedback. Setting $r(t) = \alpha|b(t)|$ with $\alpha \in [0,1]$, it follows that the controlled dissipation rate will satisfy $0 \le Q(R_c y_2; r(t)) y_2 \le \alpha |b(t)\| y_2|$ as required. Since $Q(R_c y_2; r(t))$ is continuous in y_2, it is impossible to stabilize the origin of Σ_Y when $b(t)$ is a nontrivial T-periodic tremor (as it was with the discontinuous feedback). However, it will now be shown that it is possible to obtain an estimate similar to (5.1.9).

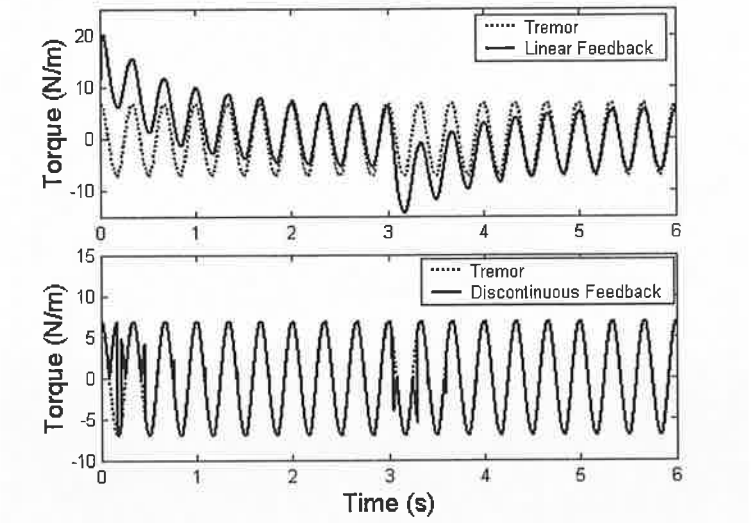

Fig 5.5 Comparison of linear $\Theta(y_2;t) = R_c y_2$ and discontinuous $\Theta(y_2;t) = |b(t)|\mathrm{SGN}(y_2)$, feedbacks

Recall that the operator $P(R_c y_2; r(t))$, given by $P(R_c y_2; r(t)) = R_c y_2 - Q(R_c y_2; r(t))$, satisfies the variational inequality $\langle P(R_c y_2; r(t)), Q(R_c y_2; r(t)) - \varphi \rangle \geq 0, \forall |\varphi| \leq r(t)$. Inserting $\Theta(y_2;t) = Q(R_c y_2; r(t))$ into (5.1.8) gives

$$\begin{aligned}
\dot{H}_Y(y) &= -Ry_2^2 - Q(R_c y_2; r(t)) y_2 + b(t) y_2, \\
&\leq -\frac{R}{2} y_2^2 + \frac{(1-\alpha)^2}{2R} b^2(t) + \frac{1}{R_c} \left(Q(R_c y_2; r(t)), \alpha b(t) - Q(R_c y_2; r(t)) \right) \\
&\quad + \frac{1}{R_c} \left(P(R_c y_2; r(t)), \alpha b(t) - Q(R_c y_2; r(t)) \right), \\
&\leq -\frac{R}{2} y_2^2 + \left(\frac{(1-\alpha)^2}{2R} + \frac{\alpha^2}{4R_c} \right) b^2(t),
\end{aligned} \tag{5.1.10}$$

where the fact that $\alpha b(t) \in \alpha |b(t)| [-1,1]$ and Young's inequality have been employed. Let $\bar{y}(t)$ be a T-periodic solution of Σ_Y. Integrating (5.1.10) over $[0,T]$ and using the fact that $H_Y(\bar{y}(T)) = H_Y(\bar{y}(0))$ yields the estimate

$$\int_0^T b(s)^2 ds \left(\frac{(1-\alpha)^2}{R^2} + \frac{\alpha^2}{2RR_c} \right) \geq \int_0^T \bar{y}_2^2(s) ds > 0. \tag{5.1.11}$$

If $\alpha = 1$, then the coefficient on the left hand side of (5.1.11) is $1/(2RR_c)$, implying that the average kinetic energy can be made arbitrarily small, by making R_c suitably large. Based on inequality (5.1.11) and the fact that the controlled dissipation rate is now bounded by $\alpha |b(t)| |y_2|$, it should be possible to pick R_c and α, so as to ensure that the

controlled motions Σ_Y converge to a unique T-periodic trajectory, with a minimal degradation of the convergence rate (as compared with the natural motion).

Fig 5.6 compares the perturbed and controlled motions of Σ_Y, corresponding to the projected feedback $\Theta(y_2;t) = Q(R_c y_2;\alpha|b(t)|)$, with $\alpha = .9$ and $R_c = 10R$. Comparing Fig 5.6 and Fig 5.5 with Fig 5.4, it can be seen that the projected feedback achieves a level of disturbance attenuation close to that of the Linear Feedback, but with a convergence rate similar to the discontinuous feedback. Furthermore, it can be shown that if R_c is suitably chosen, then the controlled motions of Σ_Y will converge to a unique T-periodic trajectory. Based on the above discussion, it would seem that the feedback control $\Theta(y_2;t) = Q(R_c y_2;\alpha|b(t)|)$, is capable of achieving most of the original control objectives. The next question is, does there exists an admissible control for the EP model which will lead to similar results, when the memoryless feedback is once again replaced by a feedback interconnection with the system Σ_Z.

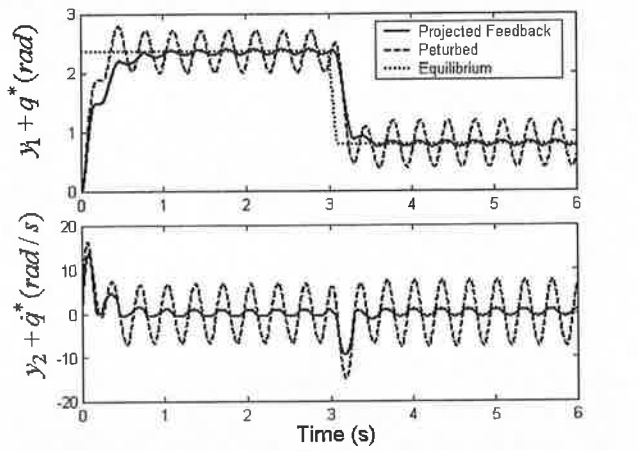

Fig 5.6 Comparison of perturbed and controlled motions of Σ_Y, corresponding to the feedback $\Theta(y_2;t) = Q(R_c y_2;\alpha|b(t)|)$, with $\alpha = .9, R_c = 10R$.

To that end, let $s(t)$ denote the solution of the EVP model introduced in §4.3 (see Fig 4.8 in §4.3),

$$\Sigma_S \begin{cases} \langle Gx_2 - Gs/R_c - \dot{s}, s - \varphi \rangle \geq 0 & \forall |\varphi| \leq r_s(t), \\ |s(t)| \leq r_s(t) & \forall t \geq 0. \end{cases} \tag{5.1.12}$$

where $r_s(t)$ is an admissible damper control. In §4.3 it was shown that $|s(t)|$ is an admissible control for the EP model and that if $r(t) = |s(t)|$ is used in (5.1.1), then

$z(t)$ will converge to $s(t)$ in finite time. Setting $r(t)=|s(t)|$ in (5.1.1), the property of finite time convergence means that for the purposes of analysis, it will be sufficient to consider the modified system

$$\Sigma_D\begin{cases}\Sigma_X\begin{cases}\dot{x}_1=x_2\\ \dot{x}_2=-Kx_1-Rx_2-h(x_1)-z+b(t),\end{cases}\\ \Sigma_Z\begin{cases}\langle Gx_2-Gz/R_c-\dot{z},z-\varphi\rangle\geq 0,\quad \forall|\varphi|\leq r_s(t),\\ |z|\leq r_s(t),\ \forall t\geq 0,\end{cases}\end{cases} \tag{5.1.13}$$

with $r_s(t)=\alpha|b(t)|$ acting as the damper control. The subscript D is used to emphasise the fact that a dissipation shaping control is being used. Note that the rate at which energy is dissipated by Σ_Z is now given by

$$\Phi(t)=\begin{cases}x_2z-\dot{H}_Z(r_s(t)), & \text{if } H_Z(z)=H_Z(r_s(t)) \text{ and } \langle x_2-z/R_c,z\rangle>\dot{H}_Z(r_s(t)),\\ z^2/R_c, & \text{otherwise},\end{cases} \tag{5.1.14}$$

so that even if $r_s(t)=\alpha|b(t)|$, the dissipation rate need not be upper bound by $\alpha|b(t)\|x_2|$. However, the rate at which energy is transferred between Σ_X and Σ_Z is $zx_2\leq r_s(t)|x_2|=\alpha|b(t)\|x_2|$. The results obtained in §4.3 and §D.2 will now be used to obtain an estimate similar to (5.1.11) for the system Σ_D. In §D.2 it is shown that if $L<R^2$ (assumed in what follows), then picking $R_c\leq 8K/aR$ where $a=\min\{\theta\in(0,1)\mid\theta(2-\theta)R^2>L\}$, is sufficient to ensure that Σ_D has a unique, GES T-periodic trajectory $(\bar{x}(t),\bar{z}(t))$. Furthermore since $\|\bar{b}\|_\infty\leq\bar{A}$ and $\|r_s\|_\infty\leq\bar{A}$, this solution satisfies $\|\bar{x}\|_\infty\leq\gamma\bar{A}$ for some constant $\gamma>0$, which is independent of G and R_c. Substituting $\|\bar{x}\|_\infty\leq\gamma\bar{A}$ into (5.1.13) gives $\|\dot{\bar{x}}\|_\infty\leq(2+\gamma R\gamma+K\gamma+L\gamma)\bar{A}=\kappa_X$, implying that the Lipschitz constant κ_X is also independent of G and R_c. Define the error variable $p(t)=\bar{z}(t)-Q(R_c\bar{x}_2(t);r_s(t))$ and substituting it into (5.1.13) gives

$$\Sigma_X\begin{cases}\dot{x}_1=x_2\\ \dot{x}_2=-Kx_1-Rx_2-h(x_1)-Q(R_cx_2;r_s(t))-p(t)+b(t).\end{cases} \tag{5.1.15}$$

It was shown in §4.3 that the T-periodic function $p(t)$ satisfies the bound $\|p\|_\infty\leq\left(R_c^2\kappa_X+R_c\kappa_r\right)/G$ (see inequality (4.3.33)), where κ_r is a Lipschitz constant for the control $r_s(t)$. Using an argument identical to that used to obtain (5.1.11), yields the estimate

$$\int_0^T \bar{x}_2^2(s)ds \le \left(\frac{(1-\alpha)^2}{R^2}+\frac{\alpha^2}{2RR_c}\right)\int_0^T b(s)^2 ds + \int_0^T |p(s)\|\bar{x}_2(s)|ds$$
$$\le \left(\frac{(1-\alpha)^2}{R^2}+\frac{\alpha^2}{2RR_c}\right)T\bar{A}^2 + \frac{\gamma\bar{A}T}{G}\left(R_c^2\kappa_X + R_c\kappa_r\right), \tag{5.1.16}$$

which approaches (5.1.11) as $R_c^2/G \to 0$ (with $\bar{y}_2$ replaced by $\bar{x}_2$) . It follows that the level of disturbance attenuation obtainable through feedback interconnection with the EVP model (5.1.12) (with $r_s(t) = \alpha|b(t)|$) approaches that of the memoryless feedback $Q(R_c x_2; \alpha|b(t)|)$ as $R_c^2/G \to 0$. Note that $R_c \le 8K/aR$ with $a = \min\{\theta \in (0,1) \mid \theta(2-\theta)R^2 > L\}$ is also a sufficient condition for Σ_Y (with $\Theta(y_2;t) = Q(R_c y_2; r_s(t))$), to have a GES T-periodic trajectory $\bar{y}(t)$. Furthermore in §4.3 it was shown that the distance between T-periodic trajectories $\bar{x}(t)$ and $\bar{y}(t)$ of Σ_D and Σ_Y respectively, satisfy the estimate (see arguments preceding inequality (4.3.39) for details)

$$\|\bar{x}-\bar{y}\|_\infty \le \frac{\eta}{G}\left(R_c^2\kappa_X + R_c\kappa_r\right),$$
$$\|\bar{z}-Q(R_c\bar{y}_2; r_s)\|_\infty \le \frac{\eta}{G}\left(R_c^2\kappa_X + R_c\kappa_r\right), \tag{5.1.17}$$

for some positive $\eta > 0$, which is independent of G and R_c. Inequality (5.1.17) implies that for a given value of R_c, the controlled periodic trajectory of Σ_D is contained in a cylinder surrounding the periodic function $(\bar{y}(t), Q(R_c\bar{y}_2(t); r_s(t)))$, the radius of which can be made arbitrarily small for suitably large values of G.

Fig 5.7 and Fig 5.8 compare the controlled motions of Σ_Y with ($\Theta(y_2;t) = Q(R_c y_2; r_s(t))$) and Σ_D, using the control $r_s(t) = \alpha|b(t)|$ in both cases. It can be seen that for small $\varepsilon = R_c/G$, the motions are almost indistinguishable. A quick glance over the previous developments, starting at (5.1.10), reveals that all of the arguments remain valid if the dynamic control $r_s(t) = \alpha|b(t)|$ is replaced by the static control $r_s(t) = \alpha A$ (recall $b(t) = A\sin(\omega t + \varphi)$). Fig 5.9 compares the controlled motions of Σ_D corresponding to the dynamic control $r_s(t) = .9|b(t)|$ and the static control $r_s(t) = 0.8A$ (since $\text{avg}_{[0,T]}|b| < A$). Fig 5.10 compares a portion of the corresponding motions of Σ_Z. It can be seen that the static control achieves a level of performance

comparable with the dynamic control (even if the steady state periodic trajectory of Σ_X is a bit more complex).

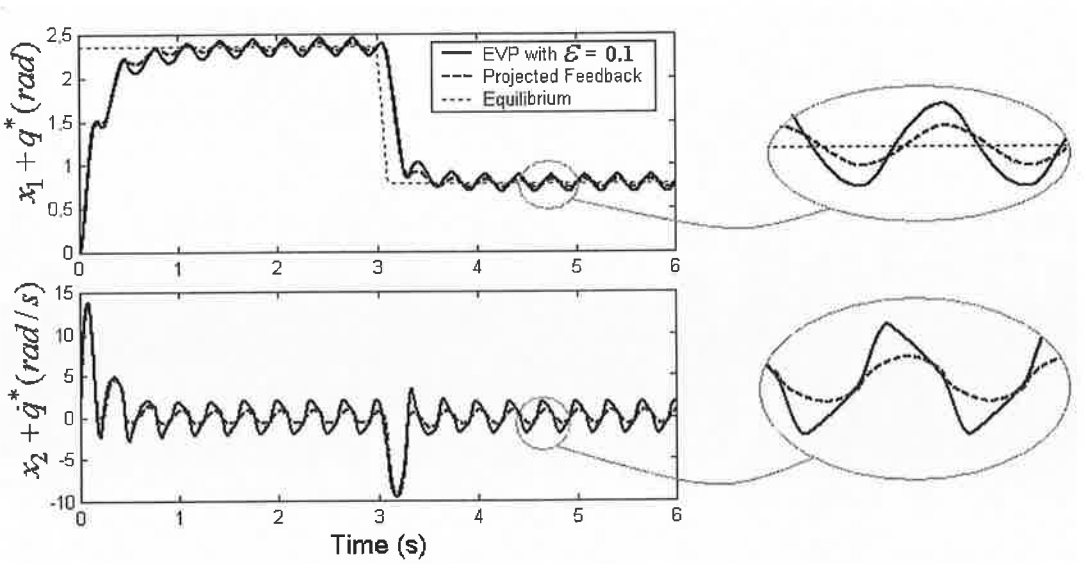

Fig 5.7 Comparison of controlled motions of Σ_Y with feedback $\Theta(y_2;t) = Q(R_c y_2; r_s(t))$, and of Σ_D with control $r_s(t) = \alpha|b(t)|$. In both cases $\alpha = .9, R_c = 10R$ and $\varepsilon = R_c/G = 0.1$.

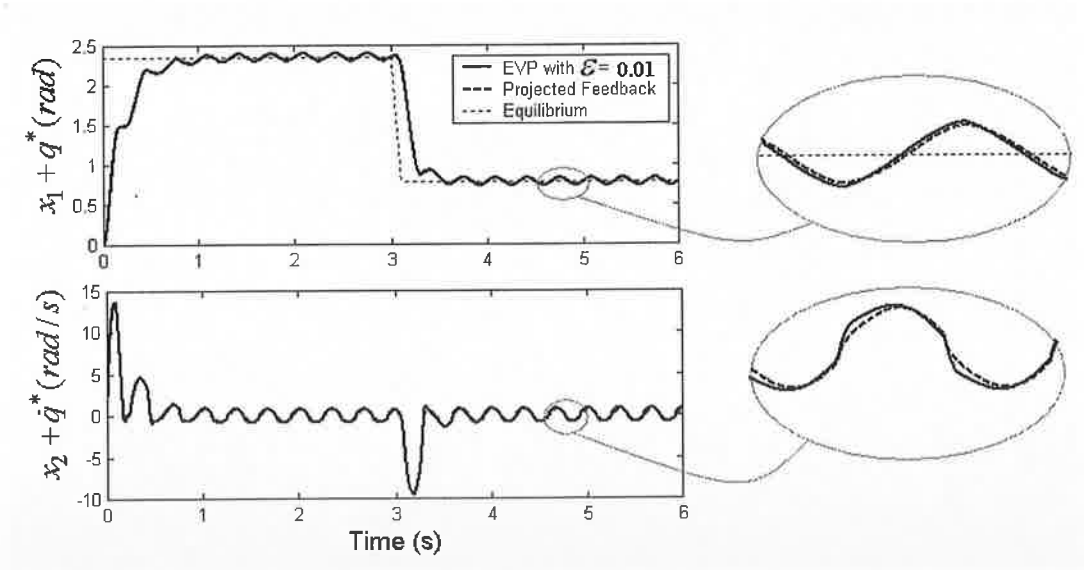

Fig 5.8 Comparison of controlled motions of Σ_Y with feedback $\Theta(y_2;t) = Q(R_c y_2; r_s(t))$, and of Σ_D with control $r_s(t) = \alpha|b(t)|$. In both cases $\alpha = .9, R_c = 10R$ and $\varepsilon = R_c/G = 0.01$.

So why bother with the more complex dynamic control ? One reason is the instantaneous upper bound on the rate of energy transfer between Σ_X and Σ_Z, is more conservative for the static control ($zx_2 \le \alpha|x_2|A$ for static as opposed to $zx_2 \le \alpha|x_2||b(t)|$ for the dynamic control), implying that use of the static control may result in a slower convergence rate.

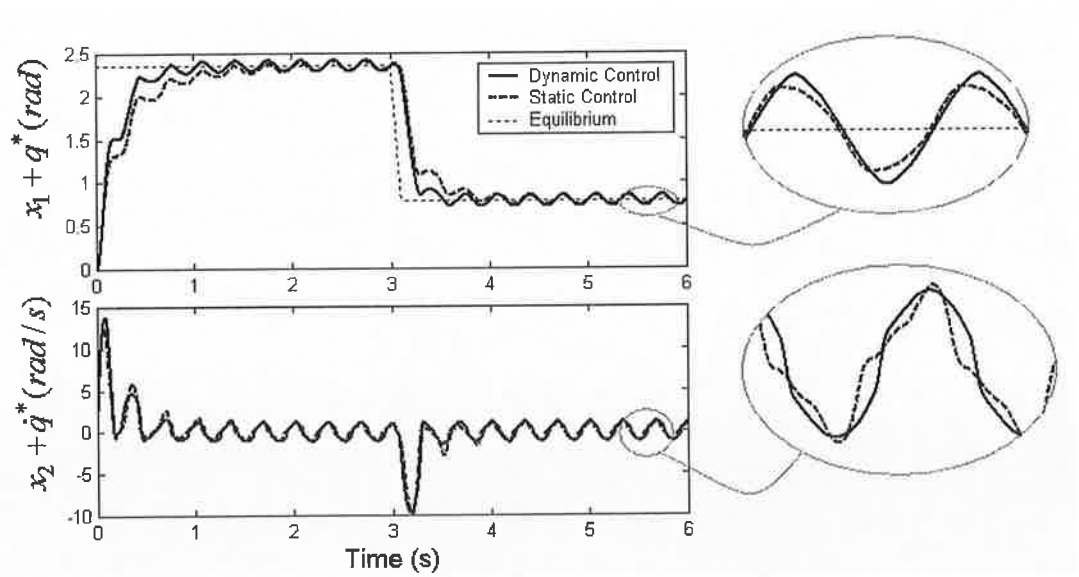

Fig 5.9 Controlled motions of Σ_D corresponding to the dynamic control $r_s(t) = .9|b(t)|$ and the static control $r_s(t) = 0.8A$.

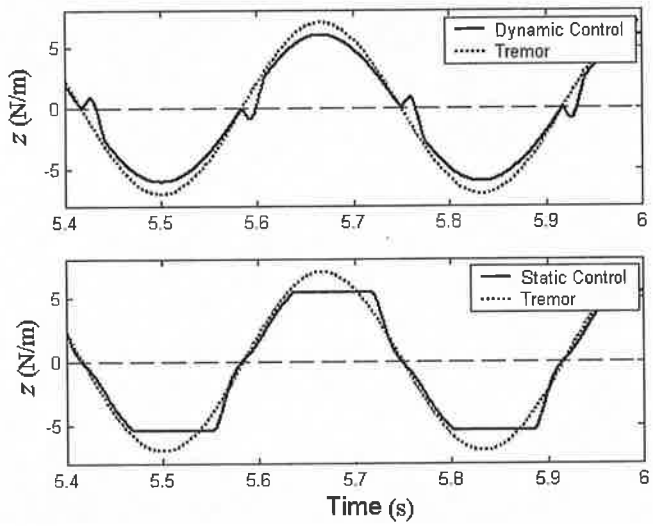

Fig 5.10 Comparison of the trajectories of the EVP model corresponding to the dynamic control $r_s(t) = .9|b(t)|$ and the static control $r_s(t) = 0.8A$.

Now, in all of the developments so far it has been assumed that complete knowledge of the tremor $b(t) = A\sin(\omega t + \varphi)$ was available. In reality, this will hardly be the case. Indeed, the parameters A, ω and φ, characterizing $b(t)$ will probably be time varying (see §1.1) . Consider first the case where only a rough estimate, $\hat{A}$, of the amplitude is available. If $\hat{A} < A$, the steady state attenuation of the tremor will be degraded, however, there will also be less of an effect on the transient motion. As a result, the controlled motion should still be an improvement on the perturbed motion. If $\hat{A} > A$, then although there may be some additional attenuation of the tremor when the system

is in steady state (converged to periodic trajectory), the transient motion may be greatly slowed down.

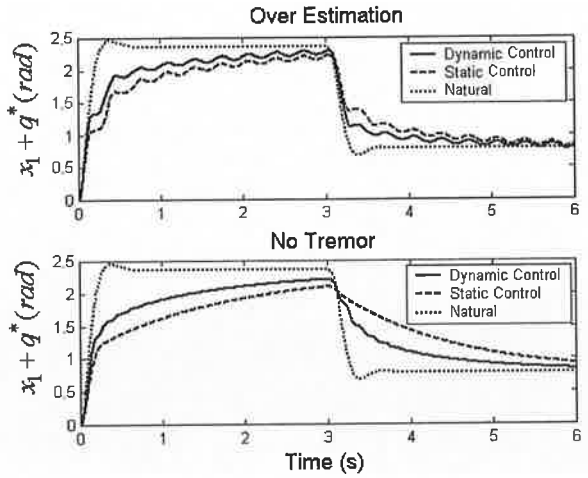

Fig 5.11Comparison of natural and controlled motions of Σ_D corresponding to the control's and $r_s(t) = 0.8\hat{A}$, for the cases in which $\hat{A} > A$ and $b(t) \equiv 0$.

Fig 5.11 compares the natural motion Σ_X with of controlled motions of Σ_X (only x_1 shown) corresponding to the dynamic control $r_s(t) = .9\left|\hat{b}(t)\right| = 0.9\hat{A}\left|\sin(\omega t + \varphi)\right|$ and the static control $r_s(t) = 0.8\hat{A}$. In the first case the estimate is given by $\hat{A} = 1.5A$ and in the second case, the same value of $\hat{A}$ is used but there is no tremor (i.e. $b(\cdot) \equiv 0$). The importance of a good estimate of A is clearly evident. Furthermore, if at some instant, the tremor should vanish, the damper control should then tend to zero rapidly. If this could be achieved, then the controlled motion would converge to the natural motion.

Before moving on, the notion of a limit trajectory will be introduced. Let $b(t) = A\sin(\omega t + \varphi)$, with $A \in [0, \overline{A}]$ and let $r_s(t)$ be an admissible but otherwise arbitrary control such that $\|r_s\|_\infty = \bar{r} \le \overline{A}$. Let $x_a(t) = \big(x(t), z(t)\big)$ and $\hat{x}_a(t) = \big(\hat{x}(t), \hat{z}(t)\big)$ be two controlled motions of Σ_D, with arbitrary initial conditions $x_a(0) \in \Re^2 \times [-r(0), r(0)]$ and $\hat{x}_a(0) \in \Re^2 \times [-r(0), r(0)]$ respectively. Set $a = \min\left\{\theta \in (0,1) \mid \theta(2-\theta)R^2 > L\right\}$ and assuming that $R_c \le 8K/aR$, then inequality (D.2.27) implies that there exists two constants $\lambda, c > 0$ such that

$$\left|x_a(t) - \hat{x}_a(t)\right| \le \lambda \left|x_a(0) - \hat{x}_a(0)\right| e^{-ct}. \tag{5.1.18}$$

Since $x_a(t)$ and $\bar{x}_a(t)$ are arbitrary controlled motions of Σ_D, inequality (5.1.18) implies that all controlled motions of Σ_D are GES. Combining this with the fact that all

motions of Σ_D satisfy the estimate (5.1.2), it is possible to infer the existence of a controlled limit, or "steady state" trajectory, $\bar{x}_a(t) = (\bar{x}(t), \bar{z}(t))$, of Σ_D,which is GES and satisfies $|\bar{x}(t)| \le \gamma\bar{A}$ for all $t \ge 0$. Note that if $r_s(t)$ is T-periodic ($T = 2\pi/\omega$), then the limit trajectory corresponds with the unique GES T-periodic trajectory of Σ_D.

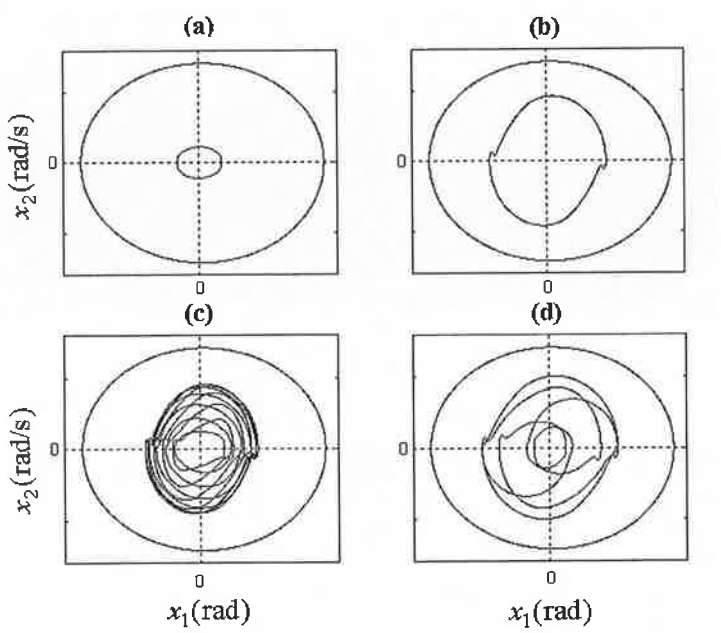

Fig 5.12 Comparisons of the phase portraits of the limit trajectories of Σ_X under various conditions. (a) perturbed and controlled trajectories with correct estimates of ω and φ. (b) perturbed and controlled trajectories with a phase error of $\pi/2$. (c) and (d) compare the perturbed and controlled trajectories $\hat{\omega} = 1.05\omega$ and $\hat{\omega} = 0.8\omega$ respectively.

While errors in estimates of the parameters ω and φ will not effect the performance of the static damper control, they will have a large effect on the controlled motions of Σ_D, when using the dynamic damper control. It was found that errors in ω and φ have little effect on the transient portions of the controlled motions (as one might expect).

As a result the following examples consider only the controlled limit trajectories of Σ_D, with $q^* = 0$ and the dynamic control $r_s(t) = 0.9A|\sin(\hat{\omega}t + \hat{\varphi})|$. Fig 5.12 compares the phase portraits of the limit trajectories of Σ_X under various conditions. Fig 5.12 compares the phase portrait perturbed trajectory with that of the controlled trajectory assuming exact knowledge of ω and φ. Fig 5.12(b) compares the phase portrait perturbed trajectory with that of the controlled trajectory corresponding to a phase error

of $\pi/2$. Finally, Fig 5.12(c) and (d) compare the phase portrait perturbed trajectory with that of the controlled trajectory corresponding to the case where $\hat{\omega}=1.05\omega$ and $\hat{\omega}=0.8\omega$ respectively. Fig 5.13 and Fig 5.14**Error! Reference source not found.** show portions of the limit trajectories of Σ_Z and the acceleration $\ddot{x}_2(t)$ corresponding to each of the cases described above.

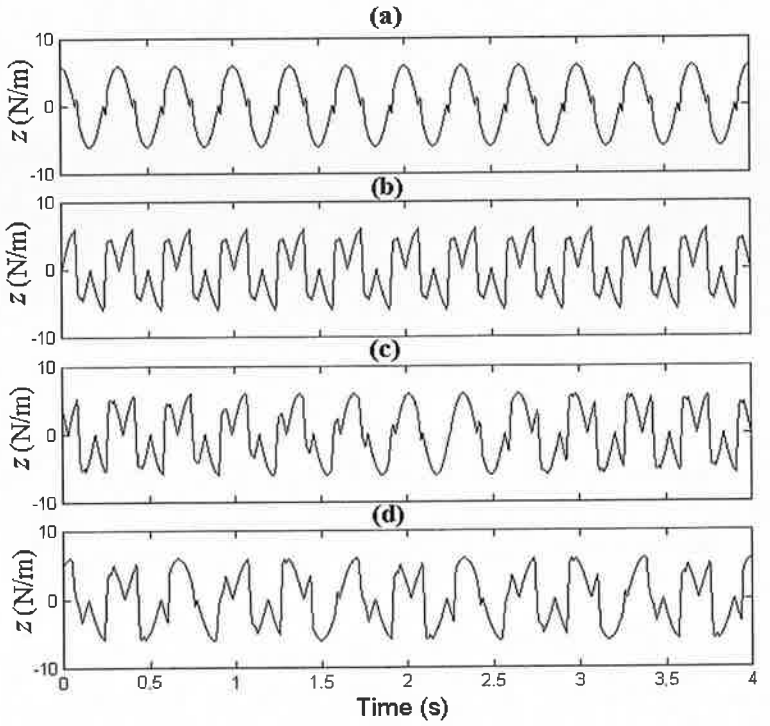

Fig 5.13 Portions of the trajectories of Σ_Z (a) correct estimates of ω and φ, (b) phase error of $\pi/2$. (c) $\hat{\omega}=1.05\omega$, (d) $\hat{\omega}=0.8\omega$.

Note that in the case where there is an error in the phase but the frequency is correct, the limit trajectory of Σ will still be T-periodic ($T=2\pi/\omega$). On the other hand, if there is an error in the frequency, then $r_s(t)$ need not be T-periodic (depends on the error) so that periodicy of the corresponding limit trajectory cannot be assumed. Preliminary investigations would suggest that when $b(t)$ and $r_s(t)$ are periodic, but with different periods, it should be possible to prove that the corresponding limit trajectories are almost periodic (or at least recurrent). Further discussions on this point will be given in the discussions chapter of the thesis (§6.2).

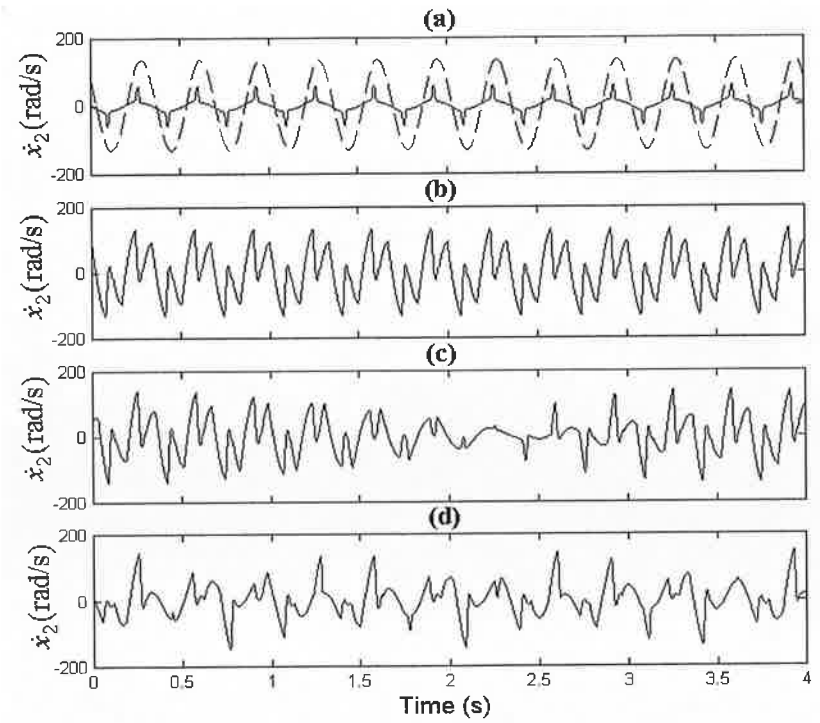

Fig 5.14 Portions of the acceleration $\dot{x}_2(t)$. (a) Perturbed (dash) and controlled with correct estimates of ω and φ, (b) phase error of $\pi/2$,(c) $\hat{\omega} = 1.05\omega$, (d) $\hat{\omega} = 0.8\omega$.

From examination of Fig 5.12 it can be seen that even with errors in the frequency and phase, the controlled trajectories of Σ_X are contained in a smaller neighbourhood of the origin than the perturbed trajectory. That said, examination of the corresponding accelerations shows that the controlled trajectories, without exact knowledge of ω and φ, are far more complex than the perturbed trajectory. In this case, a person with tremor may find that the controlled motions are less useful than the perturbed. Imagine trying to hold a glass of water while your hand is subjected to each of the acceleration profiles of Fig 5.14. These examples should be enough to convince the reader that if the dynamic controller is to be used, then the ability to obtained accurate estimates of ω and φ is vital.

To recap, it has been shown by first applying a feedforward model of the form (5.1.12) and then using the dynamic control $r_s(t) = \alpha|b(t)|$, the effect of tremor on the motions of Σ_X can be significantly attenuated, while remaining in a neighbourhood of the natural motion. However, these results rely crucially on the ability to obtain an accurate estimate of the tremor, $b(t)$. Let $(\bar{x}(t), \bar{z}(t)) = (\bar{x}(t; \bar{x}_a(0), r_s(\cdot), b(\cdot)), \bar{z}(t; \bar{x}_a(0), r_s(\cdot), b(\cdot)))$ be the GES T-periodic solution of Σ_D corresponding to the T-periodic input $b(t)$ and

control $r_s(t) = \alpha|b(t)|$. Suppose that $\hat{x}_a(t) = (\hat{x}(t), \hat{z}(t))$ is an arbitrary solution of Σ_D corresponding to the T-periodic input $b(t)$ and estimated control $\hat{r}_s(t) = \alpha|\hat{b}(t)|$, that is $(\hat{x}(t), \hat{z}(t)) = \left(\hat{x}(t; \hat{x}_a(0), \hat{r}_s(\cdot), b(\cdot)), \hat{z}(t; \hat{x}_a(0), \hat{r}_s(\cdot), b(\cdot))\right)$. It is shown in §D.2 that if R_c satisfies the usual assumptions, then the distance between these two solutions satisfy the estimate (see inequality (D.2.40))

$$\begin{aligned} |\hat{x}_a(t) - \bar{x}_a(t)| &\le \beta|\hat{x}_a(0) - \bar{x}_a(0)|e^{-\sigma t} + \gamma\left(\int_0^t e^{-\sigma(t-s)}|r_s(s) - \hat{r}_s(s)|ds\right)^{1/2}, \\ &\le \beta|\hat{x}_a(0) - \bar{x}_a(0)|e^{-\sigma t} + \gamma\left(\alpha\int_0^t e^{-\sigma(t-s)}|b(s) - \hat{b}(s)|ds\right)^{1/2}, \end{aligned} \tag{5.1.19}$$

for some constants $\gamma, \beta > 0$. It follows from Lemma.5 in §B.2 that if it were possible to obtain an estimate of $b(t)$ such that $\lim_{n\to\infty} \hat{b}(t + nT) = b(t)$, then $\hat{x}(t)$ will converge to the periodic trajectory $\bar{x}(t)$, for which the estimate (5.1.16) holds. This is useful result and justifies the search for suitable online estimation schemes. Some further discussion is given in §6.2.

5.2 Summary

The control objective was stated in Chapter 2 as follows : Devise a control strategy for an ER damper which will reduce the oscillations caused by the tremor, without adversely affecting the intentional motion. In this chapter the feasibility of achieving this objective, for periodic tremor, was investigated using results from the analysis in Chapter 4 and Appendix D. In order to simplify the discussions, when the EP model is removed and the tremor is zero, the motions of the forearm model were referred to as natural motions. When the tremor was nonzero, the resulting motions were referred to as perturbed motions. Finally when the forearm was coupled with the EP model the resulting motion of the forearm model are referred to as controlled.

After examining simulations of the natural and perturbed motions the control objective was restated as follows: To select a damper control so as to ensure that the controlled motions of the forearm converge to a periodic trajectory which is contained in a neighbourhood of the desired equilibrium, and which has smaller oscillation than the perturbed motion. Furthermore, the rate at which the controlled motion of converges to

the periodic trajectory, should be close to the rate at which natural motion converges to the desired equilibrium.

The first step in the control design was to use the dissipation shaping control in order to make the EP model behave like the EVP model. Then using the results from appendix D, the viscous coefficient associated with the EVP model was chosen so as to ensure that the system has a unique GES periodic solution. This choice of control also ensures that if the tremor should disappear, then the state of the coupled system will converge to zero exponentially. It was argued that in order to avoid slowing down the rate of convergence to the periodic solution, the rate at which energy is transferred between the forearm model and the damper model should be upper bound by the rate at which energy is supplied to the system by the tremor. This was achieved by assuming that the tremor was know and then setting the controllable yield stress of the EVP model equal to the absolute value of the tremor.

Simulations showed that using the control scheme described above, the controlled motion does indeed converge to a periodic trajectory contained in a neighbourhood of the desired equilibrium and which has smaller oscillation than the perturbed motion. The simulations also showed that the rate of convergence to this periodic trajectory was close to the rate at which natural motion converged to the desired equilibrium. Theoretical justification for the decrease in the oscillation of the controlled motion, when compared to the perturbed motion, was also presented using the singular perturbation type analysis from Section 4.3.

Finally, it was shown that the success of this control scheme relies on some knowledge of tremor. As knowledge of the tremor would not be a realistic assumption in practice, a scheme for obtaining good estimate of the tremor is required if this control scheme is to be of any practical value. Some further discussion on this point is given in the final chapter of the thesis.

Chapter 6

Conclusions and future research

6.1 Summary and conclusions

It is well established that the application of viscous damping can significantly reduce the oscillations caused by severe pathological tremor, but that concurrent suppression of voluntary motion may also occur. The use of controllable dampers constructed using ER fluids has been identified as a possible means of overcoming this problem. It has been argued that in order to investigate the feasibility of using an ER damper to suppress tremor, models are required which capture the highly nonlinear behaviour exhibited by ER fluid dampers and which are well suited for analysis and control design. A survey of the literature on ER fluids revealed that many of the models which have appeared in the literature fail to meet these requirements. An analysis of experimental results and physics based micromechanical models for ER fluids, revealed that the qualitative mechanical behaviour of ER fluids in shear resembles that of elastic-plastic or viscoplastic solid, with electric field dependent yield stress. It is now widely accepted that the behaviour of many elastic-plastic and viscoplastic materials can be successfully modelled using the theory of "thermomechanics with internal variables". One objective of the thesis was to show that this theory also provides an approach for modelling the mechanical behaviour of ER fluid dampers, which:

- Captures the qualitative mechanical behaviour displayed by ER fluid dampers.
- Is intuitive and easy to apply.
- Defines a passive map from the imposed velocity to the resistive force produced by the damper.
- Are wellposed and numerically friendly.
- Are easily coupled with models for other mechanical systems.
- Are well suited for analysis using traditional qualitative methods for ordinary differential equations.

A simplified version of the theory of "thermomechanics with internal variables" was presented along with the necessary tools from convex analysis. Through the use of examples, it was shown that a simple and intuitive approach to applying the theory is to

initially construct a phenomenological model which conceptually captures the mechanical behaviour of a given damper using idealised rheological elements such as spring and friction elements. This model is then used to construct two functions, representing the energy stored in the rheological elements (free energy) and the rate at which energy is dissipated by the elements (dissipation function). Then, applying a systematic procedure to these two functions, one obtains an evolution equation for the phenomenological damper model. It is also shown that if the electric field (control variable) only appears as a parameter in the dissipation function, the resulting model will automatically define a passive map from the imposed velocity to the resulting force. Depending on the manner in which viscosity has been incorporated, the resulting equations will either take the form of a Lipschitz ordinary differential equation, or a variational inequality.

An advantage of using well established modelling techniques is that there is a wealth of results available for establishing wellposedness and developing integration algorithms, for the resulting models. Unfortunately, many of the results relating to wellposedness of variational inequalities are presented in such general form that they are inaccessible to those without prior acquaintance with the theory. As a consequence, some simple results for establishing wellposedness of the damper models were presented, which are accessible to those with some knowledge of ordinary differential equations.

The simplest of the damper models, consisting of a spring and controllable friction element in series, was then coupled with a forced second order oscillator, representing the forearm/elbow subject to tremor. A detailed analysis of the internal and external stability properties of the coupled system was then performed, using traditional energy based and Liapunov type techniques. Conditions for the existence and stability of periodic solutions of the coupled system were also studied in detail, using fixed point theorems and Liapunov analysis.

An outgrowth of this analysis was the development of a new approach to the control of ER dampers, referred to as dissipation shaping. The idea is to use a suitably chosen feedforward control to endow the damper model with a more desirable dissipation function (rate). The idea itself is very simple and can be viewed as a form of global model reference control. Finally the dissipation shaping control and some relevant results on periodic solutions were used to assess the feasibility of using an ER damper

to suppress tremor at the elbow, with minimal degradation of the intentional motion. The theoretical results were quite favourable and were supported by numerous simulation results. In conclusion, the use of an ER fluid damper to suppress periodic tremor at the elbow, with a minimal degradation of the intentional motion is very feasible.

Existing models reviewed in Chapter 1:

Model/Formulation (reference)	Equation	Figure	Passive	Fluid/ solid	Viscoelastic in preyield	Existence, uniqueness
Bingham plastic [26]	(1.2.1)	1.5	yes	solid	no	yes
Biviscous [20],[29]	(1.2.3)	N/A	yes	fluid	no	trivial
Extended Bingham (fixed stiffness coefficients) [31],[32]	(1.2.4)	1.5	yes	solid	yes	unclear
[33]	(1.2.6)	1.6	no	solid	yes	unclear
[30]	N/A	N/A	yes	fluid	no	trivial
Bouc-type models [23],[35]	(1.2.7)	N/A	no	solid	yes	trivial
Nonlinear Viscoelastic-plastic [36],[29]	(1.2.9)	N/A	no	solid	yes	trivial

Table 6.1

Models formulated in Chapter 3:

Model/Formulation (abbreviation)	Equation	Figure	Passive	Fluid/ solid	Viscoelastic preyield	Existence, uniqueness
Elastic-plastic, (EP)	(3.4.35)	3.10	yes	solid	yes	yes
Multiple element (Π(EP))	(3.6.3) (3.6.7)	3.19	yes	solid	yes	yes
Viscoplastic, (VP)	(3.5.10)	3.14	yes	solid	yes	trivial
Modified viscoplastic, (MVP)	(3.5.15)	3.17	yes	solid	yes	yes
Extended Bingham (GnF)	(3.5.25)	3.18	yes	solid	yes	trivial

Table 6.2

Tables 6.1 and 6.2 list some attributes of the ER /MR damper models surveyed in §1.2 and the damper models formulated in §3. A model was classified as passive if it defines a passive map from the imposed velocity to the predicated damper force, according to the definition given in §2.1. The models were classified as solid models if they are capable of sustaining a non-zero force when the imposed velocity is zero and as fluid

models otherwise. The models were deemed to exhibit viscoelastic behaviour in preyield if they behave like a viscoelastic solid (linear or nonlinear) when the predicted force is less than the yield force. When evaluating the existence and uniqueness of solutions, the damper models were assumed to be coupled with the nonlinear second order oscillator from §4.1. It was also assumed that the controllable damper parameters were Lipschitz continuous functions of time. Note that the references cited in Table 6.2 do not consider questions of existence and uniqueness of solutions. Existence and uniqueness of solutions has been classified as trivial if the results can be obtain by applying well known theorems for ordinary differential equations (for example [96],[97]). The classification "unclear" has been used where existence of solutions was unobtainable, using methods known to the author. Existence of solutions for the oscillator coupled with Bingham plastic model was obtained by applying standard theorems for ordinary differential inclusions, [98]. The remaining cases in Table 6.2 were obtained by applying Corollary C.3.1.

In conclusion, the original contributions of this thesis were:

(1) To show that the theory of "thermomechanics with internal variables" provides an intuitive and systematic approach for modelling the mechanical behaviour of ER fluid dampers . It was also shown that under mild conditions the resulting model will define a passive map from the imposed velocity to the resulting force.

(2) To present theorems providing sufficient conditions for the existence and uniqueness of solutions of the damper models. The proofs for these theorems were greatly simplified, so as to make them accessible to those with a working knowledge of existence and uniqueness theory for ordinary differential equations.

(3) To show that the models are easily coupled with models for other mechanical systems and that traditional energy based and Liapunov type techniques can be used to analyse the qualitative behaviour of the coupled system in detail.

(4) To show that by using a suitably chosen feedforward control, the EP model can be made to behave exactly like another rheological model consisting of a series combination of a linear spring with the same stiffness and a dissipative element with a more desirable dissipation function (dissipation shaping).

To the best knowledge of the author the work presented in this thesis is the first in the literature to accomplish (1) to (4) above.

6.2 Some topics for future research

It is the purpose of this section to briefly outline some of the topics/ extensions which the author is presently investigating and plans to investigate in the future.

To begin with, some possible extensions of the work in §3 will be considered. Two of the major simplifications assumed in §3, were that the polarization/chain formation occurs instantaneously upon application of the electric field and that the imposed flow conditions have no effect on the magnitude of the yield stress. Consider the case where an electric field is initially applied to a static (no flow/stress) ER fluid. It is generally accepted that the chain formation in a static ER fluid takes place on at least two time scales. When the field is first applied, most of the particles will rapidly form into chains running parallel to the field. This is then followed by a much slower thickening of the chains and possibly coalescing of thinner chains. Combining this with the hypothesis that the thicker the chain the greater the stress/strain required to induce rupture, implies that that the minimum stress required to induce unbounded flow in an activated suspension will depend on how long the field had been applied before the suspension is disturbed (mechanically). This minimum stress is often referred to as the static yield stress. Now consider the case where the electric field has been applied for a sufficient amount of time for chain formation to reach steady state. Then one of the electrodes is made to translate at a constant velocity. When the stress in the fluid reaches the static yield stress, a steady shear flow will be induced and the particle chains will begin the continual process of breakage and reformation. During flow, only a percentage of the chains will be intact at any moment. In addition the hydrodynamic forces due to the shearing flow will cause some fragmentation of the chains, making them thinner. As a result the stress in the fluid will decrease, implying that the dynamic yield stress will be lower than the static yield stress. This phenomena has been reported in numerous studies where the ER fluid is subjected to very low frequency oscillatory shear.

From a practical point of view other electric phenomena are also of considerable interest. For example, the relationship between electric field, shear flow and the leakage current in an ER fluid is vitally important, as it will govern the power consumption of a device. As one would expect, the current through a static ER fluid does not obey ohms

law. In fact numerous experimental studies have concluded that the conduction current through an ER fluid varies in proportion with E^2, though only after E has exceeded some threshold E_T. Also, there is an increase in the leakage current observed in static ER fluids, as compared to fluids in shear. Given that the particles are generally more conductive than the base fluid, the main source of leakage current will be through the electrode spanning chains. It follows that the thicker chains present in a stationary fluid would conduct more current than the degraded chains in a flowing fluid.

The modelling of electrical phenomena can be performed in much the same manner as in §3. Simply replace stresses and strains by electric fields and charges, and replace rheological elements such as springs and friction elements by their circuital analogs, capacitors and diodes etc. The coupling of electrical and mechanical phenomena is a bit more difficult. One approach would to first develop separate phenomenological models for the electrical and mechanical systems using circuital and rheological elements. The total thermodynamic state will then consist of the strain, mechanical internal variables, electric field and electric internal variables. The coupling between the models would then be performed by allowing the dissipation function to depend on the entire thermodynamic state. It is thought that a unified modelling procedure could be developed based on the material in the excellent text [38].

The next logical step would be to validate the models using experimental data from an ER fluid damper. To do this, parameter identification algorithms need to be developed for the, models. It is thought that it may be possible to use the identification methods developed in [84],[85]. These methods are ideally suited for systems involving variational inequalities. The basic idea is to first formulate the identification problem as a constrained convex optimization problem. The solution of this optimization is then formulated as the stable equilibrium set for a system of differential equations. An integration algorithm is also presented in [84], which could be used to implement the identification method on a digital signal processor.

In order to use the damper models for online identification and control implementation, efficient integration algorithms are needed. In §D.2 justification for a mixed implicit-explicit solver was presented. In practice it was found that this scheme was only suited for integration over short time periods. A form of mixed midpoint-implicit algorithm was found to be much better behaved, particularly when integrating more complex models, such as the GnF model coupled with a model for a smooth mechanical system. It would certainly be worthwhile performing a detailed analysis of the stability and

convergence properties of this and other algorithms. A wealth of information on integration algorithms can be found in [41].

In Appendix C it was noted that a sufficient condition for the viscoplastic type models, to have a unique Lipschitz continuous solution is that the input (strain) is Lipschitz continuous and the control (yield stress) is essentially bounded. In contrast, for models involving a variational inequality, such as the EP model, to have a Lipschitz continuous solution requires that both the input $x(t)$ and control $r(t)$ are Lipschitz continuous. This is a particular disadvantage of the EP model, as on/off type controls may be of interest in applications such as vibration control. The conditions on $r(t)$ cannot be weakened without redefining the notion of solution. For example, using the methods in [40] it can be shown that if $r(t)$ and $x(t)$ are continuous and of bounded variation, then the EP model will have a solution which is continuous and of bounded variation. It is thought that if the EP model were reformulated as a hysteresis operator, it may be possible to use the theorems in [86], to shown that if $r(t)$ and $x(t)$ are piecewise continuous, then the EP model will have a unique piecewise continuous solution.

Next some possible extensions of the work in §4 and §D will be discussed. Appendix D presented some sufficient conditions for the existence of a periodic solution for the coupled system $\sum$ (EP model and forced second order oscillator). This of course assumes that the input $b(t)$ and control $r(t)$ are both periodic, with the same period. It was noted in §5, that in applications such as tremor suppression, it is unlikely that $b(t)$ and $r(t)$ will be periodic, but will be some superposition of periodic functions, with different, independent periods. In this case the notion of an almost periodic solution is more natural. Recall that a solution $x(t)$ of the differential equation $\dot{x} = F(x,t)$ is said to be T-periodic if $x(t) = x(t+T)$ for all $t \geq 0$. A solution $x(t)$ is said to be almost periodic if for each $\varepsilon > 0$ there exists a number $L(\varepsilon) > 0$, such that every closed interval in $\Re_+$ with length $L(\varepsilon)$, contains a number τ such that $|x(t+\tau) - x(t)| < \varepsilon$ for all $t \geq 0, t+\tau \geq 0$. A more general notion, which contains both periodic and almost periodic solutions, is that of a recurrent solution. A solution is said to be recurrent if for each $\varepsilon > 0$ there exists a number $L(\varepsilon) > 0$, such that for every $t \in \Re_+$ and every interval $\mathrm{I} \subset \Re_+$ of length greater than $L(\varepsilon)$, there exists a $\tau \in \mathrm{I}$ such that $|x(t) - x(\tau)| < \varepsilon$. The author is presently investigating the possibility of using the results in the excellent

papers [87] and [88], to prove the existence of almost periodic and recurrent solution of Σ. If existence can be proved, then stability of the solutions follows exactly as in §D.

In §4.3, a feedforward control was used to transform the EP model into the EVP model (dissipation shaping). A natural question is, could a feedback control be used to endow the EP model with more desirable behaviour (dissipation rate). Unfortunately this is difficult to show. Recall that the solution of the EP model z, satisfies $|z(t)| \le r(t)$ for all $t \ge 0$. If the control r is chosen as $r(t) = L|z(t)|$, two possibilities could occur. If $L \in [0,1)$, then $|z(t)| \le L|z(t)|$ implies $z(t) = 0$ for all $t \ge 0$. If $L \ge 1$, then $|z(t)| \le L|z(t)|$ holds for all $z \in \Re$ and the EP model will behave like a spring. For more general nonautonomous controls $r(t) = \Theta(z(t), t) \ge 0$, the existence and uniqueness results in §C.2 can no longer be applied. Establishing uniqueness is actually the most difficult problem. A detailed discussion on existence and uniqueness of variational inequalities with state dependent constraints can be found in [89]. The author is presently trying to establish if a feedback control would be "useful", and if so, what restrictions need to be placed on the feedback function $\Theta : \Re \times \Re_+ \to \Re_+$ so as to ensure existence and uniqueness. As usual, the viscoplastic models display much more regular behaviour. As an example, recall that the simple viscoplastic model from Fig.13 in §3 is given by

$$\dot{\sigma}(t) = G\dot{e}(t) - \frac{G}{\eta_p} P(\sigma(t); r(t)), \tag{6.2.1}$$

where $P(\sigma; r) = \max(\sigma - r, \min(\sigma + r, 0))$. If the control r is chosen as $r(t) = L|\sigma(t)|$, and $L \ge 1$, then $\dot{\sigma}(t) = G\dot{e}(t)$ for all $t \ge 0$ (a spring).

However if $L \in [0,1)$ then (6.2.1) becomes

$$\dot{\sigma}(t) = G\dot{e}(t) - \frac{G}{\eta_p}(1 - L)\sigma(t), \tag{6.2.2}$$

which is equivalent to a Maxwell model with controllable viscosous coefficient $\eta_c = \eta_p/(1-L)$. The controllable coefficient η_c can be varied over the interval $[\eta_p, \infty)$ by varying L over the interval $[0,1)$.

In section §4.2 it was mentioned that for T small enough, certain $0T$-recurrent controls

have the effect of transforming the EP model into a memoryless function of the velocity x_2, in an averaged sense. The idea is similar in spirit to the use of dither to linearize or smoothen, discontinuous control systems [90],[91].

For example, consider partitioning $\Re_+$ into intervals $T[n,n+1]$ for $n=0,1,2\ldots$ and implementing the control

$$r(t)=\begin{cases}\bar{r}/\varepsilon\left(t-nT\right) & for \quad t\in[nT,nT+\varepsilon),\\ \bar{r} & for \quad t\in[nT+\varepsilon,(n+1)T-\varepsilon),\\ \bar{r}/\varepsilon\left((n+1)T-t\right) & for \quad t\in[(n+1)T-\varepsilon,(n+1)T),\end{cases} \tag{6.2.3}$$

where $\bar{r}$ and ε are positive constants. It can be shown that for ε and T small enough and $\bar{r}$ large enough, the averaged response of the EP model $z_{av}(t)=\frac{1}{T}\int_t^{t+T} z(s)ds$ approximates $GTx_2(t)/2$. Which is to say that the averaged damper response is close to that of a linear viscous damper, with coefficient $GT/2$. This estimation was backed up by numerous simulations of the system Σ, carried out by the author. Unfortunately the author has been so far unable to obtain rigorous bounds on the error $z_{av}(t)-GTx_2(t)/2$. It would also be of interest to investigate the averaging effect of other types of $0T$-recurrent controls and to maybe formulate some sort of procedure for constructing $0T$-recurrent controls.

Finally, some possible topics of future research into tremor suppression are discussed. In §5 it was shown by first transforming the EP model into the EVP model and then using the dynamic control $r_s(t)=\alpha|b(t)|$, the effect of tremor on the motions of Σ_X can be significantly attenuated. However, these results rely crucially on the ability to obtain an accurate estimate of the tremor, $b(t)$. The need to estimate and reject periodic disturbances with unknown frequency arises in various important applications such as active noise control and vibration suppression. As a result numerous techniques and algorithms have been developed for just this purpose, some examples of which can be found in [92],[93],94].The author has developed a number of robust estimators, for continuously estimating the tremor, $b(t)$. The estimator's are developed on the assumption that the tremor can be represented as the output of the following dynamic system

$$\dot{q} = \begin{bmatrix} 0 & \omega(t) \\ -\omega(t) & 0 \end{bmatrix} q + \begin{bmatrix} 0 \\ 1 \end{bmatrix} \delta(t) \tag{6.2.4}$$

with $b(t) = q_2(t)$. The function $\delta \in C(\Re_+, \Re)$ represents variations in the tremor amplitude and $\omega \in C(\Re_+, \Re_+)$ represents the unknown time varying "frequency". Note that the system in (6.2.4) defines a passive map form $\delta(t)$ to $q_2(t)$. This property greatly facilitates the development of estimators and the subsequent stability analysis. The idea now is to estimate the state of the system (2.4) based on measurements of the velocity, $x_2(t)$. The estimators developed by the author are essentially a constrained version of the passive observers developed in [95]. The result is a system of differential equations coupled with a variational inequality, not that dissimilar to $\sum$. The theoretical and numerical investigations performed so far, show that the estimators are extremely well behaved and under certain conditions, can obtain an exponentially convergent estimate of $b(t)$. The author is currently attempting to develop estimators for more general tremor representations than (6.2.4). It is hoped that these estimators will also account for more complex intentional motions than the point-to-point motions considered in §5. Another worthwhile topic under investigation is the simultaneous suppression of tremor in the elbow and shoulder, using two ER fluid dampers.

References

[1] A. Anouti, W. Koller. "Tremor disorders: diagnosis and managment". Western Journal of Medicine, vol.162, pp. 510-513, 1995.

[2] G. Cooper, R. Rodnitzky. "The many forms of tremor: precise classification guides selection of therapy". Postgraduate Medicine, vol.108, pp. 57-70, July 2000.

[3] P. Charles, G. Esper, T. Davis, D. Mactunas, D. Robertson. "Classification of tremor and update on treatment". American Family Physician, pp.1567-1576, 1999.

[4] L. Smedman. "Tremor". Multiple Sclerosis Basic Facts Series, National Multiple Sclerosis Society, 2004,

[5] S. Alusi, S. Glickman, T. Aziz, P. Bain, "Tremor in multiple sclerosis" (editorial). Journal of Neurology, Neurosurgery and Psychiatry, vol.68, pp. 131-134, 2000.

[6] C. Riviere, N. Thakor. "Modeling and canceling tremor in human machine interfaces". IEEE Engineering in Medicine and Biology. vol.15, pp.29-36, 1996.

[7] C. Riviere, R. Rader, N. Thakor. "Adaptive canceling of physiological tremor for improved precision in microsurgery". IEEE Transactions on Biomedical Engineering, vol. 45, pp. 839-846, 1998.

[8] J. Gonzalez, E. Heredia, T. Rahman, K. Barner, G. Arce. Filtering Involuntary Motion of People with Tremor Disability Using Optimal Equalization. IEEE International Conference on Systems, Man and Cybernetics, Oct 1995.

[9] M. Rosen, J. Gesink, D. Rowell. "Suppression of intention tremor by application of viscous damping". 4th Annual New England bioengineering Conference, pp. 391-394, 1976.

[10] M. Aisen, A. Arnold, I. Baiges, S. Maxwell, M. Rosen. "The effect of mechanical damping loads on disabling action tremor". Neurology, vol. 43, pp.1346-1350, 1993.

[11] Neater Solutions Ltd. Web site: http://www.neater.co.uk/

[12] S. Pledgie, K. Barner, S. Agrawal, T. Rahman. "Tremor suppression through impedance control". IEEE Transactions on Rehabilitation Engineering, vol.8, pp.53 -59, 2000.

[13] M. Rosen, A. Arnold, I. Baiges, M. Aisen, S. Elgowstein. "Design of a controlled-energy-dissipation orthosis for functional suppression of intention tremors". Journal of Rehabilitation Research and Development, vol. 32, pp.1-16, 1995.

[14] S. Beringhause, M. Rosen, N. Berube, M. Aisen. "Evaluation of a damped joystick for people disabled by tremor". Conference on Rehabilitation Technology, New Orleans, pp.41-42, 1989.

[15] J. Kotovsky, M. Rosen. "A wearable tremor-suppression orthosis". Journal of Rehabilitation Research and Development, vol. 35, pp. 373-387, 1998.

[16] M. Manto, M. Topping, M. Soede, J. Sanchez-Lacuesta, W. Harwin, J. Pons, J. Williams, S. Skaarup. L. Normie. "Dynamical Responsive Intervention For Tremor Suppression". IEEE Engineering in Medicine and Biology Magazine, vol.22, pp.120-123, 2003.

[17] E. Rocon, A. Ruiz, J. Pons, J. Belda-Lois, J. Sanchez-Lacuesta. "Rehabilitation robotics: a wearable exo-skeleton for tremor assessment and suppression". Proceedings of the IEEE International Conference on robotics and Automation, Spain, pp. 2271-2276, 2005.

[18] R. Loureiro, J. Belda-Lois, E. Lima, J. Pons, J. Sanchez-Lacuesta, W. Harwin. "Upper limb tremor suppression in ADL via an orthosis incorporating a controllable double viscous beam actuator". Proceedings of the IEEE 9th International Conference on Rehabilitations Robotics, USA, pp.119-121, 2005.
[19] R. Loureiro, W. Harwin. "Improvements in or relating to damping mechanisms", International patent number WO 2006/051301 A1, 18 May, 2006.
[20] R. Stanway, J. Sproston, A. El-Wahed. "Applications of electrorheological fluids in vibration control: a survey". Smart Materials and Structures, vol.5, pp.464-482, 1996.
[21] R. Bonnzecaze, J. Brady, "Yield stresses in electrorheological fluids". Journal of Rheology, vol.36, pp.73-114, 1992.
[22] G. Yang. Large-scale magnetorheological fluid damper for vibration mitigation: modeling, testing and control. Ph.D dissertation, University of Notre Dame, 2001.
[23] B. Spencer, S. Dyke, M. Sain, J. Carlson. "Phenomenological model of a magnetorheological damper". ASCE Journal of Engineering Mechanics, vol.123, pp.230-238, 1997.
[24] T. Butz, O. von Stryk. "Modelling and simulation of electro- and magnetorheological Fluid Dampers". ZAMM, vol.82, pp.3-20, 2001.
[25] F. Gandhi, W. Bullough, "On the phenomenological modelling of electrorheological and magnetorheological fluid preyield behaviour". Journal of Intelligent Material Systems and Structures, vol.16, pp.237-248, 2005.
[26] W. Bullough, M. Foxon. ''A proportionate coulomb and viscously damped isolation system''. Journal of Sound and Vibration, vol.56, pp.35-44, 1978.
[27] H. Gavin. "Multi-duct ER Dampers". Journal of Intelligent Material Systems and Structures,vol.12, pp.353-366, 2001.
[28] L. Bitman, Y. Choi, S Choi, N. Wereley. "Electrorheological damper analysis using an eyring-plastic model". Smart Materials and Structures, vol.14, pp.237-246, 2005.
[29] R. Snyder, G. Kamath, N. Wereley. "Characterization and analysis of magnetorheological damper behaviour under sinusoidal loading". AIAA Journal, vol. 39, pp.1240-1253, 2001.
[30] N. Sims, N. Holmes, R. Stanway. ''A unified modelling and model updating procedure for electrorheological and magnetorheological vibration dampers,'' Smart Materials and Structures, vol.13, pp.100-121, 2004.
[31] D. Gamota, F. Filisko. ''Dynamic mechanical studies of electrorheological materials: moderate frequencies''. Journal of Rheology, vol.35, pp.399-426, 1991.
[32] R. Ehrgott, S. Masri. "Modeling the oscillatory dynamic behaviour of electrorheological fluids in shear". Smart Materials and Structures, vol.1, pp.275-285, 1992.
[33] N. Sims, D. Peel, R. Stanway, A. Johnson, W. Bullough. ''The electrorheological long stroke damper: A new modelling technique with experimental validation,'' Journal of Sound and Vibration, vol.229, pp.207-227, 2000.
[34] R. Bouc. "Modèle mathématique d'hystérésis". Acustica , 24 , pp.16-22, 1971.
[35] L. Jansen, S. Dyke. "Semi-active control strategies for mr dampers :a comparative study" . ASCE Journal of Engineering Mechanics, vol.126, pp. 795-803, 2001.

[36] G. Kamath, N. Wereley. ''A nonlinear viscoelastic-plastic model for electrorheological fluids,'' Smart Materials and Structures, vol. 6, pp.351-358, 1997.
[37] G. Maugin. The thermomechanics of plasticity and fracture. Cambridge University Press, Cambridge U.K., 1992.
[38] G. Maugin. The thermomechanics of nonlinear irreversible behaviours. World Scientific, Singapore, 1999.
[39] H. Ziegler. An introduction to thermomechanics, 2nd Ed. North-Holland Amsterdam, 1983.
[40] P. Krejci. Evolution variational inequalities and multidimensional hysteresis operators. In: Nonlinear Differential Equations, Research Notes in Mathematics, Chapman and Hall/CRC, London, 1999.
[41] J. Simo, T. Hughes. Computational inelasticity.
[42] N. Hogan. "Adaptive control of mechanical impedance by coactivation of antagonist muscles". IEEE Transactions on Automatic Control, vol.29, pp.681-690, 1984.
[43] C. Abul-Haj, N. Hogan. "Functional assessment of control systems for cybernetic elbow prostheses-part1: description of technique". IEEE Transactions on Biomedical Engineering, vol.37, pp.1025-1036, 1990.
[44] M. Kawato. "Internal models for motor control and trajectory planning". Current Opinion in Neurobiology, vol.9, pp.718-727, 1999.
[45] P. Gribble, D. Ostry, V. Sanguineti, R. Laboissiere. "Are complex control signals required for human arm movement". The American Physiological Society, pp.1409-1424, 1998.
[46] R. Shadmehr. "The equilibrium point hypothesis for control of posture, movement and manipulation". Handbook of Brian Theory and Neural Networks, MIT Press, 1995.
[47] R. Shadmehr, F. Mussa-Ivaldi. "Adaptive representation of dynamics during learning of a motor task". The Journal of Neuroscience, vol.14, pp.3208-3224 1994.
[48] C. Byrnes, A. Isidori, J. Willems. "Passivity, feedback equivalence, and the global stabilization of minimum phase nonlinear systems" . IEEE Transactions on Automatic Control, vol.36, pp.1228-1240, 1991.
[49] W. Winslow. "Translating electrical impulses into mechanical force". US Patent no.2,417,85, 1947.
[50] W. Winslow. "Induced fibration of suspensions". Journal of Applied Physics . vol.20, pp.1137-1140, 1949.
[51] Y. Han, S. Lim, H. Lee, S. Choi, H.Choi. "Hysteresis identification of polymethylaniline based ER fluid using the preisach model". Materials and Design, vol.24, pp.943-956, 2003.
[52] R. Larson. The structure and rheology of complex fluids. Oxford University Press, 1999.
[53] M. Parthasarathy, D. Klingenburg. "Electrorheology: mechanisms and models", Materials Science and Engineering. R17, pp.57-103, 1996.
[54] J. Furusho, M. Sakaguchi, N. Takesue, K. Koyanagi. "Development of ER brake and its application to passive force display". Journal of Intelligent Material Systems and Structures, vol. 13, pp.425-429, 2002.
[55] H. Gavin. "Control of seismically excited vibration using electrorheological materials and lyapunov methods". IEEE Transactions on Control Systems Technology, vol.9, pp.27-36, 2001.

[56] R. Bonnzecaze, J. Brady. "Dynamics simulation of an electrorheological fluid". Journal of Chemical Physics, vol.96, pp. 2183-2202, 1992.
[57] Smart technology Ltd. Electrorheological Fluid LID 3354, Technical Information Sheet. United Kingdom, 1998.
[58] J. Stangroom. "Electrorheological fluids: an introduction". ER fluids Developments Ltd., United Kingdom, 1992.
[59] J. Martin, J. Odinek, T. Halsey, R. Kamien. "Structure and dynamics of electrorheological fluids". Physical Review E., pp.756–775, 1998.
[60] M. Parthasarathy, D. Klingenberg. "Large amplitude oscillatory shear of ER suspensions". Journal of Non-Newtonian Fluid Mechanics, pp.83-104, 1999.
[61] C. Lee, C. Cheng, "Complex moduli of electrorheological material under oscillatory shear". International Journal of Mechanical Sciences, vol.42, pp. 561-573, 2000.
[62] K. Rajagopal, M. Ruzicka. "Mathematical modelling of electrorheological materials". Continuum Mechanics and Thermodynamics, vol.13, pp.59-78, 2001.
[63] G. Gully, R. Tao. "Static shear stress of an electrorheological fluid". Physical Review E, vol.48, pp.2987–2990 ,1993.
[64] G. Houlsby, A. Puzrin. "Rate-dependent plasticity models derived from potential functions". Journal of Rheology, vol.46, pp.113-126, 2001.
[65] R. Eve, B. Reddy, R. Rockafellar. "An internal variable theory of elastoplasticity based on the maximum plastic work inequality". Quarterly of Applied Mathematics, pp. 59-83, 1990.
[66] G. Batchelor. "The stress system in a suspension of force free particles". Journal of Fluid Mechanics, vol.41, pp.545, 1970.
[67] P. Krejci. "Reliable solutions to the problem of periodic oscillations of an elastoplastic beam". International Journal of Non-Linear Mechanics, vol.37, pp.1337-1349, 2002.
[68] A. Visintin. Differential models of hysteresis. Springer-Verlag, Berlin Heidelberg, 1994.
[69] M. Whittle, R. Atkin, W. Bullough. "Fluid dynamic limitations on the performance of an electrorheological clutch". Journal of Non-Newtonian Mechanics, vol.21, pp.61-81, 1995.
[70] J. Powell. "Modelling the oscillatory response of an electrorheological fluid". Smart Materials and Structures, vol.3, pp. 416-438, 1994.
[71] L. Hatvani, T. Krisztin, V. Totik. "A necessary and sufficient condition for the asymptotic stability of the damped oscillator", Journal of Differential Equations, vol.119, pp. 209-223, 1995.
[72] P. Sain, M. Sain, B. Spencer. "Models of hysteresis and applications to structural control". Proceedings American Control Conference, June, pp.16-20, 1997.
[73] P. Dupont, P. Kasturi, A. Stokes. "Semi-active control of friction dampers". Journal of Sound and Vibration. , vol.202, pp. 203-218, 1997.
[74] R. Nitsche, L. Gaul. "Lyapunov design of damping controllers". Archive of Applied Mechanics, vol.72, pp.865-874, 2002.
[75] G. Yao, F. Yap, G. Chen, W. Li, S. Yeo. "MR damper and its application for semi-active control of vehicle suspension system". Mechantronics, vol. 12, pp.963-973, 2002.
[76] S. Erlicher, N. Point. "Thermodynamic admissibility of Bouc–Wen type hysteresis models". Comptes Rendus Mecanique, vol. 332, pp.51-57, 2004.
[77] P. Dahl. "A solid friction model". Technical Report TOR-0158H3107–18I-1, The Aerospace Corporation, El Segundo, CA, 1968.

[78] N. Sims, R. Stanway, A. Johnson, D. Peel, W. Bullough. "Smart Fluid Damping: Shaping the Force/Velocity Response through Feedback Control". Journal of Intelligent Material Systems and Structures, vol. 11, pp. 945-958, 2000.
[79] S. Marathe, K. Wang, F. Gandhi. "Feedback linearization control of magnetorheological fluid damper based systems with model uncertainty". Smart Materials and Structures. vol.13, pp.106-116, 2004.
[80] G. Maganti, S. Singh, W. Yim. "On absolute stability and semi-active control of a magnetorheological Fluid Vibration Suppression System". Proceedings of the 18th International Conference on Systems Engineering, pp.100-105, 2005.
[81] K. Byeonghwa , P. Roschke, "Linearization of magnetorheological behaviour using a neuralnetwork", American Control Conference, vol.6, pp.4501-4505, 1999.
[82] H. Khalil. Nonlinear Systems, 3rd Ed. Prentice Hall, Upper Saddle River, N.J., 2002.
[83] Simulink/Matlab. The MathWorks, Inc, Natick, Massachusetts, 1999.
[84] K. Kuhnen. P. Krejci. "Identification of linear error-models with projected dynamical systems". Mathematical and Computer Modeling of Dynamical Systems, vol.10, pp. 59-91, 2004.
[85] K. Kuhnen, Modeling, identification and compensation for complex hysteretic nonlinearities: a modified prandtl-ishlinskii approach". European Journal of Control, vol.9, pp. 407-421, 2003.
[86] H. Logemann, A. Mawby. "Extending hysteresis operators to spaces of piecewise continuous functions". Journal of Mathematical Analysis and Applications, vol.282, pp. 107-127, 2003.
[87] M. Brokate, I. Collings, A. Pokrovskii, F. Stagnitti. "Asymptotically stable almost-periodic oscillations in systems with hysteresis nonlinearities". Institute for Nonlinear Science, University College Cork, report 99-002, 1999.
[88] A. Pokrovskii, K. Abodayeh and J. McInerney. "Recurrent oscillations in systems with hysteresis nonlinearities".
Institute for Nonlinear Science, University College Cork,, report 99-008, 1999.
[89] M. Brokate, P. Krejci, H. Schnabel. "On uniqueness in evolution quasivariational inequalities".
Journal of Convex Analysis, vol.11, pp.111-130, 2004.
[90] G. Zames, N. Shneydor. "Structural stabilization and quenching by dither in nonlinear systems".
IEEE Transactions on Automatic Control, vol.22, pp.352-361, 1977.
[91] L Iannelli, K Johansson, U Jonsson, F Vasca . "Dither for smoothing relay feedback systems". IEEE Transactions on Circuits and Systems, Part I, vol.50, pp. 1025-1035, 2003.
[92] M. Bodson. S. Douglas. "Adaptive algorithms for the rejection of sinusoidal disturbances with unknown frequency".
Automatica, vol.33, pp. 2213–2221, 1997.
[93] R. Marino, G. Santosuosso, P. Tomei. "Robust adaptive compensation of biased sinusoidal disturbances with unknown frequency".
Automatica, vol.39, pp.1755-1761, 2003.
[94] L. Brown, Q. Zhang. "Periodic disturbance cancellation with uncertain frequency". Automatica, vol. 40, pp.631-637, 2004.
[95] M. Krstic, P. Kokotovic, I. Kanellakopoulos. Nonlinear and Adaptive Control Design. John Wiley & Sons, New York, 1995.
[96] R. Miller, A. Michel. Ordinary differential equations. Academic Press, NY, 1982.

[97] J. Hale. Ordinary differential equations, second edition. Krieger Publishing Company, Malabar, Florida, 1980.
[98] G. Smirnov. Introduction to the theory of differential inclusions. American Mathematical Society, 2002.

Appendix A

Functions and convex analysis

Section.1 of this appendix presents some standard definitions and classifications for functions of a real variable, while Section.2 presents a summery of some results from convex analysis, which will be used throughout this thesis.

A.1 Function Spaces

The purpose of his section is recall some definitions and classifications for functions of a real variable. The material is standard enough and can be found in most texts on real analysis, for example [1].

In what follows, $\Re^n$ is used to denote the n-dimensional real Euclidean space with scalar product $\langle x, y\rangle = x^{\mathrm{T}} y$ and norm $|x| = \sqrt{\langle x, x\rangle}$ for $y, x \in \Re^n$. The one dimensional Euclidian space consists of all real numbers and is denoted by $\Re$. The subset of $\Re$ consisting of all nonnegative real numbers is denoted by $\Re_+$. The subset $[a,b] \subset \Re$ is the closed interval $a \le x \le b$, $(a,b) \subset \Re$ is the open interval $a < x < b$ and $[a,b) \subset \Re$ is the half-open interval $a \le x < b$.

Let $J \subset \Re$ be some interval. A subset $\mathrm{I} \subset J$ is said to have measure zero if for each $\varepsilon > 0$ there exists a countable family of intervals I_i with length $\varepsilon_i > 0$ such that $\mathrm{I} \subset \bigcup_{i=1}^{\infty} \mathrm{I}_i$ and $\sum_{i=1}^{\infty} \varepsilon_i < \varepsilon$. Two functions $f, g : J \mapsto \Re^n$ are said to be equal almost everywhere (a.e.) if the set $\{t \in J \mid f(t) \neq g(t)\}$ has measure zero. In general a property is said to hold almost everywhere or a.e., provided it only fails on a set of measure zero. For example, a sequence of functions $\{f_i\}$ is said to converge to a function $f : J \mapsto \Re^n$ almost everywhere if the set $\{t \in J \mid f_i(t) \not\mapsto f(t)\}$ has measure zero. A function $f : J \mapsto \Re^n$ is said to be measurable if there exits a sequence of piecewise constant functions $\{f_i\}$, such that $\{f_i\}$ converges to f almost everywhere as $i \to \infty$. The reader unfamiliar with Lebesque integration can substitute "piecewise continuous

functions" for "measurable functions" and interpret "almost everywhere" as "everywhere except at most on a countable number of points".

A function $f : J \mapsto \Re^n$ is said to be essentially bounded if it is measurable and there exists a compact set $X \subset \Re^n$ (closed and bounded) such that $f(t) \in X$ for almost all $t \in J$. The space of essentially bounded measurable functions $f : J \mapsto \Re^n$ is denoted $L_\infty(\mathrm{I};\Re^n)$, with associated norm $\|x\|_\infty = \inf\{\sup(|x(t)|, t \in J \setminus M) | M \subset J, meas(M) = 0\}$.

For a measurable function $f : J \mapsto \Re^n$, $f : J \mapsto \Re^n$, the Lebesque integral $\int_a^b f(s)ds$ can be defined via the limits of integrals of suitable sequences of approximating piecewise constants functions. An integrable function is one for which $\int_a^b |f(s)|ds$ is finite. $L_1(J;\Re^n)$ is the space of integrable functions $f : J \mapsto \Re^n$ endowed with norm, $\|f\|_1 = \int_a^b |f(s)|ds$. Similarly $L_p(J;\Re^n)$, $p \in (1,\infty)$ consists of all measurable functions $f : J \mapsto \Re^n$ functions such that $\|f\|_p = \left(\int_a^b |f(s)|^p ds\right)^{\frac{1}{p}}$.

A function $f : J \mapsto \Re^n$ is said to be continuous at a point $t \in J$, if for each $\varepsilon > 0$, there exists a $\delta(\varepsilon,t) > 0$ so that $|f(t) - f(\tau)| < \varepsilon$ for all $\tau \in J$, such that $|t - \tau| < \delta(\varepsilon,t)$. A function $f : J \to \Re^n$ is said to be continuous on J or $f \in C(J;\Re^n)$, if it is continuous at each point of the interval J. It is said to be uniformly continuous on J if $\delta(\varepsilon,t) > 0$ in the above definition depends only on $\varepsilon > 0$. The space $C^m(J;\Re^n)$ consists of continuous functions $f : J \mapsto \Re^n$, with continuous derivatives or order m, i.e. $d^m f/dt^m \in C(J;\Re^n)$.

A function $f : J \mapsto \Re^n$ is said to be locally Lipschitz continuous if for each $t \in J$ there exists two constants $\kappa_f, \delta > 0$, so that $|f(t) - f(\tau)| \le \kappa_f |t - \tau|$ for all $\tau \in J$ such that $|t - \tau| < \delta$. It is said to be Lipschitz continuous, or $f \in C^{0,1}(J;\Re^n)$ if there exists a constant $\kappa_f > 0$ such that $|f(t) - f(\tau)| \le \kappa_f |t - \tau|$ for all $t, \tau \in J$. If $f \in C^1(J;\Re^n)$ then f is at least locally Lipschitz continuous. If also J is compact, then

$f \in C^{0,1}(J;\Re^n)$. The space $f \in C^{m,1}(J;\Re^n)$ consists of the functions $f \in C^m(J;\Re^n)$ for which the m^{th} derivative is Lipschitz continuous. Lipschitz continuous have the pleasant property that they are differentiable almost everywhere.

A function $f: J \mapsto \Re^n$ defined on a compact interval $f: J \mapsto \Re^n$ is said to be absolutely continuous if for each $\varepsilon > 0$, there exists a $\delta > 0$ such that $\sum_{k=1}^{n} |f(b_k) - f(a_k)| < \varepsilon$ for every system of pairwise disjoint subintervals $(a_k, b_k) \subset J$ with $\sum_{k=1}^{n} (b_k - a_k) < \delta$. The space of absolutely continuous functions $f: J \mapsto \Re^n$ is denoted $AC(J;\Re^n)$. If J is semi-infinite, say $\Re_+$, then $f: \Re_+ \mapsto \Re^n$ is said to belong to $AC(\Re_+;\Re^n)$ if the above definition holds on each compact subinterval $J_k \subset \Re_+$. For every absolutely continuous function $f: J \mapsto \Re^n$ and on each subinterval $[a,b] \subset J$, there exits a function $\dot{f} \in L_1([a,b];\Re^n)$ such that $\dot{f}(t) = \lim_{h \to 0} (f(t+h) - f(t))/h$ for almost all $t \in [a,b]$. Or equivalently $f(t) - f(\tau) = \int_\tau^t \dot{f}(s)ds$ for all $t, \tau \in [a,b]$. For compact intervals $J = [a,b]$, the norm associated with $AC(J;\Re^n)$ is given by $\|f\|_{AC} = |f(a)| + \int_a^b |f(s)|ds$. Note that a Lipschitz function $f: J \mapsto \Re^n$ is absolutely continuous and an absolutely continuous function is Lipschitz if it has an essentially bounded derivative.

The following two inequalities will prove useful in studying stability properties in §4 and §5.

Young's inequality: Suppose that $p, q \in (1, \infty)$ and $1/p + 1/q = 1$. Then

$$|xy| \le \frac{1}{p} K^p |x|^p + \frac{1}{qK^q} |y|^q, \quad \forall x, y \in \Re, \ \forall K > 0.$$

Holders's Inequality: Let $p, q \in [1, \infty]$ and $1/p + 1/q = 1$ (note if $p = 1$ take $q = \infty$). Let $f \in L_p(\Re_+;\Re^n)$ and $g \in L_q(\Re_+;\Re^n)$ then for all $t \in \Re_+$

$$\int_0^t |f(s)g(s)|ds \le \left(\int_0^t |f(s)|^p ds \right)^{\frac{1}{p}} \left(\int_0^t |g(s)|^q ds \right)^{\frac{1}{q}}.$$

In proving some of the existence results in §C the following well known results will be needed. The first is the well know Arzela compactness theorem. Recall that a family of real valued functions $X \in C([a,b];\Re^n)$ is called equicontinuous if, given $\varepsilon > 0$, there exits a $\delta > 0$ such that $|x^n(a') - x^n(b')| < \varepsilon$ for each $x^n \in X$ whenever $a', b' \in [a,b]$ and $|a'-b'| < \delta$

Theorem A.1.1 [1] (Arzela) If a set $X \subset C([a,b];\Re^n)$ is uniformly bounded and equicontinuous, then it contains a uniformly convergent subsequence $x^n \in X, n = 1,2\ldots$; that is, there exists $x \in C([a,b];\Re^n)$ such that $\|x^n - x\|_\infty \to 0$ as $n \to \infty$.

Theorem A.1.2 [2] Let $A \subset \Re^n$ be a convex compact set. Assume that $x^n \in AC([a,b];\Re^n)$ is a sequence such that $x^n(t) \to x(t)$ for all $t \in [a,b]$ and $\dot{x}^n(t) \in A$ for almost all $t \in [a,b]$.Then $x \in AC([a,b];\Re^n)$ and $\dot{x}(t) \in A$ almost everywhere.

The next two results are know as the continuous and discrete Gronwall inequalities and can be found in most books dealing with ordinary differential equations.

Theorem A.1.3 [3] If r, α are real valued and continuous for all $t \in [a,b]$, $\beta(t) \geq 0$ is integrable on $[a,b]$ and

$$r(t) \leq \alpha(t) + \int_a^t \beta(s) r(s) ds, \quad \forall t \in [a,b]$$

then

$$r(t) \leq \alpha(t) + \int_a^t \beta(s)\alpha(s) \exp\left(\int_s^t \beta(u)du\right) ds, \quad \forall t \in [a,b].$$

Theorem A.1.4 [3] If $r_0, r_1, r_2, \ldots r_n$ is a nonnegative sequence of numbers with and $\delta_k \geq 0$,

$\Delta_k \geq 0$ for $k = 0,1,2,\ldots,n-1$, the if

$$r_{k+1} \leq (1+\delta_k) r_k + \Delta_k, \qquad k = 0,1,2,\ldots,n-1$$

it follows that if $r_0 = 0$ then

$$r_n \leq \left(\exp\left(\sum_{k=0}^{n-1} \delta_k\right)\right) \sum_{k=0}^{n-1} \Delta_k.$$

A.2 Elements of convex analysis

The purpose of this section is to recall some basic definitions and results from convex analysis. The material present below is taken from [4], [5] and [6].

Let $\mathbf{C}$ be a subset of $\Re^n$. The interior, closure and boundary of $\mathbf{C}$ are denoted by $\text{int}\mathbf{C}$, $\text{cl}\mathbf{C}$ and $\text{bd}\mathbf{C}$. A nonempty subset $\mathbf{C} \subset \Re^n$ is said to be convex if for any $x, y \in \mathbf{C}$ and $\alpha \in [0,1]$ then $x\alpha + (1-\alpha)y \in \mathbf{C}$. A nonempty subset $\mathbf{K} \subset \Re^n$ is said to be a cone if along with any element $x \in \mathbf{K}$ it contains the element $\alpha x \in \mathbf{K}$ for all $\alpha \geq 0$.

Let $\mathbf{C} \subset \Re^n$ be a closed convex set such that $0 \in \mathbf{C}$. For each $x \in \Re^n$ there exists a point $z \in \mathbf{C}$ such that $|x-z| = \text{dist}(x;\mathbf{C}) = \min\{|x-y| \mid y \in \mathbf{C}\}$. It is thus possible to define the projection operator $Q(\cdot;\mathbf{C}) : \Re^n \to \mathbf{C}$ and its complement $P(x;\mathbf{C}) = x - Q(x;\mathbf{C})$ for all $x \in \Re^n$, by the formulae $Q(x;\mathbf{C}) \in \mathbf{C}$ and $|P(x;\mathbf{C})| = \text{dist}(x;\mathbf{C})$ for all $x \in \Re^n$. These operators have the following useful properties

$$\begin{cases} (i)\langle P(x;\mathbf{C}), Q(x;\mathbf{C}) - \varphi \rangle \geq 0, \quad \forall \varphi \in \mathbf{C}, \\ (ii)\langle P(x;\mathbf{C}) - P(y;\mathbf{C}), Q(x;\mathbf{C}) - Q(y;\mathbf{C}) \rangle \geq 0, \\ (iii)|Q(x;\mathbf{C}) - Q(y;\mathbf{C})| \leq |x-y|, \\ (iv)|P(x;\mathbf{C}) - P(y;\mathbf{C})| \leq |x-y|. \end{cases} \tag{A.2.1}$$

When considering $\Re$, the closed convex subsets are the closed intervals $[-r,r] \subset \Re, r > 0$. For simplicity the corresponding projection pair will be denoted $Q(x;r)$ and $P(x;r)$. In this case the following formulae hold $Q(x;r) = \min(r, \max(-r,x))$ and $P(x;r) = \max(x-r, \min(x+r,0))$ along with the properties , for $x, y \in \Re$ and $s, r > 0$

$$\begin{cases} (v)|Q(x;r) - Q(y;s)| \leq |x-y| + |r-s|, \\ (vi)|P(x;r) - P(y;s)| \leq |x-y| + |r-s|. \end{cases} \tag{A.2.2}$$

Convex functions will be considered next. It will be convenient to consider the extended real numbers $\overline{\Re} = \Re \cup \{\infty\} \cup \{-\infty\}$. For each function $f : \Re^n \mapsto \overline{\Re}$, the set $\text{dom}(f) = \{x \in \Re^n \mid f(x) < \infty\}$ is called the effective domain of f. The epigraph of f denoted $\text{epi}(f)$ is the set of ordered pairs $\text{epi}(f) = \{(x,\alpha) \in \Re^n \times \Re \mid f(x) \leq \alpha\}$. A function $f : \Re^n \mapsto \overline{\Re}$ is called proper if $f(x) < \infty$ for at least one point $x \in \Re^n$ and

$f(x) > -\infty$ for all $x \in \Re^n$. A function $f : \Re^n \mapsto \overline{\Re}$ is said to be positively homogenous of degree $p > 0$ if $f(\alpha x) = \alpha^p f(x)$ for all $\alpha > 0$ and $x \in \Re^n$. A function $f : \Re^n \mapsto \overline{\Re}$ is said to be convex if epi(f) is a convex set in $\Re^n \times \Re$. Equivalently, a proper function $f : \Re^n \mapsto \overline{\Re}$ is said to be convex if

$$f(\theta x + (1-\theta)y) \le \theta f(x) + (1-\theta) f(y), \tag{A.2.3}$$

for all $x, y \in \Re^n$ and $\alpha \in [0,1]$. Furthermore, a convex function is said to lower semicontinuous or lsc if epi(f) is a closed convex set in $\Re^n \times \Re$.

Two very useful, though unusual, convex functions are the indicator function of the convex set $\mathbf{C} \subset \Re^n$

$$I(x;\mathbf{C}) = \begin{cases} 0, & x \in \mathbf{C}, \\ +\infty, & x \notin \mathbf{C}, \end{cases} \tag{A.2.4}$$

and the support function of the convex set $\mathbf{C} \subset \Re^n$

$$S(x;\mathbf{C}) = \sup\{\langle x, \tilde{x} \rangle \mid \tilde{x} \in \mathbf{C}\}. \tag{A.2.5}$$

Clearly the support function is positively homogeneous of degree one.

An important aspect of convex analysis is that of duality. For a proper, lsc convex function $f : \Re^n \mapsto \overline{\Re}$, the conjugate function f^* of f (or Legendre or Legendre-Fenchel transform) is defined by

$$f^*(x^*) = \sup\{\langle x^*, x \rangle - f(x) \mid x \in \Re^n\} \tag{A.2.6}$$

If f is a proper, lsc convex function, then so is f^* and $(f^*)^* = f^{**} = f$. For example, if $f(x) = 1/p \sum_{i=1}^n |x_i|^p$, $p \in (1, \infty)$, then $f^*(x^*) = 1/q \sum_{i=1}^n |x_i^*|^q$ with $1/q + 1/p = 1$. Also the support function of the convex set $\mathbf{C} \subset \Re^n$ (A.2.5) is the conjugate of the indicator function (A.2.4) and vice versa.

The calculus of convex functions will be considered next.. Let $f : \Re^n \mapsto \overline{\Re}$ be a convex function finite at $x \in \Re^n$, the set (possibly empty)

$$\partial f(x) = \{z \in \Re^n \mid f(y) - f(x) \ge \langle z, y - x \rangle, \forall y \in \Re^n\}, \tag{A.2.7}$$

is the subdifferential of f at $x \in \Re^n$. The elements of $\partial f(x)$ are called the subgradients of f at $x \in \Re^n$. If f is differentiable at x then $\partial f(x) = \nabla f(x)$.

If f convex and finite at $x \in \Re^n$, then $\partial f(x)$ is a closed convex set. If in addition f is continuous at $x \in \Re^n$, then $\partial f(x)$ is nonempty, compact, convex set. Similar to Fermat's theorem for differentiable functions, a point $\bar{x} \in \Re^n$ minimises the convex function if and only if $0 \in \partial f(\bar{x})$. Another important property is that the subdifferential of a convex function is a monotone operator, in the sense that

$$\langle \partial f(x) - \partial f(y), x - y \rangle \geq 0, \quad \forall x, y \in \Re^n. \tag{A.2.8}$$

A very important result in convex calculus is the Moreau-Rockafellar theorem which states that ; if f_1 and f_2 are two convex, lsc functions and there exists a point where both functions are finite and at least one is continuous, then

$$\partial(f_1(x) + f_2(x)) = \partial f_1(x) + \partial f_2(x) \tag{A.2.9}$$

for all $x \in \text{dom}(f_1) \bigcap \text{dom}(f_2)$.

In terms of conjugate functions, if f^* is the conjugate of the a proper, lsc, convex function f given by (A.2.6), then

$$x^* \in \partial f(x) \Leftrightarrow x \in \partial f^*(x^*). \tag{A.2.10}$$

This result provides a useful means of constructing the conjugate function f^*. That is , calculate $\partial f(x)$, invert it and then integrate to find f^*.

For the special case of the indicator function (A.2.4), the subdifferential $\partial I(x;\mathbf{C})$ corresponds with the normal cone $N(x;\mathbf{C})$, to the convex set $\mathbf{C}$ at x

$$N(x;\mathbf{C}) = \left\{ z \in \Re^n \mid \langle z, x - \varphi \rangle \geq 0, \forall \varphi \in \mathbf{C} \right\}. \tag{A.2.11}$$

If $x \in \text{int}\,\mathbf{C}$ then $N(x;\mathbf{C}) = 0$, where as if $x \in \text{bd}\mathbf{C}$, then $N(x;\mathbf{C})$ consists of the cone of outward normal's to $\mathbf{C}$ at x. For sets of the form $[-r,r], r \geq 0$, the normal cone will be denoted by $N(x;r)$.

References

[1] A. Kolmogorov, S. Fomin. Introductory real analysis.
Dover Publications Inc., NY, 1975.

[2] G. Smirnov. Introduction to the theory of differential inclusions.
American Mathematical Society, 2002.

[3] F. Clarke, Y. Ledyaev, R. Stern. P. Wolenski.
Nonsmooth analysis and control theory. Springer-Verlag, NY, 1998.

[4] P. Krejci. "Evolution variational inequalities and multidimensional hysteresis operators". In: Nonlinear Differential Equations, Research Notes in Mathematics, Chapman and Hall/CRC, London, 1999.

[5] G. Magaril-Il'yaev, V. Tikhomirov. Convex analysis: theory and applications.
American Mathematical Society, 2003.

[6] R. Eve, B. Reddy, R. Rockafellar. " An internal variable theory of elastoplasticity based on the maximum plastic work inequality".
Quarterly of Applied Mathematics, vol.XLVIII, pp.59-83, 1990.

Appendix B

Liapunov stability: principle theorems and definitions

B.1 Principle Liapunov theorems

The purpose of this appendix is to briefly summarize the main stability definitions and theorems relating to stability in the sense of Liapunov. The material to be presented has be taken from the excellent textbooks [1], [2] and [3], to which the reader is referred to for the proofs and further details. All the results will be presented for the nonautonomous differential equation

$$\dot{x} = F(t,x) \tag{B.1}$$

where $F:\Re_+ \times \Re^n \mapsto \Re^n$. The differential equation is assumed to have a unique solution $x(t) = x(t;t_0,x(t_0))$, $x(0;t_0,x(t_0)) = x(t_0)$,defined for $\forall t \geq 0$. The origin is said to be an equilibrium point for (B.1), if $F(t,0) = 0$ for all $t \geq 0$.

The principle Liapunov stability definitions, can be stated as follows.

Definition B.1: The equilibrium point $x = 0$ of (B.1) is

- **S:** stable, if for each $\varepsilon > 0$, there exists a $\delta(\varepsilon,t_0) > 0$ such that

$$|x(t_0)| \leq \delta(\varepsilon,t_0) \Rightarrow |x(t)| \leq \varepsilon, \quad \forall t \geq t_0 \geq 0 \tag{B.2}$$

- **US:** uniformly stable, if for each $\varepsilon > 0$, there exists a $\delta(\varepsilon) > 0$, independent of t_0, such that (B.2) holds.
- **AS:** asymptotically stable, if there exists a positive constant $c = c(t_0)$, such that $x(t) \to 0$ as $t \to \infty$, for all $|x(t_0)| < c$.
- **UAS:** uniformly asymptotically stable, if it is uniformly stable and there is a positive constant c, independent of t_0, such that for each $\eta > 0$, there exists a $T(\eta) > 0$ such that

$$|x(t)| < \eta, \quad \forall t \geq t_0 + T(\eta), \ \forall |x(t_0)| < c \tag{B.3}$$

- **GAS:** globally asymptotically stable, if it is stable and every solution of (B.1) tends to zero as $t \to \infty$.
- **GUAS:** globally uniformly asymptotically stable if, if it is uniformly stable and for any positive constants $c, \eta > 0$, there exists a $T(\eta, c) > 0$ such that $|x(t)| < \eta, \quad \forall t \geq t_0 + T(\eta, c), \forall |x(t_0)| < c$.
- **ES:** exponentially stable, if there exists positive constants ρ, η and σ such that

$$|x(t)| \leq \eta |x(t_0)| e^{-\sigma(t-t_0)}, \quad \forall t \geq t_0 \geq 0, \quad \forall |x(t_0)| \leq \rho. \tag{B.4}$$

- **GES:** globally exponentially stable, if (4) is satisfied for any initial state $x(t_0)$.
- For autonomous and periodic systems stability and asymptotic stability are equivalent to uniform stability and uniform asymptotic stability respectively. (the same holds for global notions).

The principle theorems relating to Liapunov-like stability are greatly simplified using the notions of class K and class KL functions.

Definition B.2: A continuous function $\alpha : [0, a) \mapsto [0, \infty)$ is said to belong to class K, if it is increasing and $\alpha(0) = 0$. It is said to belong to class K_∞ if $a = \infty$ and $\alpha(r) \to \infty$ a $r \to \infty$.

Definition B.3: A continuous function $\beta : [0, a) \times [0, \infty) \mapsto [0, \infty)$ is said to belong to class KL if, for each fixed s, the mapping $\beta(r, s)$ belongs to class K with respect to r and , for each fixed r, the mapping $\beta(r, s)$ is a decreasing function of s and $\beta(r, s) \to 0$ as $s \to \infty$. It is said to belong to class KL_∞ if, in addition, for each fixed s, the mapping $\beta(r, s)$ belongs to class K_∞ with respect to r.

Definition B.4: A function $V : \Re^n \times \Re_+ \mapsto \Re$ is said to be locally positive definite if it is continuous, $V(0, t) = 0, \forall t \geq 0$ and if there exists a constant $r > 0$ and a function α_1 of class K, such that $\alpha_1(|x|) \leq V(x, t), \forall t \geq 0, \forall x \in \mathbf{B}(0; r)$. V is positive definite if the previous definition holds with $r = \infty$. V is radially unbounded if it is positive definite and α_1 is of class K_∞. V is negative definite if $-V$ is positive definite. V is decrescent if there exists a constant $r > 0$ and a function α_2 of class K, such that $V(x, t) \leq \alpha_2(|x|), \forall t \geq 0, \forall x \in \mathbf{B}(0; r)$.

Definition 5 Let $V:\Re^n \times \Re \mapsto \Re$ be continuously differentiable with respect to all of its arguments and let ∇V denote the gradient with respect to x. Then the function $\dot{V}:\Re^n \times \Re_+ \to \Re$ is defined by

$$\dot{V}(x,t) = \frac{\partial V}{\partial t}(x,t) + \nabla V(x,t)F(t,x) \tag{B.5}$$

and is called the derivative V along the trajectories of Σ.

The main Liapunov stability theorems used in this thesis can be stated as follows.

Theorem B.1 (Liapunov Stability) Let $x = 0$ be an equilibrium point for (B.1) and $D = \{x \in \Re^2 \mid |x| < r\}$. Let $V: D \times \Re_+ \mapsto \Re_+$ be a continuously differential function such that for $\forall t \geq 0, \forall x \in D$

$$\alpha_1(|x|) \leq V(x,t) \leq \alpha_2(|x|) \tag{B.6}$$

$$\dot{V}(x,t) \leq -\alpha_3(|x|) \tag{B.7}$$

Then the equilibrium $x = 0$ is

- **US,** if $\alpha_1, \alpha_2 \in \mathrm{K}$ on $[0,r)$ and $\alpha_3(\cdot) \geq 0$ on $[0,r)$;
- **UAS,** if α_1, α_2 and $\alpha_3 \in \mathrm{K}$ on $[0,r)$;
- **ES,** if $\alpha_i(y) = \eta_i y^a$ on $[0,r)$ with $\eta_i > 0, a > 0, i = 1,2,3$;
- **GUS,** if $D = \Re^n$ and $\alpha_1, \alpha_2 \in \mathrm{K}_\infty$ and $\alpha_3(\cdot) \geq 0$ on $\Re_+$;
- **GUAS,** if $D = \Re^n$ and $\alpha_1, \alpha_2 \in \mathrm{K}_\infty$ and $\alpha_3 \in \mathrm{K}$ on $\Re_+$;
- **GES,** if $D = \Re^n$ and if $\alpha_i(y) = \eta_i y^a$ on $\Re_+$ with $\eta_i > 0, a > 0, i = 1,2,3$.□

Even when the differential equation in (1), has no equilibrium points, Liapunov analysis can still be used to obtain useful estimates relating to the boundedness of solutions. The definitions which follow are along this line.

Definition B.6 The solutions of (B.1) are

- **LUB,** locally uniformly bounded, if there exists a positive constant ρ, independent of $t_0 \geq 0$, and for every $c \in (0, \rho)$, there is a $\beta(c) > 0$, independent of t_0, such that $\forall t \geq t_0$

$$|x(t_0)| \leq c \Rightarrow |x(t)| \leq \beta, \forall t \geq t_0. \tag{B.8}$$

- **UB,** uniformly bounded if (8) holds for arbitrarily large c.

- **LUUB,** locally uniformly bounded with ultimate bound B, if there exists positive constants ρ, B, independent of $t_0 \geq 0$, and for every $c \in (0, \rho)$, there is a $T(c, \mathrm{B}) > 0$, independent of t_0, such that $\forall t \geq T + t_0$

$$|x(t_0)| \leq c \Rightarrow |x(t)| \leq \mathrm{B}, \forall t \geq T(c, \mathrm{B}) + t_0. \tag{B.9}$$

- **UUB,** uniformly ultimately bounded if (B.8) holds for arbitrarily large c.

The next theorem provides a Liapunov characterisation of boundedness of solutions.

Theorem B.2(Boundedness) Let $D = \{x \in \Re^2 \mid |x| < r\}$. Let $V : D \times \Re_+ \mapsto \Re_+$ be a continuously differential function such that for $\forall t \geq 0, \forall x \in D$

$$\alpha_1(|x|) \leq V(x,t) \leq \alpha_2(|x|) \tag{B.10}$$

$$\dot{V}(x,t) \leq -\alpha_3(|x|), \quad \forall |x| \geq R > 0, \tag{B.11}$$

where $\alpha_i, i = 1,2,3$ are class K functions. Suppose that $R < \alpha_2^{-1} \circ \alpha_1(r)$ and $|x(t_0)| < \alpha_2^{-1} \circ \alpha_1(r)$, then there exists a class KL function β and $T \geq 0$ (independent of R and $x(t_0)$) such that

$$|x(t)| \leq \beta(|x(t_0)|, t - t_0), \quad \forall t_0 \leq t \leq t_0 + T, \tag{B.12}$$

$$|x(t)| \leq \alpha_1^{-1} \circ \alpha_2(R), \quad \forall t \geq t_0 + T, \tag{B.13}$$

That is $|x(t)|$ is LUB for $t \geq t_0$ and LUUB with ultimate bound $\alpha_1^{-1} \circ \alpha_2(R)$. Furthermore, if $D = \Re^n$ and $\alpha_1, \alpha_2 \in \mathrm{K}_\infty$, then (B.10) and (B.11) hold for any initial state, $x(t_0)$ with no restriction on how large R is. That is $|x(t)|$ is UB for $t \geq t_0$ and UUB with ultimate bound $\alpha_1^{-1} \circ \alpha_2(R)$. □

The following comparison lemma is an extremely useful tool for obtaining estimates for the solutions of differential equations. Recall that the upper right Dini derivative of $y(t)$ is defined by $D^+x(t) = \limsup_{t \to 0^+} [x(t+h) - x(t)]/h$. Note that if $x \in C^1(\Re_+; \Re)$, then $D^+x(t) = \dot{x}(t)$.

Lemma B.1 (Comparison Lemma) Consider the scalar differential equation $\dot{y} = F(t, y), y(t_0) = y_0$, where $F(t, y)$ is continuous in t and locally Lipschitz in y, for $t \geq t_0$ and all $y \in I \subset \Re$. Let $[t_0, T)$ (T could be infinity) be the maximal interval of existence of the solution $y(t)$ and suppose $y(t) \in I$ for all $t \in [t_0, T)$. Now let $x(t)$ be a continuous function, whose upper right Dini derivative satisfies the inequality $D^+x(t) \leq F(t, x(t))$ with $x(t_0) \leq y_0$ and $x(t) \in I$ for all $t \in [t_0, T)$. Then $x(t) \leq y(t)$ for all $t \in [t_0, T)$. □

B.2 Asymptotic behaviour of Solutions

The theorems to be presented in this section enable one to obtain estimates pertaining to the asymptotic behaviour of solutions of ordinary differential equations, under far less restrictive conditions than those required by Theorem B.1. The material presented below is based on the excellent text [1] and the innovative paper [4]. These theorems make use of the notion of a ω-limit point, of the solution $x(t; t_0, x(0))$ of the differential equation Σ. Following [4], it was found to be useful to define the concept of a ω-limit point, in terms of arbitrary $\Re^n$- valued functions.

Definition B.7 Let $x : \Re_+ \mapsto \Re^n$ be an arbitrary function. A point $p \in \Re^n$ is said to be a ω-limit point of x, if there exists an unbounded sequence $\{t_n\}$ in $\Re_+$, such that $x(t_n) \to p$ as $n \to \infty$. The (possible empty) ω-limit set of x, denoted $\Omega(x)$, is the set of all ω-limit points of x.

The following lemma collects some useful properties of ω-limit sets.

Lemma B.2 The following hold for any function $x : \Re_+ \to \Re^n$;

- $\Omega(x)$ is closed.
- $\Omega(x)$ is empty if $|x(t)| \to \infty$ as $t \to \infty$.
- If x is continuous and bounded, then $\Omega(x)$ is nonempty, compact, and connected, is approached by x, and is the smallest closed set so approached.
- If x is continuous and $\Omega(x)$ is nonempty and bounded, then x is bounded and x approaches $\Omega(x)$.

Possibly the most useful tool for the characterisation $\Omega(x)$, is a lemma known as Barbalat's lemma. Before stating Barbalat's lemma, it will prove useful to recall some definitions from advanced calculus. A function $x:\Re_+ \mapsto \Re^n$ is said to be Riemann integrable on $\Re_+$, if the improper integral $\lim_{t\to\infty} \int_0^t x(s)ds$ exists and is finite. Let $x:\Re_+ \mapsto \Re^n$ be a Lebesgue measurable function, then $x \in L_p(\Re_+;\Re^n)$, for some $p \in [1,\infty)$ if the function $t \to |x(t)|^p$ is Lebesgue integrable. If the function $t \mapsto |x(t)|$ is essentially bounded, then $x \in L_\infty(\Re_+;\Re^n)$. Finally note that if $x \in C^{0,1}(\Re_+;\Re^n)$, then x is uniformly continuous on $\Re_+$ by definition.

Lemma B.3 (Barbalat's lemma 1) If $x:\Re_+ \mapsto \Re^n$ is uniformly continuous and Riemann integrable on $\Re_+$, then $x(t) \to 0$ as $t \to \infty$.

Corollary B.1 For $x:\Re_+ \mapsto \Re^n$, if $x, \dot{x} \in L_\infty(\Re_+;\Re^n)$ and $x \in L_p(\Re_+;\Re^n)$ for some $p \in [1,\infty)$ then $x(t) \to 0$ as $t \to \infty$.

The next corollary is a direct consequence of Lemma B.2 and Lemma B.3.

Corollary B.2 Let G be a nonempty closed subset of $\Re^n$ and let $\gamma: G \to \Re$ be a continuous function. Assume that $x:\Re_+ \to \Re^n$ is uniformly continuous with $x(t) \in G, \forall t \in \Re_+$. If $\gamma(x)$ is Riemann integrable, then $\Omega(x) \subset \{x \in G \mid \gamma(x) = 0\}$.

Lemma B.4 (Barbalat's lemma 2) If $x \in C^{1,1}(\Re_+;\Re^n)$ has a finite limit as $t \to \infty$, then $\dot{x}(t) \to 0$ as $t \to \infty$.

Finally, another simple lemma which will prove useful for analysing the asymptotic behaviour of solutions.

Lemma B.5 Let σ be a positive constant and let $x: C(\Re_+;\Re^n)$. If $|x(t)|$ is Riemann integrable or $|x(t)| \to 0$ as $t \to \infty$, then $\int_0^t e^{-\sigma(t-s)}|x(s)|ds \to 0$ as $t \to \infty$.

Combining Corollary B.2 and Theorem B.2, one obtains the following Liapunov-type theorem.

Theorem B.3 (Liapunov-like theorem) Consider the differential equation (B.1) and suppose that for bounded x, $F(t,x)$ is bounded uniformly in t. Let $V:\Re^n\times\Re_+\mapsto\Re_+$ be a continuously differential function such that for $\forall t\geq 0,\forall x\in\Re^n$

$$\alpha_1(\|x\|)\leq V(x,t)\leq\alpha_2(\|x\|) \tag{B.14}$$

$$\dot{V}(x,t)\leq-\gamma(\|x\|)\leq 0 \tag{B.15}$$

where $\alpha_1,\alpha_2\in K_\infty$ and γ is a continuous function. Define the set $E=\{x\in\Re^n\mid\gamma(x)=0\}$. Then all solutions of (B.1) are UB and $\Omega(x)\subset E$.□

If the system Σ is T-periodic, that is $F(t,x)=F(t+T,x),\forall x\in\Re^n,\forall t\geq 0$, then it is possible to sharpen the results presented above, using the notion of an invariant set.

Definition B.8 A set $M\subseteq\Re^n$ is called a positively invariant set for (B.1), if for some $t_0\geq 0$ and each $x(t_0)\in M$, the resulting solution $x(t;t_0,x(t_0))$, satisfies $x(t;t_0,x_0)\in M,\forall t\geq t_0$.

Lemma B.6 Suppose the system Σ is periodic and let. If the solution $x(t;t_0,x(t_0))$ is bounded for all $t\geq t_0\geq 0$, then $\Omega(x)$ is an invariant set for (B.1).

The following theorems are simplified versions, of what are commonly referred the Krasovskii-LaSalle stability theorems [1].

Theorem B.4 (Krasovskii-LaSalle) Suppose that (B.1) is T-periodic, and that for bounded x, $F(t,x)$ is bounded uniformly in t. Let $V:\Re^n\times\Re_+\mapsto\Re_+$ be a continuously differential T- periodic function, such that for $\forall t\geq 0,\forall x\in\Re^n$

$$\alpha_1(\|x\|)\leq V(x,t)\leq\alpha_2(\|x\|) \tag{B.16}$$

$$\dot{V}(x,t)\leq 0 \tag{B.17}$$

where $\alpha_1,\alpha_2\in K_\infty$. Define the set $E=\{x\in\Re^n\mid\dot{V}(x,t)=0\}$ and let M denote the largest invariant set for Σ contained in E. Then all solutions of Σ are uniformly bounded and $\Omega(x)\subset M$.□

Theorem B.5 (Krasovskii-LaSalle) Suppose that (B.1) is T-periodic, and that for bounded x, $F(t,x)$ is bounded uniformly in t. Define $D=\{x\in\Re^2 \mid |x|<r\}$ and let $V:\Re^n\times D\mapsto\Re_+$ be a continuously differential T- periodic function and such that for $\forall t\geq 0, \forall x\in D$

$$\alpha_1(\|x\|)\leq V(x,t)\leq\alpha_2(\|x\|) \tag{B.18}$$

$$\dot{V}(x,t)\leq 0 \tag{B.19}$$

where $\alpha_1,\alpha_2\in \mathrm{K}$. Define the set $\mathrm{E}=\{x\in\Re^n \mid \dot{V}(x,t)=0\}$. Let $x=0$ be an equilibrium point for Σ, suppose that no solution of Σ can stay identically in E, other than $x(t;t_0,0)\equiv 0, t>t_0$. Then the equilibrium $x=0$ is UAS. Furthermore if all of the above conditions hold with $D=\Re^n$ and $\alpha_1,\alpha_2\in \mathrm{K}_\infty$, then the equilibrium $x=0$ is GUAS.□

References

[1]. M. Vidyasagar. Nonlinear Systems Analysis, 2nd Ed. Prentice Hall, Englewood Cliffs, 1993.

[2]. H. Khalil. Nonlinear Systems, 3rd Ed. Prentice Hall, Upper Saddle River, N.J., 2002.

[3]. R. Miller, A. Michel. Ordinary differential equations. Academic Press, NY, 1982.

[4]. H. Lodgemann, E. Ryan. "Asymptotic behavior of nonlinear systems". American Mathematical Monthly, vol.111, pp. 864-889, 2004.

Appendix C

Wellposedness of damper models

C.1 Introduction

The main purpose of this appendix is to present some simple results establishing wellposedness of the models presented in §3. As the reader may be unfamiliar with the concept of a well-posed model, it would seem worthwhile to take a few seconds to explain the basic idea. Consider the following model of a simple pendulum

$$\ddot{q}(t) + c\dot{q}(t) + \sin(q(t)) = 0 \qquad \text{(C.1.1)}$$

with initial conditions $q(0) = q_0$ and $\dot{q}(0) = \dot{q}_0$. Now suppose it was intended to use this model to determine the motion of a physical pendulum. Unlike its linear counter part, the spring mass damper (C.1.1) cannot be solved in terms of simple trigonometric functions. In fact, does it even have a solution. It would not be a very good model if it didn't, since an actual pendulum certainly does move. Thus for the mathematical model of a physical processes to be of any use, it should at least have a solution. This is the problem of existence of solutions.

Suppose the actual pendulum is released from the initial conditions $q(0) = \pi/3$ and $\dot{q}(0) = 0$ and is allowed to swing about for a bit. Now, suppose the same experiment is repeated the next day, with the same initial conditions and under same environmental conditions. Experience would suggest that the resulting motion will be identical with that of the previous experiment. This is the usual notion of determinism, or in the terminology of differential equations, uniqueness of solutions. In reality it is impossible to repeat such an experiment exactly, there will always be some small variations in the initial conditions or in the experimental setup itself. However if the experiment is repeated under almost the same conditions, then it is reasonable to expect that the resulting motions of the pendulum would be almost the same. That is, small errors in the data cause only small errors in the solution. If the solutions of a mathematical model exhibit this sort of behaviour, then it is said that the solution depends continuously on the data of the problem (this idea is very closely related to stability).

To recap, a mathematical model, along with a family of initial conditions is said to be wellposed, if the following can be proved

- Existence : the problem has at least one solution
- Uniqueness : the problem cannot have more than one solution.
- Continuous dependence on the data : small variations in the data, will only result in small variations in the solution.

Section.2 presents some standard results for ordinary differential equations, which are sufficient for the analysis of the viscoplastic models. Section.3 presents some results relating to solutions of the EP model in isolation and when coupled with an ordinary differential equation.

C.2 Differential Equations

The purpose of this section is to present some standard results from the theory of ordinary differential equations and to illustrate their application to the viscoplastic models form §3.5.

As noted in §3.5, when a viscous element is placed in parallel with a friction element it has the effect of "smoothing out" the corresponding evolution equations (as compared to the EP type models). The reason for this is that the stress response is no longer confined to a closed set, $[-r,r] \subset \Re$. In terms of the evolution equations themselves, the variational inequality can be replaced by an ordinary differential equation. This means that existence and uniqueness results can be obtained using the standard theorems for ordinary differential equations. The material in this section is based on the excellent text books [1], [2] and [3], to which the reader is referred for further details.

Consider the ordinary differential equation

$$\dot{x}(t) = F(x(t), u(t)) \tag{C.2.1}$$

where $t \in \Re_+$, $x \in \Re^n$ represent the state variables , $u : \Re_+ \mapsto \Re^m$ is a vector of forcing terms and time varying parameters and $F : \Re^n \times \Re^m \mapsto \Re^n$. By a classical solution of the differential equation (C.2.1) on an interval $[0,T] \subset \Re_+$ is meant a continuously differentiable function $x(t)$, which along with $\dot{x}(t)$, its derivative with respect to t, satisfies (C.2.1) for all $t \in [0,T]$. In general the initial condition $x(0) = x_0$ and input $u(t)$ will be specified. When there is need to emphasize the dependence of a solution of

(C.2.1) on u and x_0, the notation $x(t) = x(t; x_0, u(\cdot))$ will be used. If $x(t)$ is a solution of (C.2.1) and $F(x(t), u(t))$ is integrable with respect to t, then (C.2.1) is equivalent to the integral equation,

$$x(t) = x(0) + \int_0^t F(x(s), u(s))ds, \quad \forall t \in [0,T]. \tag{C.2.2}$$

Suppose the input $u(t)$ is continuous and bounded on $\Re_+$ and $F(x,u)$ is defined and continuous on $\Re^n \times \Re^m$, then a classical result states that (C.2.1) has at least one solution $x(t)$, defined on a small interval $[0,a] \subset [0,T]$. If it can be shown that for every $x_0 \in \Re^n$, all resulting solutions of (C.2.1) remain bounded, then each solution of (C.2.1) can be continued over the entire interval $[0,T]$. This theorem says nothing about uniqueness or continuity with respect to the data. A sufficient condition for (C.2.1) to have a unique solution, which depends continuously on $x(0) = x_0$ and $u(t)$ is that $F(x,u)$ is locally Lipschitz on $\Re^n \times \Re^m$. Which is to say that for each $(\bar{x}, \bar{u}) \in \Re^n \times \Re^m$, there exists two constants $\delta > 0$ and $\beta > 0$ such that

$|F(x_1,u_1) - F(x_2,u_2)| \le \beta(|x_1 - x_2| + |u_1 - u_2|)$, for all x_i and u_i such that

$|x_i - \bar{x}| \le \delta, |u_i - \bar{u}| \le \delta, i = 1,2$.

The continuity assumption on the input $u(t)$ is too restrictive for many applications, particularly if $u(t)$ represents some sort of control. A more useful assumption would be that $u(t)$ is integrable and essentially bounded, i.e. $u \in L_\infty([0,T];\Re^m)$. In this case, even if $F(x,u)$ on $\Re^n \times \Re^m$ is continuous, it cannot be assumed that $F(x,u(t))$ is continuous on $\Re^n \times \Re_+$, and hence it cannot be assumed that the solutions of (C.2.1) are continuously differentiable. By a Caratheodory solution of (C.2.1) on an interval $[0,T] \subset \Re_+$ is meant an absolutely continuous function $x(t) = x(t; x_0, u(\cdot))$, which satisfies (C.2.1) for almost every $t \in [0,T]$, or equivalently which satisfies (C.2.2) for all $t \in [0,T]$. The terminology for almost every $t \in [0,T]$, or for a.e. $t \in [0,T]$ means, for all $t \in [0,T]$ except on a set of Lebesque measure zero (see §A.1). Recall also that a function $x : [0,T] \to \Re^n$ is said to be absolutely continuous or an element of $AC([0,T];\Re^n)$, if it can be expressed in the form $x(t) = x(0) + \int_0^t \vartheta(s)ds$, for some integrable function ϑ; it follows then that $\dot{x}(t) = \vartheta(t)$ for a.e. $t \in [0,T]$. Most theorems on the existence and uniqueness of classical solution cans be carried over to the

Caratheodory case with a little modification [2]. Note that by a solution defined on $\Re_+$, is meant a solution defined on $[0,T]$ for each $T \in \Re_+$.

The following global existence theorem is not very general and has been tailored to the specific requirements of this thesis. For its proof and a more general discussion on existence theorems for differential equations, the reader is referred to [1],[2] and [3].

Theorem C.1 Suppose that $F(0,0) = 0$ and for all $(x,u),(\bar{x},\bar{u}) \in \Re^n \times \Re^m$ there exists a positive constant β such that

$$|F(x,u) - F(\bar{x},\bar{u})| \le \beta|x-\bar{x}| + \beta|u-\bar{u}|. \tag{C.2.3}$$

Then for each $x_0 \in \Re^n$ and $u \in L_\infty([0,T];\Re^m)$, $T \in \Re_+$

(i) The differential equation (C.2.1) has a unique absolutely continuous solution $x(t) = x(t;x_0,u(\cdot))$ (i.e. $x \in AC([0,T];\Re^n)$) which satisfies

$$|x(t) - x_0| \le \left(e^{\beta t} - 1\right)\left(|x_0| + \|u\|_\infty\right), \quad \forall t \in [0,T]. \tag{C.2.4}$$

Let $x(t) = x(t;x_0,u(\cdot))$ and $\bar{x}(t) = \bar{x}(t;\bar{x}_0,\bar{u}(\cdot))$ be the unique solution of (C.2.1) corresponding to the initial conditions and inputs $x_0 \in \Re^n, u \in L_\infty([0,T];\Re^m)$ and $\bar{x}_0 \in \Re^n$, $\bar{u} \in L_\infty([0,T];\Re^m)$ respectively, then

$$|x(t) - \bar{x}(t)| \le |x_0 - \bar{x}_0|e^{\beta t} + \left(e^{\beta t} - 1\right)\|u - \bar{u}\|_\infty, \tag{C.2.5}$$

for all $t \in [0,T]$ (continuous dependence on the data).

(ii) If $u \in C([0,T];\Re^m)$ then $x \in C^1([0,T];\Re^n)$ (classical solution).

(iii) If $u \in C([0,\infty);\Re^m)$ or $u \in L_\infty([0,\infty);\Re^m)$ then $x \in C^1([0,\infty);\Re^n)$ or $x \in AC([0,\infty);\Re^n)$ respectively (see §A1 for remarks on semi-infinite intervals).

(iv) If $u \in C^{0,1}([0,\infty);\Re^m)$ and all solutions of (C.2.1) are uniformly bounded (see §B.1) then $x \in C^{1,1}([0,\infty);\Re^n)$. □

To demonstrate the application of the theorem, the GnF model given by equation (3.5.22), will be considered as a representative example. For simplicity, setting $z_1 = \sigma$, $z_2 = H\alpha_1$, $u_1 = \dot{e}, u_2 = r$ and $\eta = \eta_e = \eta_p$ in equation (3.5.25) yields the ordinary differential equation

$$\begin{aligned} \dot{z}_1 &= Gu_1(t) - \frac{G}{\eta}(z_1 - z_2) - \frac{G}{\eta}P(z_1; u_2(t)), \\ \dot{z}_2 &= \frac{H}{\eta}(z_1 - z_2). \end{aligned} \tag{C.2.6}$$

It is assumed that $|u_1(t)| < \infty$ and $u_2(t) \in [0, \bar{r}]$ for almost all $t \in \Re_+$. Recall that $P(z_1; u_2) = z_1 - Q(z_1; u_2)$, where $Q(z_1; u_2)$ is the projection onto the interval $[-u_2, u_2]$ and $|P(z_1; u_2) - P(\bar{z}_1; \bar{u}_2)| \le |z_1 - \bar{z}_1| + |u_2 - \bar{u}_2|$ for all $(z_1, u_2), (\bar{z}_1, \bar{u}_2) \in \Re \times \Re_+$ (see §A2). Defining $z = (z_1, z_2) \in \Re^2$ and $u = (u_1, u_2) \in \Re \times \Re_+$, it can be seen that the right hand side of (C.2.6) satisfies (C.2.3) and so (i)-(iii) of Theorem C.1 can be applied. The growth estimates (C.2.4) and (C.2.5) are very conservative as they don't account for the external stability properties of the differential equation. To illustrate this, consider the system energy $H(z) = 0.5(z_1^2/G + z_1^2/H)$. The derivative of $H(z)$ along the solution of (2.6) satisfies

$$\begin{aligned} \dot{H}(z) &= -\frac{1}{\eta}\left(z_1^2 - 2z_1 z_2 + z_2^2\right) - \frac{1}{\eta} z_1 P(z_1; u_2(t)) + z_1 u_1(t), \\ &\le -\frac{1}{\eta}\left(2z_1^2 - 2z_1 z_2 + z_2^2\right) + \frac{1}{\eta} z_1 Q(z_1; u_2(t)) + z_1 u_1(t), \\ &\le -\frac{1}{\eta}\left(1.5z_1^2 - 2z_1 z_2 + z_2^2\right) + \frac{1}{\eta} u_2^2(t) + \eta u_1^1(t). \end{aligned} \tag{C.2.7}$$

In the final inequality, the term in brackets is positive definite, which when combined with the fact that $H(z)$ is quadratic and positive definite implies the existence of two constants $\gamma, p > 0$ such that

$$|z(t)|^2 \le \beta |z_0|^2 e^{-pt} + \beta \|u\|_\infty^2 \left(1 - e^{-pt}\right). \tag{C.2.8}$$

Inequality (C.2.8) is clearly much better than (C.2.4). In particular, it implies that that all solution of (C.2.6) are uniformly bounded, so that from (iv) of Theorem B.1, if also $u \in C^{0,1}([0,\infty); \Re^2)$ then $z \in C^{1,1}([0,\infty); \Re^2)$.

C.3 The EP model

The purpose of this section is to establish existence, uniqueness and regularity results for the simple EP model from §3.4, when in isolation and when coupled with an ordinary differential equation. Before presenting the main results, some equivalent representations of the EP model will be presented. For the initial discussion, the elastic modulus is assumed to be constant and equal to one, $G=1$. As such, no distinction will be made between stresses and elastic strains. In §3.4, it was shown that the evolution of the EP model is completely described by the variational inequality

$$\Sigma_Z \begin{cases} \langle \dot{x}(t)-\dot{z}(t), z(t)-\varphi \rangle \geq 0, \quad \forall |\varphi| \leq r(t), \\ |z(t)| \leq r(t), \quad \forall t \geq 0. \end{cases} \tag{C.3.1}$$

where $x(t)$ is the displacement input and $r(t) \in [0,\bar{r}]$ is the time varying yield stress. As noted in §3.4, (C.3.1) can be interpreted as a special form of the maximum dissipation principle. Indeed, multidimensional versions of (C.3.1) play a central role in the theory of elastoplastic materials [4]. Recall that the normal cone to the set $[-r(t),r(t)]$ at the point z is given by $N(z;r(t)) = \{\alpha \in \Re \mid \langle \alpha, z-\varphi \rangle \geq 0, \forall |\varphi| \leq r(t)\}$. Comparing this with (C.3.1) it can be seen that the EP model can also be written in the form of a differential inclusion

$$\begin{aligned} &\dot{x}(t)-\dot{z}(t) \in N(z(t);r(t)) \\ &|z(t)| \leq r(t), \quad \forall t \geq 0. \end{aligned} \tag{C.3.2}$$

A differential inclusion can be seen as a generalization of the notion of an ordinary differential equation. They frequently occur when modelling nonsmooth mechanical and electrical system and play an important role in modern control theory [5]. Now, defining the new evolution variable $\xi(t)$ and the time dependent closed convex set $C(t)$ by

$$\xi(t) = z(t) - \int_0^t \dot{x}(s)ds, \quad C(t) = [-r(t),r(t)] - \int_0^t \dot{x}(s)ds, \tag{C.3.3}$$

yields

$$-\dot{\xi}(t) \in N(\xi(t);C(t)). \tag{C.3.4}$$

Evolution problems formulated in the form (C.3.4) are usually referred as a (Moreau's) sweeping process [6]. The name comes from the fact that in the multidimensional setting (C.3.4) describes the movement of a point $\xi(t)$ in some (Hilbert) space, as it is swept along by the convex set $C(t)$. The sweeping process can be used to model all sorts

of physical systems which are subject to inequality constrains, a review of such applications can be found in [7].

All three of the above formulations can be used to investigate conditions for existence and uniqueness of solutions of the EP model. Applying the standard theory of differential inclusions to (C.3.2) requires a lot of work. On the other hand existence theory for the variational inequality (C.3.1) and the sweeping process have been developed specifically for physical models such as the EP model. Indeed, the results in [7] and [8] can be used to show that under mild assumptions on the functions $r(t)$ and $x(t)$, the EP model has a unique solution. The results in these works admit the infinitely dimensional case and as such, are not readily accessible to those without a working knowledge of Hilbert spaces and convex analysis. If the models developed in this thesis are to gain acceptance in the ER fluid community, the results need to be accessible to those with only a working knowledge of existence theory for ordinary differential equations. This is not an unrealistic goal as the EP model is only one dimensional.

The results given below hopefully go some way towards achieving this goal. Before stating the first theorem, the actual problem needs to be defined more precisely.

Problem EP

For some $T > 0$, given the functions $x \in C^{0,1}([0,T];\Re)$, $r \in C^{0,1}([0,T];\Re_+) \bigcap [0,\bar{r}]$ and an initial condition $|z_0| \le r(0)$, find a function $z \in C^{0,1}([0,T];\Re)$ such that

(i) $|z(t)| \le r(t)$ for all $t \in [0,T]$,

(ii) $\langle \dot{x}(t) - \dot{z}(t), z(t) - \varphi \rangle \ge 0$ for all $|\varphi| \le r(t)$ and a.e. $t \in [0,T]$.

The following theorem and proof is based on a simplification of the ideas in [4] and [8], in particular Proposition 4.1 of [8]. The idea behind the proof is to first construct and discrete time approximate solution and to show that this discrete solution converges to the actual solution as the time step tends to zero. The construction of the discrete approximated solution is not obvious. Suppose the interval $[0,T]$ is partitioned into n equal subintervals by the partition $0 = t_0 < t_1 \ldots < t_n = T$ with $h = T/n$ and $t_k = kh, k = 0,1\ldots,n.$

Now, at time t_{k+1}, approximating the derivatives on the left hand side of (C.3.2) by $(x(t_{k+1})-x(t_k))/h$ and $(z(t_{k+1})-z(t_k))/h$ yields the implicit Euler type scheme

$$x(t_{k+1})-x(t_k)-z(t_{k+1})+z(t_k)\in hN(z(t_{k+1});r(t_{k+1})). \tag{C.3.5}$$

Note that the positive factor h is immaterial as the right hand side of (C.3.5) is a cone. The next step is to solve (C.3.5) for $z(t_{k+1})$. Let $Q(y;r)$ denote the projection of $y\in\Re$ onto the set $[-r,r]$. A classical result from convex analysis is that $y-z\in N(z;r)$ is equivalent to $z=Q(y;r)$, [4], [6]. Applying this result to (C.3.5) yields the solution

$$z(t_{k+1})=Q\big(z(t_k)+x(t_{k+1})-x(t_k);r(t_{k+1})\big) \tag{C.3.6}$$

Theorem C.3.1

For every $x\in C^{0,1}([0,T];\Re)$, $r\in C^{0,1}([0,T];\Re_+)\cap[0,\bar{r}]$ and initial condition $|z_0|\le r(0)$, problem EP has a unique solution $z(t)=z(t;z_0,x(\cdot),r(\cdot))$ such that $z\in C^{0,1}([0,T];\Re)$.

(let κ_x, κ_r denote the Lipschitz constants of x and r respectively)

Proof:

As outlined above, the proof of existence is based on the construction of an approximate solution using a simple time discretization. For each $n\in\mathrm{N}$, form a partition $0=t_0<t_1\ldots<t_n=T$ with $h=T/n$ and $t_k=kh, k=0,1\ldots,n.$ Let $Q(y;r)$ be the projection operator defined in §A.2 and $P(y;r)=y-Q(y;r)$. For $k=0,1,\ldots,n$ define the nodes $x_k^n=x(t_k)$, $r_k^n=r(t_k)$ and for $k=1,2\ldots,n$, define

$$z_k^n=Q(z_{k-1}^n+x_k^n-x_{k-1}^n;r_k^n)\ , \tag{C.3.7}$$

starting from the given initial condition z_0. Note that the projection operator ensures that each node satisfies $|z_k^n|\le r_k^n$. Now construct a set of piecewise linear Euler arcs on $[0,T]$ using

$$\begin{cases} x^n(t)=x_{k-1}^n+\dfrac{1}{h}(t-t_{k-1})(x_k^n-x_{k-1}^n),\\ r^n(t)=r_{k-1}^n+\dfrac{1}{h}(t-t_{k-1})(r_k^n-r_{k-1}^n),\\ z^n(t)=z_{k-1}^n+\dfrac{1}{h}(t-t_{k-1})(z_k^n-z_{k-1}^n), \end{cases} \tag{C.3.8}$$

for $t\in[t_{k-1},t_k), k=1,2\ldots,n$, continuously extended to $t=T$. It follows that $x^n\to x$ and $r^n\to r$ uniformly in $C([0,T];\Re)$ as $n\to\infty$. To make the equations a bit shorter the

following notation is introduced $\Delta x_k^n = x_k^n - x_{k-1}^n$, $\Delta r_k^n = r_k^n - r_{k-1}^n$ and $\Delta z_k^n = z_k^n - z_{k-1}^n$. Now, using the identity $P(y;r) = y - Q(y;r)$ yields $\Delta x_k^n - \Delta z_k^n = P(z_{k-1}^n + x_k^n - x_{k-1}^n; r_k^n)$ and applying inequality (A.2.1) in §A.2 leads to

$$\left\langle \Delta x_k^n - \Delta z_k^n, z_k^n - \varphi \right\rangle \geq 0 \quad \forall\, |\varphi| \leq r_k^n, \tag{C.3.9}$$

for all $k = 1,2\ldots,n$. Since $\left|Q(z_{k-1}^n; r_k^n)\right| \leq r_k^n$ by definition, it follows from (C.3.9) that

$$\left\langle \Delta x_k^n - \Delta z_k^n, z_k^n - Q(z_{k-1}^n; r_k^n) \right\rangle \geq 0, \tag{C.3.10}$$

and hence

$$\begin{aligned} \left|\Delta x_k^n - \Delta z_k^n\right|^2 &= \left\langle \Delta x_k^n - \Delta z_k^n, \Delta x_k^n \right\rangle - \left\langle \Delta x_k^n - \Delta z_k^n, z_k^n - Q(z_{k-1}^n; r_k^n) \right\rangle \\ &\quad + \left\langle \Delta x_k^n - \Delta z_k^n, z_{k-1}^n - Q(z_{k-1}^n; r_k^n) \right\rangle, \\ &\leq \left|\Delta x_k^n - \Delta z_k^n\right|\left|\Delta x_k^n\right| + \left|\Delta u_k^n - \Delta z_k^n\right|\left|P(z_{k-1}^n; r_k^n)\right| \\ &\leq \left|\Delta u_k^n - \Delta z_k^n\right|\left(\left|\Delta u_k^n\right| + \left|\Delta r_k^n\right|\right). \end{aligned} \tag{C.3.11}$$

where (C.3.10) and the fact that $\left|z_{k-1}^n\right| \leq r_{k-1}^n \Rightarrow \left|P(z_{k-1}^n; r_k^n)\right| \leq \left|r_k^n - r_{k-1}^n\right|$ have been used. Simplifying (C.3.11) yields

$$\begin{aligned} \left|\Delta x_k^n - \Delta z_k^n\right| &\leq \left|\Delta x_k^n\right| + \left|\Delta r_k^n\right| \leq \int_{t_{k-1}}^{t_k} \left(|\dot{x}| + |\dot{r}|\right)(s)\,ds, \\ \left|\Delta z_k^n\right| &\leq 2\left|\Delta x_k^n\right| + \left|\Delta r_k^n\right| \leq h(2\kappa_x + \kappa_r), \end{aligned} \tag{C.3.12}$$

for all $k = 0,1,2\ldots,n$. It is now possible to obtain a uniform bound on $\left|\dot{z}^n(t)\right|$, using (C.3.8) and (C.3.11), for $t \in [t_{k-1}, t_k)$,

$$\left|\dot{z}^n(t)\right| = \frac{1}{h}\left|z_k^n - z_{k-1}^n\right| \leq (2\kappa_u + \kappa_r) = \kappa_z, \tag{C.3.13}$$

and hence $\left\|\dot{z}^n\right\|_\infty \leq \kappa_z$ for all $t \in [0,T]$. Recall that $\left|z_k^n\right| \leq r_k^n \leq \bar{r}$ for all k. Combining this with the fact that $z^n(t)$ is a convex combination of the values taken by two successive nodes, leads to the conclusion that $\left\|z^n\right\|_\infty \leq \bar{r}$. To recap, as $n \to \infty$ the Euler arcs on $[0,T]$ all satisfy

$$z^n(0) = z_0, \quad \left\|z^n\right\|_\infty \leq \bar{r}, \quad \left\|\dot{z}^n\right\|_\infty \leq \kappa_z. \tag{C.3.14}$$

It follows that the sequence $\{z^n\}$ is uniformly bounded and equicontinuous and so by the theorem of Arzela (Theorem A.1.1 in §A.1), some subsequence of $\{z^n\}$ converges uniformly to a continuous function $z : [0,T] \to \Re$. From Theorem A.1.2, the limiting

function will inherit the Lipschitz rank κ_z on $[0,T]$ and hence $z \in C^{0,1}([0,T];\Re)$. Next it is shown that $z(t)$ satisfies EP(i). Referring back to (C.3.8) it can be seen that for $t \in [t_{k-1}, t_k)$, $z^n(t)$ satisfies

$$|z^n(t)| \le \alpha |z_k| + (1-\alpha)|z_{k-1}| \le \alpha r_k + (1-\alpha) r_{k-1}, \tag{C.3.15}$$

for some $\alpha \in [0,1)$. Combining (C.3.15) with the equality $r(t) - \alpha r(t) - (1-\alpha) r(t) = 0$, yields

$$\left|z^n(t)\right| \le r(t) + \alpha \left|r(t) - r_k^n\right| + (1-\alpha)\left|r(t) - r_{k-1}^n\right|, \tag{C.3.16}$$

for $t \in [t_{k-1}, t_k)$ and hence

$$\left|z^n(t)\right| \le r(t) + \kappa_r h = r(t) + \frac{1}{n}\kappa_r (b-a), \tag{C.3.17}$$

for all $t \in [0,T]$. Selecting a convergent subsequence of $\{z^n\}$ and passing to the limit as $n \to \infty$, shows that EP (i) is satisfied. The next step is to show that EP (ii) is satisfied as $n \to \infty$. Pick some $\varphi \in C([0,T];\Re)$ such that $|\varphi(t)| \le r(t)$ for all $t \in [0,T]$, then for a.e. $t \in (t_k, t_{k-1})$

$$\begin{aligned} \left\langle \dot{x}^n(t) - \dot{z}^n(t), z^n(t) - \varphi(t) \right\rangle &= \frac{1}{h}\left\langle \Delta x_k^n - \Delta z_k^n, z^n(t) - \varphi(t) \right\rangle, \\ &= \frac{1}{h}\left\langle \Delta x_k^n - \Delta z_k^n, z_k^n - Q(\varphi(t); r_k^n) \right\rangle \\ &\quad - \frac{1}{h}\left\langle \Delta x_k^n - \Delta z_k^n, z_k^n - z^n(t) + P(\varphi(t); r_k^n) \right\rangle. \end{aligned} \tag{C.3.18}$$

From (C.3.9), it can be seen the first term on the right is positive, so using (C.3.12) leads to

$$\begin{aligned} \left\langle \dot{x}^n(t) - \dot{z}^n(t), z^n(t) - y(t) \right\rangle &\ge -\frac{1}{h}\left|\Delta x_k^n - \Delta z_k^n\right|\left(\left|z^n(t) - z_k^n\right| + \left|r(t) - r_k\right|\right), \\ &\ge -2(\kappa_x + \kappa_r)\left|\Delta x_k^n - \Delta z_k^n\right| \ge -2h(\kappa_x + \kappa_r)^2, \end{aligned} \tag{C.3.19}$$

and so for every $\tau, t \in [0,T], t > \tau$,

$$\int_\tau^t \left\langle \dot{x}^n(s) - \dot{z}^n(s), z^n(s) - \varphi(s) \right\rangle ds \ge -2(\kappa_u + \kappa_r)^2 hT \ge -2T^2(\kappa_u + \kappa_r)^2 \frac{1}{n}. \tag{C.3.20}$$

Setting $\alpha^n(t) = x^n(t) - z^n(t)$, (C.3.20) can be equivalently written as a Riemann-Stieltjes integral

$$\int_\tau^t \left\langle z^n(s) - \varphi(s), d\alpha^n(s) \right\rangle \ge -2T^2(\kappa_u + \kappa_r)^2 \frac{1}{n}. \tag{C.3.21}$$

As it has already been established that a subsequence of $\{z^n\}$ converges to a Lipschitz function $z(t)$ uniformly in $C([0,T];\Re)$ and $\{x^n\}$ converges to $x(t)$ uniformly in $C^{0,1}([0,T];\Re)$, it follows that a subsequence of $\{\alpha^n\}$ converges to a Lipschitz function $\alpha(t)$ uniformly in $C([0,T];\Re)$. Thus, inserting the convergent subsequences into (C.3.21), it is possible to pass to the limit as $n \to \infty$ [9], to obtain

$$0 \le \int_\tau^t \langle z(s) - \varphi(s), d\alpha(s) \rangle = \int_\tau^t \langle \dot{x}(s) - \dot{z}(s), z(s) - \varphi(s) \rangle ds. \qquad \text{(C.3.22)}$$

for every $\tau, t \in [0,T], t > \tau$ and $\varphi \in C([0,T];\Re)$ such that $|\varphi(t)| \le r(t)$, which is equivalent to EP(ii). The next step is to establish the uniqueness of solutions on $[0,T]$. Let $z(t) = z(t; z_0; x(\cdot), r(\cdot))$ and $s(t) = s(t; s_0; y(\cdot), r(\cdot))$ be two solutions of EP, corresponding to the inputs $x, r \in C^{0,1}(\Re_+;\Re)$ and $y, r \in C^{0,1}(\Re_+;\Re)$ and initial conditions $|z_0| \le r(0)$ and $|s_0| \le r(0)$ respectively. Testing the corresponding variational inequalities with $\varphi = (s(t) + z(t))/2$ and adding gives

$$\frac{1}{2}\frac{d}{dt}(z(t) - s(t))^2 \le \langle z(t) - s(t), \dot{x}(t) - \dot{y}(t) \rangle, \qquad \text{(C.3.23)}$$

and hence

$$|z(t) - s(t)| \le |z_0 - s_0| + \int_0^t |\dot{x}(s) - \dot{y}(s)| ds \qquad \text{(C.3.24)}$$

for all $t \in [0,T]$. Setting $z_0 = s_0$ and $x(t) = y(t)$, implies $z(t) = s(t)$ and hence uniqueness of the solution follows. While (C.3.24) does prove continuous dependence on the initial conditions and on $\dot{x}(t)$, establishing continuous dependence of the solution on $r(t)$ is a little trickier and will be taken up next. □

A more general version of this theorem, requiring only $x, r \in AC([0,T];\Re)$, can be obtained from the author on request. The effect of viscoplastic regularization becomes apparent when the result above is compared with Theorem C.2.1, where the inputs were only required to be in $L_\infty([0,T];\Re)$. The next step in establishing wellposedness of the EP model, is to establish continuous dependence the solutions on $r(t)$ and $x(t)$. The proof of the following proposition is essentially the same as the proof of Proposition 2.3.4 in [10].

Proposition C.3.1 For some $T > 0$, let $z(t) = z(t; z(0); x(\cdot), r(\cdot))$ and $s(t) = s(t; s(0); y(\cdot), p(\cdot))$ be two solutions of EP corresponding to the inputs $(x, r) \in C^{0,1}(\Re_+; \Re) \times C^{0,1}(\Re_+; \Re) \cap [0, \bar{r}]$, and $(y, p) \in C^{0,1}(\Re_+; \Re) \times C^{0,1}(\Re_+; \Re) \cap [0, \bar{r}]$ and initial conditions $|z(0)| \le r(0)$ and $|s(0)| \le p(0)$ respectively. Then the following Lipschitz-type estimate holds

$$|z(t) - s(t)| \le |z(0) - s(0)| + 2 \sup_{\tau \in [0,t]} |x(t) - y(t)| + \sup_{\tau \in [0,t]} |r(t) - p(t)|, \qquad \text{(C.3.25)}$$

for all $t \in [0, T]$.

Proof: Proceeding as in the proof of Theorem C.3.1, one obtains the recursions $z_k^n = Q(z_{k-1}^n + x_k^n - x_{k-1}^n; r_k^n)$. Recall that the projection operator is given by $Q(y; r) = \min(r, \max(-r, y))$ (see §A.2). Defining $\alpha_k^n = x_k^n - z_k^n$, then

$$\begin{aligned} \alpha_k^n &= x_k^n - Q(z_{k-1}^n + x_k^n - x_{k-1}^n; r_k^n), \\ &= x_k^n - Q(x_k^n - \alpha_{k-1}^n; r_k^n), \\ &= \max\left(x_k^n - r_k^n, \min\left(x_k^n + r_k^n, \alpha_{k-1}^n\right)\right). \end{aligned} \qquad \text{(C.3.26)}$$

Similarly defining $\eta_k^n = y_k^n - s_k^n$ one obtains

$$\eta_k^n = \max\left(y_k^n - p_k^n, \min\left(y_k^n + p_k^n, \eta_{k-1}^n\right)\right). \qquad \text{(C.3.27)}$$

Now for any $a, b, c, d \in \Re$, the following inequities holds [10],

$$\begin{aligned} |\max(a, b) - \max(c, d)| &\le \max(|a - c|, |b - d|), \\ |\min(a, b) - \min(c, d)| &\le \max(|a - c|, |b - d|). \end{aligned} \qquad \text{(C.3.28)}$$

Thus combining (C.3.26)-(C.3.27) one obtains the inequality

$$\begin{aligned} |\alpha_k^n - \eta_k^n| &\le \max\left(|x_k^n - y_k^n| + |r_k^n - p_k^n|, |\alpha_{k-1}^n - \eta_{k-1}^n|\right), \\ &\le \max\left(\sup_{\tau \in [0,T]} |x^n(\tau) - y^n(\tau)| + \sup_{\tau \in [0,T]} |r^n(\tau) - p^n(\tau)|, |\alpha_{k-1}^n - \eta_{k-1}^n|\right), \end{aligned} \qquad \text{(C.3.29)}$$

for all $k = 1, \ldots, n$. Using a simple induction argument on (C.3.29) and the interpolation formulas in (C.3.8) with $\alpha^n(t) = x^n(t) - z^n(t)$ and $\eta^n(t) = y^n(t) - s^n(t)$, it can be show that

$$|\alpha^n(t) - \eta^n(t)| \le \max\left(\sup_{\tau \in [0,T]} |x^n(\tau) - y^n(\tau)| + \sup_{\tau \in [0,T]} |r^n(\tau) - p^n(\tau)|, |\alpha(0) - \eta(0)|\right), \qquad \text{(C.3.30)}$$

for all $t \in [0, T]$. Using $|z^n(t) - s^n(t)| \le |x^n(t) - y^n(t)| + |\alpha^n(t) - \eta^n(t)|$ for all $t \in [0, T]$ and (C.3.30) gives

$$
\begin{aligned}
&\left|z^n(t)-s^n(t)\right| \le \left|x^n(\tau)-y^n(\tau)\right| \\
&+\max\left(\sup_{\tau\in[0,T]}\left|x^n(\tau)-y^n(\tau)\right|+\sup_{\tau\in[0,T]}\left|r^n(\tau)-p^n(\tau)\right|, \left|z(0)-s(0)\right|+\left|x(0)-y(0)\right|\right), \quad \text{(C.3.31)} \\
&\le \left|z(0)-s(0)\right|+\sup_{\tau\in[0,T]}\left|x^n(\tau)-y^n(\tau)\right|+\sup_{\tau\in[0,T]}\left|r^n(\tau)-p^n(\tau)\right|.
\end{aligned}
$$

Since EP has a unique solution, the entire sequences $\{z^n(t)\}$ and $\{s^n(t)\}$ converge uniformly to $z(t)$ and $s(t)$ restively as $n\to\infty$. Passing to the limit as $n\to\infty$ in (C.3.31) yields

$$
\left|z(t)-s(t)\right| \le \left|z(0)-s(0)\right|+\sup_{\tau\in[0,T]}\left|x(\tau)-y(\tau)\right|+\sup_{\tau\in[0,T]}\left|r(\tau)-p(\tau)\right|, \qquad \text{(C.3.32)}
$$

which due to causality is equivalent to (C.3.25). □

Interestingly, it can be shown that the solution is locally Lipschitz dependent in $AC([0,T];\Re)$. There are some restrictions however. The estimate is only valid for some interval $[0,T]\subset\Re_+$, on which $r(t)$ is nonzero, i.e. $r(t)\ge\delta>0,\forall t\in[0,T]$. This is not as bad as it seems however, since if on some interval, $r(t)=0$, then $z(t)=0$ and the question of dependence is moot. The following theorem is based on Theorem.7.1 of [8] and shows that if $r(t)$ satisfies $0<\delta\le r(t)\le\bar{r},\forall t\in[0,T]$, then the solution $z(t;z_0,x(\cdot),r(\cdot))$ is Lipschitz dependent on u and r, in the $AC([0,T];\Re)$ norm. The proof is rather long and has been omitted for brevity. The proof of the multidimensional version can be found in [8].

Proposition C.3.2 For some $T>0$, let $z(t)=z(t;z(0);x(\cdot),r(\cdot))$ and $s(t)=s(t;s(0);y(\cdot),p(\cdot))$ be two solutions of EP corresponding to the inputs $(x,r)\in C^{0,1}(\Re_+;\Re)\times C^{0,1}(\Re_+;\Re)$ and $(y,p)\in C^{0,1}(\Re_+;\Re)\times C^{0,1}(\Re_+;\Re)$ and initial conditions $z(0)=Q(x(0);r(0))$ and $s(0)=Q(y(0);p(0))$ respectively. If $0<\delta\le r(t),s(t)\le\bar{r},\forall t\in[0,T]$, then the following inequality holds

$$
\begin{aligned}
&\int_0^T\left|\dot{z}(\tau)-\dot{s}(\tau)\right|ds+\left|z(0)-s(0)\right| \\
&\le K_0 e^{K_0K_1T}\left(\left|x(0)-y(0)\right|+\left|r(0)-p(0)\right|+\int_0^T\left|\dot{x}(\tau)-\dot{y}(\tau)\right|+\left|\dot{r}(\tau)-\dot{p}(\tau)\right|ds\right).
\end{aligned} \qquad \text{(C.3.33)}
$$

The positive constant K_0 depends only on δ and $\bar{r}$, while $K_1=\max(\kappa_x,\kappa_r,\kappa_y,\kappa_p)$ where $\kappa_x,\kappa_r,\kappa_y$ and κ_p are the Lipschitz constants for x,r,y and p respectively. □

Following Proposition.2.3.7 in [10], Proposition C.3.2 can be strengthened to global Lipschitz continuity with respect to x, and without insisting that r is nonzero.
The proof is identical to the proof of proposition.2.3.7 in [10] and so has been omitted.

Proposition C.3.3 For some $T>0$, let $z(t)=z(t;z(0);x(\cdot),r(\cdot))$ and $s(t)=s(t;s(0);y(\cdot),r(\cdot))$ be two solutions of EP with the same control $r\in C^{0,1}([0,T];\Re_+)\cap[0,\bar{r}]$, but with inputs $x\in C^{0,1}(\Re_+;\Re)$ and $y\in C^{0,1}(\Re_+;\Re)$ and initial conditions $z(0)=Q(x(0);r(0))$ and $s(0)=Q(y(0);r(0))$ respectively. Then the following inequality holds

$$\int_0^T|\dot{z}(\tau)-\dot{s}(\tau)|ds+|z(0)-s(0)|\le 2|x(0)-y(0)|+2\int_0^T|\dot{x}(\tau)-\dot{y}(\tau)|ds. \quad \text{(C.3.34)}$$

□

Before moving on lets take a look at the implications of Theorem C.3.1 for models based on the simple EP element. Consider first the multiple element model form §3.6, with constant elastic moduli. An $\prod$(EP) model, consisting if n EP elements arranged in parallel can be written in variational form as

$$\begin{aligned} &z(t)=G_T\sum_{i=1}^{n}\beta_i z_i(t), \\ &\langle\dot{x}(t)-\dot{z}_i(t),z_i(t)-\varphi_i\rangle\ge 0, \quad \forall|\varphi_i|\le r(t)\tau_i \quad i=1,\ldots,n. \end{aligned} \quad \text{(C.3.35)}$$

where $0=\tau_0<\ldots<\tau_n<\infty$ define the relative magnitudes of the individual yields strains, $r(t)\in[0,\bar{r}]$ controls the instantaneous values yields strains and $\beta_i>0$, $\sum_i\beta_i=1$ are the stiffness distribution coefficients. Obviously if $x,r\in C^{0,1}([0,T];\Re)$ then by Theorem C.3.1, each of the individual elements will have a unique solution $z_i\in C^{0,1}([0,T];\Re)$. Since $C^{0,1}([0,T];\Re)$ is a normed linear space, it is closed under addition and hence $z=G_T\sum_{i=1}^{n}\beta_i z_i\in C^{0,1}([0,T];\Re)$ will also unique. Now, what if G_T is also a time varying function. If $G_T(t)\in[0,\overline{G}],\forall t\in[o,T]$ and $G_T\in C^{0,1}([0,T];\Re)$, then z will still be unique and Lipschitz continuous. While the first remark is fairly obvious, to see that the second is true note

$$\begin{aligned} |G_T(t)z(t)-G_T(s)z(s)|&\le|G_T(s)\|z(t)-z(s)|+|z(t)\|G_T(t)-G_T(s)|, \\ &\le\overline{G}\kappa_z|t-s|+\bar{r}\kappa_G|t-s|, \end{aligned} \quad \text{(C.3.36)}$$

where κ_z and κ_G are Lipschitz constants for $z(t)$ and $G_T(t)$ respectively.

The final question to be explored is, if the EP model is coupled with an ordinary differential equation, can the existence of a solution still be assumed. Consider the following system

$$\Sigma\begin{cases}\Sigma_Z\{\dot{x}(t)=F(x(t),z(t),u(t))\\ \Sigma_Z\begin{cases}\langle G\dot{x}(t)-\dot{z}(t),z(t)-\varphi\rangle\geq 0, & \forall|\varphi|\leq r(t),\\ |z(t)|\leq r(t), & \forall t\geq 0.\end{cases}\end{cases} \tag{C.3.37}$$

where $x\in\Re^n, z\in\Re$, $u:\Re_+\mapsto\Re^m$ is a vector of forcing terms, $r:\Re_+\to\Re_+$ is the damper control, $F:\Re^n\times\Re\times\Re^m\mapsto\Re^n$ and $G\in\Re^n$ is a vector with $|G|=1$ for simplicity. If F is Lipschitz in all its arguments, then it is possible to prove a very general theorem like Theorem C.1.1 using the contraction mapping theorem and Propositions C.3.2 and C.3.4. A nice example of this sort is given in [11]. Instead a less general theorem will be given, the proof of which is based on a mixed explicit-implicit Euler discretization of Σ. It is basically a combination of Theorem C.3.1 and the classical Peano existence theorem for ordinary differential equations [1],[9].

Corollary C.3.1 Suppose that $F(0,0,0)=0$ and for all $(x,z,u),(\bar{x},\bar{z},\bar{u})\in\Re^n\times\Re\times\Re^m$ there exists a positive constant β such that

$$|F(x,z,u)-F(\bar{x},\bar{z},\bar{u})|\leq\beta|x-\bar{x}|+\beta|z-\bar{z}|+\beta|u-\bar{u}|. \tag{C.3.38}$$

Then for each $x_0\in\Re^n$, $|z_0|\leq r(0)$, $r\in C^{0,1}([0,T];\Re_+)$, $u\in C([0,T];\Re^m)$ and $\|u\|_\infty,\|r\|_\infty<R$, $T\in\Re_+$

(i) The system Σ has a unique solution $x(t)=x(t;x_0,z_0,r(\cdot),u(\cdot))$, $z(t)=z(t;x_0,z_0,r(\cdot),u(\cdot))$ such that $z\in C^{0,1}([0,T];\Re)$, $x\in C^1([0,T];\Re^n)$ and

$$|x(t)-x_0|\leq te^{\beta t}\big(|x_0|+2R\big),\quad\forall t\in[0,T]. \tag{C.3.39}$$

Let $x(t)=x(t;x_0,z_0,r(\cdot),u(\cdot))$, $z(t)=z(t;x_0,z_0,r(\cdot),u(\cdot))$ and $\bar{x}(t)=\bar{x}(t;\bar{x}_0,\bar{z}_0,\bar{r}(\cdot),\bar{u}(\cdot))$, $\bar{z}(t)=\bar{z}(t;\bar{x}_0,\bar{z}_0,\bar{r}(\cdot),\bar{u}(\cdot))$ be the unique solutions of Σ corresponding to the initial conditions, controls and inputs (x_0,z_0,r,u) and $(\bar{x}_0,\bar{z}_0,\bar{r},\bar{u})$ respectively (both sets satisfying the conditions above), then

$$\begin{aligned}|x(t)-\bar{x}(t)|+|z(t)-\bar{z}(t)|\leq\big(&|x(0)-\bar{x}(0)|+|z(0)-\bar{z}(0)|\big)e^{\beta_1 t}\\&+\beta_2 e^{\beta_1 t}\big(\|u-\bar{u}\|_\infty+\|r-\bar{r}\|_\infty\big).\end{aligned} \tag{C.3.40}$$

for some constants $\beta_1, \beta_2 > 0$ and for all $t \in [0,T]$ (continuous dependence).

(ii) If also $u \in C([0,\infty);\Re^m)$ and $r \in C^{0,1}([0,\infty);\Re_+)$, the solution of Σ admits the extension then $x \in C^1([0,\infty);\Re^n)$ and $z \in AC([0,\infty);\Re)$.

(iii) If also $u \in C^{0,1}([0,\infty);\Re^m)$ and all solutions of Σ are uniformly bounded, then $x \in C^{1,1}([0,\infty);\Re^n)$ and $z \in C^{0,1}([0,\infty);\Re)$.

Proof

For each $n \in \mathrm{N}$, form a partition $0 = t_0 < t_1 \ldots < t_n = T$ with $h = T/n$ and $t_k = kh, k = 0,1\ldots,n.$ For $k = 0,1,\ldots,n$ define $r_k^n = r(t_k)$ and $u_{k-1}^n = u(t_k)$ for $k = 1,2\ldots,n$, construct a set of nodes spanning $[0,T]$ using the following mixed explicit-implicit Euler scheme

$$\begin{aligned} x_k^n &= x_{k-1}^n + hF\left(x_{k-1}^n, z_{k-1}^n, u_{k-1}^n\right), \\ z_k^n &= Q\left(z_{k-1}^n + Gx_k^n - Gx_{k-1}^n; r_k^n\right), \end{aligned} \tag{C.3.41}$$

starting from the given initial conditions z_0 and x_0 .Now construct the piecewise linear Euler arcs on $[0,T]$ using

$$\begin{cases} x^n(t) = x_{k-1}^n + \dfrac{1}{h}(t - t_{k-1})(x_k^n - x_{k-1}^n), \\ z^n(t) = z_{k-1}^n + \dfrac{1}{h}(t - t_{k-1})(z_k^n - z_{k-1}^n), \end{cases} \tag{C.3.42}$$

for $t \in [t_{k-1}, t_k), k = 1,2\ldots,n$, continuously extended to $t = T$. It follows $r^n \to r$ in $C([0,T];\Re)$ as $n \to \infty$. To simplify the equations a bit, define $\Delta x_k^n = x_k^n - x_{k-1}^n$, $\Delta z_k^n = z_k^n - z_{k-1}^n$ etc. Recall that $\left|z_k^n\right| \le r_k^n$ for all k, due to the projection in (C.3.41). Using this knowledge it is possible to obtain an explicit bound on the nodes x_k^n by using (C.3.38) and (C.3.41),

$$\left|x_k^n - x_{k-1}^n\right| \le h\beta\left(\left|x_{k-1}^n\right| + \left|z_{k-1}^n\right| + \left|u_{k-1}^n\right|\right) \le h\beta\left|x_{k-1}^n\right| + h\beta\left(\bar{r} + \|u\|_\infty\right), \tag{C.3.43}$$

and hence

$$\begin{aligned} \left|x_k^n - x_0\right| &\le \left|x_k^n - x_{k-1}^n\right| + \left|x_{k-1}^n - x_0\right| \le h\beta\left|x_{k-1}^n\right| + h\beta\left(\bar{r} + \|u\|_\infty\right) + \left|x_{k-1}^n - x_0\right|, \\ &\le (1 + h\beta)\left|x_{k-1}^n - x_0\right| + h\Delta, \end{aligned} \tag{C.3.44}$$

where $\Delta = \beta\left(\left|x_0\right| + \bar{r} + \|u\|_\infty\right)$.

Application of Theorem A.1.4 in §A.1 gives

$$\left\|x_k^n - x_0\right\| \le \Delta T \mathrm{e}^{\beta T} = m. \tag{C.3.45}$$

for $k=1,\ldots,n$. Thus all of the nodes x_k^n, are contained in the ball $\mathrm{B}(x_0;m)$ and due to the fact that $x^n(t)$ is a convex combination of successive nodes, $x^n(t)\in \mathrm{B}(x_0;m), \forall t\in[0,T]$. Now for $t\in(t_{k-1},t_k)$, taking the derivative of $x^n(t)$ and using (C.3.43) and (C.3.45) yields,

$$\left\|\dot{x}^n\right\|_\infty \le \beta\left(m+|x_0|+\bar{r}+\|u\|_\infty\right)=\kappa_x. \tag{C.3.46}$$

Therefore $x^n(t)$ is Lipschitz of rank κ_x on $[0,T]$. Putting all this together, it can be seen that the family of Euler arcs $\{x^n\}$ are equicontinuous and uniformly bounded. Then by Arzela's theorem (see §A.1), $\{x^n\}$ contains a subsequence, say $\{x^m\}$ which converges uniformly on $[0,T]$ to a continuous function $x(t):[0,T]\to R^n$. By Theorem A.1.2 in §A.1, the limiting function will inherit the Lipschitz rank κ_x and in consequence $x\in C^{0,1}([0,T];\Re^n)$. Furthermore the limit function inherits the estimate (C.3.45). Of coarse this implies that $\{Gx^m\}$ is Lipschitz continuous and converges uniformly on $[0,T]$ to a function $Gx\in C^{0,1}([0,T];\Re^n)$. Using the sequence $\{Gx^n\}$ in the proof of Theorem C.3.1, it can be concluded that $\{z^n\}$ contains a subsequence $\{z^m\}$, which converges uniformly on $[0,T]$ to a function $z\in C^{0,1}([0,T];\Re)$. Furthermore the limiting functions Gx and z, satisfies the variational inequality Σ_Z in (C.3.37).

The next step is to show that the limit functions x and z satisfy Σ_X in (C.3.37). Since $u\in C([0,T];\Re^m)$, it is uniformly continuous on $[0,T]$. Thus, for any ζ there exists a δ such that $|u(t)-u(\tau)|\le\zeta$ for all $t,\tau\in[0,T], |t-\tau|<\delta$. Now, for m large enough and for any point t which is not one of the point where $x^m(t)$ is a node, then $\dot{x}^m(t)=F\left(x^m(\tau),z^m(\tau),u(\tau)\right)$, for some τ such that $|t-\tau|<\delta$. For any $\varepsilon>0$ pick m large enough to ensure that δ and ζ satisfy $L\kappa_x\delta+L\kappa_z\delta+L\zeta<\varepsilon$ and hence

$$\left|F\left(x^m(\tau),z^m(\tau),u(\tau)\right)-F\left(x^m(t),z^m(t),u(t)\right)\right|\le Lk_x\delta+Lk_z\delta+L\zeta<\varepsilon. \tag{C.3.47}$$

It follows that for any $t\in[0,T]$

$$\begin{aligned}&\left|x^m(t)-x^m(0)-\int_0^t F\left(x^m(s),z^m(s),u(s)\right)ds\right|\\ &\qquad\le\left|\int_0^t \dot{x}^m(s)-F\left(x^m(s),z^m(s),u(s)\right)ds\right|<\varepsilon T.\end{aligned} \tag{C.3.48}$$

Thus letting $m \to \infty$ one obtains

$$\left| x(t) - x(0) - \int_0^t F\big(x(s), z(s), u(s)\big) ds \right| \le \varepsilon T. \tag{C.3.49}$$

Since ε is arbitrary, it follows

$$x(t) = x(0) + \int_0^t F\big(x(s), z(s), u(s)\big) ds, \tag{C.3.50}$$

which implies that $x \in C^1([0,T];\Re^n)$ and $\dot{x}(t) = F\big(x(t), z(t), u(t)\big)$ for all $t \in (0,T)$.

The next step is to establish uniqueness and continuous dependence of solutions. Let $s(t)$ be a solution of the variational inequality $\langle G\dot{x}(t) - \dot{s}(t), s(t) - \varphi \rangle \ge 0, \forall |\varphi| \le \bar{r}(t)$ and $|s(t)| \le \bar{r}(t)$ such that $s_0 = z_0$ (if $r(0) > \bar{r}(0)$ use $\dot{\bar{x}}$ and $\bar{r}$ instead). So applying Proposition C.3.1 gives $|z(t) - s(t)| \le \|r - \bar{r}\|_\infty, \forall t \in [0,T]$. Define $V(t) = 0.5|x(t) - \bar{x}(t)|^2 + 0.5|s(t) - \bar{z}(t)|^2$. Using the Lipschitz condition (C.3.38) and $|z(t) - s(t)| \le \|r - \bar{r}\|_\infty$ it can be shown that the directional derivative of $V(t)$ along the solutions (x,s) and $(\bar{x},\bar{z})$ satisfies

$$\begin{aligned} \dot{V}(t) &\le \beta\Big(|x - \bar{x}|^2 + 2|x - \bar{x}||s - \bar{z}| + |s - \bar{z}|^2\Big) + \\ &\quad \beta\big(|x - \bar{x}| + |s - \bar{z}|\big)\big(\|u - \bar{u}\|_\infty + \|r - \bar{r}\|_\infty\big), \\ &\le 3\beta\Big(|x - \bar{x}|^2 + |s - \bar{z}|^2\Big) + \frac{\beta}{2}\big(\|u - \bar{u}\|_\infty + \|r - \bar{r}\|_\infty\big), \\ &\le 6\beta V(t) + \frac{\beta}{2}\big(\|u - \bar{u}\|_\infty + \|r - \bar{r}\|_\infty\big). \end{aligned} \tag{C.3.51}$$

Integrating the final inequality in (C.3.50) and using $|z(t) - s(t)| \le \|r - \bar{r}\|_\infty$, $s_0 = z_0$ yields (C.3.40) and also uniqueness of solutions. Since Σ has a unique solution, the entire sequences $\{x^n\}$ and $\{z^n\}$ converge to the actual solution. Thus providing some justification for the use of (C.3.41) and (C.3.42) as an integration algorithm.

If also $u \in C([0,\infty);\Re^m)$ and $r \in C^{0,1}([0,\infty);\Re)$, then (C.3.39) and $\|z\|_\infty \le \beta$ imply that the solutions of Σ cannot become unbounded in finite time, and can therefore be continued over the semi-infinite interval $[0,\infty)$. Since $\dot{x}$ may not be uniformly bounded, it can only be concluded that z is locally Lipchitz and thus absolutely continuous, proving (ii).

If all solutions of Σ are uniformly bounded, then for each $(x_0, z_0) \in \Re^n \times \Re$, there exists a $b \geq 0$, such that $\|x\|_\infty \leq b$. Thus $\|\dot{x}\|_\infty \leq \beta(b + 2R)$, so that it can be concluded that $z \in C^{0,1}([0,\infty);\Re)$. If also $u \in C^{0,1}([0,\infty);\Re^m)$, then using (3.38) it follows that for any $t, \tau \in \Re_+$, $|\dot{x}(t) - \dot{x}(\tau)| \leq \beta(\|\dot{x}\|_\infty + \kappa_z + \kappa_u)|t - \tau|$, where κ_z and κ_u are Lipschitz constants for z and u respectively. This shows that $x \in C^{1,1}([0,\infty);\Re^n)$ and proves (iii).□

References

[1] R. Miller, A. Michel. Ordinary differential equations. Academic Press, NY, 1982.

[2] J. Hale. Ordinary differential equations, second edition. Krieger Publishing Company, Malabar, Florida, 1980.

[3] F. Clarke, Y. Ledyaev, R. Stern, P. Wolenski. Nonsmooth analysis and control theory. Springer-Verlag, NY, 1998.

[4] P. Krejci. "Evolution variational inequalities and multidimensional hysteresis operators". In: Nonlinear Differential Equations, Research Notes in Mathematics, Chapman and Hall/CRC, London, 1999.

[5] G. Smirnov. Introduction to the theory of differential inclusions. American Mathematical Society, 2002.

[6] J. Moreau. "Numerical aspects of the sweeping process". Computer Methods in Applied Mechanics and Engineering, vol.177, pp.329-349, 1999.

[7] M. Kunze, M. Monterio Marques. "An introduction to Moreau's sweeping process". In: Impacts in mechanical systems-Analysis and modelling, (B. Brogliato ed.), Springer-Verlag, 2000.

[8] M. Brokate, P. Krejci, H. Schnabel. "On uniqueness in evolution quasivariational inequalities". Journal of Convex Analysis, vol.11, pp.111-130, 2004.

[9] A. Kolmogorov, S. Fomin. Introductory real analysis. Dover Publications Inc., NY, 1975.

[10] M. Brokate, J. Sprekels. Hysteresis and phase transitions. Springer-Verlag, NY, 1996.

[11] M. Brokate, A. Pokorovskii. "Asymptotically stable oscillations in systems with hysteresis nonlinearities". Journal of Differential Equations, vol.150, pp.98-123, 1998.

Appendix D

Periodic Solutions

D.1 Periodic solutions of the EP model

The purpose of this section and the next section is to establish some existence and stability results relating to periodic solutions of the controllable EP model in isolation and when coupled with a simple second order system. So why the interest in periodic solutions. Referring back to Fig 1.2, Fig 2.2 and Fig 3.2, it can be seen that when an ER damper is subjected to a periodic displacement (zero mean) the resulting force-displacement plots which form closed or asymptotically closed hysteresis loops, clearly indicative of a periodic response. It follows for a model of ER damper to be of any use it should respond in a similar manner. Unfortunately the author was unable to find experimental results, in which the applied displacement and controllable yield were varied periodically. However, in this case the magnitude of the models response is bounded by a continuous periodic function, would seem to be even more suggestive of the existence of a periodic solution.

As discussed in §1, the involuntary motion resulting from human tremor is approximately periodic in nature. In §4.1 it was shown that, complete cancellation of the effect of the tremor cannot be achieved using a controllable damper. Thus, the ideal situation would be if a control scheme could be devised for the damper, which would guarantee that the response of the coupled system would converge to a periodic motion, of smaller amplitude than in the absence of the damper. Indeed, if a chaotic or undeterministic motion were to result from the coupling, the effect could be more debilitating than the tremor itself.

From a purely analytic point of view, if it can be shown that all solutions of the system converge asymptotically to a periodic solution, then a certain orderliness emerges, in what may otherwise seem like a highly complex situation. To quote [1], "Among all the qualitative properties of solutions of differential equations, none is quite so satisfying aesthetically as that of periodicity ".

In §C.2 it is shown that for a given input $x \in C^{0,1}(\Re_+;\Re)$ and control $r \in C^{0,1}(\Re_+;\Re_+) \cap [0,\bar{r}]$, the variational inequality

$$\Sigma_Z \begin{cases} \langle G\dot{x}(t) - \dot{z}, z - \varphi \rangle \geq 0, & \forall |\varphi| \leq r(t), \\ |z(t)| \leq r(t), & \forall t \geq 0. \end{cases} \tag{D.1.1}$$

with initial condition $z(0) = z_0 \in r(0)[-1,1]$, has a unique solution $z \in C^{0,1}(\Re_+;\Re)$, which depends continuously on the initial condition. Through out this section, inputs and controls satisfying the above conditions will be referred to as admissible. Similar to the idea of a *0T*-recurrent control, introduced in §4.2, a control will be referred to as *0T*-perioidic if it is an admissible, non-trivial T-periodic function, for which there is at least one $\tau \in [0,T)$ such that $r(\tau) = 0$ (and hence $r(\tau + nT) = 0, \forall n = 0,1,2,\ldots$).

The purpose of this section is to present some simple results relating to the existence and uniqueness of periodic solutions of Σ_Z, when x and r are themselves T-periodic.

If x and r are T-periodic, then Σ_Z is T-periodic and it follows from uniqueness of solutions, that for all $|z_0| \leq r(0)$ and all positive integers n, $z(t + nT; nT, z_0) = z(t;0,z_0)$ for all $t \geq 0$. That is, solutions of Σ_Z are invariant with respect to time shifts which are integer multiples of T. A necessary and sufficient condition for (D.1.1) to have a T-periodic solution, is that the map $\mathrm{P}(z_0) = z(T;0,z_0)$ have at least one fixed point in the interval $[-r(0), r(0)]$, see [1] for details. Sufficiency is easily established by setting $\mathrm{P}(z_0) = z_0$, then $z(t+T;0,z_0) = z\big(t+T;T,z(T,0,z_0)\big) = z(t;0,z_0)$. Due to continuous dependence of solutions on the initial conditions, $\mathrm{P}(\cdot)$ is a continuous function, mapping the closed interval $[-r(0), r(0)]$ into itself. The existence of a fixed point can be deduced from a simple fixed point theorem, which states that a continuous function mapping a closed interval into itself has at least one fixed point [1]. Due to perioidicity of Σ_Z and the boundedness of solutions, the positive limit set $\Omega(z)$ is nonempty, compact, an invariant set for Σ_Z and is approached by $z(t)$ as $t \to \infty$ (see §B.2). Let $\bar{z}(t)$ be a T-periodic solution of Σ_Z and $z(t)$ an arbitrary solution of Σ_Z. Adding up the corresponding variational inequalities, $\langle G\dot{x}(t) - \dot{z}(t), z(t) - \bar{z}(t) \rangle \geq 0$ and $\langle G\dot{x}(t) - \dot{\bar{z}}(t), \bar{z}(t) - z(t) \rangle \geq 0$, gives

$$\frac{d}{dt}\big(z(t) - \bar{z}(t)\big)^2 = 2\langle \dot{z}(t) - \dot{\bar{z}}(t), z(t) - \bar{z}(t) \rangle \leq 0. \tag{D.1.2}$$

It follows that the periodic solution $\bar{z}(t)$ is uniformly stable and that the difference $|z(t)-\bar{z}(t)|$ is nonincreasing as a function of time. Since $|z(t)-\bar{z}(t)|$ is nonincreasing and bounded below by zero it has a definite limit as $t \to \infty$.

That is $\lim_{t\to\infty}|z(t)-\bar{z}(t)| = a$. Furthermore, defining $r_m = \min_{t\in[0,T)} r(t)$, it must be that $a \le 2r_m$. Invariance of $\Omega(z)$ implies that $|z(t)-\bar{z}(t)| = a$ whenever $z(t) \in \Omega(z)$.

Clearly if there exists a time $\tau \ge 0$ such that $z(\tau) = \bar{z}(\tau)$, then $z(t) = \bar{z}(t), \forall t \ge \tau$ and $\Omega(z) = \bar{z}([0,T])$. If this is not the case, then by continuity the difference $z(t)-\bar{z}(t)$ must be sign definite and hence $z(t) = \bar{z}(t) + a\,\mathrm{sgn}(z(t)-\bar{z}(t))$ whenever $z(t) \in \Omega(z)$. But periodicy of $\bar{z}(t)$ means that $\bar{z}(t)+a\,\mathrm{sgn}(z(t)-\bar{z}(t))$ is T-periodic, implying that once again $\Omega(z)$ contains a T-periodic solution of Σ_Z.

Let $\bar{z}_1(t)$ and $\bar{z}_2(t)$ be any two T-periodic solutions of Σ_Z, then there exists a constant a, with $|a| \le 2r_m$, such that $\bar{z}_1(t) = \bar{z}_1(t) + a, \forall t \in [0,T)$. If r is a $0T$-periodic control, then $r_m = 0$ and hence $\bar{z}_1(t) = \bar{z}_2(t)$, implying that Σ_Z has a unique T-periodic solution $\bar{z}(t)$. If $z(t)$ is an solution of Σ_Z, and r is a $0T$-periodic , then by assumption, there exists a $\tau \in [0,T)$ such that $r(\tau) = 0$, implying $z(\tau) = \bar{z}(\tau) = 0$, and hence $z(t) = \bar{z}(t), \forall t \ge \tau$. For clarity the above conclusions are stated in the following proposition.

Proposition D.1.1

Let $x \in C^{0,1}(\Re_+;\Re)$ and $r \in C^{0,1}(\Re_+;\Re) \cap [0,\bar{r}]$ be T-periodic functions. Then the following statements hold;

(i) The system Σ_Z has at least one T-periodic solution.

(ii) Let z be a solution of Σ_Z with (arbitrary) initial condition $|z(0)| \le r(0)$, then there exists a T-periodic solution of Σ_Z, say $\bar{z}(t)$, such that $\lim_{n\to\infty}|z(t+nT)-\bar{z}(t)| = 0$

(iii) Let $\bar{z}_1(t)$ and $\bar{z}_2(t)$ be two T-periodic solutions of Σ_Z and define $r_m = \min_{t\in[0,T)} r(t) > 0$. Then there exists a constant a, with $|a| \le 2r_m$, such that $\bar{z}_1(t) = \bar{z}_2(t) + a, \forall t \in [0,T)$.

(iv) If r is a $0T$-periodic control, then the system Σ_Z has a unique T-periodic solution, say $\bar{z}(t)$, such that for each $|z_0| \le r(0)$, the corresponding solution reaches $\bar{z}(t)$, within the time interval $[0,T)$. (if $r(\cdot) \equiv 0$ the question of solutions is moot). □

As a simple example, let $r(t) = r_m + |\sin(t)|$ and $\dot{x}(t) = \cos(t)/G$, then $z_\lambda(t) = \lambda + \sin(t)$, with $\lambda \in [-r_m, r_m]$, is a family of T-periodic solutions for the variational inequality (D.1.1). Before stating the next result, the following definition is required. Define the oscillation of a T-periodic function $x : \Re_+ \mapsto \Re$ by

$$\operatorname{osc}_T x = \sup_{t,\tau \in [0,T)} |x(t) - x(\tau)| = \sup_{t \in [0,T)} x(t) - \inf_{t \in [0,T)} x(t) \ge 0 \qquad \text{(D.1.3)}$$

The following proposition is based on the results presented in [2].

Proposition D.1.2

Let $z_1(t)$ be an arbitrary solution of Σ_Z corresponding to the admissible input $x_1(t)$ and admissible T-periodic control $r(t)$. Let $z_2(t)$ be a T-periodic solution of Σ_Z corresponding to the admissible T-periodic input $x_2(t)$ and the same T-periodic control $r(t)$. If the T-periodic input $x_2(t)$ is such that $\operatorname{osc}_T x_2 - 2\bar{r}/G > 0$ where $\bar{r} = \max_{t \in [0,T)} r(t)$, then there exists a positive constant $p > 0$ such that

$$|z_1(t) - z_2(t)| \le |z_1(0) - z_2(0)| e^{pT} e^{-pt} + e^{2pT} G \int_0^t e^{-p(t-s)} |\dot{x}_1(s) - \dot{x}_2(s)| ds. \qquad \text{(D.1.4)}$$

Proof: Define the functions $\alpha_1(t) = Gx_1(t) - z_1(t)$ and $\alpha_2(t) = Gx_2(t) - z_2(t)$. Clearly if $x_2(t)$ and $z_2(t)$ are T-periodic, then so is $\alpha_2(t)$. Consider the closed interval $[-r, r]$, with $r \in [0, \bar{r}]$. If $z_1, z_2 \in [-r, r]$, then a simple calculation shows that an interval of length $(z_1 - z_2)^2/(4\bar{r})$, centred at $(z_1 + z_2)/2$, is also contained in $[-r, r]$.

Since $|z_1(t)| \le r(t)$ and $|z_2(t)| \le r(t)$ for all $t \ge 0$, it is possible to define the function

$$d(z_1(t), z_2(t); r(t)) := \min_{|\varphi| = r(t)} \left| \frac{z_1(t) + z_2(t)}{2} - \varphi \right| \ge \frac{1}{4\bar{r}} (z_1(t) - z_2(t))^2. \qquad \text{(D.1.5)}$$

Define $z^*(t) = (z_1(t) + z_2(t))/2$ and let $\operatorname{sgn}(x)$ denote the usual signum function. Now, testing the variational inequality for $z_1(t)$ with

$\varphi_1(t) = z^*(t) + d(z_1(t), z_2(t); r(t)) \operatorname{sgn}(\dot{\alpha}_1(t))$ with $|\varphi_1(t)| \le r(t)$ gives

$$\begin{aligned}&\langle G\dot{x}_1(t)-\dot{z}_1(t), z_1(t)-\varphi_1(t)\rangle \\ &= 0.5\langle G\dot{x}_1(t)-\dot{z}_1(t), z_1(t)-z_2(t)\rangle - |\dot{\alpha}_1(t)|d(z_1(t),z_2(t);r(t)) \geq 0.\end{aligned} \tag{D.1.6}$$

Similarly, testing the variational inequality for $z_2(t)$ with

$\varphi_2(t) = z^*(t) + d(z_1(t), z_2(t); r(t))\,\mathrm{sgn}(\dot{\alpha}_2(t))$ gives

$$0.5\langle G\dot{x}_2(t)-\dot{z}_2(t), z_2(t)-z_1(t)\rangle - |\dot{\alpha}_2(t)|d(z_1(t),z_2(t);r(t)) \geq 0. \tag{D.1.7}$$

Setting $\tilde{z}(t) = z_1(t) - z_2(t)$ and $\tilde{x}(t) = x_1(t) - x_2(t)$, summing inequalities (D.1.6), (D.1.7) and using (D.1.5) gives

$$\begin{aligned}\frac{d}{dt}(\tilde{z})^2 &\leq -4\left(|\dot{\alpha}_1(t)| + |\dot{\alpha}_2(t)|\right)d(z_1,z_2;r(t)) + 2G|\tilde{z}||\dot{\tilde{x}}(t)|, \\ &\leq -\frac{1}{\bar{r}}|\dot{\alpha}_2(t)|(\tilde{z})^2 + +2G|\tilde{z}||\dot{\tilde{x}}(t)|,\end{aligned} \tag{D.1.8}$$

and hence

$$\frac{d}{dt}|\tilde{z}| \leq -\frac{1}{2\bar{r}}|\dot{\alpha}_2(t)||\tilde{z}| + G|\dot{\tilde{x}}(t)|. \tag{D.1.9}$$

Applying the comparison principle in §B to (D.1.9) yields

$$\begin{aligned}|\tilde{z}(t)| &\leq |\tilde{z}(0)|\Phi(t) + G\Phi(t)\int_0^t \Phi(s)|\dot{\tilde{x}}(s)|ds, \\ \Phi(t) &= \exp\left(-\frac{1}{2\bar{r}}\int_0^t |\dot{\alpha}_2(\tau)|d\tau\right).\end{aligned} \tag{D.1.10}$$

On the assumption that $\alpha_2(t)$ is T-periodic, define the positive constant

$$\begin{aligned}p &:= \frac{1}{2T\bar{r}}\int_0^T |\dot{\alpha}_2(\tau)d\tau| =: \frac{1}{2T\bar{r}}\,\mathrm{var}_T\,\alpha_2, \\ &\geq \frac{1}{2T\bar{r}}\,\mathrm{osc}_T\alpha_2 \geq \frac{1}{2T\bar{r}}\left(G\,\mathrm{osc}_T x_2 - \mathrm{osc}_T z_2\right), \\ &\geq \frac{1}{2T\bar{r}}\left(G\,\mathrm{osc}_T x_2 - 2\bar{r}\right) > 0,\end{aligned} \tag{D.1.11}$$

by assumption on x_2. Set

$$Q(t) = \Phi(t)e^{pt} = \exp\left(-\frac{1}{2\bar{r}}\int_0^t |\dot{\alpha}_2(s)|ds + \frac{t}{2T\bar{r}}\int_0^T |\dot{\alpha}_2(s)|ds\right). \tag{D.1.12}$$

Since $\alpha_2(t) = \alpha_2(t+T), \forall t \in \Re_+$, it is easily seen that $Q(t) = Q(t+T), \forall t \in \Re_+$ and $e^{-pT} \leq Q(t) \leq e^{pT}$. Finally, putting (D.1.12) into (D.1.10) gives

$$\begin{aligned}|\tilde{z}(t)| &\leq |\tilde{z}(0)|Q(t)e^{-pt} + GQ(t)\int_0^t Q^{-1}(s)e^{-p(t-s)}|\dot{\tilde{x}}(s)|ds, \\ &\leq |\tilde{z}(0)|e^{pT}e^{-pt} + e^{2pT}G\int_0^t e^{-p(t-s)}|\dot{\tilde{x}}(s)|ds,\end{aligned} \tag{D.1.13}$$

which is the required result.□

Let $z(t)$ be an arbitrary solution of Σ_Z corresponding to the admissible T-periodic input $x(t)$ and admissible T-periodic control $r(t)$. Let $\bar{z}(t)$ be a T-periodic solution of Σ_Z corresponding to the same input and control. If $\operatorname{osc}_T x > 2\bar{r}/G$, then setting $x_1 = x_2 = x$ in (D.1.4) yields $|z(t) - \bar{z}(t)| \le |z(0) - \bar{z}(0)| e^{pT} e^{-pt}$. It follows that the T-periodic solution $\bar{z}(t)$ is exponentially stable. Furthermore, the fact that all solutions converge to $\bar{z}(t)$ means that it must be the unique T-periodic solution of Σ_Z.

Now consider the EVP model from §4.3

$$\Sigma_S \begin{cases} \langle G\dot{x} - Gs/R_c - \dot{s}, s - \varphi \rangle \ge 0 \quad \forall |\varphi| \le r_s(t), \\ |s(t)| \le r_s(t) \qquad \forall t \ge 0. \end{cases} \tag{D.1.14}$$

where $x(t)$ is an admissible T-periodic input and $r_s(t)$ is an admissible T-periodic control. Existence of a T-periodic can be established using the same reasoning as for Σ_Z. Let $s(t)$ be an arbitrary solution of Σ_S and let $\bar{s}(t)$ be a T-periodic solution of Σ_S. The directional derivative of the error function $V(\tilde{s}(t)) = \tilde{s}^2(t) = (s(t) - \bar{s}(t))^2$ satisfies

$$\begin{aligned} \dot{V}(\tilde{s}) &= \langle \dot{s} - \dot{\bar{s}}, s - \bar{s} \rangle, \\ &\le \langle \dot{s} + Gs/R_c - G\dot{x}, s(t) - \bar{s}(t) \rangle + \langle \dot{\bar{s}} + G\bar{s}/R_c - G\dot{x}, \bar{s}(t) - s(t) \rangle - G(s - \bar{s})^2/R_c \\ &\le -G(s - \bar{s})^2/R_c . \end{aligned} \tag{D.1.15}$$

implying that the T-periodic solution $\bar{s}(t)$ is exponentially stable. Since $s(t)$ is an arbitrary solution of Σ_S, it follows that all solutions of Σ_S converge to $\bar{s}(t)$, implying that $\bar{s}(t)$ is the unique T-periodic solution of Σ_S. To sum up, for a given admissible T-periodic input $x(t)$ and control $r_s(t)$, Σ_S has a unique exponentially stable T-periodic solution, $\bar{s}(t)$. Following the same reasoning as before, if $r_s(t)$ is $0T$-periodic, then all solutions converge to $\bar{s}(t)$ within the time interval $[0, T)$. It is quite clear that Σ_S is a much better behaved system than Σ_Z and that its behaviour is also far easier to analyze. This alone would seem to make the dissipation shaping control an interesting option.

D.2 Periodic solutions of the coupled system

The objective here will be to extend some of the results from the previous section, to the case where the Σ_Z and Σ_S are coupled with a simple second order differential equation. The question of existence and stability of periodic solutions for differential equations coupled with models of hysteresis is by no means new and continues to be a very active area of research. Some resent results on this topic can be found in [2]-[5]. A fundamental difference between the present investigation and most of the research to date, is that the constraints placed on the output of the hysteresis model, are now permitted to be time varying. That said, many of the previously obtained results can be extended to the present case, once it has been shown that the system is well-posed. While the systems considered in [2] are far more general than those considered here, the method of analysis is probably the closest in "spirit", to that presented below. The idea is to first establish sufficient conditions for the existence of at least one periodic solution using a suitable fixed point theorem and to then study the stability of these solutions using Liapunov type analysis.

So as to include the case where a dissipation shaping control has been used, consider the system

$$\Sigma\begin{cases}\Sigma_X\begin{cases}\dot{x}_1 = x_2\\ \dot{x}_2 = -Rx_2 - Kx_1 - h(x_1) - z + b(t)\end{cases}\\ \Sigma_Z\begin{cases}\langle Gx_2 - \eta Gz - \dot{z}, z - \varphi\rangle \geq 0, \quad \forall|\varphi| \leq r(t),\\ |z(t)| \leq r(t), \quad \forall t \geq 0.\end{cases}\end{cases} \tag{D.2.1}$$

with state $x_a = (x, z)$, where $G, K, R > 0$ and $\eta \geq 0$ are constants and the nonlinear function $h : \Re \to \Re$ satisfies $h(0) = 0$ and the inequality

$$0 \leq (h(x_1) - h(y_1), x_1 - y_1) \leq L(x_1 - y_1)^2. \tag{D.2.2}$$

for some constant $L \geq 0$. Unless stated otherwise it will be assumed that $r \in C^{0,1}(\Re_+; \Re_+)$ is T-periodic and $b \in C^{0,1}(\Re_+; \Re)$ is a non-constant T-periodic function. Also setting $\bar{r} = \|r\|_\infty$ and $\bar{b} = \|b\|_\infty$, it will be assumed that $\bar{r} \leq \bar{b}$. Any input b and control r satisfying these conditions will henceforth be referred to as admissible. Using inequality (4.1.5) it follows that for initial conditions $x(0) \in \Re^2$ and $|z(0)| \leq r(0)$, any solution of Σ will satisfy $|z(t)| \leq r(t) \leq \bar{b}$

$$|x(t)| \le \beta |x(0)| e^{-ct} + \gamma \bar{b}\left(1 - e^{-ct}\right), \tag{D.2.3}$$

for some constants $\beta, \gamma, c > 0$. Applying Corollary C.3.1 it can be concluded that Σ has a unique solution $x_a(t; x_a(0), r(\cdot), b(\cdot)) = \left(x(t; x_a(0), r(\cdot), b(\cdot)), z(t; x_a(0), r(\cdot), b(\cdot))\right)$ such that $x \in C^{1,1}(\Re_+; \Re^2)$ and $z \in C^{0,1}(\Re_+; \Re)$. Moreover, the solution depends continuously on the initial conditions $x_a(0)$ and the functions $r(t), b(t)$ (inputs). When this dependence is clear the notation $x_a(t) = \left(x(t), z(t)\right) = x_a(t; x_a(0), r(\cdot), b(\cdot))$ will be used to refer to the state of Σ at time $t \ge 0$.

The first step in the analysis will be to show that satisfaction of inequality (D.2.3) is sufficient to ensure that Σ has at least one T-periodic solution. While there are many approaches to solving this problem, a very appealing one is to apply a suitable fixed point theorem, [1][6]. Define the map $\mathrm{P}(x(0), z(0)) = \left(x(T), z(T)\right)$. Due to uniqueness of solutions, a necessary and sufficient condition for the existence of a T-periodic, is that the map P, have at least one fixed point in the admissible solution space. Following [1], the existence of a fixed point will be established using an asymptotic fixed point theorem from [7]. Before stating the theorem, the following definition will be required. Let S be a subset of $\Re^n$ and define by $U(S, \varepsilon)$ the ε-neighbourhood of S in $\Re^n$. If $S_0 \subset S_1 \subset S_2$ are subsets of $\Re^n$, then S_1 is said to be a neighbourhood of S_0 relative to S_2 if there exist an $\varepsilon > 0$ such that $S_1 = S_2 \bigcap U(S_0, \varepsilon)$.

Theorem D.2.1 ([7], Lemma.5)

Let $S_0 \subset S_1 \subset S_2$ be bounded convex subsets of $\Re^n$, such that S_0 and S_2 are closed and S_1 is a neighbourhood of S_0, relative to S_2. Let $\mathrm{P} : S_2 \mapsto \Re^n$ be a continuous map such that for some integer $m > 0$,

$$\mathrm{P}^j(S_1) \subset S_2, \quad 1 \le j \le m-1,$$
$$\mathrm{P}^j(S_1) \subset S_0, \quad m \le j \le 2m-1,$$

then P has at least one fixed point in S_0.

Proposition D.2.1

Suppose that for all admissible initial conditions $x_a(0) = (x(0), z(0)) \in \Re^2 \times [-r(0), r(0)]$, $x(t)$ is UB and UUB with ultimate bound B, then Σ has at least one T-periodic solution $(\bar{x}(t), \bar{z}(t))$, such that $|\bar{x}(t)| \le B, \forall t \ge 0$.

Proof:

Under the above assumptions, the proof can be completed by appropriately defining the sets $S_0 \subset S_1 \subset S_2$, and then applying Theorem D.2.1. Due to the fact that x is UB, there exist positive constants B_1, B_2, such that $B_2 > B_1 > B$ and

$$\begin{aligned} |x(0)| \le B &\Rightarrow |x(t)| < B_1, \forall t \ge 0, \\ |x(0)| < B_1 &\Rightarrow |x(t)| \le B_2, \forall t \ge 0. \end{aligned} \tag{D.2.4}$$

Using the fact that x is also UUB, there exists a positive constant $K = K(B_1, B)$, such that $|x(0)| < B_1 \Rightarrow |x(t)| \le B, \forall t \ge K$. Note that periodicy of r implies $|z(nT)| \le r(0)$ for each nonnegative integer n. Define

$$\begin{aligned} S_0 &= \{(x, z) \in \Re^2 \times \Re \,|\, |x| \le B, |z| \le r(0)\}, \\ S_1 &= \{(x, z) \in \Re^2 \times \Re \,|\, |x| < B_1, |z| \le r(0)\}, \\ S_2 &= \{(x, z) \in \Re^2 \times \Re \,|\, |x| \le B_2, |z| \le r(0)\}. \end{aligned} \tag{D.2.5}$$

The sets $S_0 \subset S_1 \subset S_2$ are cylinders, centred at the origin in $\Re^3$. The lateral surfaces are the same in each case, while the radii are increasing. Clearly S_1 is a neighbourhood of S_0 relative to S_2. Due to uniqueness $\mathrm{P}^j(x(0), z(0)) = (x(jT), z(jT))$, for each nonnegative integer j. Now letting m be the smallest positive integer such that $mT \ge K(B_1, B)$, it follows that $\mathrm{P}^j(S_1) \subset S_2, \forall j > 0$ and $\mathrm{P}^j(S_1) \subset S_0, \forall j \ge m$. Continuity of P follows from the continuity of the solutions of Σ with respect to the initial conditions. Theorem.1 can now be applied to infer that $\mathrm{P} : S_2 \mapsto (\Re^2 \times \Re)$, has at least one fixed point $(\bar{x}(0), \bar{z}(0)) \in S_0$. Finally, since $\bar{x}(t)$ is periodic and ultimate bounded by B it must satisfy $|\bar{x}(t)| \le B, \forall t \ge 0$. □

The next step in the analysis will be to obtain sufficient conditions for Σ to have a GAS and hence unique T-periodic solution. Note that GAS and GUAS are equivalent for T-periodic systems. For the general parameterization in (D.2.1), this task is by no means trivial. However there are certain special cases for which the task is greatly simplified.

Consider first the case where $r([0,T))=0$ (and hence $z(\Re_+)=0$) and $L=0$. In this case Σ reduces to the linear second order system $\dot{x}_1=x_2, \dot{x}_2=-Rx_2-Kx_1+b(t)$, which is easily shown to have a GES T-periodic solution. All of the cases which follow can be seen as nonlinear perturbations of this linear system.

Next the case where $r([0,T))=0$ and $L>0$, so that Σ reduces to Σ_X. It has already been stated in §2.2, that sufficient conditions for Σ_X to have a GES T-periodic solution is that either $L<R^2$ or that Σ_X has a T-periodic solution $\bar{x}(t)$ such that $\|\bar{x}_2\|_\infty < 2RK/L$. Since any T-periodic of Σ_X must satisfy $\|\bar{x}\|_\infty \le \gamma\bar{b}$, the latter condition is trivially satisfied if $\bar{b}$ is sufficiently small.

When $r([0,T))\neq 0$ and $L=0$, one obtains the semi -linear system

$$\Sigma_L\begin{cases}\dot{x}_1=x_2\\ \dot{x}_2=-Rx_2-Kx_1-z+b(t)\\ \langle Gx_2-\eta Gz-\dot{z},z-\varphi\rangle\ge 0, \quad \forall|\varphi|\le r(t),\\ |z(t)|\le r(t), \quad \forall t\ge 0.\end{cases} \tag{D.2.6}$$

Let $(\bar{x}(t),\bar{z}(t))$ be a T-periodic solution of Σ_L and let $(x(t),z(t))$ be an arbitrary solution of Σ_L. Setting $y(t)=x(t)-\bar{x}(t)$ and $\vartheta(t)=z(t)-\bar{z}(t)$, the directional derivative of the error energy

$$V(y,\vartheta)=0.5\left(Ky_1^2+y_2^2+\vartheta^2/G\right) \tag{D.2.7}$$

along the solutions $(\bar{x}(t),\bar{z}(t))$ and $(x(t),z(t))$ satisfies

$$\begin{aligned}\dot{V}(y,\vartheta)&=-Ry_2^2-\eta\vartheta^2+\left\langle\vartheta,\dot{\vartheta}+\eta G\vartheta-G\dot{y}_2\right\rangle/G,\\ &\le -Ry_2^2-\eta\vartheta^2\le 0,\end{aligned} \tag{D.2.8}$$

from which it follows that the T-periodic solution $(\bar{x}(t),\bar{z}(t))$ is uniformly stable. Consider first the case where $\eta=0$. Then (D.2.8) and (D.2.6) imply that $y_2\in L_2(\Re_+;\Re)\cap C^{0,1}(\Re_+;\Re)$, so that Barbalat's lemma (§B.2) can be used to conclude that $y_2(t)\to 0$ as $t\to\infty$, or equivalently $\lim_{n\to\infty}x_2(t+nT)=\bar{x}_2(t)$. Since Σ_L is periodic and has all solutions bounded, the positive limit set $\Omega(x,z)$ is nonempty, compact, invariant and attractive. Furthermore $\Omega(x,z)$ must be contained in the largest invariant subset of $\mathbf{E}=\left\{(x,z)\in\Re^2\times\Re \mid x_2(t)=\bar{x}_2(t),\forall t\ge 0\right\}$. Define $r_m=\min_{t\in[0,T]}r(t)$. Any solution of Σ_L remaining identically in E must satisfy $x_1(t)=\bar{x}_1(t)+a/K$ and $z(t)=\bar{z}(t)-a$, where a is some constant such that $|a|\le 2r_m$. Using the above

mentioned properties of $\Omega(x,z)$, it can thus be conclude that all solutions of $\sum_L$ converge to a T-periodic solution. If $r(t)$ is $0T$-periodic, then $r_m = 0$, implying that $(\bar{x}(t),\bar{z}(t))$ is the unique T-periodic solution $\sum_L$, which is GAS (it can actually be shown that $(\bar{x}(t),\bar{z}(t))$ is GES) . If $r(t)$ is not $0T$-periodic but $\sum_L$ has a T-periodic solution such that $\text{osc}_T \bar{x}_1 - 2\bar{r}/G > 0$, then applying Proposition D.1.2 one obtains the inequality

$$|z(t)-\bar{z}(t)| \le |z(0)-\bar{z}(0)|e^{pT}e^{-pt} + e^{2pT}G\int_0^t e^{-p(t-s)}|x_2(s)-\bar{x}_2(s)|ds, \qquad \text{(D.2.9)}$$

for some constant $p > 0$. Applying Lemma B.5 in §B.2 to (D.2.9), it can be seen that $\lim_{n\to\infty} x_2(t+nT) = \bar{x}_2(t)$ implies $\lim_{n\to\infty} z(t+nT) = \bar{z}(t)$. In this case $\Omega(x,z)$ must be contained in the largest invariant subset of,
$\mathbf{E} = \{(x,z) \in \Re^2 \times \Re \mid x_2(t) = \bar{x}_2(t), z(t) = \bar{z}(t), \forall t \ge 0\}$. Since no solution of $\sum_L$ can remain in $\mathbf{E}$ other than $(\bar{x}(t),\bar{z}(t))$, it can be concluded that the T-periodic solution $(\bar{x}(t),\bar{z}(t))$ is GAS. Now consider the case where $a = 1/R_c > 0$. Then using the same arguments as above, it can be concluded that $\lim_{n\to\infty} x_2(t+nT) = \bar{x}_2(t)$ and $\lim_{n\to\infty} z(t+nT) = \bar{z}(t)$. But then $\Omega(x,z)$ must be contained in the largest invariant subset of $\mathbf{E} = \{(x,z) \in \Re^2 \times \Re \mid x_2(t) = \bar{x}_2(t), z(t) = \bar{z}(t), \forall t \ge 0\}$, once again implying that the T-periodic solution $(\bar{x}(t),\bar{z}(t))$ is GAS.

Based on the above analysis it can be seen that $\sum_L$ is a very well behaved system which is quite amenable to analysis. This is rather surprising considering that $\sum_Z$ is highly nonlinear. Indeed, it will shortly be shown that the rather innocent looking nonlinearity $h(x_1)$ is far trickier to deal with than $\sum_Z$. An important point about the situations considered so far is that a rather complete characterisation of the periodic solutions of were obtained without the need to place restrictions on the magnitudes of the positive constants R, K, G or in the period T. In the more general cases, such an analysis will be far more difficult, if not impossible (using the simple techniques employed here).

Consider now the case where $r([0,T)) \neq 0$, $\eta = 0$ and $L > 0$, so that one obtains the familiar system

$$\Sigma \begin{cases} \Sigma_X \begin{cases} \dot{x}_1 = x_2 \\ \dot{x}_2 = -Rx_2 - Kx_1 - h(x_1) - z + b(t) \end{cases} \\ \Sigma_Z \begin{cases} \langle Gx_2 - \dot{z}, z - \varphi \rangle \geq 0, \quad \forall |\varphi| \leq r(t), \\ |z(t)| \leq r(t), \quad \forall t \geq 0. \end{cases} \end{cases} \tag{D.2.10}$$

Let $(\bar{x}(t), \bar{z}(t))$ be a T-periodic solution of Σ and let $(x(t), z(t))$ be an arbitrary solution of Σ. The distance between solutions $y(t) = x(t) - \bar{x}(t)$ and $\vartheta(t) = z(t) - \bar{z}(t)$ satisfy

$$\begin{aligned} &\dot{y}_1 = y_2 \\ &\dot{y}_2 = -Ry_2 - Ky_1 - \bar{h}(y_1; \bar{x}_1(t)) - \vartheta, \\ &\langle Gy_2 - \dot{\vartheta}, \vartheta \rangle \geq 0, \\ &|\vartheta(t)| \leq 2r(t), \quad \forall t \geq 0, \end{aligned} \tag{D.2.11}$$

where $\bar{h}(y_1; \bar{x}_1) = h(y_1 + \bar{x}_1) - h(\bar{x}_1)$. Due to (D.2.2) $\bar{h}(y_1; \bar{x}_1)$ satisfies the inequality

$$0 \leq \left(\bar{h}(y_1; \bar{x}_1), y_1\right) \leq L(y_1)^2, \tag{D.2.12}$$

for all $\bar{x}_1, y_1 \in \Re$. Note also that $y(t)$ is uniformly bounded due to the boundedness of $x(t)$ and $\bar{x}(t)$. Viewing (D.2.11) as the model of a physical system, it can be seen that the term $\bar{h}(y_1; \bar{x}_1)$ acts like a time-varying, nonlinear stiffness, with the capability of introducing energy into the system. It is for this reason that simple energy-like functions, such as (D.2.7) cannot be used to provide a unified analysis of the possible periodic solutions of (D.2.10). As a result the author has been able to prove GAS, only after placing certain restrictions on the periodic solutions themselves and on the relative magnitude of the system parameters R, K, G and L. Rather than detail all of the possibilities, only a few specific cases will be discussed. It will be assumed throughout that $L < R^2$, which is a sufficient condition for Σ_X to have a GES T-periodic solution when $r([0,T)) = 0$. Consider the Liapunov function,

$$V_1(y, \vartheta) = 0.5\left(2K + aR^2\right)y_1^2 + aRy_1y_2 + y_2^2 + \vartheta^2/G, \tag{D.2.13}$$

Which is positive definite for $a \in (0,2)$. Taking the directional derivative of $V_1(y, \vartheta)$ along the solutions $(\bar{x}(t), \bar{z}(t))$ and $(x(t), z(t))$

$$\begin{aligned}
\dot{V}_1(y,\vartheta) &\le -(2-a)Ry_2^2 - aRKy_1^2 - aR\bar{h}(y_1;\bar{x}_1)y_1 - 2\bar{h}(y_1;\bar{x}_1)y_2 - aRy_1\vartheta, \\
&\le -(2-a)Ry_2^2 - aRKy_1^2 - \frac{aR}{L}\bar{h}(y_1;\bar{x}_1)^2 - 2\bar{h}(y_1;\bar{x}_1)y_2 - aRy_1\vartheta, \\
&\le -(2-a)Ry_2^2 - aRKy_1^2 - \frac{L}{aR}y_2^2 - aRy_1\vartheta, \qquad \text{(D.2.14)} \\
&\le -\frac{1}{aR}\left(a(2-a)R^2 - L\right)y_2^2 - \frac{1}{2}aRKy_1^2 + \frac{1}{2K}aR\vartheta^2, \\
&\le -\left(\frac{1}{aR}\left(a(1-a)R^2 - L\right)y_2^2 + \frac{1}{2}aRKy_1^2 + \frac{1}{2K}aR\vartheta^2\right) + R\left(\frac{a}{K}\vartheta^2 - y_2^2\right),
\end{aligned}$$

where Young's inequality $bc \le \theta b^2/2 + c^2/2\theta, \forall \theta > 0$ has been used repeatedly. Due to the assumption that $L < R^2$, the exists a constant $a \in (0,1)$ such that $a(1-a)R^2 - L > 0$. Picking $a = \min\left\{\theta \in (0,1) \mid \theta(1-\theta)R^2 - L > 0\right\}$ and owing to the fact that $V_1(y,\vartheta)$ is quadratic and positive definite, there exits a constant $c > 0$ such that

$$\dot{V}_1(y,\vartheta) \le -cV_1(y,\vartheta) + R\left(\frac{a}{K}\vartheta^2 - y_2^2\right), \qquad \text{(D.2.15)}$$

and hence

$$V_1(y(t),\vartheta(t)) - V_1(y(0),\vartheta(0)) \le -c\int_0^t V_1(y(\tau),\vartheta(\tau))d\tau + R\int_0^t\left(\frac{a}{K}\vartheta^2(\tau) - y_2^2(\tau)\right)d\tau. \qquad \text{(D.2.16)}$$

Now suppose that $r(t)$ is $0T/m$-periodic for some positive integer m. Assume for simplicity that $r(0) = 0$, then following the same reasoning as in §4.2 (see equations (4.2.10)-(4.2.16)), one obtains the inequality

$$\int_0^t \vartheta^2(\tau)d\tau \le \frac{G^2T^2}{m^2}\int_0^t y_2^2(\tau)d\tau. \qquad \text{(D.2.17)}$$

Inserting (D.2.17) into (D.2.16) gives

$$V_1(y(t),\vartheta(t)) - V_1(y(0),\vartheta(0)) \le -c\int_0^t V_1(y(\tau),\vartheta(\tau))d\tau + R\left(\frac{aG^2T^2}{Km^2} - 1\right)\int_0^t y_2^2(\tau)d\tau. \qquad \text{(D.2.18)}$$

If $m^2 > aG^2T^2/K$, then the second term on the right hand side of (D2.18) will be negative , so that (D.2.18) can be used to conclude that

$$V_1(y(t),\vartheta(t)) \le V_1(y(0),\vartheta(0))e^{-ct}, \qquad \text{(D.2.19)}$$

implying that the periodic solution $(\bar{x}(t),\bar{z}(t))$ is GES and hence unique. Given that the elastic modulus G is assumed to very large, this condition will be very restrictive unless L is very small. If Σ has a T-periodic solution such that $\mathrm{osc}_T\bar{x}_1 - 2\bar{r}/G > 0$

($r(t)$ need not be $0T$-periodic), then applying Proposition D.2 one obtains inequality (D.1.4). Applying Holder's inequality (§A.1) to (D.1.4) and integrating, one obtains the inequality

$$\int_0^t \vartheta^2(\tau)d\tau \le \vartheta^2(0)\frac{e^{2pT}}{2p} + \frac{e^{4pT}G^2}{p^2}\int_0^t y_2^2(\tau)d\tau, \tag{D.2.20}$$

where p is a positive constant (see proof of Proposition D.2 for definition). Assuming that $a<2$, then $V_1(y,\vartheta)$ is quadratic and positive definite, implying the existence of a positive constant C, such that $V_1(y,\vartheta) \ge C\left(|y|^2 + |\vartheta|^2\right)$. Inserting inequality (D.2.20) into (D.2.16) and rearranging, one obtains (recall that $V_1(y(t),\vartheta(t))$ is uniformly bounded)

$$\begin{aligned}\int_0^t \left(|y(\tau)|^2 + |\vartheta(\tau)|^2\right)d\tau \le \frac{1}{cC}V_1(y(0),\vartheta(0)) + \frac{e^{2pT}aR}{2cCKp}|\vartheta(0)|^2 \\ + \frac{R}{cC}\left(\frac{aG^2e^{2pT}}{Kp^2} - 1\right)\int_0^t y_2^2(\tau)d\tau.\end{aligned} \tag{D.2.21}$$

If $a \le Kp^2/\left(G^2e^{2pT}\right)$, then the integral term on the right hand side of (D.2.21) will be negative, so that (D.2.21) can be used to concluded that $y \in L_2(\Re_+;\Re^2)$ and $\vartheta \in L_2(\Re_+;\Re)$. Assuming this to be the case, since $(\bar{x}(t),\bar{z}(t))$ and $(x(t),z(t))$ are Lipschitz continuous, so are $y(t)$ and $\vartheta(t)$. Barbalat's lemma can be used to conclude that $\lim_{n\to\infty} x(t+nT) = \bar{x}(t)$ and $\lim_{n\to\infty} z(t+nT) = \bar{z}(t)$, which, because $(x(t),z(t))$ is an arbitrary solution, implies that the periodic solution $(\bar{x}(t),\bar{z}(t))$ is GUAS. The condition $a \le Kp^2/\left(aG^2e^{2pT}\right)$ can also be seen as a condition that L is sufficiently small, since $a = \min\left\{\theta \in (0,1) \mid \theta(1-\theta)R^2 - L > 0\right\}$.

In an attempt to reduce the restrictions placed on L, specific bounds on the possible periodic solutions of Σ will now be considered. To that end consider the nonautonomous Liapunov function Consider the Liapunov function

$$V_2(y,\vartheta;t) = V_1(y,\vartheta) + 2\int_0^{y_1}\bar{h}(s;\bar{x}_1(t))ds, \tag{D.2.22}$$

where $V_1(y,\vartheta)$ is given in (D.2.15). Assuming that $a<2$ in (D.2.13), the using (D.2.12) it can be shown that there exists two constants $c_2 \ge c_1 > 0$ such that $c_1(y^2+\vartheta^2) \le V_2(y,\vartheta) \le c_2(y^2+\vartheta^2)$. Taking the directional derivative of $V_2(y,\vartheta;t)$ along the solutions $(\bar{x}(t),\bar{z}(t))$ and $(x(t),z(t))$ gives

$$\dot{V}_2(y,\vartheta;t) \le -(2-a)Ry_2^2 - aRKy_1^2 - aRy_1\vartheta + \bar{x}_2(t)\int_0^{y_1} \frac{\partial \bar{h}(s;\bar{x}_1(t))}{\partial \bar{x}_1}\,ds. \qquad \text{(D.2.23)}$$

Using $\bar{h}(y_1;\bar{x}_1) = h(y_1+\bar{x}_1) - h(\bar{x}_1)$ and the definition of $h(x_1)$ given in equation (D.2.2.6) it can be shown that $\left|\partial \bar{h}(y_1;\bar{x}_1)/\partial \bar{x}_1\right| \le 0.5L|y_1|$ for all $\bar{x}_1, y_1 \in \Re$, so that

$$\begin{aligned}\dot{V}_2(y,\vartheta;t) &\le -(2-a)Ry_2^2 - \left(aRK - 0.5L\|\bar{x}_2\|_\infty\right)y_1^2 - aRy_1\vartheta \\ &\le -(1-a)Ry_2^2 - \frac{1}{2}\left(aRK - L\|\bar{x}_2\|_\infty\right)y_1^2 - \frac{aR}{2K}\vartheta^2 + R\left(\frac{a}{K}\vartheta^2 - y_2^2\right).\end{aligned} \qquad \text{(D.2.24)}$$

Now suppose that $r(t)$ is $0T/m$-periodic for some positive integer m, then inequality (D.2.27) holds. Picking $a \le \min(1, Km^2/(GT)^2)$, if Σ has a periodic solution $(\bar{x}(t), \bar{z}(t))$ such that $\|\bar{x}_2\|_\infty \le aRK/L$, then the same reasoning as used to obtain (D.2.19), can be used to show that $(\bar{x}(t), \bar{z}(t))$ is a GES periodic solution of Σ. Recall that any periodic solution of Σ must satisfy $\|x\|_\infty \le \gamma\bar{b}$, for some constant $\gamma > 0$ independent of $\bar{b}$.

It follows that the conditions above can be restated as follows. If r is $0T/m$-periodic and $\bar{b}$ is sufficiently small, then Σ will have a GES T-periodic solution. It would be interesting to try and develop a control $r(t)$ which would ensure that $\|\bar{x}_2\|_\infty \le m^2RK^2/\left(LG^2T^2\right)$. This would obviously be quite difficult, but might be a worthwhile research topic for the future. Unfortunately, the author has been unable to convincingly combine the condition $\mathrm{osc}_T\bar{x}_1 - 2\bar{r}/G > 0$ with the a smallness condition on $\|\bar{x}_2\|_\infty = \|\dot{\bar{x}}_1\|_\infty$. This is another possible topic for future research. To recap on some of the results obtained above.

Proposition D.2.2

(i). If r and b are admissible T-periodic input and control respectively, the system (D.2.10) has at least one T-periodic solution.

(ii). On the assumption that $L < R^2$ and r is $0T/m$-periodic for some positive integer m, if $m^2 > aG^2T^2/K$, where $a = \min\left\{\theta \in (0,1) \mid \theta(1-\theta)R^2 - L > 0\right\}$, then the system (D.2.10) has a unique GES T-periodic solution.

(iii). On the assumption that r is $0T/m$-periodic for some positive integer m, if (D.2.10) has a T-periodic solution $(\bar{x}, \bar{z})$ such that $\|\bar{x}_2\|_\infty \le aRK/L$, where $a \le \min(1, Km^2/(GT)^2)$, then this solution is GES for (D.2.10).

Finally consider the case where $r([0,T)) \neq 0$, $\eta = 1/R_c > 0$ and $L > 0$, so that one obtains the system

$$\Sigma_D \begin{cases} \Sigma_X \begin{cases} \dot{x}_1 = x_2 \\ \dot{x}_2 = -Rx_2 - Kx_1 - h(x_1) - z + b(t) \end{cases} \\ \Sigma_Z \begin{cases} \langle Gx_2 - Gz/R_c - \dot{z}, z - \varphi \rangle \geq 0, \quad \forall |\varphi| \leq r_s(t), \\ |z(t)| \leq r_s(t), \quad \forall t \geq 0. \end{cases} \end{cases} \tag{D.2.25}$$

The system Σ_D arises when the control $r(t) = |s(t)|$, with $s(t)$ being the solution of system Σ_S in (D.1.14), has been applied to the system in (D.2.10). The subscript D is used as a reminder that a dissipation shaping control is being considered. It is assumed that the new control $r_s(t)$ is admissible and $T-$periodic. Similar to the previous case, the distance between solutions $y(t) = x(t) - \bar{x}(t)$ and $\vartheta(t) = z(t) - \bar{z}(t)$ satisfy

$$\begin{aligned} &\dot{y}_1 = y_2 \\ &\dot{y}_2 = -Ry_2 - Ky_1 - \bar{h}(y_1; \bar{x}_1(t)) - \vartheta, \\ &\langle Gy_2 - G\vartheta/R_c - \dot{\vartheta}, \vartheta \rangle \geq 0, \\ &|\vartheta(t)| \leq 2r(t), \quad \forall t \geq 0, \end{aligned} \tag{D.2.26}$$

where $\bar{h}(y_1; \bar{x}_1) = h(y_1 + \bar{x}_1) - h(\bar{x}_1)$ satisfies the inequality in (D.2.12). Let $(\bar{x}(t), \bar{z}(t))$ be a T-periodic solution of Σ_D and let $(x(t), z(t))$ be an arbitrary solution of Σ_D. It should be clear that the stability conditions obtained for Σ also apply to the solutions of Σ_D. Consider the Liapunov function $V_1(y, \vartheta)$ in (D.2.13). The directional derivative of $V_1(y, \vartheta)$ along the solutions $(x(t), z(t))$ and $(\bar{x}(t), \bar{z}(t))$ of Σ_D now satisfy (see (D.2.14))

$$\dot{V}_1(y, \vartheta) \leq -\frac{1}{aR}\left(a(2-a)R^2 - L\right)y_2^2 - aRKy_1^2 - aRy_1\vartheta - \frac{2}{R_c}\vartheta^2, \tag{D.2.27}$$

On the assumption that $L < R^2$, the exists a constant $a \in (0,1)$ such that $a(1-a)R^2 - L > 0$. Picking $a = \min\{\theta \in (0,1) \mid \theta(1-\theta)R^2 - L > 0\}$, the quadratic term $aRKy_1^2 + aRy_1\vartheta + 2\vartheta^2/R_c$, will be positive definite if R_c is chosen such that $R_c < 8K/aR$. Choosing a and R_c as above, the left hand side of (D.2.27) will be negative definite, thus implying that the periodic solution $(\bar{x}(t), \bar{z}(t))$ is GES. Note that the upper bound on R_c tends to infinity as L tends to zero. Now consider the Liapunov function $V_2(y, \vartheta; t)$ given in (D.2.21). Using the inequality $|\partial \bar{h}(y_1; \bar{x}_1)/\partial \bar{x}_1| \leq 0.5L|y_1|$, the directional derivative of $V_2(y, \vartheta; t)$ along the solutions Σ_D satisfies

$$\begin{aligned}\dot{V}_2(y,\vartheta;t) &\le -(2-a)Ry_2^2 - \left(aRK - \frac{1}{2}L\|\bar{x}_2\|_\infty\right)y_1^2 - aRy_1\vartheta - \frac{2}{R_c}\vartheta^2 \\ &\le -(2-a)Ry_2^2 - \frac{1}{2}\left(aRK - L\|\bar{x}_2\|_\infty\right)y_1^2 - \left(\frac{2}{R_c} - \frac{aR}{2K}\right)\vartheta^2.\end{aligned} \tag{D.2.28}$$

Suppose Σ_D has a T-periodic solution $(\bar{x}(t),\bar{z}(t))$, such that $\|\bar{x}_2\|_\infty < 2RK/L$. Setting $a = \min\{\theta \in (0,2) \mid \theta > L\|\dot{x}_2\|/RK\}$, if $R_c < 4K/aR$ then the right hand side of (D.2.27) will be negative definite, implying that $(\bar{x}(t),\bar{z}(t))$ is GES and hence unique. Since any periodic solution of Σ_D must satisfy $\|x\|_\infty \le \gamma\bar{b}$, for some constant $\gamma > 0$ independent of $\bar{b}$, it can be seen that bound on R_c tends to infinity as $\bar{b}$ tends to zero. Note that that the two conditions given above only require that the control $r(t)$ is T-periodic. The discussion above establishes the following.

Proposition D.2.6

(i). If r and b are an admissible T-periodic input and control respectively, the system (D.2.25) has at least one T-periodic solution.

(ii). On the assumption that $L < R^2$, set $a = \min\{\theta \in (0,1) \mid \theta(1-\theta)R^2 - L > 0\}$. If $R_c < 8K/aR$ then the system (D.2.25) has a unique GES T-periodic solution.

(iii). If (D.2.25) has a T-periodic solution $(\bar{x},\bar{z})$ such that $\|\bar{x}_2\|_\infty \le aRK/L$, where $a \le \min(2, 4K/(RR_c))$, then this solution is GES for (D.2.25)

The conditions derived for the uniqueness and stability of the periodic solutions of Σ and Σ_D are only sufficient and by no means necessary. It is thought that with further investigation and by employing different techniques of analysis, that the restrictions on the $0T/m$-periodic control and the magnitude of the parameter R_c may be significantly weakened. Some possible directions of investigation and techniques are discussed in the conclusions and discussions chapter of this thesis.

In what follows it will be assumed that $L < R^2$ and that R_c has been chosen so as to ensure that Σ_D has a GES T-periodic solution

$(\bar{x}(t),\bar{z}(t)) = \left(\bar{x}(t;\bar{x}_a(0),r_s(\cdot),b(\cdot)),\bar{z}(t;\bar{x}_a(0),r_s(\cdot),b(\cdot))\right)$.

Let $\hat{r}_s(t)$ and $\hat{b}(t)$ be an admissible control and input, which converge to the T-periodic functions $r_s(t)$ and $b(t)$ respectively, in the sense that $\lim_{n\to\infty}\hat{r}_s(t+nT)=r_s(t)$ and $\lim_{n\to\infty}\hat{b}(t+nT)=b(t)$ for all $t\in[0,T]$. Suppose that $(\hat{x}(t),\hat{z}(t))$ is an arbitrary solution of Σ_D corresponding to the control and input $\hat{r}_s(t)$ and $\hat{b}(t)$, that is $\hat{x}(t)=\hat{x}(t;\hat{x}_a(0),\hat{r}_s(\cdot),\hat{b}(\cdot))$ and $\hat{z}(t)=\hat{z}(t;\hat{x}_a(0),\hat{r}_s(\cdot),\hat{b}(\cdot))$. It will now be shown that under the conditions stated above that $\lim_{n\to\infty}(\hat{x}(t+nT),\hat{z}(t+nT))=(x(t),z(t))$. Let $z^*(t)$ denote the solution of the variational inequality

$$\begin{aligned}&\left\langle G\hat{x}_2-Gz^*/R_c-\dot{z}^*,z^*-\varphi\right\rangle\geq 0,\quad \forall|\varphi|\leq r(t),\\&\left|z^*\right|\leq r(t),\ \forall t\geq 0.\end{aligned}\tag{D.2.29}$$

For simplicity it will be assumed that $r(0)\geq\hat{r}(0)$, so that $z^*(0)=\hat{z}(0)$ is an admissible initial condition. Set $a=G/R_c$, $\hat{w}(t)=G\hat{x}_2(t)-a\hat{z}(t)-\dot{\hat{z}}(t)$ and $w^*(t)=G\hat{x}_2(t)-az^*(t)-\dot{z}^*(t)$. It can be shown that $\left\|w^*\right\|_\infty,\left\|\hat{w}\right\|_\infty\leq G\kappa_X+a\bar{r}+\kappa_r\equiv B/4$, where κ_X is a Lipschitz constant for $\hat{x}(t)$ and κ_r is a Lipschitz constant for $r(t)$ and $\hat{r}(t)$. Testing the variational inequality defining $z^*(t)$ with $\varphi=Q(\hat{z};r(t))$ yields

$$\left\langle G\hat{x}_2-az^*-\dot{z}^*,z^*-Q(\hat{z},r(t))\right\rangle=\left\langle G\hat{x}_2-az^*-\dot{z}^*,z^*-\hat{z}\right\rangle+w^*P(\hat{z};r(t))\geq 0,\tag{D.2.30}$$

which implies (see §A2 for the properties of the operators $Q(\hat{z};r(t))$ and $P(\hat{z};r(t))$)

$$\left\langle G\hat{x}_2-az^*-\dot{z}^*,z^*-\hat{z}\right\rangle+B/4\left|r(t)-\hat{r}(t)\right|\geq 0.\tag{D.2.31}$$

Similarly, testing the variational inequality defining $\hat{z}(t)$ with $\varphi=Q(z^*;\hat{r}(t))$ yields

$$\left\langle G\hat{x}_2-a\hat{z}-\dot{\hat{z}},\hat{z}-z^*\right\rangle+B/4\left|r(t)-\hat{r}(t)\right|\geq 0.\tag{D.2.32}$$

Define $\rho=\hat{z}-z^*$ and $\tilde{r}=r-\hat{r}$. Now adding (D.2.31) and (D.2.32), and then rearranging gives

$$\left\langle\dot{\rho},\rho\right\rangle\leq-a\rho^2+B/2\left|\tilde{r}(t)\right|.\tag{D.2.33}$$

Integrating (D.2.32) over the interval $[0,\tau]$ and using $\rho(0)=0$ gives

$$\rho^2(\tau)\leq B\int_0^\tau e^{-2a(\tau-s)}\left|\tilde{r}(s)\right|ds.\tag{D.2.34}$$

For some $\sigma>0$ such that $\sigma<2a$ and $t\geq\tau$ multiplying (D.2.34) by $e^{-\sigma(t-\tau)}$ and integrating up to t gives

$$\begin{aligned}\int_0^t e^{-\sigma(t-\tau)}\rho^2(\tau)d\tau &\le B\int_0^t e^{-\sigma(t-\tau)}\int_0^\tau e^{-2a(\tau-s)}|\tilde{r}(s)|dsd\tau,\\ &\le B\int_0^t e^{-\sigma t}e^{-2as}|\tilde{r}(s)|\int_s^\tau e^{(\sigma-2a)\tau}d\tau ds,\\ &\le \frac{B}{\sigma-2a}\int_0^t|\tilde{r}(s)|\left(e^{-2a(t-s)}-e^{-\sigma(t-s)}\right)ds\\ &\le \frac{R_cB}{2G-R_c\sigma}\int_0^t e^{-\sigma(t-s)}|\tilde{r}(s)|ds.\end{aligned} \tag{D.2.35}$$

An estimate in terms of $|\rho(t)|$ rather than $\rho^2(t)$ can be obtained by application of Holder's inequality to (D.2.35)

$$\begin{aligned}\int_0^t e^{-\sigma(t-s)}|\rho(s)|ds &\le \left(\int_0^t e^{-\sigma(t-s)}\rho^2(s)ds\right)^{1/2}\left(\int_0^t e^{-\sigma(t-s)}ds\right)^{1/2},\\ &\le \left(\frac{1}{\sigma}\int_0^t e^{-\sigma(t-s)}\rho^2(s)ds\right)^{1/2},\\ &\le \left(\frac{R_cB}{\sigma(2G-R_c\sigma)}\int_0^t e^{-\sigma(t-s)}|\tilde{r}(s)|ds\right)^{1/2},\\ &= \tilde{B}\left(\int_0^t e^{-\sigma(t-s)}|\tilde{r}(s)|ds\right)^{1/2}.\end{aligned} \tag{D.2.36}$$

Now setting $y(t)=\hat{x}(t)-\bar{x}(t)$, $\vartheta(t)=z^*(t)-\bar{z}(t)$, $\tilde{b}(t)=\hat{b}(t)-b(t)$ and using (D.2.25), the distance between solutions satisfies

$$\begin{aligned}&\dot{y}_1 = y_2\\ &\dot{y}_2 = -Ry_2-Ky_1-\bar{h}(y_1;\bar{x}_1(t))-\vartheta-\rho(t)+\tilde{b}(t),\\ &\left\langle Gy_2-G\vartheta/R_c-\dot{\vartheta},\vartheta\right\rangle \ge 0,\\ &|\vartheta(t)|\le 2r(t),\quad \forall t\ge 0.\end{aligned} \tag{D.2.37}$$

The directional derivative of $V_1(y,\vartheta)$ along the solutions $(\hat{x}(t),z^*(t))$ and $(\bar{x}(t),\bar{z}(t))$ satisfies

$$\begin{aligned}\dot{V}_1(y,\vartheta) \le &-\left(\frac{1}{aR}\left(a(2-a)R^2-L\right)y_2^2+aRKy_1^2+aRy_1\vartheta+\frac{2}{R_c}\vartheta^2\right)\\ &+\left(aR|y_1|+2|y_2|\right)\left(|\rho(t)|+|\tilde{b}(t)|\right)\end{aligned} \tag{D.2.38}$$

As in pervious developments, on the assumption that $L<R^2$, and R_c and a can be chosen so as to ensure $V_1(y,\vartheta)$ and the first term in brackets on the right hand side of (D.2.38) are positive definite. Assuming this to be the case and following the usual procedures one obtains the estimate

$$|y_\vartheta(t)| \le \beta|y_\vartheta(0)|e^{-\sigma t}+\gamma\int_0^t e^{-\sigma(t-s)}\left(|\rho(s)|+|\tilde{b}(s)|\right)ds, \tag{D.2.39}$$

where $y_\vartheta(t) = (y(t), \vartheta(t))$ and for some constants $\beta, \gamma, \sigma > 0$. Inserting (D.2.36) into (D.2.39) one obtains (one can assume that $\sigma < 2a$, by taking a smaller σ if necessary)

$$|y_\vartheta(t)| \le \beta |y_\vartheta(0)| e^{-\sigma t} + \gamma \int_0^t e^{-\sigma(t-s)} |\tilde{b}(s)| ds + \gamma \tilde{B} \left(\int_0^t e^{-\sigma(t-s)} |\tilde{r}(s)| ds \right)^{1/2}. \quad \text{(D.2.40)}$$

It follows from Lemma B.5 in §B.2 that if $\tilde{r}, \tilde{b} \in L_1(\Re_+; \Re)$ or if $\lim_{n\to\infty} \hat{r}(t+nT) = r(t)$ and $\lim_{n\to\infty} \hat{b}(t+nT) = b(t)$, then $\lim_{n\to\infty} \hat{x}_a(t+nT) = \bar{x}_a(t)$. This property implies that the solutions of Σ_D "forget" their initial conditions and converge to a "steady state" solution which is determined by the asymptotic behaviour of $b(t)$ and $r(t)$. Equivalently, the structure of the positive limit set $\Omega(x,z)$ is independent of the initial conditions and depends only on the positive limit sets of the functions $b(t)$ and $r(t)$.

References

[1] T. Burton. Stability and periodic solutions of ordinary and functional differential equations. Academic Press, Orlando, 1985.

[2] M. Brokate, A. Pokrovskii. "Asymptotically stable oscillations with hysteresis nonlinearities". Journal Differential Equations, vol.150, pp. 98-123, 1998.

[3] P. Krejci. "Reliable solutions to the problem of periodic oscillations of an elastoplastic beam", International Journal of Nonlinear Mechanics, vol.31, pp.1337-1349 , 2002.

[4] P. Bliman, A. Krasnosel'skii, M. Sorine, A. Vladimirov. "Nonlinear resonance in systems with hysteresis". Nonlinear Analysis, Theory, Methods and Applications. vol. 27, pp.561-577, 1996.

[5] C. Comain. "On a class of non-smooth oscillators". Dynamical Systems, vol. 18, pp.1-22, 2003.

[6] T. Yoshizawa. Stability theory and the existence of periodic and almost periodic solutions. Springer-Verlag, 1973.

[7] W. Horn. "Some fixed point theorems for compact maps and flows in Banach spaces". Transactions of the American Mathematical Society, vol. 149, pp.391-404, 1970.